Investigation of *Plasmodium falciparum* Aminopeptidases and Characterisation of the M17 Leucine Aminopeptidase

A thesis submitted for the degree of Doctor of Philosophy

by

Eithne Cunningham

Moyne Institute of Preventive Medicine

School of Genetics and Microbiology

Trinity College

University of Dublin

October 2007
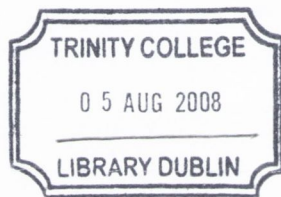
DECLARATION

This is to certify that the experimentation recorded herein represents my own work, unless otherwise stated, and has not been submitted for higher degree at this or any other university.

This thesis may be lent or copied at the discretion of the librarian, Trinity College.

Eithne Cunningham

Eithne Cunningham

October, 2007

SUMMARY

Plasmodium falciparum spends part of its life cycle residing in human erythrocytes, during which time it digests much of the host cell haemoglobin to provide a source of amino acids for synthesis of its own proteins. The final stages of digestion are thought to be carried out by aminopeptidases that cleave amino acids from the N-termini of peptides. The inhibition of aminopeptidase activity can disrupt parasite development, implicating this group of enzymes as a possible drug target. Novel targets for antimalarial drugs are greatly needed due to the high rate of mortality associated with the disease and the emergence of resistance to existing treatments.

The gene for an M1-family aminopeptidase (*PfAP-M1*) has previously been identified. This study identified the presence of three additional, putative (non-methionine) metallo-aminopeptidases: PfAP-M17, PfAP-M18 and PfAP-M24. Northern blotting and PCR amplification of DNA confirmed expression of the four genes in asexual, erythrocytic parasites. Stage-specific Northern blotting showed maximal transcription of *PfAP-M17* in immature stage parasites. Western blotting and fluorescence microscopy of parasites with green fluorescent protein (GFP)-tagged *PfAP-M17* demonstrated the presence of similar levels of PfAP-M17 throughout the intra-erythrocytic cycle. GFP fluorescence located PfAP-M17 in the parasite cytosol and this was confirmed by immunofluorescence studies. Experiments attempting to produce transgenic parasites under-expressing *PfAP-M17*, including one using an antisense method, were unsuccessful.

Production of the aminopeptidases as maltose binding protein (MBP)-fusion proteins (including two truncates of PfAP-M1) in *Escherichia coli* using their native gene sequences was unsuccessful. Production of PfAP-M17 and a truncated protein lacking the low-complexity N-terminal region, tPfAP-M17, (both codon-optimised for yeast expression) as hexahistidine-tagged proteins in *E. coli* produced weakly active enzymes but a more stable and active truncated enzyme was produced in baculovirus-infected insect cells. The protein was purified from these cells and characterised. It was found to form hexamers, had a neutral pH optimum and was most active against a substrate with an N-terminal leucine residue but unexpectedly had negligible activity against an alanine substrate. It was activated by metal ions, especially Co^{2+}, and was inhibited by metal chelators and by bestatin.

The antimalarial and anti-aminopeptidase activities of a series of compounds designed to inhibit M17 aminopeptidases (α-aminoalkylphosphonates and phosphonopeptides) and of a series designed to inhibit M1 aminopeptidases (3-amino-2-

tetralone and 3-amino-benzosuberone derivatives) were assessed. A correlation was found between the inhibition of parasite growth and of M17 leucine aminopeptidase activity by the former, indicating that inhibition of this enzyme could be a basis for the design of new drugs. Although the second group contained compounds with both good antimalarial and good anti-aminopeptidase activities, no direct relationship between the two activities was observed.

Overall, this work has furthered our knowledge about the *P. falciparum* aminopeptidases and their possible importance for the parasites. In particular the characterisation of PfAP-M17 is reported and evidence is presented that helps to validate this enzyme as an antimalarial drug target.

ACKNOWLEDGEMENTS

PUBLICATIONS ORIGINATING FROM THIS STUDY

1. Stack C. M., J. Lowther, E. Cunningham, S. Donnelly, D. L. Gardiner, K. R. Trenholme, T. S. Skinner-Adams, F. Teuscher, J. Grembecka, A. Mucha, P. Kafarski, L. Lua, A. Bell and J. P. Dalton. (2007) Characterization of the *Plasmodium falciparum* M17 leucyl aminopeptidase. A protease involved in amino acid regulation with potential for antimalarial drug development. J Biol Chem **282**: 2069-80.

2. Cunningham E., M. Drag, P. Kafarski and A. Bell. (2008) Chemical target validation studies of aminopeptidase in malaria using alpha-aminoalkylphosphonate and phosphonopeptide inhibitors. Antimicrob Agents Chemother. In press.

TABLE OF CONTENTS

x

Chapter 3 Investigation of aminopeptidase genes and gene expression in *Plasmodium falciparum*

Chapter 4 Recombinant expression of *P. falciparum* aminopeptidases including purification and functional analysis of the M17 aminopeptidase

Chapter 5 Anti-malarial and anti-aminopeptidase activities of M17 aminopeptidase inhibitors

List of Figures

List of Tables

Key to Abbreviations

AAP	alanine aminopeptidase activity
AMA	apical membrane antigen
AMC	amino-methyl-coumarin
Amp	ampicillin
AMT	acetate/MES/Tris
APAD	3-acetyl pyridine adenine dinucleotide
APN	aminopeptidase N
APS	ammonium persulphate
bp	base pair
BSA	bovine serum albumin
cDNA	complementary deoxyribonucleic acid
Cm	chloramphenicol
CS	circumsporozoite
CSPD	disodium 3-(4-methoxyspiro-(1,2-dioxethane-3-2'-(5'-chloro)-tricyclo (3.3.1.)decane-4-yl) phosphate
ddH$_2$O	double deionised water
DEPC	diethyl pyrocarbonate
DIG	digoxigenin
DMSO	dimethylsulphoxide
DPAP	dipeptidyl aminopeptidase
DTT	dithiothreitol
EC	Enzyme Commission
ED	experiment discontinued
EDTA	ethylenediaminetetraacetic acid

EGTA	etheleneglycolbis(aminoethyl)-tetra-acetic acid
EK	enterokinase
GFP	green fluorescent protein
h	hour
HAP	histo-aspartic peptidase
HEPES	4-(2-hydroxyethyl)-1-piperazineethanesulphonic acid
HPLC	high performance liquid chromatography
IC_{50}	median inhibitory concentration
ICP-MS	inductively coupled plasma mass spectrometry
IPTG	isopropyl-β-D-thiogalactopyranoside
Kan	kanamycin
kbp	kilobase pair
LAP	leucine aminopeptidase activity
LTA_4H	leukotriene A_4 hydrolase
LDH	lactate dehydrogenase
MBP	maltose binding protein
MCAC	metal-chelate affinity chromatography
MCS	multiple cloning site
MES	2-(N-morpholino)ethanesulfonic acid
min	minute
MSP	merozoite surface protein
NBT	nitroblue tetrazolium

NR	not reported
NS	not specified
PAGE	polyacrylamide gel electrophoresis
PBS	phosphate buffered saline
PCR	polymerase chain reaction
PES	phenazine ethosulphate
PIGPA	phosphate-inosine-glucose-pyruvate -adenine
PIPES	piperazine-N,N'-bis [2-ethanesulphonic acid]
PfLDH	parasite lactate dehydrogenase
pkLAP	porcine kidney leucine aminopeptidase
PMSF	phenylmethylsulphonyl fluoride
PVDF	polyvinylidene fluoride
rEK	recombinant enterokinase
rpm	revolutions per minute
RT-PCR	reverse transcriptase polymerase chain reaction
s	second
SDS	sodium dodecyl sulphate
SDS-PAGE	sodium dodecyl sulphate- polyacrylamide gel electrophoresis
SEM	standard error of the mean
Str	streptomycin
SSC	saline sodium citrate

TAE	Tris-acetate-EDTA
TBE	Tris-borate-EDTA
TCA	trichloroacetic acid
TE	Tris-EDTA
TEMED	N, N, N', N'-tetramethyl-ethylenediamine
Tet	tetracycline
Tris	tris(hydroxymethyl)aminomethane
UV	ultraviolet
YFP	yellow fluorescent protein

Chapter 1

General Introduction

1.1. MALARIA

1.1.1. Malaria: an introduction

Malaria is caused by the protozoal, apicomplexan parasite *Plasmodium* and is transmitted to humans by the female *Anopheles* mosquito, with 60 of the 400 species acting as vectors (22). Of greater than 120 species of *Plasmodium*, there are at least 4 species that infect humans: *P. falciparum*, *P. vivax*, *P. ovale* and *P. malariae*, with the first two of these the most common but *P. falciparum* by far responsible for the majority of deaths, due to the development of severe malaria (104). Recent reports have also documented infection of humans in Southeast Asia by *P. knowlesi*, previously thought to infect only primates (148).

Approximately 40% of the world's population is at risk of malaria, living in tropical and subtropical malaria endemic regions. Most cases and deaths occur in Africa but areas of Asia, Latin America, the Middle East and Europe are also at risk. An estimated 500 million people become infected with malaria every year, resulting in more than a million deaths, with young children and pregnant women most affected. In Africa it is responsible for one in five childhood deaths (22) and it is estimated that a child dies of malaria every 30 seconds (173). The high rate of mortality associated with the disease and the emergence of resistance to existing treatments means that new drugs and new drug targets are in great demand (44).

1.1.2. The developmental cycle of *P. falciparum*

The life cycle of *P. falciparum* (illustrated in Figure 1.1 (175)) is quite complex and involves both the human host and the mosquito vector and a number of distinct stages. Transmission of the parasite to humans occurs via the salivary glands of the female *Anopheles* mosquito during a blood-meal, required for the gestation of the mosquito's eggs. Between 5 and 20 sporozoites (133) are injected into the bloodstream or the tissue of the human host. Within minutes some of these sporozoites will have found their way to the liver and invaded hepatocytes where they multiply asexually to develop initially into hepatic (exoerythrocytic) trophozoites and then into schizonts. This exoerythrocytic schizogony produces thousands of merozoites that are released following rupture of the infected hepatocyte, six to sixteen days after infection. The merozoites then invade the host erythrocytes where they undergo asexual multiplication (intra-erythrocytic schizogony), are released and invade new erythrocytes, over a period of ~48 h (described in more detail in section 1.1.3). Some merozoites differentiate into sexual micro (male)- and macro

1

(female)- gametocytes that are taken up by the mosquito while feeding. In the mosquito's stomach the macrogametocytes escape from the erythrocytes and develop into macrogametes, while the microgametocytes undergo nuclear division and formation of motile microgametes. Penetration of the macrogametes by the microgametes results in the fertilisation of the former and generation of the diploid zygote. This form develops further into the motile and elongated ookinete that penetrates the midgut wall of the mosquito where it develops into the oocyst stage. Expansion and nuclear division of the oocyst generates thousands of haploid sporozoites that migrate to the salivary glands and can be transmitted to humans, completing the parasite life-cycle. This mosquito stage of sexual sporogony takes approximately 12 days (57).

1.1.3. Intra-erythrocytic stages of *P. falciparum* development

The asexual phase of the *P. falciparum* life-cycle (illustrated in Figure 1.2) occurs in the host red blood cells and lasts for approximately 48 h. The merozoites attach to the erythrocyte and orientate themselves such that the apical region can contact the cell surface and induce the formation of the parasitophorous vacuole to enable entry into the cell. The parasites develop into a biconcave disc or cup shape called the ring stage (92) (because of their appearance by Giemsa staining) that feeds on the host cell (haemoglobin and nutrients) through a cytosome and carries out processes including the synthesis and export of ring-stage specific molecules to the erythrocyte surface (38, 151). The following stage of development, the trophozoite stage, is the most active in terms of growth and development. The parasite enlarges, the large, acidic digestive vacuole is formed and more parasite proteins are exported to the cell surface. During the schizont phase the parasite undergoes nuclear division producing up to 24 nuclei that are incorporated into new merozoites and the parasite is now termed a segmenter. The merozoites are released and can invade more erythrocytes (12). The export of molecules to the surface of the erythrocyte results in the adhesion of the mature parasite-infected erythrocyte to uninfected cells (termed rosetting) and to the walls of the blood vessels (cytoadherence). This, along with other factors, can lead to severe malaria that is often fatal (104). This erythrocytic stage of the parasite's life-cycle is associated with the clinical symptoms of malaria, i.e. fever, chills etc. and is the target of most antimalarial drugs (15).

1.2. PEPTIDASES

1.2.1. Peptidases: introduction and classification
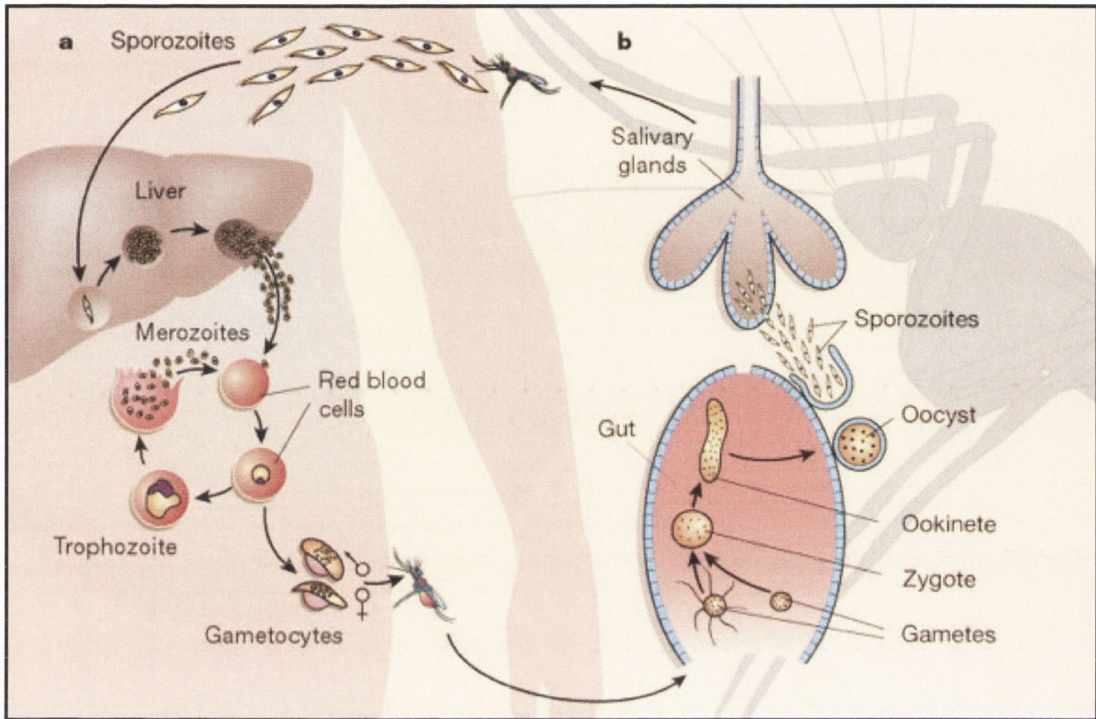
Figure 1.1. The developmental cycle of *P. falciparum*. Anti-clockwise from the top, parasites are injected into the human host (a) by the female *Anopheles* mosquito (b) as sporozoites during a blood-meal. Sporozoites quickly invade hepatocytes and develop through hepatic trophozoites and schizonts (liver stage) to release merozoites that invade erythrocytes. It is here that the ~ 48-h, asexual development through the ring, trophozoite and schizont stage to new merozoites takes place (erythrocyte stage, see Figure 1.2). The released merozoites invade fresh erythrocytes or differentiate into the sexual gametocytes that are taken up by the mosquito. The gametocytes develop into gametes in the insect gut and penetration of the macrogamete by the motile microgamete produces the diploid zygote. This develops further into an ookinete that penetrates the mosquito midgut wall. Here it develops into an oocyst that divides to produce sporozoites that can infect another human host. From Wirth, 2002 (175)
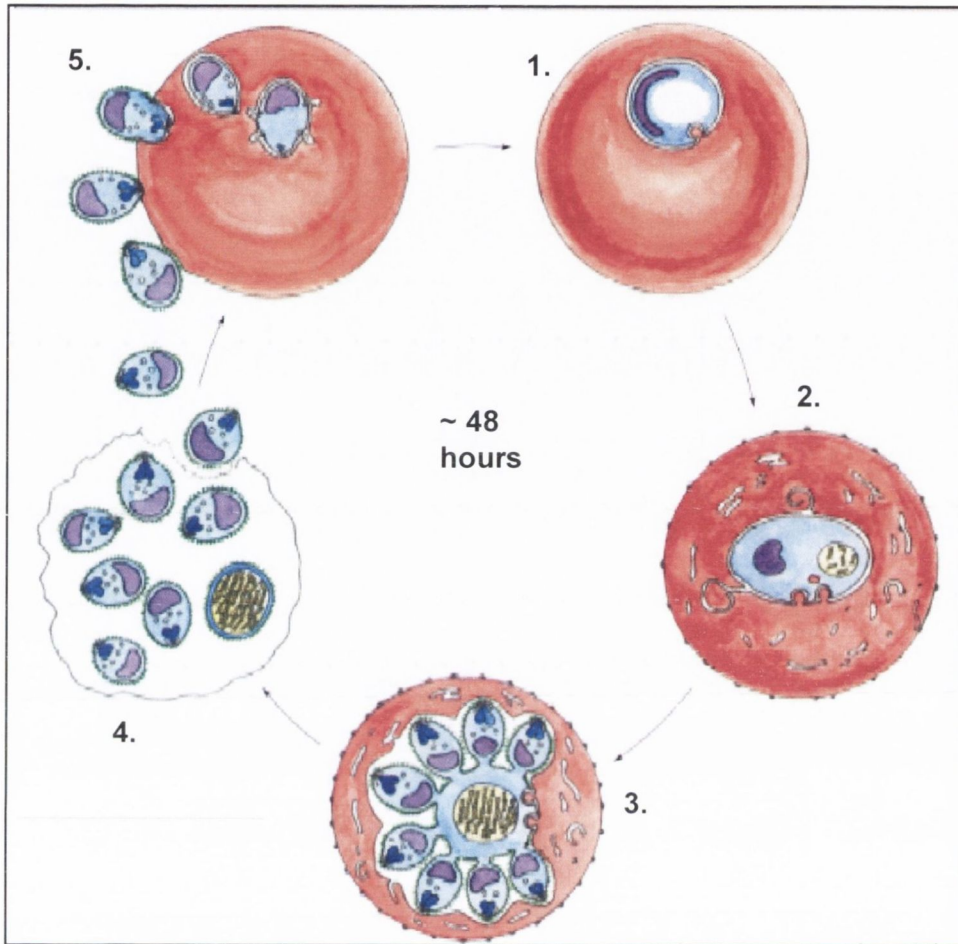
Figure 1.2. The asexual, intra-erythrocytic phase of the *P. falciparum* life-cycle. The merozoites develop through the ring stage (1) and trophozoite stage (2) to form erythrocytic schizonts (3) and, finally, more merozoites (4) that are released and can invade more erythrocytes (5) completing the cycle. Adapted from Bannister *et al*, 2003 (12).

Peptidases (also called proteases) belong to the hydrolase group of enzymes and catalyse the breakdown of proteins by hydrolysing peptide bonds. They are classed as the group EC 3.4 according to the Enzyme Commission (EC) scheme for numbering, where 3 indicates the hydrolase group and 4 indicates the peptidase sub-group (8). They are a large group of enzymes accounting for 10% of those listed by the EC (13) and are important for a great range of processes, including protein synthesis and regulation, growth, cell cycle control, immunological processes and cell differentiation and death, in a variety of organisms ranging from viruses and bacteria to eukaryotes including mammals (97). This importance is reflected in the fact that they represent approximately 2% of the genes products of all organisms that have had their genomes sequenced (130). Peptidases can be defined depending on the position of the peptide bond, in the particular substrate, that they cleave, termed the scissile bond. Endopeptidases cleave internal bonds while exopeptidases cleave N-terminal residues (aminopeptidases) or C-terminal residues (carboxypeptidases). Other peptidases include dipeptidases that cleave dipeptides into two separate amino acids and dipeptidyl and tripeptidyl peptidases that cleave dipeptides and tripeptides, respectively, from the N-termini of substrates (131).

Peptidases are also classed into catalytic groups based on their chemical mechanism of catalysis, i.e. serine, cysteine, threonine, aspartic, glutamic and metallo peptidases (and a few that are classed as unknown). The first three groups use a covalent catalysis where the nucleophile that targets the peptide bond is part of the particular amino acid and a histidine normally acts as a base. The non-covalent mechanism of action of the other three groups involves the activation of a water molecule to act as the nucleophile while the aspartate, glutamate or metal ion function as acids and bases (162).

The most recent classification system is the basis of the construction of the MEROPS database and web site (131). It groups peptidases into families (nearly 200 so far) based on similarity between their molecular structures, particularly in the region involved in catalysis. The member of a family is named by a letter indicating its catalytic type (e.g. M for metallo), followed by an arbitrarily assigned number. A clan then consists of a group of families that demonstrate some evolutionary relationship to each other, indicated by their tertiary structures or by the arrangement of catalytic-site residues. They are named with the letter representing their catalytic type followed by another letter. In some cases families and clans are also be further divided into sub-families and sub-clans (129, 131).

1.2.2. Peptidase Inhibitors

As the activity of peptidases is very important for the correct functioning of various cells and processes they do need to be carefully regulated and, therefore, a number of proteins exist to prevent their action. Peptidase inhibitors have been classified similarly to peptidases, although differences, like inhibitors having much smaller active units (as little as 14 amino acids) than peptidases (generally up to 200), made the classification more difficult. They have been divided into 55 families based on homologous amino acid sequences, particularly in the inhibitory subunit, and 41 of these have been classified into 32 clans, groups containing families that show an evolutionary relationship, primarily through similar tertiary structure (132). There are also a large number of small-molecule peptidase inhibitors listed on the MEROPS website that are not included in this classification system (131).

The importance of peptidase inhibitors is confirmed by the variety of diseases associated with excessive levels of proteolysis, including cancers, cardiovascular and inflammatory disorders and a number of microbial diseases. Similarly, a number of disorders (often genetic) have been associated with decreased peptidase activity, e.g. epilepsy (132). The correct functioning of peptidase activity is clearly an important area and as a result peptidases and their inhibitors are under investigation as novel drugs in a variety of areas (162).

1.2.3. Metallopeptidases

Metallopeptidases are the most diverse of the different catalytic types of peptidases. They require the presence of a metal co-factor in their active site for activity, which is often zinc but may be other metals including manganese and cobalt. Metallopeptidases can contain a single zinc (166) (or other metal) ion or two ions (165) depending on their type. In the case of the latter, both metals may be needed for full enzyme activity or the second (usually less tightly bound) may only be involved in regulation of the catalytic activity. Both the mononuclear and dinuclear metal centres aid in catalysis by providing substrate binding sites, by activating the nucleophile and by helping to stabilise the transition state of the reaction (103).

The metallopeptidase catalytic group contains 53 (M) families divided between 15 clans (131). About half of them are in families divided between the MA and MM clans that are characterised by the sequence motif originally designated the His-Glu-Xaa-Xaa-His (where Xaa is any amino acid) (HEXXH) motif that was subsequently extended to the larger sequence Xaa-Xbb-Xcc-His-Glu-Xbb-Xbb-His-Xbb-Xdd where Xaa is hydrophobic

or Thr, Xbb is uncharged, Xcc is any amino acid except Pro, and Xdd is hydrophobic (83). This motif is important for metal binding and plays a role in enzyme activity.

Metallopeptidases have been found to be involved in processes including protein maturation and degradation, cell-cycle control and tissue repair. They have also been associated with a variety of diseases and disorders ranging from cancers and neurological disorders to infectious diseases including HIV infection and as such have been suggested as targets for drug development (77). The most common metallopeptidase inhibitors are metal chelators (e.g. EDTA, 1,10-phenanthroline) that inhibit the enzyme by binding to the metal needed for catalytic activity.

1.2.4. Aminopeptidases

Aminopeptidases are peptidases that catalyse the hydrolysis of single amino acids from the N-termini of proteins or peptides. They are found in a wide variety of organisms, from animals and plants to protozoa and prokaryotes, and are involved in a diverse range of functions including protein degradation and maturation, cell-cycle control, regulation of protein and hormone levels and regulation of amino acid supply. Their altered expression and/or activity have been found to be associated with conditions ranging from cataracts and aging to cancers and leukemias (157). The majority of aminopeptidases are metallopeptidases. Apart from being divided into families of this catalytic type aminopeptidases can also be classified in terms of their Enzyme Commission (EC) numbers. They are in the group EC 3.4.11, where the number 11 indicates the cleavage of an amino-terminal amino acid, and they are numbered further from 3.4.11.1 to 3.4.11.23 depending on what reaction they catalyse (see Table 1.1 (8)). Aminopeptidases are also referred to in terms of the relative efficiency with which they remove different residues and many were initially named accordingly when discovered. They are also sometimes classified by their subcellular locations, according to their susceptibility to inhibitors and to the pH at which they display maximal activity (156). Aminopeptidases of the M1, M17, M18 and M24B families are of particular interest in this thesis and are discussed further below.

Bestatin (2-(3-amino-2-hydroxy-4-phenyl-butanoyl)amino-4-methyl-pentanoic acid) is a small, naturally occurring, slow/tight-binding, reversible inhibitor of aminopeptidases. It is produced by *Streptomyces* bacteria and was first discovered as an inhibitor of aminopeptidase B (164), an M1 aminopeptidase (see section 1.2.4.1). Its immunomodulatory effects together with its low toxicity have resulted in its use in the treatment of cancer. Bestatin is an analogue of the dipeptide of phenylalanine and leucine

(Phe-Leu) and differs by the addition of a secondary alcohol in between two carbon atoms of the phenylalanine (Figure 1.3). It inhibits a variety of Zn^{2+} metallopeptidases, especially aminopeptidases belonging to the M1, M17 and M28 families but it also has activity against the M16 family endopeptidase, nardilysin (141). Synthetic forms of bestatin are available and derivatives have been generated that have different activities, e.g. nitrobestatin (120), including some substituted compounds that demonstrate activity against different targets e.g. apstatin inhibits M24B aminopeptidases (128).

1.2.4.1. M1 aminopeptidases

M1-family peptidases are one of thirty members of the MA clan of metallopeptidases and one of eighteen of the MA(E) sub-clan (129), a group also referred to as the gluzincins (78). They require a zinc ion for catalytic activity and most of them are aminopeptidases. They contain the Xaa-Xbb-Xcc-His-Glu-Xbb-Xbb-His-Xbb-Xdd sequence (the HEXXH motif) as discussed in section 1.2.3 (83). The catalytic activity of the enzyme involves the glutamate (E) of the motif and a water molecule, bound by the zinc, acting as a nucleophile. The two histidine (H) residues act as ligands for the zinc ion along with a third ligand, a glutamate in the case of the MA(E) sub-clan. M1 aminopeptidases (EC number 3.4.11.2, see Table 1.1) have been termed alanyl aminopeptidase but they can often hydrolyse a variety of amino acids from the N-termini of proteins. M1 aminopeptidases are known to be inhibited by bestatin and amastatin, and by metal chelators like EDTA and 1,10-phenanthroline (131). The most studied example is probably the mammalian aminopeptidase N (APN), a transmembrane enzyme found in a wide variety of tissues and cells. Its upregulation is associated with a range of diseases especially cancers and inflammatory conditions and as a result has been the subject of extensive investigation of novel inhibitors (reviewed in (14, 179)).

1.2.4.2. M17 aminopeptidases

The M17 peptidase family is the only one of the MF clan of metallopeptidases (129) and the majority of them are aminopeptidases. These peptidases were the first metallopeptidases identified to need two co-catalytic metal ions for activity. These ions, normally zinc, are liganded by five residues: one lysine, three aspartates and a glutamate, with the latter binding to both ions. They form homo-hexamers with each monomer binding two metal ions. M17 aminopeptidases (EC number 3.4.11.1) were originally termed leucyl aminopeptidases due to their usual preference for leucine at the N-termini of substrates. However, they will usually hydrolyse most other substrates, especially small,

6
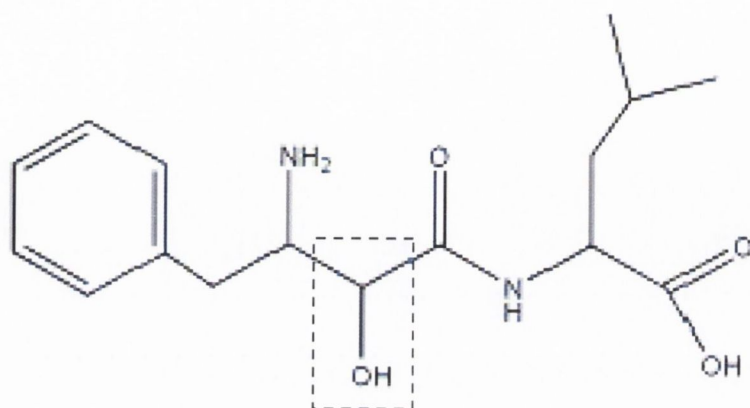
Figure 1.3. Structure of bestatin (2-(3-amino-2-hydroxy-4-phenyl-butanoyl)amino-4-methyl-pentanoic acid). Bestatin is a naturally occurring analog of the Phe-Leu dipeptide, differing by the addition of a secondary alcohol (outlined by the dashed box) between the two carbon atoms of the carbonyl and amino groups of the phenylalanine.

TABLE 1.1. Aminopeptidases listed according to their Enzyme Commission (EC) numbers

EC number	Common Name	Peptidase family[a]	N-terminal amino acid released
3.4.11.1	Leucyl aminopeptidase	M17	Preferably Leu but may be others, including Pro. Not Arg or Lys
3.4.11.2	Membrane alanyl aminopeptidase	M1	Preferably Ala but may be most, including Pro
3.4.11.3	Cystinyl aminopeptidase	M1	Cys
3.4.11.4	Tripeptide aminopeptidase	M9	From a tripeptide
3.4.11.5	Prolyl aminopeptidase	S33	Pro
3.4.11.6	Aminopeptidase B	M1	Arg and Lys (except when attached to Pro)
3.4.11.7	Glutamyl aminopeptidase	M1	Glu (and Asp to lesser extent)
3.4.11.9	Xaa-Pro aminopeptidase	M24B	Any linked to Pro, including Pro
3.4.11.10	Bacterial leucyl aminopeptidase	M17 and M28	Preferably Leu. Not Glu or Asp
3.4.11.13	Clostridial aminopeptidase	NR[b]	Any including Pro (except when attached to Pro)
3.4.11.14	Cytosol alanyl aminopeptidase	NR	Preferably Ala

TABLE 1.1 Aminopeptidases listed according to their Enzyme Commission (EC) numbers (continued)

EC number	Common Name	Peptidase family[a]	N-terminal amino acid released
3.4.11.15	Aminopeptidase Y	M28B	Preferably Lys
3.4.11.16	Xaa-Trp aminopeptidase	NR	Variety linked to Trp (or Phe or Tyr), especially Glu and Leu
3.4.11.17	Tryptophanyl aminopeptidase	NR	Preferably Trp
3.4.11.18	Methionyl aminopeptidase	M24A	Preferably Met
3.4.11.19	D-stereospecific aminopeptidase	S12	D-amino acid, preferably Ala, Ser or Thr
3.4.11.20	Aminopeptidase Ey	M1	Broad specificity
3.4.11.21	Aspartyl aminopeptidase	M18	Asp or Glu (preferably Asp)
3.4.11.22	Aminopeptidase I	M18	Neutral or hydrophobic
3.4.11.23	PepB aminopeptidase	M17	Preferably Glu or Asp but may be others including Leu, Met, His, Cys and Gln

[a]M and S refer to metallo and serine peptidases, respectively

[b]NR = not reported

hydrophobic residues but they will generally not cleave residues linked to proline. Similarly to the M1 aminopeptidase, they are inhibited by bestatin and amastatin and by metal chelators (131). The best studied is that of the bovine lens and work on this enzyme has provided much of the information about M17 aminopeptidases. Crystallisation of this enzyme has enabled the examination of its structure and interactions with inhibitors like bestatin (25, 26).

1.2.4.3. M18 aminopeptidases

The M18 peptidase family contains only metalloaminopeptidases and is one of four members of the MH clan (129). This group of enzymes also require two cocatalytic metal ions that bind the water nucleophile and are liganded by five amino acids: histidine/aspartate, aspartate (binds two metal ions), glutamate, aspartate/glutamate and histidine. M18 aminopeptidases (EC number 3.4.11.21) have been found to exist as homo-dodecamers (131).

1.2.4.4. M24B aminopeptidases

M24B peptidases are a sub-family of the M24 family, the only member of the MG clan (129). This clan contains metalloexopeptidases that have a water nucleophile bound by two metal ions, normally cobalt or manganese. These metals are liganded by five residues: two aspartates, one histidine and two glutamates (131). M24B aminopeptidases (EC number 3.4.11.9) cleave any amino acid at the N-terminus linked to proline and are inhibited by apstatin (128).

1.3. *PLASMODIUM FALCIPARUM* PEPTIDASES

1.3.1. Peptidases of *Plasmodium*

Peptidases are involved in the pathogenesis of the diseases caused by a variety of parasites including helminths and kinetoplastid and apicomplexan protozoa. Cysteine, aspartyl, serine and metallopeptidases have all been found to play important roles in establishing and maintaining the infection of parasites through processes like tissue and cell invasion, immune evasion and nutrient degradation (110).

Peptidases of the five major catalytic types (i.e. serine, cysteine, threonine, aspartic and metallo) have been identified in *P. falciparum*. The initial annotation identified 25 putative peptidases belonging to 10 families but more recent data-mining of the genome identified a total of 92 putative peptidase homologues classified into 27 families across the

five types (177). *Plasmodium* peptidases are suggested to be involved in a range of functions in the parasite including progression through the various life cycle stages, processing of surface antigens and invasion of and escape from host cells (17). During the eythrocytic stage of the life-cycle, peptidases are involved during the processes of merozoite invasion of red cells and their subsequent release. There are also a range of peptidases involved in the process of haemoglobin degradation during this intra-erythrocytic stage that are dealt with in more detail in section 1.4. Some of these peptidases may also play roles in cell invasion and rupture (135).

1.3.2. Aminopeptidases in *Plasmodium*

Aminopeptidases in *Plasmodium* have been suggested to play roles in both haemoglobin degradation and erythrocyte invasion. Various aminopeptidase activities have been reported in different *Plasmodium* species (Table 1.2). In *P. falciparum* these include a ~186-kDa neutral peptidase found to have aminopeptidase activity (73) along with ~100-kDa (167) and ~63-kDa (169) activities. The 186-kDa peptidase was seen to have maximal aminopeptidase activity against substrates with alanine at their N-termini but was also active against leucine and lysine substrates. It had a pH optimum of 7.5 and a pI of 6.05 and was inhibited by 1 mM Hg^{2+}, Zn^{2+} and Cd^{2+} and to some degree by 1 mM Cu^{2+} and Co^{2+}, and by leupeptin, a serine peptidase inhibitor. The activity was also inhibited by antimalarial compounds including chloroquine and primaquine (at 1 mM). The 63-kDa aminopeptidase was also inhibited by chloroquine.

Partial purification of the 100-kDa aminopeptidase (by HPLC) yielded an enzyme with activity against alanine and leucine, with higher activity against the former (167). The pI of the aminopeptidase was 6.8 and it was maximally active at a pH of ~8.5. The activity was inhibited by bestatin, to some degree by metal chelators, 1,10-phenanthroline and EDTA, and by 1 mM Hg^{2+}, Zn^{2+} or Co^{2+}. The enzyme was inhibited by chloroquine, mefloquine and quinacrine, with K_i values of 410, 280 and 20 µM, respectively, but not by quinine or primaquine.

Between one and four aminopeptidases have been reported in rodent *Plasmodium* species. Among the first reports was that of a ~90-kDa aminopeptidase activity in *P. chabaudi* and *P. yoelii nigeriensis* (28). Parasite extract was seen to be active against alanine, leucine and lysine substrates, demonstrating about twice as much activity against the alanine than the other two substrates. Both enzymes had pH optima of 7.5 and temperature optima of 40–50 °C. Isoelectric focusing revealed a major peak for the *P. yoelii* aminopeptidase corresponding to a pI of 5.3 but with the possibility of two

8

Plasmodium species	Number present	Molecular mass (kDa)[a]	Substrates	Non-substrates	pH optimum	pI	Temp optimum (°C)	Inhibitors	Ref
P.chabaudi	4?	90	Ala, Leu, Lys	Gly, Tyr, Pro	7.5	5.5, 5.6, 5.7, 5.85	40-50	Hg^{2+}, Zn^{2+}, Co^{2+}, Mn^{2+}, 1,10-phenanthroline, chloroquine, quinacrine, primaquine	(28)
P. yoelii	1–3?					5.2, 5.3, 5.4			
P. falciparum	1	186	Ala, Leu, Lys	-	7.5	6.05	-	Hg^{2+}, Zn^{2+}, Cd^{2+}, Cu^{2+}, Co^{2+}, chloroquine, primaquine, leupeptin	(73)
P. falciparum	1	100	Ala, Leu	-	8.5	6.8	-	Hg^{2+}, Zn^{2+}, Co^{2+}, bestatin, chloroquine, mefloquine, quinacrine	(167)
P. falciparum	1	63	Ala	-	7.5	-	-	Chloroquine	(169)
P. falciparum *P.c.chabaudi* *P. berghei*	1	80	Ala, Leu, Arg, Asn, Lys, Gly	His, Pro	7.2	-	45-55	1,10-phenanthroline, Hg^{2+}, Cd^{2+}, Mn^{2+}, bestatin	(34)
P. chabaudi	1?	80	Leu	-	7.2	-	-	Bestatin, nitrobestatin	(120)
P. falciparum	1?	56, 66, 97	Leu	-	7.2	-	-	Bestatin, nitrobestatin	(60)

TABLE 1.2. Overview of reported aminopeptidase activities in *Plasmodium* (continued)									
Plasmodium species	Number present	Molecular mass (kDa)[a]	Substrates	Non-substrates	pH optimum	pI	Temp optimum (°C)	Inhibitors	Ref
P. falciparum	1	122, 96, 68	Leu	-	6.8-7.1	-	-	-	(54)
P. falciparum	1	120, 115, 110, 96, 68	Lys, Ala, Arg, Leu (also Phe, Tyr, Ser, Asn)	Glu, Asp	7.4	-	-	1,10-phenanthroline, bestatin, amastatin	(3)

[a]corresponds to the molecular mass or apparent molecular mass of bands in purified or partially-purified preparations

- indicates data not specified

additional enzymes with peaks at 5.2 and 5.4. Four peaks were observed for the *P. chabaudi* extract corresponding to pI's 5.5, 5.6, 5.7 and 5.85. The activity was inhibited by 1,10-phenanthroline and by some metal ions including Hg^{2+} and Zn^{2+} but less so by Co^{2+} and Mn^{2+}. It was inhibited by some quinoline antimalarials including chloroquine and primaquine (at 1 mM).

A single ~80-kDa metallo-aminopeptidase was subsequently reported in each of *P. chabaudi chabaudi, P. berghei* and *P. falciparum* (34), demonstrating very similar properties to each other. These enzymes had a preference for leucine or alanine as the N-terminal amino acid of the substrate but could also cleave arginine, asparagine, lysine and glycine substrates. The enzymes had pH optima of 7.2 and temperature optima of 45–55 °C and were inhibited by bestatin, 1,10-phenanthroline and 1 mM Mn^{2+}, Cd^{2+} or Hg^{2+}. Reactivation of the apoenzyme (protein deactivated by removal of metal ions by treatment with 1,10-phenanthroline) was partially achieved in the presence of Mn^{2+}, Ca^{2+} or Mg^{2+}.

This enzyme was partially purified from *P. c. chabaudi* by gel filtration and affinity chromatography. One major peak of activity was eluted and one band was seen when assayed by fluorography but a number of protein bands, running at ~80 kDa, were observed when analysed by SDS-PAGE (120). The enzyme was inhibited by bestatin and nitrobestatin but not by chloroquine as was reported for some other aminopeptidase activities.

Partial purification of the ~80 kDa aminopeptidase from *P. falciparum* (by affinity and gel-exclusion chromatography) yielded four bands with apparent molecular masses between 56 and 97 kDa, including one at ~66 kDa. Bestatin and nitrobestatin, known metallo-aminopeptidase inhibitors, inhibited the enzyme and blocked the growth of intraerythrocytic parasites, with the late ring/early trophozoite stage most susceptible. The aminopeptidase demonstrated maximal activity at neutral pH and no detectable activity at acidic pH (60).

Further information on *Plasmodium* aminopeptidases came from the identification of the gene encoding an M1 family zinc metallopeptidase (referred to here as PfAP-M1) (3, 54). The protein appeared to be processed from its predicted size of 126 kDa (through two intermediates of sizes 115 and 110 kDa) to two, smaller, active proteins of apparent molecular masses of 96 and 68 kDa. Analysis of these truncates using anti-peptide antibodies, generated against residues 111-123 and 163-175, indicated that both were N-terminal truncates. Neither was recognised by the first antibody but both were by the second, suggesting that their protein sequences began somewhere between residues 123 and 163. The 68-kDa protein is then presumed to be processed further at its C-terminal end

giving rise to the shorter protein. Partially purified enzyme was found to have a preference for lysine at the N-terminus of peptide substrates but also rapidly hydrolysed alanine, arginine and leucine substrates (with activities of 86, 77 and 42 %, respectively, of that seen for lysine). It had some activity against phenylalanine, tyrosine, serine and asparagine (25, 11, 10 and 9 %, respectively, of the activity seen for lysine) but none against aspartate or glutamate. It had a neutral pH optimum of 7.4. The aminopeptidase was not detected in early ring stages by immunofluorescence but it was present in the trophozoite stage, in the cytosol but not in the digestive vacuole. It was also detected in the schizont stage and was observed as concentrated spots in free merozoites leading the authors to suggest that it might be associated with invasion. The apoenzyme was reactivated best by addition of Zn^{2+} but activity was partially restored by Hg^{2+}, Mg^{2+}, Co^{2+} and Mn^{2+}. The enzyme was inhibited by bestatin and amastatin and by 1,10-phenanthroline as expected for a metallo-aminopeptidase.

This study includes work on the characterisation of an M17 aminopeptidase from *P. falciparum* encoded by the *PfAP-M17* gene (153). Additional work on this gene product includes the description of transgenic parasites, carrying an extra copy of *PfAP-M17*, designed to over-express the protein (58). Transgenic parasites displayed increased aminopeptidase activity against leucine and alanine substrates and decreased susceptibility to bestatin, supporting the idea of this enzyme as a target of this metallo-aminopeptidase inhibitor.

1.4.   HAEMOGLOBIN DEGRADATION BY *P. FALCIPARUM*

1.4.1. Haemoglobin degradation: an introduction

During the intra-erythrocytic phase of their life-cycle, *P. falciparum* parasites digest up to 75% of the host cell haemoglobin (102). The parasite engulfs portions of erythrocyte cytoplasm and transports them via the cystosome organelle to the acidic digestive vacuole (124) where the haemoglobin is processed to small peptides by a process that appears to employ the action of a number of peptidases described in more detail in the following sections (proposed model outlined in Figure. 1.4). Incubation of haemoglobin and digestive vacuole extract yielded peptides as small as approximately 8 amino acids in length but did not produce single amino acids. This, together with the inability to detect any exopeptidase activity in food vacuoles, has led to the proposal that the small peptides produced by the action of the preceding peptidases are transported out of the digestive vacuole into the parasite cytosol for processing to free amino acids (87). The haem
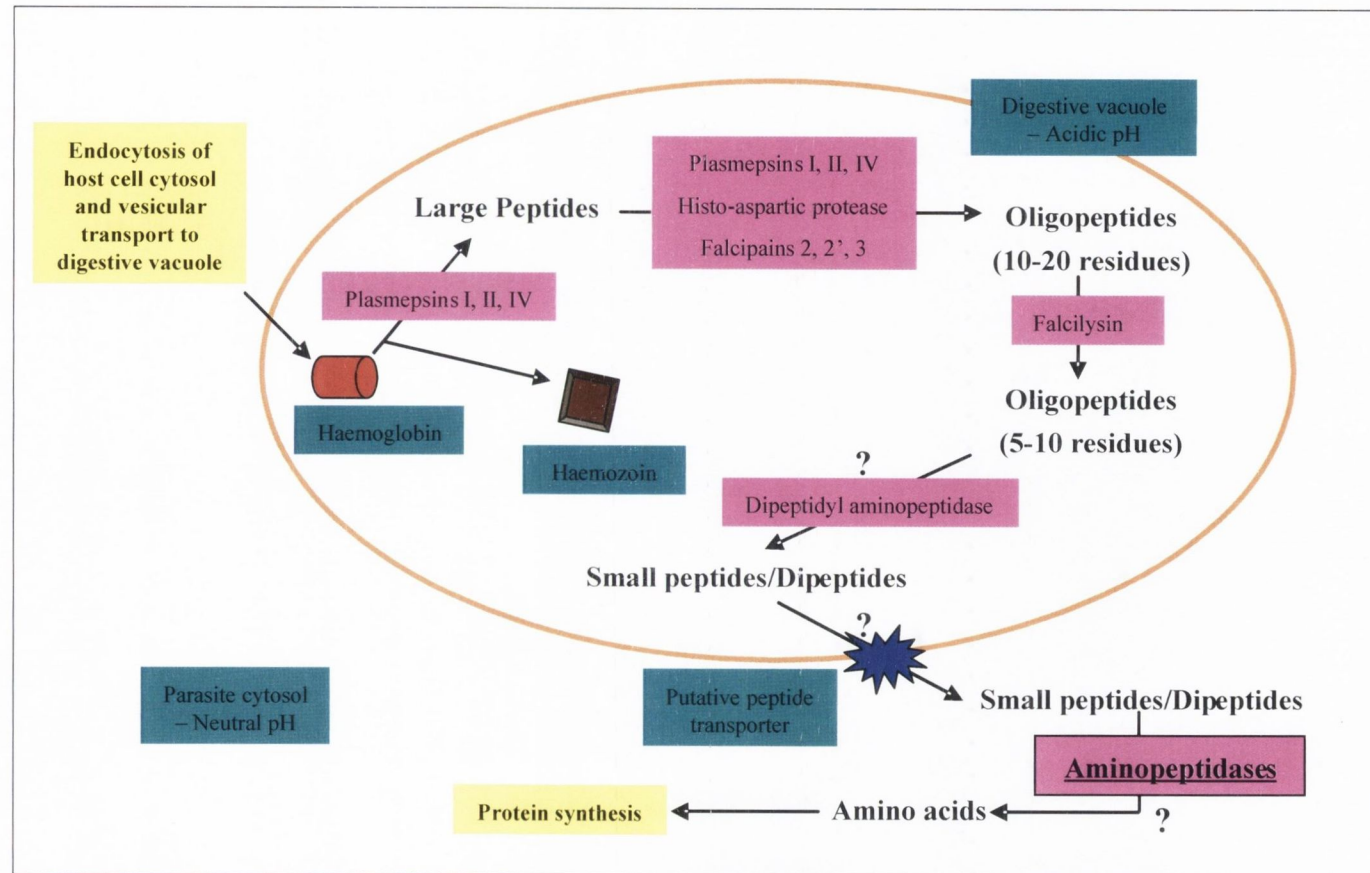
Figure 1.4. Proposed model of the steps involved in processing haemoglobin to haemozoin and free amino acids. Globin is digested to small peptides by the concerted action of plasmepsins I, II and IV, falcipains, falcilysin and, possibly, a histo-aspartic protease and a dipeptidyl aminopeptidase. Small peptides (and/or dipeptides) may be acted on by aminopeptidases, after transport out of the digestive vacuole into the cytosol, to yield free amino acids.

released by the process of haemoglobin degradation is detoxified via a process of biomineralisation into an insoluble crystalline complex termed haemozoin (malarial pigment) (125).

It is not yet fully clear why *Plasmodium* parasites digest haemoglobin and a number of functions have been suggested for this process. The most obvious of these is that the parasites digest haemoglobin to generate free amino acids for incorporation into newly synthesised proteins. This has been supported by findings of incorporation of radiolabelled haemoglobin-derived amino acids into parasite proteins (10) and by the parasites' ability to survive in medium containing only one to five amino acids that are not found or are rare in haemoglobin (40, 100), despite their limited ability to synthesise amino acids themselves (144). The excretion of a proportion of the haemoglobin-derived amino acids out of the erythrocyte and the confirmation that only ~16% are incorporated into parasite proteins (88) has lead to the suggestion of alternative or additional roles for the process of degradation. These include the maintenance of osmotic stability to prevent host cell lysis (98) and providing room inside the erythrocyte for parasite growth (64).

1.4.2. Aspartic peptidases

The initial cleavage of host cell haemoglobin is mediated by a number of aspartic peptidases called plasmepsins that appear to cleave around the hinge region (residues 33 and 34) of the alpha chain of haemoglobin (65, 67, 178). The *P. falciparum* genome codes for ten of these proteins in total but only four of them, plasmepsins I, II and IV and a histo-aspartic peptidase (HAP), seem to play a part in the haemoglobin digestion pathway (11). The histo-aspartic peptidase (previously called plasmepsin III) is ~60% identical to plasmepsins I and II but it has a histidine residue in place of one of the catalytic aspartates in its active site and has been suggested to represent a new class of peptidases. It displayed different susceptibility to inhibitors, increasing its attractiveness as a drug candidate. The apparent preference for HAP and plasmepsin IV to cleave globin fragments and their expression profile has led to the suggestion that they are more involved in the later stages of degradation (11). Recent work demonstrated that parasite growth is seriously affected by knocking out all four plasmepsins in tandem (20), illustrating their importance for parasite growth. However, the fact that the knock-out parasites did grow to some extent shows that other peptidases can take over the function of these enzymes in haemoglobin degradation and the apparent lack of effect on parasites with one or two plasmepsins knocked out also confirms an element of redundancy between these enzymes (126).

1.4.3. Cysteine peptidases

The other major group of peptidases involved in the degradation process is the *P. falciparum* cysteine peptidases, the falcipains. There are four encoded by the genome: falcipain 1, falcipains 2 and 2' (two nearly identical copies of the same protein) and falcipain 3 (136, 143, 147, 149). Falcipains 2 and 3 are found in the digestive vacuole in trophozoites and degrade haemoglobin, although probably only if it has first been denatured. This may mean that they can only cleave haemoglobin that has been unfolded to some degree, possibly following cleavages by other peptidases (65, 142). Knock-out of the falcipain 2 enzyme results in a decrease in haemoglobin degradation but no lethal phenotype whereas falcipain 3 does appear to be essential for parasite survival (146). Falcipains 1 and 2' also appear not to be essential for parasite growth and the former may actually play a role in merozoite invasion rather than haemoglobin digestion (145, 146).

1.4.4. Falcilysin

Falcilysin is an M16A family zinc metalloendopeptidase (containing the HXXEH inverted active-site motif) that was purified from digestive vacuoles and is suggested to cleave the peptides produced by the plasmepsins and falcipains, as it was found to be capable of cleaving haemoglobin-derived peptides but not haemoglobin or denatured globin. At acidic pH it preferentially cleaved at polar sites in peptides 11–15 residues in length but could cleave those up to 20 amino acids long (45). It may also be involved in other processes, separate to haemoglobin degradation, as it was located outside the food vacuole and found to be active at neutral pH, with a preference for more charged residues (119).

1.4.5. Dipeptidyl aminopeptidase

The 5–10 residue products of falcilysin cleavage were thought to be end products of proteolytic degradation in the digestive vacuole, due to the lack of exopeptidase activity detected there (87). However, a homologue of mammalian dipeptidyl aminopeptidase (cathepsin C, a cysteine peptidase), i.e. an enzyme that cleaves dipeptides from the N-termini of proteins, was found in the *P. falciparum* genome. Purification of the parasite protein, dipeptidyl aminopeptidase 1 (DPAP-1) yielded an enzyme with the ability to cleave dipeptides from substrates. The enzyme was detected in the trophozoite and schizont stages and was mostly located in the digestive vacuole but was also seen in vesicles outside the parasite, generally quite close to the parasitophorous vacuole membrane, in the erythrocyte cytosol. The inability to disrupt the sequence of the gene

encoding the DPAP-1 enzyme indicated that it is important for parasite growth (86). Two more putative dipeptidyl aminopeptidase homologue genes are also present in the *P. falciparum* genome (177).

1.4.6. Aminopeptidases

As already mentioned the lack of amino acids generated by the action of the digestive vacuole lysates and the inability to detect exopeptidase activity there has led to the belief that the small peptides or dipeptides produced by the other peptidases are transported into the parasite cytosol before being degraded to free amino acids, presumably by aminopeptidases. A number of aminopeptidase activites detected in *Plasmodium* have already been detailed above (section 1.3.2). Their involvement with the process of the terminal stages of haemoglobin has yet to be definitively confirmed but previous work has provided evidence consistent with such a role.

Studies with the partially-purified *P. falciparum* aminopeptidase showed that it was most active against leucine and alanine substrates, the most common amino acids in haemoglobin (76). The enzyme demonstrated greatest activity in cultured parasites at the trophozoite stage, the stage of maximal haemoglobin digestion, and it was capable of cleaving synthetic peptides corresponding to haemoglobin-derived, endopeptidase cleavage products (60). The *P. falciparum* M1 aminopeptidase also displayed significant activity against leucine and alanine substrates. It was expressed during the trophozite stage when it was found to be located in the cytosol and displayed apparent accumulation around the digestive vacuole (3). Both enzymes displayed neutral pH optima but had no activity at acidic pH supporting their involvement in the degradation of peptides in the cytosol, rather than in the digestive vacuole.

1.5. CONTROL AND TREATMENT OF MALARIA

1.5.1. Control of malaria

Methods of dealing with malaria have involved both control measures and treatment of the disease. Control of the disease aims to eliminate the vector with pesticides and/or to prevent transmission of the disease. Reduction in transmission of parasites from the mosquito to the human host through the use of insecticides and bed nets has managed to reduce mortality in some regions. However, problems exist with these methods including the cost of bed nets, the lack of their availability and/or acceptance and the possibility of emergence of resistance to the insecticides (57).

Another area being investigated is the development of a vaccine, in particular a subunit vaccine. The first indication of protection against malaria by vaccination involved immunisation with irradiated sporozoites (31). Since then a number of candidates targeting various proteins of the different life-cycle stages of the parasite have been proposed. The majority of these are sporozoite or pre-erythrocytic vaccines that aim to prevent the parasites invading hepatocytes and to clear the host of infected liver cells e.g. the RTS,S/AS02A fusion vaccine based on the circumsporozoite (CS) protein of the sporozoite (19). Erythrocytic phase vaccines generally aim to prevent invasion of cells by the merozoites and include those based on the merozoite surface proteins (MSP) (62, 122) and apical membrane antigen 1 (AMA-1) (154). Vaccines designed against gametocyte antigens, e.g. the Pfs25 protein vaccine (113), aim to prevent transmission of the parasite rather than protect the individual from malaria meaning that their use lies in controlling the spread of the disease. A number of vaccine candidates have reached clinical trials stages but difficulties remain in vaccine development, including the production of sufficient quantities of antigens, the length of time and costs involved in vaccine trials and a host of factors involving the introduction of vaccines into the areas that need them (23, 117).

1.5.2. Chemotherapeutic treatment of malaria

Treatment of malaria through chemotherapy remains the main method of managing the disease but the development of resistance (in *P. falciparum* and *P. vivax* parasites but not *P. malariae* or *P. ovale*) is a major problem. Current chemotherapeutics come from three main groups of compounds. The quinolines and derivatives include quinine (the first characterised antimalarial drug), chloroquine, mefloquine and primaquine. It is thought that these compounds exert their effect by accumulating in the digestive vacuole and preventing the polymerisation of heme into haemozoin following haemoglobin digestion (61) (except primaquine which seems to act on liver stage parasites). Chloroquine was the most effective and widely used of the quinolines and was very successful in treating malaria for decades. However, resistance to it was reported approximately 50 years ago and it has gradually emerged in almost every region where it is in use. Resistance to the other derivatives was also seen to emerge over time. Similarly, widespread resistance has been documented for the antifolate group of drugs e.g. the combination of sulfadoxine and pyrimethamine, which was very unfortunate as this was an affordable and well-tolerated alternative to chloroquine (176). Artemisinin, derived from the Chinese herb qinghao, is the most recently developed drug of the three types used. The precise mechanism of action of this compound and its derivatives (e.g. the more water-soluble, artesunate) is unclear but

it may involve the formation of free radicals via a reaction between its peroxide group and the iron released from haem during haemoglobin digestion (75). Initially, resistance to this group of compounds was only reported in *P. yoelii*, the rodent malaria parasite (171), but incidences of resistance in *P. falciparum* are beginning to be reported (81, 112).

A number of factors make the development of antimalarial drugs particularly difficult, not least the fact that most research is conducted in academic rather than commercial settings. The drugs also need to be cheap, available orally and very well tolerated. Ideally treatment would involve combination therapy to avoid the emergence of resistance and would involve a short and simple dosing regime for good compliance, for the same reason (61). Processes and targets currently under investigation for novel antimalarial agents include peptidases (discussed below), transporters, protein kinases, enzymes of the mitochondrion and the apicoplast (a plastid organelle found in apicomplexans that is homologous to the chloroplast (172)) and proteins involved in isoprenoid and membrane biosynthesis, the redox system, the shikimate pathway and the purine and pyrimidine metabolic pathways (reviewed in (82)).

1.6. PEPTIDASE INHIBITORS AS ANTIMALARIAL AGENTS

1.6.1. Peptidases as novel targets for antimalarials

Many peptidases, involved in a variety of different processes, have been considered as potential drug targets (162) and those of *Plasmodium* (and other parasites) are no exception (110). The proposed peptidases from *P. falciparum* include those involved in the invasion of and release from erythrocytes and those of the haemoglobin digestion pathway (discussed below). A range of peptidase inhibitors has been found capable of interfering with cell invasion and rupture. Suggested targets include peptidases that may be involved in the processing of surface proteins like MSP-1 and AMA-1, e.g. two subtilisin-like serine peptidases (PfSUB-1 and -2) thought to be involved in the processing of MSP-1 (18).

1.6.2. Inhibitors of the haemoglobin pathway peptidases

A number of inhibitors have been developed with a view to inhibiting the activity of the peptidases involved in the degradation of haemoglobin. Compounds with activity against the aspartic peptidases (plasmepsins I, II, IV and the HAP) that have been investigated include statine, allophenylnorstatine and diphenylurea derivatives (reviewed in (47)). Most work has focused on plasmepsin II due to its availability in recombinant form. However, while active against purified protein, the majority of the inhibitors do not

display potent inhibition of the growth of cultured parasites. It is unclear if the reason for this lies in the apparent redundancy associated with these enzymes but it may be that combinations of inhibitors would need to be applied to knock out all the plasmepsins simultaneously (32).

Similarly, inhibitors of the falcipains (the cysteine peptidases) have been studied, including fluoromethyl ketones, vinyl sulfones and chalcones (reviewed in (134)) and they appear more promising candidates. Generally, they have more activity against growth of cultured parasites and some have been found to be active in mouse malaria. Some also demonstrate synergy with plasmepsin inhibitors (137).

1.6.3. Aminopeptidase inhibitors with antimalarial activity

Bestatin has been found to inhibit the growth of *Plasmodium* parasites, including *P. falciparum* (see Table 1.3) with an IC_{50} of 2–15 µM against cultured parasites (120, 153). It has also been suggested to block reinvasion of erythrocytes by *Plasmodium* when incubated with schizonts (123), although this may be an indirect effect actually caused by the inhibition of schizont maturation (60). Nitrobestatin, a synthetic derivative, displays improved antimalarial activity, (approximately 2–5 fold) with an IC_{50} of 0.4–8 µM (120, 153). Both bestatin and nitrobestatin were found to be particularly active on late ring and trophozoite stage parasites (60). Other, related compounds, like epibestatin, amastatin, epiamastatin and apstatin did not demonstrate IC_{50} values at the highest concentrations tested, i.e. 128 µM (C. Gavigan, PhD Thesis, Trinity College Dublin, 2001 and (120)).

More recently, some quinoline hydroxamate derivatives, developed as dual inhibitors of haemozoin formation and the *P. falciparum* M1 aminopeptidase, displayed good antimalarial activity (with IC_{50} values < 1 µM) but they were also very active against the mammalian enzyme, AP-N (52). Further development of a series of malonic hydroxamates in an attempt to improve selectivity yielded less active compounds (IC_{50} = 25–60 µM) (51).

1.7. PROJECT OBJECTIVES

The work documented in this thesis was undertaken to investigate whether *P. falciparum* aminopeptidases represent a possible target for antimalarial chemotherapy, as suggested by the antimalarial activity of bestatin (a known aminopeptidase inhibitor) and its observed inhibition of parasite development. The general aim of my project was to learn more about the *P. falciparum* aminopeptidases and the role they play in the parasites, with a view to examining them as potential novel drug targets. This was to be achieved by

16

TABLE 1.3. Previously reported antimalarial activities of aminopeptidase inhibitors in *P. falciparum*

Aminopeptidase Inhibitor	IC$_{50}$ (µM)	Comment	Reference
Bestatin	2–15		(60, 153)
Nitrobestatin	0.4–8		(60, 153)
Bestatin methyl ester	21		(153)
Epibestatin	>128	Stereoisomer of bestatin	C. Gavigan[a]
Amastatin	>128		C. Gavigan
Epiamastatin	>128	Stereoisomer of amastatin	C. Gavigan
Leuhistin	>128		C. Gavigan
Apstatin	>128		C. Gavigan
4APP-33	25	Cyclic imide	
PIQ-22128	36	Cyclic imide	C. Gavigan
PIQ-0101	45	Cyclic imide	
Compound 1	0.4	Quinoline derivative	
Compound 33	0.2	Quinoline derivative	(52)
Compound 34	0.3	Quinoline derivative	
Compound 35	0.2	Quinoline derivative	
Compound 57	59	Malonic hydroxamate	(51)
Compound 66	24	Malonic hydroxamate	

[a]C. Gavigan, PhD Thesis, Trinity College Dublin, 2001

characterisation of recombinant protein, including assessment in biochemical assays, by assessment of novel inhibitors, especially those found to have antimalarial activity, and by the generation and examination of transgenic *P. falciparum* strains to investigate the expression of aminopeptidases and their importance for the parasite.

The main aims were:

1) to establish how many/which aminopeptidases are present in *P. falciparum* and to investigate their expression in the parasite.

2) to produce and characterise recombinant *P. falciparum* aminopeptidase(s).

3) to investigate putative aminopeptidase inhibitors; determining antimalarial activity and any correlation with inhibition of aminopeptidase activity to validate this enzyme as an antimalarial target and to identify possible structures/compounds with potential as therapeutic agents.

Chapter 2

Materials and Methods

2.1. CHEMICALS, REAGENTS AND INHIBITORS

All reagents were from Sigma-Aldrich (Dublin, Ireland), unless otherwise stated. All reagents used during electrophoresis were of electrophoresis grade. All chemicals used for cell culture were of cell culture grade. The grade of water used was filter-sterile, double deionised (ddH$_2$O), and was dispensed from a Milli-Q Synthesis A10 (Millipore, Billerica, Massachusetts, USA). Plasmids pHB-Pf140015-gfp, pHB-Pf140015-cmyc, pHB-Pf14Pst-cmyc, pHH1-AP14-cmyc and pHH1-DR0.28 (listed in Table 2.1) and the anti-PfAP-M17 peptide antibody were provided by Dr. Don Gardiner (Queensland Institute of Medical Research, Brisbane, Australia). WR99210 was provided by Jacobus Pharmaceutical Company Inc., Princeton, New Jersey, USA. The pTrcHisB-PfAP-M17 and pTrcHisB-tPfAP-M17 constructs were received from Prof. John Dalton (Institute for the Biotechnology of Infectious Diseases, University of Technology, Sydney, Australia). Baculovirus-infected Sf9 cell pellets carrying the tPfAP-M17 gene were purchased from the SRC Protein Expression Facility (Queensland, Australia). The α-aminoalkylphosphonates and phosphonopeptides were provided by Dr. Marcin Drag and Prof. Pawel Kafarski (Institute of Organic Chemistry, Biochemistry and Biotechnology, Wroclaw University of Technology, Poland). Stock solutions of these compounds were prepared by dissolving in phosphate-buffered saline (PBS), to concentrations of 1–5 mM, followed by filter-sterilisation. The 3-amino-2-tetralone and 3-amino-2-benzosuberone derivatives were obtained from Prof. Céline Tarnus (Laboratoire de Chimie Organique et Bioorganique, École Nationale Supérieure de Chimie de Mulhouse, Université de Haute-Alsace, France). Stock solutions of these compounds were prepared by dissolving in dimethyl sulphoxide (DMSO), to concentrations of 10–20 mM.

2.2. CULTURE OF AND EXPERIMENTS WITH *P. FALCIPARUM*

2.2.1. Routine culture of *P. falciparum*

P. falciparum strains were maintained in continuous culture in human erythrocytes (whole blood obtained from the Irish Blood Transfusion Board, Dublin or the Australian Red Cross Blood Bank Service, Brisbane, Australia) and erythrocytes extracted as described in section 2.2.2, according to the method of Trager and Jensen (160). Strain 3D7 (obtained from M. Grainger, National Institute for Medical Research, London, UK) was cultured routinely in complete medium, pH 7.0, which consisted of RPMI 1640 medium supplemented with 25 mM HEPES, gentamicin (25 µg/ml), 0.18% (w/v) NaHCO$_3$,

18

hypoxanthine (50 µg/ml) and either 0.5% (w/v) Albumax® II (Gibco, Auckland, New Zealand) or 10% (v/v) human serum (Sigma). Strain D10 (a clone of FC27, originally from Papua New Guinea) and transfected D10 strains were cultured as above or in complete medium, pH 7.0, consisting of RPMI 1640 supplemented with 25 mM HEPES, 5% (w/v) $NaHCO_3$ (Ajax Finechem, Bay Road Taren Point, NSW), gentamicin (10 µg/ml) and 10% (v/v) normal human serum (obtained from the Royal Brisbane Hospital, Queensland and prepared as described in section 2.2.3). Parasites were cultured, at 2.5% or 5% (v/v) haematocrit, in petri dishes at 37 °C in a candle jar with reduced O_2 tension or in gassed chambers in an atmosphere of 5% CO_2, 5% O_2 and 90% N_2. Parasitemia was observed by microscopic assessment of smears stained with a 1:10 dilution of Giemsa stain (Fluka Chemie AG, Buchs, Switzerland) in Giemsa buffer (1% (w/v) $Na_2HPO_4.2H_2O$, 1% (w/v) KH_2PO_4). Routine cultures were diluted with fresh erythrocytes twice a week, or as needed, and culture medium was replaced depending on parasitaemia.

2.2.2   Treatment of whole human blood

Erythrocytes were pre-treated with 10% (v/v) PIGPA (0.55% (w/v) sodium pyruvate, 1.34% (w/v) inosine, 1.8% (w/v) glucose, 7.1% (w/v) Na_2HPO_4, 0.07% (w/v) adenine, 0.9% (w/v) NaCl) at 37 °C for 1 h with periodic agitation. They were subsequently centrifuged at $500 \times g$ at 4 °C for 10 min in a Sorvall RT6000D benchtop centrifuge (Du Pont, Hertfordshire, UK) and then washed twice in sterile, cold phosphate-buffered saline (PBS) (OXOID, Hampshire, UK) and once in complete culture medium, by centrifuging as before and removing the supernatant and the buffy coat each time. Blood was washed weekly and stored at 4 °C. A sample of washed erythrocytes was added to complete medium and incubated at 37 °C for 24 h after which Giemsa-stained smears were prepared to check for the absence of yeast or bacterial contamination.

2.2.3.   Treatment of human plasma

Plasma (obtained from the Royal Brisbane Hospital, Queensland) was pooled and defibrinated by adding 0.01 M $CaCl_2$, 80 units of bovine thrombin and 2-mm sterile glass beads (Crown Scientific, Sydney, Australia) and was allowed to clot by incubating at 37 °C for 2 h. The clot was discarded, the remaining serum was heat-inactivated at 56 °C for 45 min and 50-ml amounts were stored at -20 °C.

2.2.4.   Synchronisation of *P. falciparum* cultures

TABLE 2.1. Plasmids used in this study		
Plasmid	**Source**	**Used for:**
pGEM®-T-Easy	Promega	TA cloning of PCR products
pHB-Pf140015-gfp	D Gardiner	construction of GFP-tagged PfAP-M17 transfection vectors
pHB-Pf140015-cmyc	D Gardiner	construction of cmyc-tagged PfAP-M17 transfection vectors
pHB-Pf14Pst-cmyc	D Gardiner	isolation of the truncated *PfAP-M17* gene
pHH1-AP14-cmyc	D Gardiner	isolation of the full-length *PfAP-M17* gene
pHH1-DR0.28	D Gardiner	construction of transfection vectors
pQE-30	Qiagen	cloning of aminopeptidase genes (N-terminal His_6-tagged)
pMAL-c2x	New England Biolabs	cloning of aminopeptidase genes (N-terminal MBP-tagged)[a]
pET-15b	Novagen	cloning of aminopeptidase genes (N-terminal His_6-tagged)
pET-22b	Novagen	cloning of aminopeptidase genes (C-terminal His_6-tagged)
pTrcHisB-PfAP-M17	J Dalton	production of full-length PfAP-M17 protein in *E. coli*
pTrcHisB-tPfAP-M17	J Dalton	production of truncated PfAP-M17 protein in *E. coli*

[a]MBP = *E. coli* maltose-binding protein

Synchronisation of parasites to a specific developmental stage was achieved by the method of Lambros and Vanderberg (91). Cultures were centrifuged at 650 × g at room temperature for 10 min. The resulting pellet was resuspended in pre-warmed, filter-sterilised 5% (w/v) D (-) sorbitol (Merck, Darmstadt, Germany) and left at room-temperature for 5 min to allow accumulation of sorbitol in erythrocytes infected with mature parasites and promotion of osmotic lysis. The suspension was centrifuged again, washed in pre-warmed wash medium (RPMI 1640 medium supplemented with 25 mM HEPES, 0.18% (v/v) NaHCO$_3$ and hypoxanthine (50 µg/ml)) and the resulting pellet resuspended in complete culture medium to 2.5% haematocrit and cultured as normal. One treatment resulted in cultures of ring-stage parasites only (~0–18 h post-invasion). More highly synchronised cultures were obtained by repeating the sorbitol treatment 36 h after the end of the initial treatment, followed by parasite maturation to produce rings (~0–12 h post invasion), early/mid trophozoites (~16–24 h post-invasion), mid/late trophozoites (~28–34 h post-invasion) or schizonts/segmenters (~36–44 h post-invasion).

2.2.5. Inhibition of growth of *P. falciparum*

The effects of various compounds on *P. falciparum* growth were determined using the spectrophotometeric parasite lactate dehydrogenase (LDH) assay described by Makler *et al* (106). The assay is based on measurement of the biochemical reaction in which *P. falciparum* LDH (PfLDH) has the ability to utilise 3-acetyl pyridine adenine dinucleotide (APAD) as a co-factor in the conversion of lactate to pyruvate. Human erythrocyte LDH is also able to use APAD, but only to a very small extent. Asynchronous parasites, at 2% haematocrit and 0.8% parasitaemia, were cultured in 96-well, flat-bottomed, microtitre plates (Starstedt) in complete medium supplemented with the particular inhibitor. Inhibitors were diluted in culture medium from stock solutions and serially diluted two-fold across the plate from starting high concentrations to sub-inhibitory concentrations. The effect of inhibitors was monitored after 48 and 72 h by mixing 10-µl samples with 50 µl of Malstat (Flow Inc., Portland, OR, USA). PfLDH is released by the parasites into the extracellular environment resulting in the production of pyruvate and reduced APAD. Ten µl of nitro blue tetrazolium (NBT) : phenazine ethosulfate (PES) (ratio 1 : 1 of NBT (2 mg/ml) and PES (0.1 mg/ml)), were added to each sample, forming a blue formazan product in the presence of reduced APAD that was detected with a spectrophotometer (Titertek Multiskan® Plus, Eflab, Finland) at 650 nm. The resulting absorbance is proportional to PfLDH activity, which correlates with parasite growth. Uninfected erythrocytes were used as controls to determine the background level of LDH secreted by

human erythrocytes, while parasites cultured in the absence of inhibitors were used as controls for the measurement of 100% PfLDH activity. All inhibition assays were repeated three times in duplicate and dose-response curves were constructed from absorbance readings and the median inhibitory concentrations (IC_{50}) determined.

2.2.6. Harvesting of *P. falciparum* parasites

Free parasites were released from infected erythrocytes and harvested according to the method of Zuckerman (181). Cultures of between 5 and 20% parasitemia were resuspended and washed twice in ice-cold PBS and sedimented by centrifugation at 650 × g at 4 °C for 10 min. Pellets were resuspended in an ice-cold solution of saponin (0.05% (w/v)) in saline sodium citrate (SSC) buffer (150 mM NaCl, 15 mM sodium citrate, pH 7.0) for 20 min on ice with vigorous shaking every 5 min to rupture erythrocyte membranes and to release parasites. Liberated parasites were sedimented by centrifugation for 15 min at 975 × g at 4 °C and washed twice with ice-cold SSC to remove lysed erythrocytes. Parasite pellets were resuspended in a freezing solution of PBS containing 10% (v/v) glycerol. Parasite preparations were divided, snap frozen in liquid nitrogen and stored at -70 °C.

2.2.7. Preparation of *P. falciparum* cytosolic extract

Harvested parasites were lysed by three cycles of freezing in liquid nitrogen and thawing at 37 °C. Insoluble debris was removed by centrifugation for 20 min at 4 °C at 12,000 × g. The supernatant was removed into a fresh tube and the centrifugation repeated. The resulting supernatant, defined as the crude cytosolic extract, was transferred to a fresh tube and subsequently kept at 4 °C at all times. The protein concentration was determined by the Bradford method (section 2.7.1).

2.2.8. Visualisation of *P. falciparum* expressing green fluorescent protein (GFP)-fusion protein

Live fluorescence microscopy assays were performed as described (153) using an Axioscope 2 Mot + (Zeiss, Oberkochen, Germany) equipped with a Zeiss 63x/1.4 Plan Apochromat lens using × 100 oil immersion objectives. Erythroyctes infected with asynchronous D10 parasites (expressing GFP-fused PfAP-M17 protein) were washed with PBS, before adding Hoechst dye 33342, at 0.5 µg/ml, to enable visualisation of parasite nuclei. Cells were washed in PBS again, mounted wet on a glass slide, covered by a glass coverslip, sealed and examined within 20 min at ambient temperature (maintained at 20

°C). Images were captured with an Axiocam MRm camera using Axiovision software (Zeiss) and were analysed using CorelDRAW® software (Corel Corporation, Ottawa, Canada).

2.2.9. Immunofluorescence analysis of *P. falciparum*

Immunofluorescence microscopy was performed essentially as described before (152), with asynchronous D10 parasites, using mouse anti-PfAP-M17 antiserum generated against recombinant protein or a synthetic peptide (section 2.9). Multi-well slides were pre-incubated in conconavalin A at 37 °C for 15 min and washed three times with PBS. Infected erythrocytes were fixed with 4% (v/v) formaldehyde/0.005% (v/v) glutaraldehyde or 4% (v/v) formaldehyde/0.075% (v/v) glutaraldehyde at room temperature for 30 min and washed three times with PBS. Some wells were treated with 0.1 % (v/v) Triton-X 100 to permeabilise the cells. Cells were incubated with mouse anti-PfAP-M7 antiserum in bovine serum albumin (BSA) (1/250) for 1 h and washed three times with PBS before probing with Cy2-conjugated goat anti-mouse AffiniPure antibodies (Jackson ImmunoResearch Laboratories Inc., Pennsylvania) for 1 h. Hoechst dye 33342 was also added, at 0.5 µg/ml, to enable visualisation of parasite nuclei. Wells were washed three times and parasites visualised with an Axioscope 2 Mot + (Zeiss) equipped with a Zeiss 63x/1.4 Plan Apochromat lens was using × 100 oil immersion objectives and images were captured with an Axiocam MRm camera using Axiovision software (Zeiss) and were analysed using the GIMPshop open-source graphics program (http://www.gimpshop.com).

2.3. ISOLATION AND ANALYSIS OF RNA

2.3.1. Isolation of *P. falciparum* RNA

Total RNA was isolated from cultured parasites using TRI REAGENT® (Sigma) as per the manufacturer's instructions. Briefly, cultures were centrifuged at 4 °C, at $500 \times g$, for 4 min and washed once with PBS. Ten pellet volumes of TRI REAGENT® solution were added, mixed well and, following incubation at 37 °C for 5 min, the suspension was divided into 1-ml quantities and either used immediately to isolate RNA or stored at -80 °C until needed. Chloroform was added and the mixture was shaken vigorously before centrifuging at $12,000 \times g$ at 4 °C for 15 min and the upper aqueous phase, containing RNA, was removed to a fresh tube. The RNA was precipitated by the addition of isopropanol and incubation on ice for 2 h before centrifuging at $12,000 \times g$ for 30 min. The pellet was washed with 75% (v/v) ethanol, centrifuged at $7,500 \times g$ for 5 min at 4 °C, and

the ethanol removed. The RNA was resuspended in ddH$_2$O (previously treated with 0.1% (v/v) diethylpyrocarbonate (DEPC) to inhibit RNases) with heating to 55–60 °C for 5–10 min.

2.3.2. Analysis of RNA by agarose gel electrophoresis

RNA was analysed by agarose gel electrophoresis to examine its quality and to analyse further by Northern blotting. Equipment was treated with 1% (w/v) sodium dodecyl sulphate (SDS) and 3% (v/v) H$_2$O$_2$ and/or RNase AWAY$^®$ (Molecular BioProducts Inc., San Diego, CA, USA) before use. Gels consisted of 1% agarose made up in Tris-borate-EDTA (TBE) (89 mM Tris-HCl, 89 mM boric acid, 2 mM EDTA) or Tris-acetate-EDTA (TAE) (40 mM Tris-HCl, 1 mM acetic acid, 2 mM EDTA) buffer, with the addition of 0.2–1.0 M guanidine thiocyanate, a denaturing agent, made freshly and added immediately prior to casting of the gel. RNA (2–5 µg) in formamide was denatured at 65 °C for 10 min, centrifuged briefly and placed on ice for 5 min. Samples were loaded next to a RNA ladder (Invitrogen, Carlsbad, California, USA) and 10 µl of 6x loading dye (0.25% (w/v) bromophenol blue, 0.25% (w/v) xylene cyanol FF, 30% (v/v) glycerol, 10 mM EDTA) were also loaded to act as a marker. Gels were run, in TBE or TAE buffer, at 70–100 V until the desired degree of separation was achieved (assessed visually by migration of loading buffer). Gels were stained in ethidium bromide (0.5–1.0 µg/ml) for 15–30 min, rinsed in DEPC-treated ddH$_2$O and the RNA was visualised by exposing the gel to ultraviolet (UV) light and photographed using an AlphaImager 2200 gel imaging system (Alpha Innotech Corporation, San Leandro, California, USA) or a Gel Documentation system (Bio-Rad Laboratories, Hercules, CA, USA).

2.3.3. Analysis of RNA by Northern blotting

Northern blotting was carried out using either the digoxigenin (DIG) system (Roche Diagnostics GmbH, Mannheim, Germany) according to the manufacturer's instructions or by labelling with [α-^{32}P]dATP (Amersham Biosciences, Piscataway, New Jersey, USA,) as described previously (89). After electrophoresis of RNA the gel was soaked briefly in 20 × SSC (section 2.2.6) or 50 mM NaOH, before capillary transferring to a positively charged Hybond N$^+$ membrane (Amersham) overnight in 20 × SSC or NaOH. Membranes were neutralised in 2 × SSC and following immobilisation of RNA by baking (80 °C for 2 h or 120 °C for 30 min), membranes were prehybridised for 1–4 h at 50 °C in DIG Easy-Hyb solution (Roche) or Northern Max pre-hybridization/hybridization solution (Ambion Inc., Austin, Texas, USA). They were then hybridised in the same

solution containing 50–500 ng/ml of the appropriate DIG-labelled DNA probe (that had been amplified to incorporate DIG-dUTP) or probes labelled with $[\alpha\text{-}^{32}\text{P}]$dATP by random priming (DECAprime II, Ambion) for 6–16 h at 50 °C. The primer pairs used for PCR to make the probes for *PfAP-M1*, *PfAP-M17*, *PfAP-M18* and *PfAP-M24* were PFAPM1F and PFAPM1R2 or ProbeM1 and PFAPM1R2 (probe corresponding to the last 500 bp of the gene), PFAPM17F and PFAPM17R or AntiAP14F and AntiAP14R, PFAPM18F and PFAPM18R and PFAPM24F and PFAPM24R, respectively (Table 2.2). Membranes were washed (at 50 °C) twice in low stringency buffer (2 × SSC/0.1% (w/v) SDS) and twice in high stringency buffer (0.1 × SSC/0.1% (w/v) SDS), followed by 0.1 M maleic acid/0.15 M NaCl pH 7.5/0.3% (v/v) Tween 20. Membranes probed with the DIG-labelling system were incubated with blocking solution in maleic acid buffer (0.1 M maleic acid, 0.15 M NaCl pH 7.5) for 30 min–3 h, followed by incubation with anti-DIG antibody and a chemiluminescent substrate, disodium 3-(4-methoxyspiro-(1,2-dioxethane-3-2'-(5'-chloro)-tricyclo(3.3.1.)decane-4-yl) phosphate (CSPD) (Roche). Membranes were exposed to film (Kodak) for 3–16 h before developing in a Kodak X-Omat 1000 automatic developer. If required, membranes were stripped by incubating in a solution of 0.2 M NaOH/0.1 % (w/v) SDS at 37 °C for 20 min and were re-probed with either a DIG-labelled 18S RNA probe (kindly provided by Dr. Clare Gavigan) or a $[\alpha\text{-}^{32}\text{P}]$dATP-labelled 28S RNA probe made using the primer pair Pf28SF and Pf28SR (Table 2.2) to check loading of RNA.

2.4.   ISOLATION AND ANALYSIS OF DNA

2.4.1.   Isolation of *P. falciparum* genomic DNA

Genomic DNA was isolated from harvested, asynchronous parasites using the phenol/chloroform/isoamyl alcohol method (107). Parasites were lysed in 10 volumes of lysis buffer (10 mM Tris-HCl, pH 7.5, 2 mM MgCl$_2$, 10 mM EDTA, 400 mM NaCl, 5 % (w/v) SDS, proteinase K (0.2 mg/ml) (Roche)) overnight at 37 °C. DNA was extracted by incubation with an equal volume of phenol/chloroform/isoamyl alcohol (15:14:1) for 15 min at 65 °C followed by centrifugation at 18,000 × g for 10 min. This was repeated before precipitation of the DNA by incubation with 2 volumes of ethanol at -70 °C for 30 min, followed by centrifugation at 18,000 × g for 15 min. The DNA pellet was left to air-dry and then resuspended in ddH$_2$O. In some cases DNA was extracted using the QIAamp DNA Blood kit (Qiagen, Crawley, UK) according to the manufacturer's instructions.

2.4.2. Analysis of DNA by agarose gel electrophoresis

DNA samples (PCR products, purified plasmids, restriction enzyme-treated plasmids etc.) were examined by mixing 5–10 μl of sample with 1–2 μl of 6x loading buffer (section 2.3.2) and running through a 0.8–1.0% (w/v) agarose gel prepared in TAE buffer. Gels were run, in TAE buffer, at 70–100 V until the desired degree of separation was achieved (assessed visually by migration of tracking dye). Gels were stained, visualised and photographed as for RNA gels (section 2.3.2). DNA markers (Roche or Invitrogen) were run to confirm fragment sizes.

2.4.3. Purification of DNA and PCR products

DNA and PCR products were purified using one of two kits based on affinity purification of DNA with glass fibre membranes. The High Pure® PCR product purification kit (Roche) was used for purification of DNA directly from samples, according to manufacturer's instructions. The PerfectPrep Gel Cleanup purification kit (Eppendorf, Hamburg, Germany) was used in certain cases for the purification of excised DNA from agarose gels, again according to the manufacturer's instructions.

2.4.4. Ethanol precipitation of DNA

DNA was concentrated by mixing with a 1/10 volume of 3 M sodium acetate (pH 5.5) and 2 volumes of absolute ethanol and incubating at -70 °C for 30 min–1 h or at -20 °C overnight. DNA was then pelleted by centrifugation at 12,000 × g for 10 min, the supernatant was removed and the pellet washed with 70% (v/v) ethanol. The sample was centrifuged as before, the supernatant removed, and the DNA pellet was dried at 37 °C for ~1 h, and resuspended in an appropriate volume of ddH$_2$O.

2.5. GENERATION OF TRANSGENIC *P. FALCIPARUM* CULTURES

2.5.1. Construction of full-length and truncated PfAP-M17-GFP and PfAP-M17-cmyc fusion vectors

The strategy used to produce the GFP-tagged PfAP-M17 (full-length) vector (outlined in Figure 2.1) is based on the GATEWAY® lambda phage site-specific recombination system that generates the required vector through recombination between the *att*L sites of the 'entry vector' that contains the sequence of interest and the *att*R sites on the 'destination vector' that accepts the fragment (150). A similar process was employed to produce the truncated GFP-tagged PfAP-M17 plasmid and the equivalent

TABLE 2.2. Oligonucleotide primers used in this study		
Forward and reverse primer	Product amplified	Oligonucleotide sequence (5' – 3')[a]
PFAPM1F and PFAPM1R2	*PfAP-M1*	GCGCGGATCCATGAAATTAACAAAAGGCTGTGC and GCGCGAGCTCGTTTATAATTTATTTGTTAATCTTAATAA
PFAPM17F and PFAPM17R	*PfAP-M17*	GCGCGGATCCATGTATTTTTCTTCCTTATGTAAAT and GCGCGAGCTCTTATAGAGCGTCATTGAGTACA
PFAPM18F and PFAPM18R	*PfAP-M18*	GCGCGGATCCATGGATAAGAAAGCTAGGGAATA and GCGCGAGCTCCTATTTGTCGTGGACACATGTG
PFAPM24F and PFAPM24R	*PfAP-M24*	GCGCGGATCCATGGTATTCCATTTAAATATTTTTAATA and GCGCGAGCTCTTAATTGTTATGAATCGCAATTG
ProbeM1 and PFAPM1R2	500bp probe for *PfAP-M1*	GCGCCATTCCAAATCACCATATCCATCCAATTG and GCGCGAGCTCGTTTATAATTTATTTGTTAATCTTAATAA
Pf28SF and Pf28SR	28S RNA	AATACCGGTAAGCAATTATGC and CTCACGTATTTCGCTTCAACAC
T7 Promoter and M13 Reverse	inserts in pGEM-T	TAATACGACTCACTATAGGGCGAATTG and GGAAACAGCTATGACCATG
AP14PSalF and AP14PBgR	*PfAP-M17* promoter	GTCGACATGTATTTAAAAGTGTAGAACGAAA and TTTACATAAGGAAGAAAAAGATCTCAGAAA
AntiAP14F and AntiAP14R	*PfAP-M17* anti-sense	CTGCAGATGTATTTTTCTTCCTTATGTA and AGATCTTAGAGCGTCATTGAGTACAAATTC
MBP-M1F and MBP-M1R	*PfAP-M1*	GCGCGGATCCATGAAATTAACAAAAGGCTG and GCGCAAGCTTCAATTTTGTTTATAATTTATTTGTTAATC
MBP-M1(96)F and MBP-M1R	*PfAP-M1(96)*	GCGCGGATCCATGATTACACAAGTTGATA and GCGCAAGCTTCAATTTTGTTTATAATTTATTTGTTAATC

Forward and reverse primer	Product amplified	Oligonucleotide sequence (5' – 3')[a]
	TABLE 2.2. Oligonucleotide primers used in this study (continued)	
MBP-M1(96)F and MBP-M1(68)R	*PfAP-M1(68)*	GCGCGGATCCATGATTACACAAGTTGATA and GCGCAAGCTTTTATGTTAAGTTATCCTCAATATATACTG
MBP-M17F and MBP-M17R	*PfAP-M17*	GCGCGAATTCATGTATTTTTCTTCCTTATG and GCGCCTGCAGTTATAGAGCGTCATTGAGTACA
MBP-M18F and MBP-M18R	*PfAP-M18*	GCGCGGATCCATGGATAAGAAAGCTAGGGA and GCGCCTGCAGAATTTCTATTTGTCGTGGAC
MBP-M24F and MBP-M24R	*PfAP-M24*	GCGCGAATTCATGGTATTCCATTTAAATATTTTTAATAAG and GCGCCTGCAGTACACATTAATTGTTATGAATC
pET-M17F and pET-M17R	*PfAP-M17*	GCGCCATATGTATTTTTCTTCCTTATG A and GCGCGGATCCCATTTTTTATTATACTTTTATAG
pET-M18F and pET-M18R	*PfAP-M18*	GCGCCATATGGATAAGAAAGCTAGGGA and GCGCGGATCC TTTCTATTTGTCGTGGAC

[a]Restriction sites (underlined) are *Bam*HI (GGATCC), *Sac*I (GAGCTC), *Hin*dIII (AAGCTT), *Eco*RI (GAATTC), *Pst*I (CTGCAG), *Sal*I (GTCGAC), *Bgl*II (AGATCT), *Cla*I (ATCGAT) and *Nde*I (CATATG).

cmyc-tagged PfAP-M17 plasmids. A 1.5-kb region upstream of the *PfAP-M17* gene (shown in Figure 2.2), hoped to contain the gene's promoter region (79) was amplified (from D10 parasite genomic DNA) using the primer pair AP14PSalF and AP14PBgR to incorporate *Sal*I and *Bgl*II restriction sites, respectively. This fragment (LB) was cloned into the pGEM-T Easy vector (Promega, Madison, WI, USA) via TA cloning between the Ts present in the vector and the As produced by the DNA polymerase. Colony PCR (section 2.6.7) and sequencing (using the T7 promoter and M13 Reverse primer pair) confirmed the presence of the correct insert. The LB region was then digested from this plasmid, pGEM-T-LB, (with *Sal*I and *Bgl*II), analysed by agarose gel electrophoresis and purified from the gel before cloning into the entry vectors containing *att*L sites, pHB-Pf140015-gfp and pHB-Pf140015-cmyc. These vectors contained the (irrelevant) *Pf14_0015* gene, tagged with gfp and cymc respectively, and had previously been digested with *Sal*I and *Bgl*II to remove the heat shock protein 86 promoter (HB) and analysed by agarose gel electrophoresis before being purified from the gel. Plasmids pLB-Pf140015-gfp and pLB-Pf140015-cmyc were isolated from putative transformants and digested (with *Sal*I and *Bgl*II) to confirm successful cloning. The truncated (Pf14) and full-length (AP14) *PfAP-M17* genes were digested, using *Pst*I and *Bgl*II, from pHB-Pf14Pst-cmyc and pHH1-AP14-cmyc vectors, respectively. These genes were then ligated into the pLB-Pf140015-gfp and pLB-Pf140015-cmyc vectors (described above), also digested with *Pst*I and *Bgl*II, replacing the *Pf14_0015* gene with Pf14 and AP14 to produce pLB-Pf14-gfp and pLB-AP14-gfp, pLB-Pf14-cmyc and pLB-AP14-cmyc, respectively. These plasmids were digested with *Pst*I and *Bgl*II, to confirm the presence of the correct inserts, before incubating with pHH1-DR0.28, the destination vector containing the *att*R sites, previously digested with *Nco*I. Incubation in the presence of the GATEWAY® LR clonase enzyme and buffer (Invitrogen) produced the required transfection vectors, pHH1-Pf14-gfp, pHH1-LB-AP14-gfp, pHH1-Pf14-cmyc and pHH1-LB-AP14-cmyc via recombination. These vectors were digested with *Eco*RV to confirm correct construction before transfecting into *P. falciparum* parasites.

2.5.2. Construction of PfAP-M17 anti-sense vector

The PfAP-M17 anti-sense transfection vector was similarly produced using the GATEWAY® system (outlined in Figure 2.3). The *PfAP-M17* gene was amplified using a vector containing the full-length gene as a template (pLB-AP14-cmyc) and the primer pair AntiAP14F and AntiAP14R, incorporating the restriction sites *Pst*I and *Bgl*II, respectively. The PCR product was analysed by agarose gel electrophoresis and purified from the gel

before ligating into pGEM-T Easy and transforming into *E. coli*. Colony PCR of transformants and sequencing (using the T7 Promoter and M13 Reverse primer pair) of this vector, pGEM-T-M17anti, confirmed the presence of the correct insert. The *PfAP-M17* gene was digested from pGEM-T-M17anti, using *Pst*I and *Bgl*II and cloned into pHB-Pf140015-cmyc, previously digested with *Pst*I and *Bgl*II, to remove the cmyc-tagged (irrelevant) *Pf14_0015* gene, therefore enabling its replacement with the *PfAP-M17* gene in the reverse orientation. The resulting entry vector, pHB-M17anti-cmyc, was isolated from putative transformants and digested (with *Pst*I and *Bgl*II) to confirm successful cloning. It was then incubated with the pHH1-DR0.28 destination vector (previously digested with *Nco*I), in the presence of the GATEWAY® LR clonase enzyme and buffer, to produce the pHH1-M17anti-cmyc transfection vector. Digestion with *Eco*RV confirmed that the correct construct had been made before transfecting into *P. falciparum* parasites.

2.5.3. Transfection of *P. falciparum* cultures

Transfection of *P. falciparum* was performed by electroporation of ring-stage parasites as described previously (152) except that approximately 200 µg of plasmid DNA, isolated from *E. coli* cells using the Plasmid Maxi Kit (Qiagen, Germany), were used. The DNA was ethanol precipitated and resuspended in 30 µl TE buffer before adding to 770 µl pre-warmed Cytomix (120 mM KCl, 0.15 mM CaCl$_2$, 10 mM K$_2$HPO$_4$/KH$_2$PO$_4$ pH 7.6, 25 mM HEPES pH 7.6, 2 mM EGTA, 5 mM MgCl$_2$, adjusted to pH 7.6, filter sterilised and stored at 4 °C). Parasites (250 µl of sedimented culture at ~5% parasitaemia and containing mostly ring-stage) were mixed with the DNA/Cytomix mixture and electroporated under standard *E. coli* conditions (200 Ω, 25 uF, 2.5 kV) before immediately transferring to 6 ml of warmed complete medium containing one drop of fresh erythrocytes and incubating under standard conditions. Parasites were cultured in medium containing 5 nM WR99210, either immediately or after 24 h, and were grown until parasites were detected in the culture by microscopic examination of thin blood smears (usually after 20–30 days).

2.6. CLONING OF *P. FALCIPARUM* AMINOPEPTIDASE GENES

2.6.1. Amplification of *P. falciparum* aminopeptidase genes by polymerase chain reaction (PCR)

Sequences for the four aminopeptidase genes were identified in the *P. falciparum* genome (www.plasmodb.org). The first primer pairs used to amplify *PfAP-M1*, *PfAP-M17*, *PfAP-M18* and *PfAP-M24* (PFAPM1F and PFAPM1R2, PFAPM17F and PFAPM17R,

27
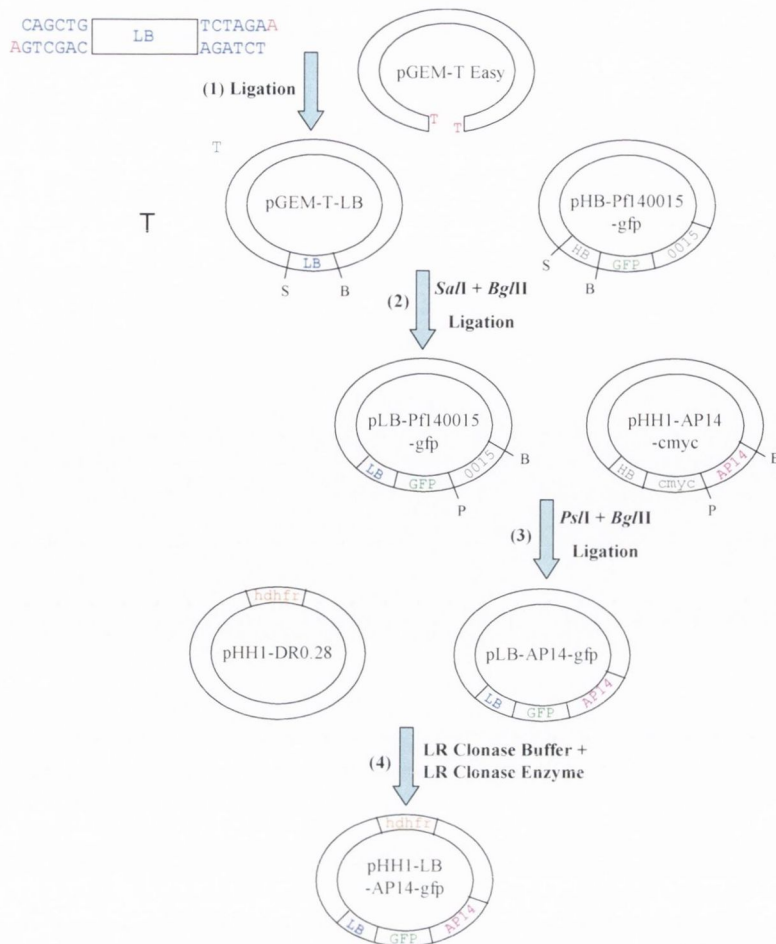
Figure 2.1. Construction of the PfAP-M17-GFP fusion vector. **(1)** The LB fragment (blue) (corresponding to the putative promoter region and shown in more detail in Figure 2.2), was amplified to incorporate *Sal*I and *Bgl*II restriction sites and was cloned into pGEM-T Easy via overhanging As and Ts (shown in red). **(2)** pGEM-T-LB and pHB-Pf140015-gfp (GFP coloured green) were digested with *Sal*I (S) and *Bgl*II (B), enabling the replacement of the heat shock protein 86 promoter (HB) with the LB fragment. **(3)** pLB-Pf140015-gfp, and vector pHH1-AP14-cmyc were digested with *Pst*I (P) and *Bgl*II (B), enabling the replacement of the *Pf14_0015* gene (labelled 0015) with the *PfAP-M17* gene (labelled AP14 and coloured purple). **(4)** pLB-AP14-gfp was incubated with the pHH1-DR0.28 vector (previously digested with *Nco*I) in the presence of LR clonase buffer and enzyme to produce pHH1-LB-AP14-gfp, i.e. a vector containing a GFP-tagged PfAP-M17 gene under the control of the PfAP-M17 promoter. The same procedure was carried out to produce pHH1-Pf14-gfp, except that step 3 involved digestion of vector pHB-Pf14Pst-cmyc with *Pst*I and *Bgl*II to replace the *Pf140015* gene with the truncated *PfAP-M17* gene (Pf14). The cmyc-tagged vectors, pHH1-AP14-cmyc and pHH1-Pf14-cmyc were constructed in a similar manner.

ATGTATTTAAAAGTGTAGAACGAAATATTTTATACTAATATATATATAATAATATATATTTATATTTACTGAG
AAAATGATAAAACAAAATTTTATTTATATTTTTAGGCATAAACTTTATTTATATATTTTTTTTTGAATTTTTT
TTCGTGAATATTGTAATTTTCTTTTTTATTATTTATATAATATATATAATATATATATAAATGTTCTTATAAA
AAAAAAATTATGTTTAATATATTATATTATAGAAAAAATATTTGTTAAAAACAAATATAACTTAAATATTATT
AACAAATAAAAAAGCATTCAATTATTTTCTATGTTCTTTATTCTTTCGAAAATCCTCATTTCACATATATAAA
TAAAAAGCCACTAAATAATTTTCGAAGGTTATATGGCATCCCTCAATATATATCCTAGTTTCTTCTTTTTTAA
TGTTATATATAATGACAAATCATATAAAAAAGAATTTCCTATATTTTTAAATTAATTCTTATATATATATATA
TATATATATATATATATGTGAAAATCACACATTGCTTATATGTAATACGCATAAAAAAAATAATATATATATG
AATATATATATATATATATATTATATTATATATATGTGTTCTTTGAATTACGGATACTATTTAAAGGGGGAAA
AATAAAATAAATAAAATGCATACATACATATATATATATATATATATATATATATATATATATATATATATTA
TATATATGTGTTCTTTGAATTACGGATACTATTTAAAGGGGAATAAATTAAATAAATAAAATACATACATATT
ATATATATAATATATATATATATATATATATATATATAATATATTTTATAATATATATATTTTTTTATAAT
ATGTTCGTTATGTAATGCTATATTATATTTATTATTTTTCCTTTTGTATACATATGTTACATTATGTATTACA
GAAATATAATACTTGCATATTTCTAATTGTACATTATTTTATTTTATATCCTAAAATCTACTATACACAGTGG
AAAAAAAAAATAAAATAAAATAAAATAAAAAAAGCCTTTGTGCATGGTTAATAATAATGTAAAATACAAAAGT
AATATAAATAAAGGAATAATTTTTATTATCTGCTTTTTAAATATTCCTTATATATTTGCTACGTATTAAAAAA
AATATATTTATTTATTATAAAAAAAAAAAATAAAAAGTCACATCTATATATATATATATATAATATATATAT
GAAATATACATGTATCATAAAAAAAATAAAATATAATATTATATATATATATATATATATATACTATATAT
ATAATACATCTTATATATACATAATTTACGTCATATAAATAATATACATACATATATATTTTATTTATATATA
TATATATATATATATACTTAAAATATATAGTATAATAAATATTATAATAATACATATAATATTTATAAATTTA
TATTTTATTATTATTTTATTATTTTTATTTTCTGATGTATTTTTCTTCCTTATGTAAATTTTTGCCAATATCT
GAAAAAGAAAGATATATTTAAATATTGTAAAAAAACGCTTCTGTAAATCAAATATATATTATAATAATAATA
ATAATAATATTATTAATTATAATAAGAGAGGTTTAAAATTTTATCCTTTTTGTAATAATTTAAAAAAAAATAT
AAATTTTGTAAATATTAATAATAAGAAGGGAATAAATTTTCATAGTATAAATAAAGAAAGAAAAATGGCAAGT
GAAGTACCACAAGTTGTTTCCTTAGATCCAACAAGTATTCCTATTGAATATAATACTCCTATACATGATATAA
AAGTTCAGGTTTATGATATAAAAGGAGGTTGTAATGTTGAAGAAGGATTAACTATTTTCTTAGTTAATAATCC
TGGTAAAGAAAATGGGCCAGTTAAAATTAGCTCAAAAGTTAATGATAAAAATGTGAGCGAATTTTTAAAAGAT
GAAAATATGGAAAAATTTAATGTTAAATTAGGAACATCAAAACATTTCTACATGTTTAATGATAATAAAAATT
CAGTTGCTGTTGGTTATGTAGGATGTGGATCAGTTGCTGATTTAAGTGAAGCTGATATGAAAAGAGTTGTATT
ATCATTAGTCACTATGTTACATGATAATAAACTTTCTAAATTAACTGTTGTTTTTGAAATTAATGTTGATAAA
AATTTATTCCGTTTTTTTCTTAGAAACATTATTTTATGAATATATGACCGATGAAAGGTTCAAATCTACTGATA
AAAATGTTAATATGGAATATATCAAACATTTAGGTGTATACATAAACAATGCTGATACTTATAAGGAAGAAGT
TGAAAAAGCTCGTGTTTATTATTTTGGTACTTATTATGCTTCTCAACTTATTGCTGCACCATCCAACTATTGT
AATCCTGTATCTTTATCTAATGCAGCTGTAGAGCTAGCTCAAAAATTAAATTTAGAATATAAAATTCTAGGAG
TAAAAGAACTTGAAGAATTAAAAATGGGAGCCTATTTATCTGTGGGTAAAGGTAGTATGTATCCAAATAAATT
TATTCATTTAACATATAAAAGCAAAGGAGATGTCAAAAAAAAAATTGCATTAGTAGGAAAAGGTATTACATTC
GATTCAGGAGGATACAATTTAAAAGCTGCTCCAGGATCTATGATAGATTTAATGAAATTTGATATGAGTGGAT
GTGCAGCCGTTTTAGGTTGTGCTTATTGTGTAGGTACACTTAAACCAGAAAATGTTGAAATTCATTTTCTAAG
TGCCGTTTGTGAAAATATGGTCTCTAAAAATTCCTATCGTCCAGGGGATATTATTACAGCATCAAATGGTAAA
ACTATAGAAGTTGGTAATACAGATGCTGAAGGAAGATTAACATTAGCTGATGCTTTAGTATATGCTGAAAAAT
TAGGTGTTGATTATATTGTAGATATAGCTACATTAACAGGTGCTATGCTATATTCATTAGGTACAAGCTATGC
TGGTGTTTTTGGTAATAATGAAGAACTTATCAATAAAATATTGAACTCTTCAAAAACTTCAAACGAACCAGTC
TGGTGGTTACCAATTATTAATGAATACAGAGCAACATTAAATTCAAAATATGCTGATATTAATAATATCTCAT
CAAGTGTTAAAGCTTCATCTATTGTGGCCTCATTATTTTTAAAAGAATTTGTTCAAAATACTGCTTGGGCACA
TATTGATATTGCTGGTGTTTCATGGAATTTCAAAGCTAGAAAACCAAAAGGTTTTGGTGTGCGTTTATTGACA
GAATTTGTACTCAATGACGCTCTATAA

Figure 2.2. Amplification of upstream region of PfAP-M17, containing the putative promoter region (LB). The DNA coding sequence of PfAP-M17 and upstream sequence showing the positions of the primers used to amplify the 1.5-kb region hoped to contain the M17 promoter are shown. The points of annealing of the forward primer (AP14PSalF) and reverse primer (AP14PBgR) used to amplify the 1.5-kb (LB) fragment are highlighted in red with the direction of PCR amplification indicated by the arrows. The start (ATG) and stop (TAA) codons for the PfAP-M17 gene are underlined and highlighted in (black) bold.
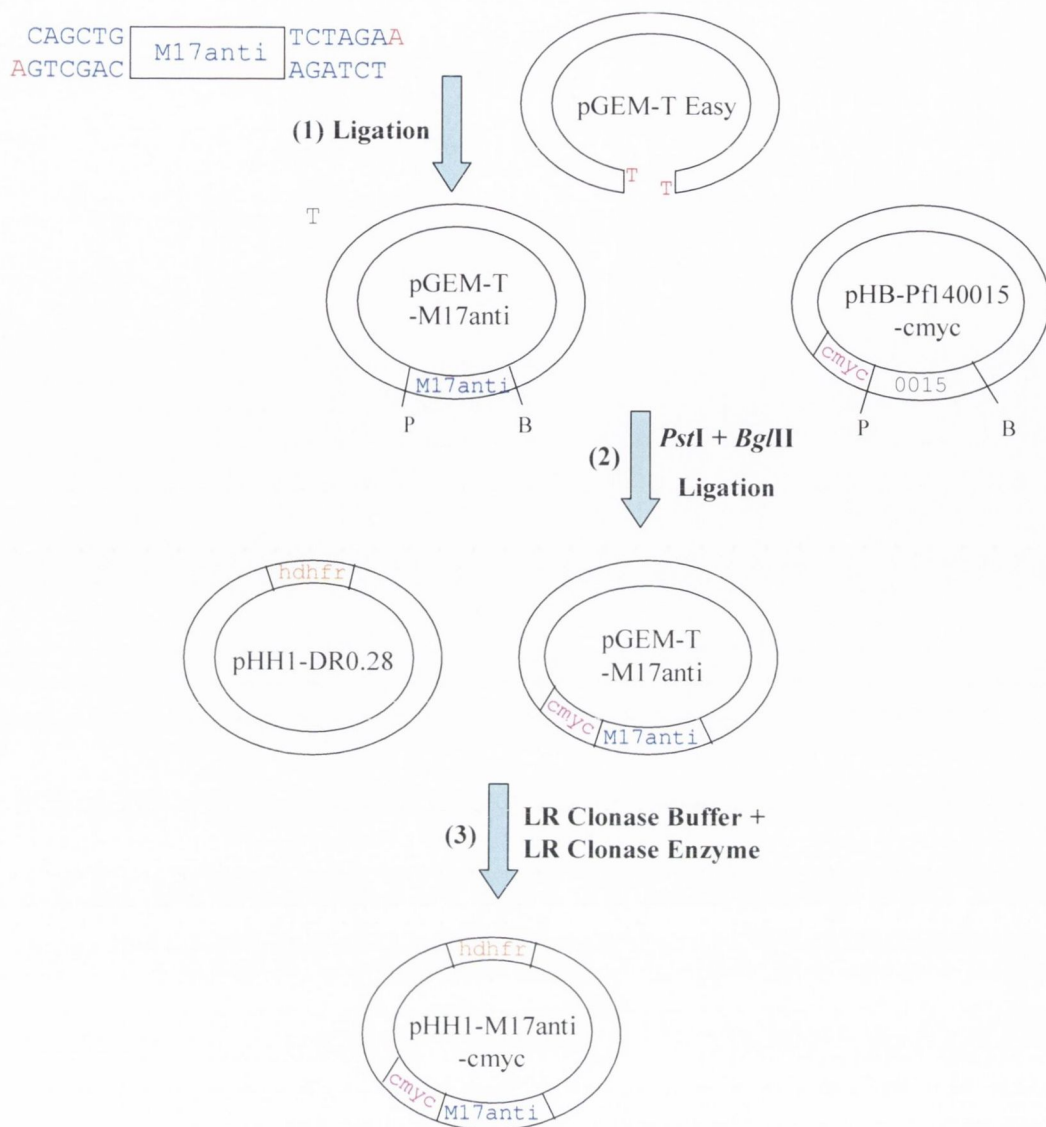
Figure 2.3. Construction of the PfAP-M17 anti-sense vector. **(1)** The *PfAP-M17* gene (blue) in the reverse orientation (amplified to incorporate *Pst*I and *Bgl*II restriction sites) was cloned into pGEM-T Easy, via overhanging As and Ts (shown in red). **(2)** pGEM-T-M17anti and pHB-Pf140015-cmyc were digested with *Pst*I (P) and *Bgl*II (B), enabling the replacement of the *Pf14_0015* gene (labelled 0015) with the *PfAP-M17* gene. **(3)** pLB-AP14-gfp was incubated with the pHH1-DR0.28 vector (previously digested with *Nco*I) in the presence of LR clonase buffer and enzyme to produce pHH1-M17antisense-cmyc, i.e. a vector containing a cmyc-tagged PfAP-M17 gene in the reverse orientation. For simplicity, the heat shock protein 86 promoter is not shown.

PFAPM18F and PFAPM18R and PFAPM24F and PFAPM24R, respectively) (Table 2.2) were designed to incorporate *Bam*HI and *Sac*I restriction endonuclease sites at the 5' and 3' ends, respectively, to facilitate subsequent cloning into the pQE-30 expression vector. "Hot-start" PCR was performed using 1–2 µg genomic DNA, 0.4 µM of the appropriate primers, 0.2 mM each of dATP, dTTP, dGTP and dCTP (Roche) and 1 unit of *Taq* DNA polymerase (Promega) or 2.5 units of *PfuTurbo*® DNA polymerase (Stratagene, Cedar Creek, Texas, USA) or a *Taq/PfuTurbo* mixture (5 units : 0.2 units) with the appropriate polymerase buffer in a Hybaid thermocycler (94 °C for 5 min, 55 °C for 1 min, 60 °C or 72 °C for 3 min; followed by 28 cycles of 94 °C for 1 min, 55 °C for 1 min, 60 °C or 72 °C for 3 min; with a final cycle of 94 °C for 5 min, 55 °C for 1 min, 60 °C or 72 °C for 5 min). The second set of primers used to amplify *PfAP-M1*, *PfAP-M17*, *PfAP-M18* and *PfAP-M24* (MBP-M1F and MBP-M1R, MBP-M17F and MBP-M17R, MBP-M18F and MBP-M18R and MBP-M24F and MBP-M24R, respectively) were designed to incorporate *Bam*HI and *Hin*dIII, *Eco*RI and *Pst*I, *Bam*HI and *Pst*I and *Eco*RI and *Pst*I restriction endonuclease sites at the 5' and 3' ends, respectively, to facilitate subsequent cloning into the pMAL-c2x expression vector (New England Biolabs, Ipswich, MA, USA). "Hot-start" PCR was performed using 1–2 µg genomic DNA, 0.4 µM of the appropriate primers and 0.2 mM each of dATP, dTTP, dGTP and dCTP (Roche) in a Hybaid thermocycler with 1 unit of *Taq* DNA polymerase (Promega) (94 °C for 4 min, 55 °C for 1 min, 60 °C or 72 °C for 3 min; followed by 28 cycles of 94 °C for 1 min, 55 °C for 1 min, 60 °C or 72 °C for 3 min; with a final cycle of 94 °C for 5 min, 55 °C for 1 min, 60 °C or 72 °C for 5-10 min) or 3.5 units of *PfuTurbo*® DNA polymerase (Stratagene) (94 °C for 1 min, 45-51 °C for 1 min, 60 °C or 72 °C for 5–7 min; followed by 28 cycles of 94 °C for 1 min, 50-67 °C for 1 min, 60 °C or 72 °C for 5–7 min; with a final cycle of 94 °C for 5 min, 50-67 °C for 1 min, 76 °C or 72 °C for 10 min) and the appropriate polymerase buffer. Two truncated forms of *PfAP-M1*, *PfAP-M1(96)* and *PfAP-M1(68)*, were amplified with primers (MBP-M1(96)F and MBP-M1R and MBP-M1(96)F and MBP-M1(68)R, respectively) designed to incorporate *Bam*HI and *Hin*dIII sites, for cloning into pMAL-c2x, using the same conditions as for the full-length gene, except that the pMAL-c2x-M1 plasmid was used as the DNA template for PCR. The primer pairs pET-M17F and pET-M17R and pET-M18F and pET-M18R were also designed to amplify *PfAP-M17* and *PfAP-M18*, respectively, incorporating *Nde*I and *Bam*HI sites to enable subsequent cloning into the pET-16b or pET-22b vectors (Novagen, Merck, KGaA, Darmstadt, Germany). *PfAP-M17* was amplified (94 °C for 1 min, 50 °C for 1 min, 60 °C for 5 min; followed by 28 cycles of 94

°C for 1 min, 62 °C for 1 min, 60 °C for 5 min; with a final cycle of 94 °C for 1 min, 62 °C for 1 min, 60 °C for 10 min) using 3.5 units of *PfuTurbo*® DNA polymerase (Stratagene).

2.6.2. Generation of pQE-30-M17

pQE-30 (Qiagen) was isolated from *E. coli* XL-1 Blue cells (Stratagene) using a Qiagen Mini plasmid purification kit. Purified pQE-30 and the *PfAP-M17* gene (amplified with a *Taq/PfuTurbo*® DNA polymerase mixture) were doubly digested with *Bam*HI and *Sac*I (Roche). Briefly, 20-μl reactions were set up using 0.4–1.0 μg DNA, 10–20 units of each enzyme, buffer A and the appropriate amount of ddH₂O to bring the reaction volumes to 20 μl and the tubes were incubated for 2–16 h in a 37 °C water bath. The DNA was purified before ligating the restricted plasmid and fragment together (in a molar ratio of 1:3) using 1 unit of T4 DNA Ligase (Roche) and ligase buffer, in 20–30 μl reactions, at 16–22 °C overnight. Competent *E. coli* XL-1 Blue cells, prepared as described in section 2.6.6, were transformed by the heat-shock method (section 2.6.7), plated out on to L-agar plates supplemented with ampicillin (100 μg/ml) and incubated overnight at 37 °C. The resulting colonies were screened for the construct of interest (pQE-30-M17) (section 2.6.8).

2.6.3. Generation of pMAL-c2x-M1, pMAL-c2x-M1(96), pMAL-c2x-M1(68), pMAL-c2x-M17, pMAL-c2x-M18 and pMAL-c2x-M24

The *PfAP-M1, PfAP-M17, PfAP-M18* and *PfAP-M24* genes were amplified with *PfuTurbo*® DNA polymerase and purified before digestion with *Bam*HI and *Hind*III, *Eco*RI and *Pst*I, *Bam*HI and *Pst*I and *Eco*RI and *Pst*I, respectively (Roche). pMAL-c2x was isolated from *E. coli* TB1 cells (New England Biolabs) using a Mini plasmid purification kit (Qiagen) and digested with the corresponding pairs of restriction enzymes to enable cloning of the aminopeptidase genes. Two constructs, pMAL-c2x-M1(96) and pMAL-c2x-M1(68) (described in section 4.2.1.2), designed to produce the MBP-fusions of the processed forms of the PfAP-M1 enzyme, were also generated as part of an undergraduate 4th-year project by L. Staunton under my supervision. These constructs were generated in a similar manner to pMAL-c2x-M1, with amplification of the fragments using *PfuTurbo*® DNA polymerase and primers designed to incorporate the same restriction sites (*Bam*HI and *Hind*III) as those for *PfAP-M1*. Digestions with *Bam*HI and *Hind*III and *Eco*RI and *Pst*I, were carried out simultaneously in buffers B and H, respectively, whereas digestion with *Bam*HI and *Pst*I required two sequential digests, in buffer B followed by buffer A, respectively, with purification of the DNA between reactions. Twenty-μl

reactions were set up using 0.4–1.0 µg DNA, 20 units of each enzyme, the appropriate buffer and the appropriate amount of ddH$_2$O to bring the reaction volumes to 20 µl. The tubes were incubated for 2–16 h in a 37 °C water bath. The DNA was purified before ligating the restricted plasmid and fragment together (molar ratio of 1:3) using 1 unit of T4 DNA Ligase (Roche) and ligase buffer, in 20–30 µl reactions, at 16-22 °C overnight. Competent *E. coli* TB1 cells, prepared as described in section 2.6.6, were transformed by the heat-shock method (section 2.6.7), plated out on to L-agar plates supplemented with ampicillin (100 µg/ml) and incubated overnight at 37 °C. The resulting colonies were screened for the constructs of interest (section 2.6.8).

2.6.4. Attempted generation of pET-16b-M17

The *PfAP-M17* gene (amplified with *PfuTurbo*® DNA polymerase) and the pET-16b (isolated from *E. coli* DH5α cells using a Mini plasmid purification kit (Qiagen)) were digested with *Nde*I and *Bam*HI (Roche). The DNA was purified before attempting ligation of the restricted plasmid and fragment together (ratio of 1:3) using 1 unit of T4 DNA Ligase (Roche) and ligase buffer, in 20-µl reactions, at 16-22 °C overnight. Competent *E. coli* DH5α cells (section 2.6.6) were transformed by the heat-shock method (section 2.6.7), plated out on to L-agar plates supplemented with ampicillin (100 µg/ml) and incubated overnight at 37 °C. The resulting colonies were screened for the constructs of interest (section 2.6.8).

2.6.5. Generation of pMAL-c2X-HisB-M17

The pTrcHisB-M17 construct was received, in *E. coli* DH5α (Invitrogen) and BL-21 (DE3) pLysS (Stratagene) cells, from Prof. John Dalton. The synthesised *PfAP-M17* gene, codon-biased for *Pichia pastoris*, had been purchased, cloned into the pPCR-Script Amp vector, from Geneart. The gene was sub-cloned into the pGEM®–T vector (Promega) before further subcloning into pTrcHisB (Invitrogen) using the *Bam*HI and *Eco*RI restriction sites, transforming into *E. coli* DH5α and BL-21 (DE3) pLysS. pTrcHisB-M17 and pMAL-c2x were isolated from *E. coli* DH5α and TB1 cells, respectively, using the GenElute mini plasmid purification kit (Sigma). Both plasmids were digested with *Bam*HI and *Hin*dIII (Roche), overnight at 37 °C, in 20-µl reactions containing 0.4–1.0 µg DNA, 10–20 units of each enzyme, buffer B and the appropriate amount of ddH$_2$O. The DNA was analysed by agarose gel electrophoresis and the restricted pMAL-c2x plasmid and PfAP-M17 fragment were purified from the gel before ligating them together (in a molar ratio of 1:3) using 1 unit of T4 DNA ligase (Roche) and ligase buffer, in 20–30 µl

reactions, at 16–22 °C overnight. Competent *E. coli* TB1 cells (section 2.6.6) were transformed by the heat-shock method (section 2.6.7), plated on L-agar plates supplemented with ampicillin (100 µg/ml) and incubated overnight at 37 °C. The resulting colonies were screened by PCR for the construct of interest (pMAL-c2x-HisB-M17) (section 2.6.8).

2.6.6. Preparation of competent *E. coli* cells

A single colony of the desired strain of *E. coli* was used to inoculate 20 ml of L-broth and the culture was grown overnight with agitation at 200 rpm at 37 °C. Five ml of overnight culture were used to inoculate 400 ml of fresh L-broth in a 2-litre baffled flask and the bacteria were then grown at 37 °C with agitation at 200 rpm until they had A_{600} of ~ 0.4. Cells were decanted into pre-chilled GSA Sorvall containers and were left on ice for 5-10 min. Cells were centrifuged at 1,600 × *g* for 7 min at 4 °C in a Sorvall RC-50 centrifuge (Du Pont Ltd., Stevenage, Herts, UK). Supernatants were discarded and pellets gently resuspended in 20 ml of ice-cold sterile $CaCl_2$ solution (60 mM $CaCl_2$, 10 mM PIPES (piperazine-N,N'-bis[2-ethanesulphonic acid]) pH 7.6, 15% (v/v) glycerol). Cells were centrifuged at 1,100 × *g* for 5 min at 4 °C and the resulting pellets resuspended in 20 ml of ice-cold $CaCl_2$ (100 mM) and incubated on ice for 30 min. Cells were sedimented and resuspended in 4 ml of ice-cold $CaCl_2$ solution, divided into pre-chilled sterile eppendorf tubes (200–500 µl volumes), snap frozen in liquid nitrogen and stored at -70 °C.

2.6.7. Transformation of competent *E. coli* strains

Competent *E. coli* cells were transformed using the heat-shock method as described by Maniatis *et al* (107). Competent cells were thawed on ice for 30 min before mixing with 2–16 µl of ligation mixture or expression plasmid alone in a sterile eppendorf tube. Samples were incubated on ice for 30 min, heat-shocked in a 43 °C water bath for 2 min and placed back on ice for a further two min. One ml of pre-warmed L-broth was added to the samples, which were then incubated in a 37 °C water bath for 1 h. After incubation, 100-µl volumes of each sample were plated in duplicate on L-agar plates containing the appropriate antibiotic and incubated overnight at 37 °C. The remaining cells in the transformation mixture were sedimented by centrifugation at 11,950 × *g* for 2 min at room temperature and most of the resulting L-broth was removed except for ~100 µl. The pellet was then resuspended in the excess L-broth and plated in duplicate on L-agar plates as previously outlined. The later step was included so to obtain the maximum possible number of transformants. Cells transformed with the parental vector alone served as

31

positive controls, while cells transformed with unligated vector, previously digested with the appropriate restriction enzyme(s), served as negative controls.

2.6.8. Screening of transformants

Putative transformants, obtained after overnight growth on L-agar, supplemented with the appropriate antibiotic, were screened for the construct of interest by a number of techniques. All of the methods involved the replica-plating of colonies onto fresh plates and using the remainder of the colony for the screening procedure. DNA sequence analysis (carried out by the Advanced Biotechnology Centre, Imperial College London, UK or the QIMR Sequencing Unit, Brisbane, Australia) was used to confirm that the constructs had the correct DNA sequence.

2.6.8.1. Rapid colony screening

If a large number of putative transformants was obtained the method of Le Gouill and Dery (93) was used for an initial, fast screen. Colonies were emulsified in microfuge tubes in 16 µl (lysis) solution I (9 vol of 10 × agarose gel loading buffer, 11 vol of water, 40 vol of solution II (0.2 M NaOH, 1% (w/v) SDS)) before adding 3 µl of solution III (3 M potassium acetate, 1.8 M formic acid). Tubes were centrifuged for 4 min at 13,000 × g to sediment cellular debris and 10–15 µl of the resulting supernatant were loaded directly onto an agarose gel for electrophoresis. Following ethidium bromide staining, constructs of interest were identified by their apparent slower migration through the gel than vector alone. These constructs were then analysed by restriction digest or PCR to confirm the presence of the required insert.

2.6.8.2. Screening by restriction endonuclease digestion

In some cases the presence of the insert in the construct of interest was investigated by the ability of restriction endonucleases, for which specific recognition sites had been introduced, to linearise the putative recombinant plasmid and/or produce a particular pattern of fragments. Putative transformants were used to inoculate 3–6 ml of L-broth supplemented with the appropriate antibiotic and cultures were grown overnight at 37 °C with agitation at 200 rpm. Putative recombinant plasmids were obtained from cultures using a plasmid purification kit. Restriction endonuclease digestion was carried out on 20-µl reactions using 20 units of the relevant enzyme in the appropriate buffer (Roche). The size and pattern produced by digestion of the putative recombinant plasmid and plasmid alone (control) were assessed by electrophoresis through an agarose gel.

2.6.8.3. Screening by PCR

PCR was performed on plasmids obtained from putative transformants to confirm the presence of the insert. Bacterial colonies were lysed by mixing with 5-10 µl of ddH$_2$O and boiling for 10 min. Following a brief spin to sediment cellular debris, 5 µl of the lysate were used as the template in a PCR using primers specific for the insert or vector regions flanking the insert. Alternatively, putative recombinant plasmids were isolated from cultures using a mini plasmid purification kit (Qiagen or Sigma) and used as the template for PCR.

2.7. ANALYSIS OF PROTEIN

2.7.1. Determination of protein concentration

Protein concentration was determined using the colourimetric assay of Bradford (21), which is based on quantitating the binding of Coomassie Brilliant Blue G250 to protein. A series of known standards of bovine serum albumin (BSA) (generally 15, 12.5, 10, 7.5, 5, 2.5 and 1 µg/ml) were made up to a total volume of 100 µl in PBS. Samples of the protein of interest were similarly prepared, at a variety of dilutions. One ml of Bradford reagent (0.01% (w/v) Coomassie Brilliant Blue G-250, 0.25% (v/v) ethanol and 10% (v/v) orthophosphoric acid, filtered and stored at 4 °C) was added to standards and samples. Solutions were mixed well and incubated at room temperature for 20 min before determination of absorbance at 595 nm in a Shimadzu UV-1601PC spectrophotometer (Shimadzu Scientific Instruments, Inc., Columbia, MD, USA). The concentrations of the samples of the protein of interest were determined from the standard curve.

2.7.2. Analysis of protein by SDS-polyacrylamide gel electrophoresis (SDS-PAGE)

Protein samples were electrophoretically separated by SDS-PAGE according to the method of Laemmli (90). For maximum resolution of the proteins of interest 10% (w/v) acrylamide mini-gels were generally used. Separating gels typically consisted of 0.375 M Tris-HCl, pH 8.8, 10% (w/v) acrylamide/bisacrylamide (37.5:1.0) (Protogel, National Diagnostics, Hull, UK), 0.1% (w/v) SDS, 0.06% (w/v) ammonium persulphate (APS) and 0.05% (v/v) N, N, N', N'-tetramethyl-ethylenediamine (TEMED). Stacking gels consisted of 0.125 M Tris-HCl, pH 6.8, 4% (w/v) acrylamide/bisacrylamide, 0.1% (w/v) SDS, 0.1% (w/v) APS, and 0.1% (v/v) TEMED. Protein samples were dissolved in an equal volume of 2x reducing SDS sample loading buffer (0.125 M Tris-HCl, pH 6.8, 4%

(w/v) SDS, 20% (v/v) glycerol, 10% (v/v) β-mercaptoethanol and 0.002% (w/v) bromophenol blue), heated to 90–100 °C for 10 min and cooled to room temperature and briefly centrifuged at 9,000 × g for 5 s before being loaded on the gel. A combination of proteins of known molecular mass (New England Biolabs) was loaded on each gel as reference standards. The protein samples (0.2–20 μl) were electrophoresed at 100 V through the stacking gel and 150-200 V through the separating gel until the sample tracking dye reached the bottom in a running buffer consisting of 0.025 M Tris-HCl, 1.9 M glycine and 0.01% (w/v) SDS.

2.7.3. Analysis of protein by native PAGE

For non-denaturing, non-reducing PAGE, gels were set up and run as described for SDS-PAGE (2.7.2) except that no SDS or β-mercaptoethanol was included in the system (i.e. separating/stacking gels, running buffer and loading buffer).

2.7.4. Fluorography

For direct visualisation of aminopeptidase activity, samples (recombinant protein or parasite extract) were separated by native PAGE. Gels were washed in PBS before being incubated with 50 μM Leu-amino-methyl-coumarin (Leu-AMC), a fluorogenic substrate, at 37 °C for 20 min as described previously (120). The presence of fluorescence was examined by visualisation under ultraviolet (UV) light with an AlphaImager 2200 gel imaging system (Alpha Innotech Corporation).

2.7.5. Staining and visualisation of polyacrylamide gels

Polyacrylamide gels were stained with Coomassie Blue reagent (0.15% (w/v) Coomassie Brilliant Blue R250 (Phiobio, Fisons Scientific Equipment, Loughborough, UK), 45% (v/v) methanol (BDH), 10% (v/v) glacial acetic acid (BDH), filtered to remove undissolved components) until the desired degree of staining was achieved (typically 1–4 h). They were subsequently destained in a solution of 20% (v/v) methanol/7.5% (v/v) glacial acetic acid until the background was clear. Gels were exposed to white light using an AlphaImager 2200 gel imaging system and photographed.

2.7.6. Concentration of protein with trichloroacetic acid (TCA)

TCA precipitation was used to concentrate dilute protein samples collected after chromatography, prior to analysis by SDS-PAGE. Protein samples were mixed with an equal volume of ice-cold 25% (w/v) TCA, incubated on ice for 5 min and centrifuged at

18,000 × *g* for 5 min at room temperature. The supernatant was removed and the protein pellet was resuspended in 15–20 μl SDS loading buffer (62.5 mM Tris-HCl pH 6.8, 1.15% (w/v) SDS, 5.0% (v/v) glycerol, 5.0% (v/v) 2-mercaptoethanol and 0.005% (w/v) bromophenol blue as a tracking dye). If the samples turned yellow upon addition of SDS loading buffer, the pH was neutralised by the addition of 2–3 crystals of Tris base. Samples were boiled for 10 min before loading on SDS-polyacrylamide gels as outlined in section 2.7.2.

2.7.7. Western immunoblotting

After electrophoresis (section 2.7.2), unstained polyacrylamide gels were soaked in transfer buffer (1.9 M glycine, 0.025 M Tris-HCl, 24% (v/v) methanol) and sandwiched with polyvinylidiene difluoride (PVDF) membrane (Roche) previously treated in 100% (v/v) methanol for 5 s. Proteins were transferred for 1 h at 100 V or overnight at 20 V, with an ice block present to keep the tank from over-heating. After transfer, the blot was blocked in 5% (w/v) skimmed milk in Towbin's buffer (0.1 M Tris-HCl, pH 7.4, 0.9% (w/v) NaCl) for 1 h or overnight. The membrane was incubated in primary antibody diluted to the required concentration in skimmed milk in Towbin's buffer (between 1: 250–1:10,000 depending on the antibody) for 1 h. The blot was washed 3–10 times for 30 min in Towbin's buffer supplemented with 0.05% (v/v) Tween-20. These steps were repeated for the secondary antibody. Maltose-binding protein (MBP)-fusion proteins were identified by probing with anti-MBP primary antibody (New England Biolabs) followed by goat anti-rabbit immunoglobin secondary antibody while His_6-tagged proteins were detected with the horseradish peroxidase (HRP)-conjugated oligo-histidine nickel probe, INDIA HisProbe® (Pierce, Rockford, IL, USA). Bands were detected using a chemiluminescence system (Roche) according to the manufacturer's instructions. The blot was exposed to X-OMAT UV film (Kodak) for the desired length of time prior to passage through a Kodak X-OMAT 1000 automatic developer.

2.7.8. Stripping and re-probing of PVDF membranes

Antibodies were removed from membranes by heating at 60 °C for 30 min in a stripping solution (62.5 mM Tris-HCl, pH 6.8, 2% (w/v) SDS, 100 mM β-mercaptoethanol). The membrane was washed three times in Towbin's/Tween solution for 10 min. After blocking with 3% (w/v) skimmed milk in Towbin's buffer, the membrane was probed with the appropriate primary antibody and processed as outlined in section 2.7.7.

2.8. PRODUCTION AND PURIFICATION OF RECOMBINANT PROTEIN

2.8.1. Expression of protein in *E. coli* cells

A variety of *E. coli* strains (Table 2.3) were assessed for their ability to express recombinant protein. Luria (L) broth (5–25 ml) supplemented with ampicillin (100 µg/ml) (Roche) (and chloramphenicol (34 µg/ml) for the BL-21 (DE3) pLysS and Rosetta® cells) was inoculated with a colony of the particular strain of *E. coli* harbouring the desired plasmid and the culture was grown overnight at 37 °C with agitation at 200 rpm. Larger volumes of L-broth (50 ml–1 l) were inoculated the following day from these overnight cultures and were grown at 37 °C to an A_{600} of 0.5–0.7. Generally, protein expression was induced by the addition of 1.0 mM isopropyl-β-D-thiogalactopyranoside (IPTG) (Melford Laboratories) and the culture was incubated for a further 3 h at 37 °C. However, many of these conditions were altered while attempting to improve the production of recombinant protein by the cells.

2.8.2. Harvesting and lysis of *E. coli* cells

Cells were harvested by centrifugation at 6,000 × g for 15 min at 4 °C in a Sorvall RC50 Plus centrifuge using a GSA rotor. Pellets were washed with PBS and then resuspended in the appropriate buffer (25 mM Na_2HPO_4, 500 mM NaCl, pH 7.4 or 10 mM Tris, pH 8.0, 150 mM NaCl), free from peptidase inhibitors (e.g. EDTA) and were either used immediately or frozen at -20 °C. The cells were lysed by the addition of lysozyme (25 µg/ml) and passage through a French pressure cell or sonication three times, for 10 s, on ice using a Sonicator 3000 Ultrasonic Liquid Processor (Misonix, NY, USA) and the resultant lysates were clarified by centrifugation at 35,000 × g or 14,000 × g for 30 min at 4 °C. The supernatant, or soluble portion, was filtered on ice through a 0.45 µm HA Millipore membrane before purification by affinity chromatography.

2.8.3. Determination of recombinant protein solubility

The solubility of recombinant protein was assessed by the method of Williams *et al* (174). Pellets obtained as outlined in section 2.8.2 were resuspended in 150 µl of lysis buffer (50 mM Tris-HCl, pH 8.0, 2 mM EDTA, lysozyme (100 µg/ml) (added immediately before use)) and the suspension was incubated for 15 min in a 30 °C water bath and sonicated with a Soniprep 150 MSE sonicator (Sanyo, Dublin) twice, for 10 s, on ice. Samples were centrifuged at 18,000 × g and supernatants (soluble protein) removed to

fresh tubes and mixed with 150 µl of 2x SDS loading buffer. Pellets (insoluble protein) were resuspended in 300 µl 2x SDS loading buffer. Samples of the soluble and insoluble extracts were analysed by SDS-PAGE.

2.8.4. Lysis of *Sf9* insect cells

Sf9 (*Spodoptera frugiperda*) cell pellets ($\sim 3.5 \times 10^6$ cells/ml) transfected with baculovirus carrying the *tPfAP-M17* gene were obtained (from the SRC Protein Expression Facility, Queensland, Australia) and were stored as ~15-ml pellets at -80 °C. The pellet was thawed on ice and re-suspended in cold PBS to a total volume of 100 ml before sonicating three times, for 10 s, on ice using a Sonicator 3000 Ultrasonic Liquid Processor (Misonix, NY, USA). This freeze/thaw and sonication was repeated a further two times. Insoluble material was sedimented by centrifugation at 14,000 × g in a Sorvall RC-5 centrifuge for 30 min at 4 °C. The supernatant, or soluble portion was filtered on ice through a 0.45 µm HA Millipore membrane before purification by affinity chromatography.

2.8.5. Nickel-chelate affinity chromatography

One of two types of nickel affinity column were used for recombinant protein purification, a nickel-nitriloacetic acid-agarose column (5 ml, HiTrap chelating column, Amersham Pharmacia) or a nickel-agarose resin column (0.5–1.0 ml, Novagen). The column was equilibrated with 10 column volumes of metal-chelate affinity chromatography (MCAC) buffer (25 mM Na_2HPO_4, 500 mM NaCl, pH 7.4 for the former column, and 50 mM Na_2HPO_4, pH 8.0, with 300 mM NaCl and 10 mM imidazole for the latter). The filtrate containing the soluble recombinant His_6-tagged protein was loaded onto the column undiluted or diluted 1:5 in MCAC buffer and passed through the column at a flow rate of 1–3 ml/min by gravity or using a peristaltic pump. The column was then washed with 10–30 column volumes of MCAC buffer supplemented with 95 mM imidazole for the former system or 20 mM imidazole for the latter. Recombinant protein was eluted from the column with 10 column volumes of MCAC buffer containing 250 mM imidazole. In some cases a range of imidazole concentrations (10–500 mM) was applied to the column and fractions were collected for analysis by SDS-PAGE. Fractions found to contain protein of the expected size were then pooled. Purified protein was dialysed at 4 °C against 1 × PBS or 50 mM Tris-HCl, with or without 10 µM $ZnCl_2$, for at least 16 hours before being concentrated by ultrafiltration through Amicon Ultra 15 concentrators (Millipore) if required.

2.8.6. Enterokinase cleavage of His$_6$-tag from fusion proteins

Removal of the tag from recombinant His$_6$-fusion protein was attempted using recombinant enterokinase (rEK) (Novagen) according to the manufacturer's instructions. Recombinant protein (7–30 µg) was incubated with 1 U of rEK at 4, 23 or 37 °C for 30 min–23 h and samples were analysed for cleavage by SDS-PAGE.

2.9.   PRODUCTION OF ANTIBODIES TO *P. FALCIPARUM* M17 AMINOPEPTIDASE

Anti-tPfAP-M17 IgG was raised in six BALB/c mice (by Dr. Sheila Donnelly, Institute for the Biotechnology of Infectious Diseases, University of Technology, Sydney, Australia) by a primary sub-cutaneous injection of 15 µg of recombinant tPfAP-M17 (produced in *E. coli* TOP 10 cells) mixed with 15 µg of the adjuvant Quil A delivered in 200 µl of saline. Subsequently, two (to three of the mice) or three (to the other three mice) booster injections were delivered three weeks apart and the mice were bled two weeks after the last immunisation. Serum was separated from clotted blood by centrifugation at 1,200 × *g* for 10 min. An anti-PfAP-M17 peptide antibody, generated against CAGVSWNFKARKPKG, was also used in these studies (provided by Dr. Don Gardiner). The peptide, corresponding to residues 577-590 plus an additional cysteine residue at the N-terminus, was synthesised (Sigma) and conjugated to diphtheria toxin (via the N-terminal cysteine). Mice were immunised with three injections three weeks apart with 30–50 µg of conjugate peptide with Freund's complete and incomplete adjuvant.

2.10.   FUNCTIONAL ANALYSIS OF RECOMBINANT *P. FALCIPARUM* M17 AMINOPEPTIDASE

2.10.1. Analysis by high performance liquid chromatography

Recombinant PfAP-M17 purified from *E. coli* cells and baculovirus-infected Sf9 cells was analysed by high performance liquid chromatography (HPLC) using a Smart System (Amersham Biosciences) equipped with a Superdex-200 gel filtration column. Samples (containing 10–20 µg protein) were run through the column at a flow rate of 40 µl per min and fractions collected every 2 min (i.e. 80 µl). Fractions were incubated in 0.5 mM CoCl$_2$ and were analysed for aminopeptidase activity against 10 µM Leu-AMC (section 2.10.2). Molecular mass standards, apo-ferritin (440 kDa), β-amylase (232 kDa), BSA (67 kDa) and carbonic anhydrase (29 kDa), were separated under the same conditions

before running samples to enable size estimation of protein. The mobile phase was PBS and elution of protein was recorded by measuring the absorbance at 215 nm and 280 nm.

2.10.2. Spectrofluorometric assay of aminopeptidase activity

Aminopeptidase activity of parasite extract or recombinant protein was determined by measuring the release of the fluorogenic leaving group, 7-amino-4-methyl-coumarin (AMC), from fluoromethyl ketone substrates essentially as described (153). Reactions (100–200 μl) were carried out in 96-well plates and were monitored over 30 min–1 h, with excitation at 370 nm and emission at 440 nm, using a spectrofluorimeter (PerkinElmer LS-50B (Waltham, MA, USA) or BioTek KC4 (Winooski, VT, USA)). In some cases reactions were carried out in 1-ml glass tubes in a 37 °C water bath with 100 μl samples removed and read in the same way. The standard reaction mixture contained PBS or 50 mM Tris-HCl pH 8.0, with or without 0.5-1.0 mM $CoCl_2$, depending on the assay, and was pre-incubated at 37 °C for 15 min before addition of Leu-AMC substrate to a final concentration of 10–20 μM.

2.10.2.1. Determination of the effects of divalent metal ions

The metal ion dependence of tPfAP-M17 was determined by assaying activity after pre-incubation of the enzyme in PBS or 50 mM Tris-HCl, pH 8, containing a given metal chloride (0.01–1 mM), for 15 min at 37 °C, before addition of Leu-AMC substrate (10–20 μM). The tPfAP-M17 apo-enzyme was produced by incubation of the enzyme with 10 mM 1,10-phenanthroline in PBS for 15 h, followed by dialysis against PBS overnight. The ability of metal cations to re-activate the apo-enzyme was determined by assaying its activity following incubation with 0.1 mM metal chlorides at 37 °C for 15 min.

2.10.2.2. Determination of substrate preference

The substrate preference of parasite extract and tPfAP-M17 was determined by assaying with different fluorogenic substrates following incubation at 37 °C for 10–15 min with PBS or 50 mM Tris-HCl with or without 0.5–1 mM $CoCl_2$. For kinetic analysis, k_{cat} and K_M values were determined using nonlinear regression analysis and initial rates were obtained over a range of substrate concentrations spanning K_M (0.2–500 μM) and at fixed enzyme concentrations (0.05–2 μM).

2.10.2.3. Determination of temperature profile and stability

The temperature dependence of tPfAP-M17 was determined by incubating the enzyme (0.1 µM) in 50 mM Tris-HCl with 1 mM $CoCl_2$, at 25–50 °C for 15 min before addition of Leu-AMC (to a final concentration of 10 µM) and measurement of fluorescence at 25–50 °C over 30 min. The temperature stability of the enzyme was assessed by incubation of enzyme (0.05 µM) in 50 mM Tris-HCl with 1 mM $CoCl_2$, at 20–80 °C for 30 min before determination of residual activity by addition of Leu-AMC (to a final concentration of 10 µM) and measurement of fluorescence at 37 °C over 30 min.

2.10.2.4. Determination of pH profile

The pH dependence of tPfAP-M17 was determined by incubation of the enzyme (0.2 µM) in 50 mM Tris-HCl pH 8, 1 mM $CoCl_2$ at 37 °C for 15 min before dilution and incubation and assaying in constant ionic strength acetate/MES(2-(N-morpholino)ethanesulfonic acid)/Tris (AMT) buffers (50 mM acetic acid, 50 mM MES, 100 mM Tris-HCl (46)) ranging from pH 4-10.5, with addition of Leu-AMC (10 µM final concentration) and measurement of fluorescence at 25–50 °C over 30 min.

2.10.2.5. Inhibition of leucine aminopeptidase activity

Inhibition of aminopeptidase activity of parasite extract and tPfAP-M17 aminopeptidase activity by classic inhibitors and novel compounds was determined by pre-incubation of the extract or enzyme with the compound (with or without 0.5–1.0 mM $CoCl_2$) for 15 min at 37 °C, before addition of fluorogenic substrate (to a final concentration of 10–20 µM) and measurement of fluorescence over 30 min–1 h. K_i values were determined by measuring the rate of tPfAP-M17 activity with a range of concentrations of inhibitor (12.2 nM–25 µM), at fixed substrate concentrations (two or more, 2–50 µM). The K_i value was determined from the x-axis coordinate of the point of intersection of Dixon plots of $1/V_s$ versus inhibitor concentration, where V_s is the final steady-state velocity of the reaction.

2.11. HOMOLOGY MODELLING OF *P. FALCIPARUM* M17 AMINOPEPTIDASE

2.11.1. Sequence alignments

The amino acid sequences of any M17 aminopeptidases that had been crystallised and the *P. falciparum* M17 aminopeptidase were obtained from the Research Collaboratory for Structural Bioinformatics (RCSB) Protein Data Bank (http://www.rcsb.org/pdb/) and

the *Plasmodium* genome database (www.plasmodb.org), respectively. The sequences were aligned and analysed using the ClustalW program (www.ebi.ac.uk/clustalw).

2.11.2. Homology modelling

The M17 aminopeptidase template structure chosen for homology modelling of the *P. falciparum* M17 leucine aminopeptidase was that of the bovine lens in complex with the phosphonate inhibitor, LeuP. This 3-D structure was obtained by X-ray crystallography (155) and is available at the RCSB Protein Data Bank (http://www.rcsb.org/pdb/), (PDB ID: 1LCP). Homology modelling was performed using the Molecular Operating Environment (MOE) 2006.08 computer software program (Chemical Computing Group Inc.). The sequences of the two proteins were aligned noting that conserved residues were correctly aligned and 10 models were built from the PfAP-M17 sequence, choosing a medium degree of minimisation and an AMBER '94 forcefield. These models were superimposed to ensure regions of variability were not in areas important for catalytic activity. The best intermediate model was chosen i.e. the model that scored best based on the packing evaluation function of MOE, it was evaluated for stereochemically unfavourable outliers and further minimisation was carried out to reduce the number of these outliers.

2.11.3. Fitting of inhibitors into the homology model active site

The chemical structure of a number of the phosphonate compounds was drawn using the MOE 2006.8 software and these structures were aligned with the LeuP inhibitor. In each case the most energetically favourable alignment was chosen for fitting with the homology model. The structure of the bovine lens leucine aminopeptidase used as the template for modelling (1LCP) and the *P. falciparum* homology model were aligned so that the LeuP molecule was in the region of the model's active site. This molecule was then replaced with the particular phosphonate compound to be analysed that had been aligned with LeuP. This enabled its placement near the active site of the model of the *P. falciparum* enzyme and subsequent assessment of its likely interactions with the residues there.

Chapter 3

Investigation of Aminopeptidase Genes and Gene Expression in *Plasmodium falciparum*

3.1. INTRODUCTION

As already described in section 1.3.2, various aminopeptidase activities (between one and four) had been reported in *Plasmodium* parasites at the beginning of this study. Among these activities is that of the PfAP-M1 enzyme (3, 54) (an M1-family aminopeptidase of *P. falciparum*) and an ~80-kDa species partially purified from *P. falciparum* (34, 60). Both aminopeptidase activities were inhibited by metal chelators and bestatin (3, 60), a metallo-aminopeptidase inhibitor that has been found to inhibit the growth of cultured parasites (120). With regard to substrate preferences, PfAP-M1 demonstrated maximal activity against those containing lysine, alanine, arginine and leucine but none against substrates containing aspartate or glutamate (3). The ~80-kDa species was active against substrates containing alanine, leucine, arginine, asparagine, lysine and glycine but had no activity against histidine or proline substrates (34).

Plasmodium aminopeptidase activity is thought to be associated only with the parasite cytosol as extracts of digestive vacuoles generated peptide fragments but no free amino acids (87) and no aminopeptidase activity was detected in these extracts (60, 87). In agreement with this, PfAP-M1 was found to be located primarily in the parasite cytosol and was seen to form condensed spots in schizonts and merozoites (3). Also, PfAP-M1 and the ~80-kDa aminopeptidase were found to be most active at neutral pH but had little or no activity at acidic pH (3, 60). All of these data have led to the suggestion that small peptides may be transported out of the vacuole for processing to single amino acids by aminopeptidases.

This chapter describes the investigation of genes coding for aminopeptidases present in *P. falciparum* genome, including their expression during the intra-erythrocytic cycle of the parasite. The location and stage-specific expression of an M17 aminopeptidase was also examined and a number of experiments involving the production of transgenic parasites under and over-expressing this enzyme were attempted.

3.2. RESULTS

3.2.1. Genomic investigation of putative aminopeptidases present in *P. falciparum*

The number and types of aminopeptidases present in *P. falciparum* were investigated by searching the malaria genome database (www.plasmodb.org) for genes annotated as aminopeptidases and for genes described as having an aminopeptidase function. The four putative methionine aminopeptidases in the *P. falciparum* genome were

not of interest in this study as they are thought to be involved in the removal of methionine residues from the N-termini of newly translated proteins (29, 180) and not to have any involvement in haemoglobin digestion. Excluding these 'house-keeping' methionine aminopeptidases, four putative aminopeptidase genes were identified: MAL13P1.56, PF14_0439, PFI1570c and PF14_0517. The first of these was the *PfA-M1* gene previously identified (54). Investigation of the gene sequences using alignment programs (e.g. BLAST) and searching protein databases (e.g. www.merops.ac.uk) to identify conserved domains and motifs revealed that the aminopeptidases belong to four different families - M1, M17, M18 and M24B. They were therefore named accordingly: PfAP-M1, PfAP-M17, PfAP-M18 and PfAP-M24. Members of these families generally have substrate preferences for alanine, leucine, aspartate and any amino acid linked to proline, respectively. A summary of their characteristics, including consensus motifs and suggested co-factors for peptidases of these families, is outlined in Table 3.1. A fifth gene, Pf14_0015, has also been annotated as a putative aminopeptidase in the *P. falciparum* genome and has been suggested to code for a proline aminopeptidase (153). However, closer examination of the gene sequence confirmed that, while it is a hydrolase, no aminopeptidase motifs or conserved domains could be identified so it was not considered in this study as one of the potential haemoglobin degrading aminopeptidases.

Orthologues of all of these aminopeptidases are found in the other *Plasmodium* species whose genome sequences are available, i.e. *P. vivax*, *P. knowlesi* and the mouse malarial parasites, *P. berghei*, *P. chaubadi chaubadi* and *P. yoelii yoelii* (Table 3.2). These genomes are not yet fully sequenced but so far at least one orthologue from each M family has been identified with up to three found in some species e.g. *P. c chaubadi* contains two putative M1 aminopeptidases and three putative M17-family ones.

3.2.2. Analysis of aminopeptidase gene expression in cultured *P. falciparum* parasites

The expression of these four putative aminopeptidase genes in parasites was assessed by Northern blotting (Figure 3.1). Total RNA was isolated from cultured asynchronous 3D7 parasites and analysed by electrophoresis before transferring to a membrane that was subsequently probed with labelled DNA fragments specific for the particular genes (as described in section 2.3.3). Blots were then stripped and re-probed with an 18S rRNA probe to ensure the RNA had been correctly transferred to the blots. A negative control of samples extract from uninfected erythrocytes in parallel with the RNA from infected cells was included. Transcripts were identified for each gene in the lanes

containing RNA (but not in the lane containing samples extracted from uninfected erythrocytes, i.e. no RNA).

The four genes were also amplified by PCR using genomic DNA isolated from 3D7 parasites (Figure 3.2) (with primers designed to allow subsequent cloning into the pQE-30 expression vector). Bands of close to the expected sizes of 3.3, 1.8, 1.7 and 2.3 kb were obtained for *PfAP-M1, PfAP-M17, PfAP-M18* and *PfAP-M24*, respectively.

3.2.3. Analysis of stage-dependent expression of PfAP-M17 during the intra-erythrocytic cycle

The expression of the *P. falciparum* M17 leucine aminopeptidase (PfAP-M17), throughout the intra-erythrocytic cycle, was investigated. D10 parasites were synchronized (by sorbitol treatment) to rings, early/mid trophozoites, mid/late trophozoites and schizonts/segmenters, (corresponding to ages of approximately 0–12, 16–24, 28–34 and 36–44 h post-invasion, respectively). Samples were taken at each stage to analyse stage-specific transcription, protein production and enzyme activity.

Expression of the *PfAP-M17* gene during the asexual stage was investigated by Northern blotting (Figure 3.3). RNA was extracted from synchronized D10 parasites and analysed by hybridizing membranes with radioactively labelled gene probes. Equal loading of RNA in each lane was confirmed by stripping the blot and re-probing for the 28S RNA subunit. Maximum transcription of *PfAP-M17* was observed in the ring and early trophozoite stage parasites and decreased throughout the cycle with very little transcription seen in the schizonts. This corresponds relatively well with data produced by whole-genome microarray studies that found that mRNA levels are maximal in ring and early trophozoite stage parasites and decrease during the latter part of the cycle (95, 101).

Expression of PfAP-M17 protein throughout the cycle was examined by SDS-PAGE of extracts of synchronised D10 parasites followed by Western blotting with mouse anti-PfAP-M17 antiserum (Figure 3.4). Equal amounts of protein (determined by the Bradford method) were loaded in each lane. Expression of PfAP-M17 was detected in all stages of the intra-erythrocytic cycle with little variation in the levels of expression between the different stages. This might be unexpected considering the results of the Northern blotting data but discrepancies between mRNA and protein levels in *P. falciparum* are well documented and have been suggested to be due to possible mechanisms of post-transcriptional control that might involve interplay of mRNA stability and degradation and/or gene-specific control of translation (94). It should also be noted

that the levels of protein expression in the schizont–stage parasite extract are somewhat questionable due to problems with high background levels on the blot in that position.

In contrast, the leucine aminopeptidase activity of parasites was seen to change over the course of the life-cycle. The activity of extracts of synchronised D10 parasites was examined by measuring the release of the fluorogenic leaving group, 7-amido-4-methyl-coumarin (AMC) from an *L*-leucine-AMC substrate (Figure 3.5). Due to the overlapping substrate profile of M1 and M17 aminopeptidases, experiments were carried out in the presence of $CoCl_2$ as this metal ion has been seen to activate PfAP-M17 activity (sections 4.2.2 and 4.2.4.3) but inhibit PfAP-M1 activity in parasite extracts (section 5.2.3 and J. Lowther, personal communication). Cytosolic extracts at each stage (containing equal amount of protein) were incubated at 37 °C in the presence of $CoCl_2$ (1 mM) for 10 min before addition of substrate. Maximum leucine aminopeptidase activity was seen in the trophozoite stages with no activity in ring-stage parasites and very little in the schizonts. While this conflicts with the western blotting data it is in good agreement with previous stage-specific analysis of leucine aminopeptidase activity (60). It may be that not all of the protein present in the parasites is active during the non-trophozoite stages when it is not needed, perhaps due to the presence of an endogenous inhibitor or the need for processing for activation.

3.2.4. Examination of transgenic parasites expressing GFP-tagged PfAP-M17

The expression of PfAP-M17 protein was also investigated using a parasite strain expressing green fluorescent protein (GFP)-tagged PfAP-M17. D10 parasites were transfected with a vector containing the *PfAP-M17* gene under the control of its native promoter and tagged with the *gfp* gene at the 3' end. The generation of this vector is described in detail in section 2.5.1 and Figures 2.1 and 2.2. A 1.5-kb region upstream of the *PfAP-M17* gene, thought likely to contain its promoter region, was amplified and cloned into the pGEM-T Easy vector, with colony PCR (Figure 3.6 A) and sequencing confirming the presence of the correct insert. (At 1.7 kb this band is larger than the original 1.5 kb size due to the use of the T7 promoter and M13 reverse primer pair that also amplifies some additional sequence contained on the pGEM-T vector.) The promoter (LB) was digested from pGEM-T-LB and cloned into pHB-Pf140015-gfp (a vector containing the *Pf14_0015* hydrolase gene tagged with *gfp*) with digestion confirming successful cloning (Figure 3.6 B).

The pLB-Pf140015-gfp vector was then digested and the insert removed before ligation of the plasmid backbone with the full-length *PfAP-M17* gene (AP14) (digested

Strain	Company	Genotype	Comments
BL-21 (DE3)	Invitrogen	F$^-$ *ompT hsd*S$_B$(r$_B^-$m$_B^-$) *gal dcm* (DE3)	
BL-21 (DE3) pLysS	Invitrogen	F$^-$ *ompT gal dcm lon hsd*S$_B$(r$_B^-$ m$_B^-$) λ(DE3) pLysS(Cm^R)	
DH5α	Invitrogen	F$^-$ *endA1 glnV44 thi-1 recA1 relA1 gyrA96 deoR nupG* Φ*80dlacZΔM15 Δ(lacZYA-argF)U169, hsdR17(r$_K^-$ m$_K^+$), λ–*	
ER2508	New England Biolabs	F$^-$ *ara-14 leuB6 fhuA2 Δ(argF-lac)U169 lacY1 lon::miniTn10*(Tet^R) *glnV44 galK2 rpsL20*(Str^R) *xyl-5 mtl-5 Δ(malB) zjc::Tn5*(Kan^R) *Δ(mcrC-mrr)*$_{HB101}$	*malE* gene (encoding maltose-binding protein) deleted
Rosetta®	Novagen	F$^-$ *ompT hsd*S$_B$(r$_B^-$ m$_B^-$) *gal dcm lacY1* pRARE2^2 (Cm^R) pAR5615 (Ap^R)	Expresses rare tRNAs; facilitates expression of genes that encode rare *E.coli* codons
TB1	New England Biolabs	F$^-$ *ara Δ(lac-proAB)* [Φ*80dlac Δ(lacZ)M15] rpsL*(Str^R) *thi hsdR*	
TOP 10	Invitrogen	F- *mcrA Δ(mrr-hsdRMS-mcrBC)* φ*80lacZΔM15 ΔlacX74 deoR nupG recA1 araD139 Δ(ara-leu)7697 galU galK rpsL* (Str^R) *endA1 λ$^-$*	
XL1-Blue	Stratagene	*recA1 endA1 gyrA96 thi-1 hsdR17 supE44 relA1 lac* [F′ *proAB lacIqZΔM15* Tn*10* (Tet^R)]	

TABLE 2.3. *E. coli* strains used in this study

	PfAP-M1	PfAP-M17	PfAP-M18	PfAP-M24

TABLE 3.1. Known and putative *P. falciparum* aminopeptidases

	PfAP-M1	PfAP-M17	PfAP-M18	PfAP-M24
Gene ID	MAL13P1.56	PF14_0439	PFI1570c	PF14_0517
Chromosome	13	14	9	14
Gene length (kb)	3.3	1.8	1.7	2.3
M Family	M1	M17	M18	M24B
Predicted number of amino acids	1085[c]	605	570	764
Predicted M_r ($\times 10^3$)	126	68	66	89
Motif/consensus sequence(s)[a]	abxHEbbHx$_{18}$E and GAMEN	[NS]-TDAEGR-[LV]	none?	[HA]-[GSYR]-[LIVMT]-[SG]-Hx-[LIV]-G-[LIVM]-x-[IV]-H-[DE]
Suggested preferred N-terminal amino acid[b]	Ala (may be most including Pro)	Leu (may be others including Pro and those linked to Pro; generally not Arg or Lys)	Asp (or Glu)	Any linked to Pro
Suggested co-factor[b]	Zinc	Zinc	Zinc	Manganese/Cobalt

[a] a = V or T, b = an uncharged amino acid, x = any amino acid

[b] Based on properties of other family members

[c] Unprocessed form

TABLE 3.2. Putative orthologues of *P. falciparum* aminopeptidases found in other *Plasmodium* species

	M1 family	M17 family	M18 family	M24B family
P. vivax	Pv122425	Pv118180	Pv087090	Pv1117760
P. knowlesi	PKH_141100	PKH_126020	PKH_073050	PKH_125210
P. berghei	PB000843.02.0	PB000863.03.0	PB000622.00.0 PB000725.01.0	PB000628.00.0 PB301269.00.0
P. chaubadi chaubadi	PC001408.02.0 PC302364.00.0	PC000352.05.0 PC000418.00.0 PC000869.01.0	PC000238.00.0	PC302381.00.0
P. yoelii yoelii	PY01557	PY01898 PY07818	PY03205	PY00855
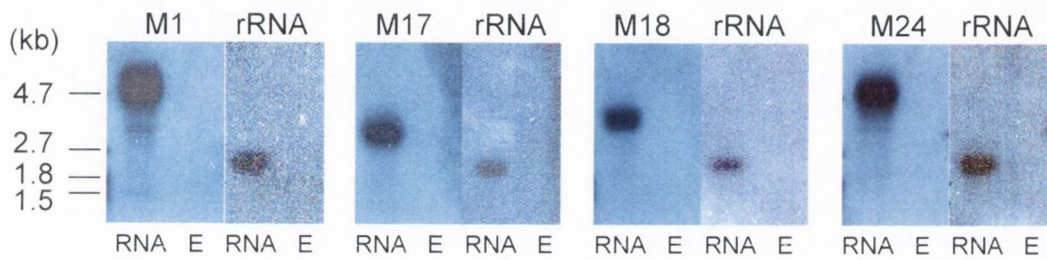
Figure 3.1. Confirmation of expression of aminopeptidase genes by Northern blotting. M1, M17, M18 and M24 refer to the probes for *PfAP-M1*, *PfAP-M17*, *PfAP-M18* and *PfAP-M24* respectively, hybridised with the particular blot, while rRNA refers to the probe for 18S ribosomal RNA applied after stripping the other probes from the blot. RNA refers to those lanes containing total RNA isolated from parasites while E refers to those that contained control samples isolated from uninfected erythrocytes (i.e no RNA). The labeled lines on the left refer to RNA molecular size markers (kb).
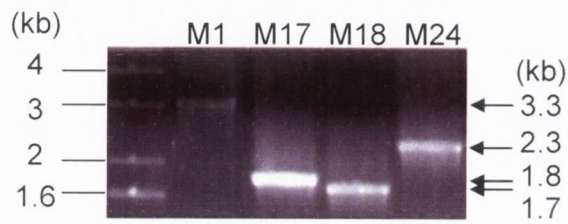
Figure 3.2. Amplification of the four known and putative *P. falciparum* aminopeptidase genes from genomic DNA using *Taq* DNA polymerase. The labelled arrows on the right refer to the bands amplified at sizes corresponding to the expected sizes of *PfAP-M1*, *PfAP-M17*, *PfAP-M18* and *PfAP-M24* genes - 3.3, 1.8, 1.7 and 2.3 kb, respectively - in lanes labelled M1, M17, M18 and M24, respectively. The labelled lines on the left refer to molecular size markers (kb).
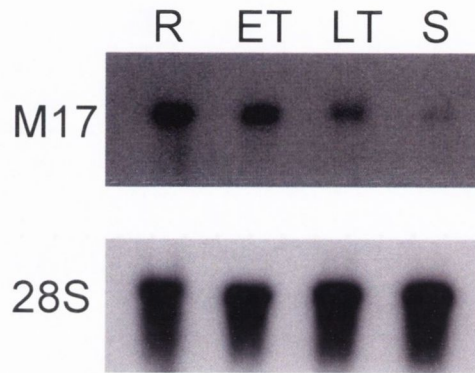
Figure 3.3. Northern blot analysis of stage-specific expression of *PfAP-M17* RNA. Samples of RNA isolated from sorbitol-synchronised D10 parasites were analysed by agarose gel electrophoresis before transferring to a membrane. M17 indicates the blot hybridised with the *PfAP-M17* gene-specific probe, while 28S refers to the blot hybridised with the 28S RNA probe used to check for equal loading, applied after stripping the blot. Lanes labelled R, ET, LT and S refer to those containing equal amounts of RNA from parasites at the ring, early trophozoite, late trophozoite and schizont stages, respectively, (aged approximately 0–12, 16–24, 28–34 and 36–44 h post-invasion, respectively).
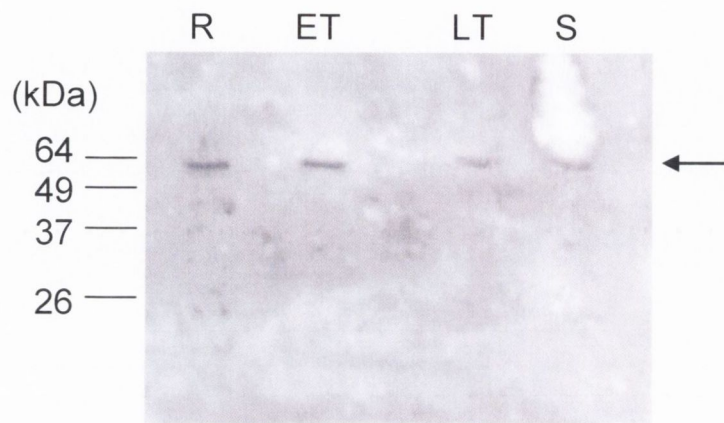
Figure 3.4. Western blot analysis of stage-specific expression of PfAP-M17 protein. Extracts of sorbitol-synchronised D10 parasites were analysed by SDS-PAGE before transferring to a membrane that was probed with mouse anti-PfAP-M17 antiserum. Lanes labelled R, ET, LT and S refer to those containing equal amounts of protein from parasites at the ring, early trophozoite, late trophozoite and schizont stages, respectively, (aged approximately 0–12, 16–24, 28–34 and 36–44 h post-invasion, respectively). The arrow indicates the band running at ~ 64 kDa, corresponding approximately to the expected size of PfAP-M17.

from vector pHH1-AP14-cmyc, a transfection vector containing the *PfAP-M17* gene under the control of the heat shock protein 86 promoter), replacing the *Pf14_0015* gene with AP14 to produce pLB-AP14-gfp, with digestion confirming the presence of the correct insert (Figure 3.7 A). pLB-AP14-gfp was then recombined with the pHH1-DR0.28 vector producing pHH1-LB-AP14-gfp, the transfection vector. This vector was digested with *Eco*RV (Figure 3.7.B) to confirm correct construction before transfecting into D10 parasites. Cultured parasites were grown in the presence of WR-99210 to select for those containing plasmids and aliquots were frozen after reaching ~ 1% parasitaemia. Parasites were assessed for expression of the GFP tag by live fluorescence microscopy.

Fluorescence due to the GFP-tagged PfAP-M17 was observed (in ring, trophozoite and schizont stage parasites, Figure 3.8), confirming the western blotting data that PfAP-M17 protein is expressed in all stages. The GFP fluorescence was located in the parasite cytosol. Extract of these transgenic parasites was analysed by western blotting (Figure 3.9) with an anti-GFP antibody to confirm that the GFP tag was not removed from the PfAP-M17 at any stage giving an incorrect impression of location. Only one band was detected at an apparent molecular mass of ~86 kDa, corresponding approximately to the combined size of the PfAP-M17 and GFP (i.e. 95 kDa) and none was seen at 27 kDa, the size of GFP alone, confirming that the tag was not processed at any point.

PfAP-M17 expression was also located in the parasite cytosol according to immunofluorescence using mouse anti-PfAP-M17 antiserum (data not shown), confirming the results seen with the transgenic PfAP-M17 GFP-fusion parasites.

3.2.5. Other transgenic experiments attempted with *P. falciparum*

A number of experiments involving the generation of transgenic parasites were attempted during this study (listed in Table 3.3 together with additional work not part of this study). These experiments were begun at the Malaria Biology Laboratory, QIMR, Brisbane, Australia and transgenic strains were frozen down in liquid nitrogen before transporting to Dublin with the aim of completing studies on them there. However, none of the strains could be revived following transport, and attempted repeated transfections with the same vectors into 3D7 or D10 parasites in medium supplemented with commercial human serum or Albumax II were unsuccessful. As a result, many of these experiments had to be discontinued.

A second transgenic strain carrying a GFP-fusion to the truncated version of PfAP-M17 was created (section 2.5.1) in parallel with the full-length fusion described above (section 3.2.4). However, these parasites did not demonstrate any fluorescence, even after

the concentration of drug (WR-99210) was increased to 10 × the usual working concentration (50 nM). It is unclear if there was a problem with the vector as no western blot analysis was carried out to confirm the expression of the GFP tag.

Two transgenic strains of *P. falciparum* were produced that contained vectors designed to over-express the full-length or truncated PfAP-M17 gene under the control of its own promoter. The generation of the transfection vectors for these strains, pHH1-AP14-cmyc and pHH1-Pf14-cmyc, respectively, was done in a very similar manner to that described for the PfAP-M17-GFP tagged strain and is described in section 2.5.1. Drug-resistant parasites were obtained following transfection but were frozen before any assays were carried out and could not be revived following transport to Dublin to allow any assessment of the different activities or susceptibility to inhibitors between parasites expressing the full-length and truncated proteins.

An attempt was made to produce a PfAP-M17 knockdown transgenic strain by transfection of parasites with an antisense vector, pHH1-M17anti-cmyc. The construction of this vector is described in section 2.5.2 and figure 2.3. Parasites were obtained following transfection but no effect on growth was observed. Increasing the concentration of WR-99210 to 50 nM (10 × usual concentration), in an effort to encourage increased production of the antisense strand, did not result in any noticeable growth defect either. However, experiments carried our by our collaborators to assess the production of the PfAP-M17 antisense strand by Northern blotting indicated that no antisense strand was being produced in the parasites (F. Teuscher, personal communication). Therefore no conclusion can be drawn from this experiment about the importance of PfAP-M17 for the parasites.

Two transgenic strains (AP13KO and AP14KO) were produced by our collaborators, by transfecting D10 parasites with vectors designed to generate single crossover knockouts of *PfAP-M1* and *PfAP-M17*, respectively (D. Gardiner, personal communication). These strains were cycled 'on' and 'off' drug (WR-99210) three times (for periods of three weeks at a time) to encourage recombination of the plasmid into the chromosome. No effect was seen on parasites when cultured with the drug i.e. no visible decrease in parasite growth was observed, possibly suggesting that integration of the vectors into the parasites' genome had occurred. However, attempted PCR of a fragment containing the 5' region of the gene in question (*PfAP-M1* or *PfAP-M17*) in tandem with the human dihydrofolate reductase (*hdhfr*) gene (only produced by homologous recombination of the vector with the chromosome), indicated that no integration had occurred (data not shown). No product corresponding to this region was amplified, using genomic DNA isolated from either strain and a pair of primers for *hdhfr* and the particular
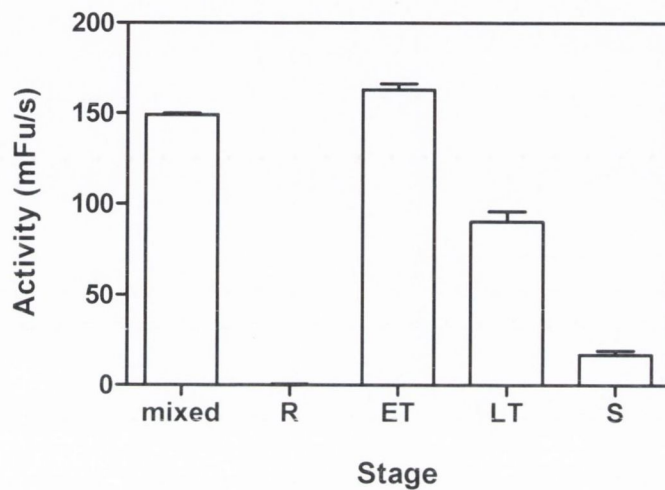
Figure 3.5. Analysis of stage-specific leucine aminopeptidase activity throughout the erythrocytic cycle. R, ET, LT and S refer to parasites at the ring, early trophozoite, late trophozoite and schizont stages, respectively, (aged approximately 0–12, 16–24, 28–34 and 36–44 h post-invasion, respectively) while mixed refers to asynchronous parasites. Extracts were incubated with $CoCl_2$ (1 mM) at 37 °C for 10 min before addition of substrate. (mFu/s = millifluorescence units per second).
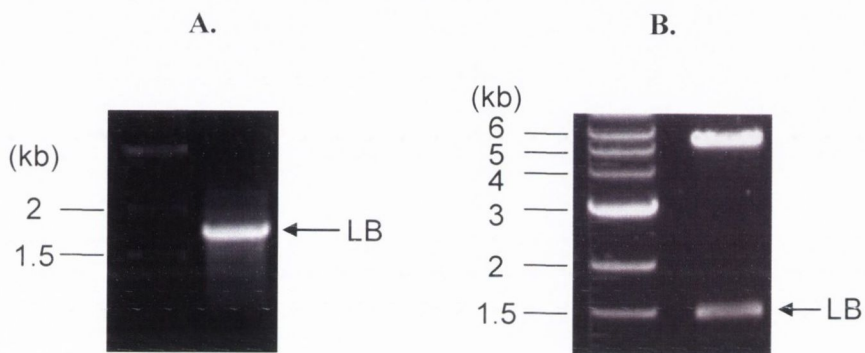
Figure 3.6. Cloning of the *PfAP-M17* promoter region. **A.** Colony PCR of the *PfAP-M17* promoter region (LB) cloned into the pGEM-T Easy vector. The arrow labelled LB indicates the band of the predicted size of ~1.7 kb amplified from pGEM-T-LB, using the T7 Promoter and M13 Reverse primer pair. **B.** Digestion of pLB-Pf140015-gfp with *Sal*I and *Bgl*II. The arrow indicates the band corresponding to the promoter region (1.5 kb). The upper band is the remainder of the vector (containing the GFP-tagged *Pf14_0015* gene). Labelled lines refer to molecular size markers (kb) contained in the lanes on the left in A and B.
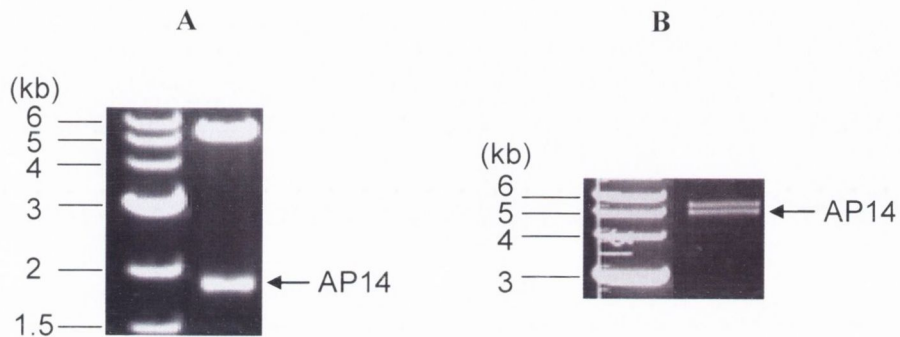
Figure 3.7. Construction of pHH1-AP14-gfp. Labelled lines refer to molecular size markers (kb). **A.** Digestion of pLB-AP14-gfp with *Pst*I and *Bgl*II. The arrow labelled AP14 indicates the band corresponding to the full-length *Pf14-M17* gene digested from pLB-AP14-gfp. The upper band (of >5 kb) is the backbone of the vector, containing the putative promoter region (LB) and the *gfp* gene. **B.** Digestion of pHH1-LB-AP14-gfp with *Eco*RV. The arrow labelled AP14 indicates a band running close to the expected size of the ~4.5 kb fragment containing the full-length *PfAP-M17* gene (plus the *PfAP-M17* promoter, LB, and an additional ~1.2 kb). The upper band (of >5 kb) is the remainder of the backbone of the vector.
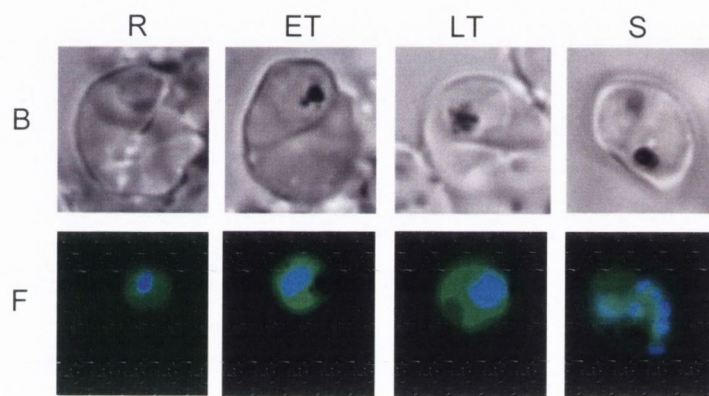
Figure 3.8. Fluorescence analysis of an asynchronous culture of PfAP-M17-GFP fusion parasites. R, ET, LT and S refers to parasites at the ring, early trophozoite, late trophozoite and schizont/segmenter stages, respectively. Panel B shows parasites viewed under bright field illumination, while panel F shows fluorescent, transgenic, GFP-tagged-PfAP-M17 parasites with nuclei visualised with Hoechst dye (blue).
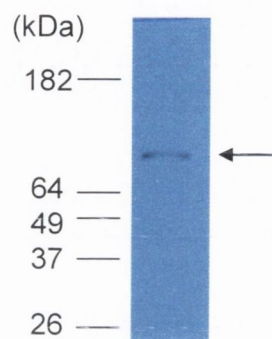
Figure 3.9. Western blot analysis of GFP-tagged PfAP-M17. Extract of parasites expressing GFP-tagged PfAP-M17 was analysed by SDS-PAGE before transferring to a membrane and probing with an anti-GFP antibody. The arrow indicates a band running at ~86 kDa, corresponding approximately to the expected position of PfAP-M17-GFP.

aminopeptidase gene. The *hdhfr* gene could be amplified from both AP13KO and AP14KO, confirming that the vector was present in the parasites.

3.3. DISCUSSION

This work in this chapter investigated the presence and expression of the aminopeptidases in *P. falciparum*. Four metallo-aminopeptidases, belonging to four different families (M1, M17, M18 and M24B) were identified and their expression confirmed by Northern blotting and PCR from genomic DNA. Originally, the PfAP-M24 protein was not annotated as an aminopeptidase on the *Plasmodium* genome website (www.plasmodb.org) but a different, fourth peptidase (*pf14_0015*) was. However, investigation of the sequences of these protein and their conserved domains and motifs made it clear that the former was an aminopeptidase homologue while the latter was not. In addition, mass spectrometric data indicates that the PfAP_0015 peptidase is only present in gametocytes (53). The four genes listed here have since been identified by other groups also (36, 177) as the four putative aminopeptidases of *P. falciparum*.

The demonstration of the expression of the aminopeptidases in intra-erythrocytic stages confirmed previous microarray data that indicated that all four genes are transcribed during these stages of the life cycle of (three strains of) *P. falciparum* (95, 101). In these studies the genes were generally expressed at higher levels in the ring and early trophozoite stages (i.e. the first twenty hours of the life-cycle). Le Roch *et al* assigned the genes to one of fifteen clusters based on expression profiles and found that there was a correlation with the function of the gene product for those proteins that were known. Clusters 5, 6 and 7 contained genes that were expressed in rings and trophozoites but demonstrated much reduced expression in schizonts and were found to contain most of the genes involved in haemoglobin degradation (e.g. falcipains and plamepsins) (95). Two of the four genes studied here were grouped into one of these clusters with PF14_0439 (encoding PfAP-M17) in cluster 6 and PF14_0517 (encoding PfAP-M24) in cluster 7. PFI1570c (encoding PfAP-M18) was in cluster 8 with genes whose expression was focused on the trophozoite stage and MAL131.56 could not be assigned to any particular cluster. Proteomic data show that the four proteins are also detected, by mass spectroscopy, throughout the life cycle of the parasite (53).

Parasites expressing GFP-tagged PfAP-M17 (and immunofluorescence studies) located the protein in the cytosol, as expected. This confirmed previous work indicating the presence of aminopeptidases outside the digestive vacuole (3, 60, 87). More recent work

48

on *P. falciparum* aminopeptidases using yellow fluorescent protein (YFP)-tagged proteins, published just before submission of this thesis, located PfAP-M17 in the cytosol but also identified concentrated spots in mature schizonts (36), not unlike the structures observed for PfAP-M1 (3). The M18 and M24 aminopeptidases were also located in the cytosol (36). Surprisingly, PfAP-M1 was located in the nucleus and, in contrast to previous suggestions it and PfAP-M24 seemed to be present in the digestive vacuole also. However, western blotting of extracts from these parasites revealed that the YFP tag was cleaved at some point. The potential reason given for this cleavage was the action of one of the many endopeptidases present in the food vacuole acting on the YFP-tagged proteins following their transport there but the possibility that the fluorescence in the food vacuole was due to the tag alone being transported there after processing from the enzymes cannot be ruled out, especially in light of previous work. However, this study also reported aminopeptidase activity in digestive vacuole extracts corresponding to activities of the M1 and M24 aminopeptidases, therefore the exact location of these enzymes remains unclear. No PfAP-M18 activity was seen and no specific assay for PfAP-M17 could be carried out as PfAP-M1 also cleaves leucine-containing substrates (36).

The western blot of the extract from parasites expressing GFP-tagged PfAP-M17 showed only one protein of ~86 kDa when probed with anti-GFP antibody, confirming that the cytosolic location of the fluorescence is not due to cleaved GFP. This apparent molecular mass is slightly lower than the expected size of the GFP-tagged PfAP-M17 (95 kDa). Interestingly, this lower apparent molecular mass was also observed by Dalal *et al* (36) in experiments involving confirmation of expression of YFP-tagged aminopeptidases, and the authors suggested that this might be due to removal of an N-terminal region of the PfAP-M17 protein. This aminopeptidase contains an asparagine-rich region at its N-terminus. Such low-complexity regions are thought to be unnecessary for the functioning of the protein. This region was removed during studies on recombinant PfAP-M17 (described in more detail in section 4.2.3 and Figure 4.8) and did not affect the activity of the enzyme. The removal of a similar region of the protein in intact parasites would correspond to a reduction in molecular mass of ~10 kDa observed here and by others.

It is unclear why reducing the expression of the PfAP-M17 using an antisense vector was unsuccessful in this case. The expression of *P. falciparum* genes has previously been knocked down using this antisense method (56), including one encoding the other aminopeptidase, PfAP-M18 (159). The reduction of expression of this gene resulted in parasites with reduced aspartate aminopeptidase activity (by ~80-fold) and apparent morphological defects. However, this antisense method is not one whose use on malarial

parasites is very widespread, suggesting that it may not work for many genes. The mechanisms by which antisense strands reduce gene expression are not fully understood but suggestions include prevention of transcription by binding to the mRNA (68) and activation of ribonucleases by the double-stranded RNA (116). All mechanisms require access to the mRNA and the ability of the antisense strand to bind to the correct region of RNA in the cell. Therefore, factors like RNA secondary structure and endogenous cell nucleases could prevent successful binding and reduction of gene expression (35). It may be that knock-out technology is the only suitable method for examination of the effects of a lack of this gene product in parasites.

In this study, drug-cycling of parasites transfected with vectors designed to interrupt the *PfAP-M1* and *PfAP-M17* genes did not result in recombination with the chromosome, as indicated by PCR. A similar result was seen by Dalal *et al* when they attempted to knock-out the *P. falciparum* aminopeptidase genes encoding the M1, M17 and M24 enzymes. Cycling of parasites transfected with vectors designed to knock out these genes did not result in recombination, causing the authors to suggest that interfering with these genes may be detrimental to the parasites (36). However, appropriate controls would need to be carried out to confirm this theory.

In contrast, Dalal *et al* did successfully knock out the gene encoding PfAP-M18 and these parasites were capable of surviving in medium supplemented with isoleucine alone (36). The lack of necessity of this enzyme for parasite survival is supported by the results of inhibitor studies (159). While some compounds were relatively efficient at inhibiting the recombinant enzyme (e.g. K_i of 0.34 µM), none of them demonstrated any antimalarial activity up to a concentration of 100 µM. It was argued that factors like the need to cross many membranes could be affecting the inhibitor activity in parasites. Indeed, as already mentioned, the results of Teuscher *et al*'s antisense knockdown of PfAP-M18 conflicts with the ability to knock out this gene with no effect on parasites. They reported that a reduction in expression of this aminopeptidase resulted in decreased aspartate aminopeptidase activity and a corresponding effect on the growth and morphology of the transgenic parasites (159). Therefore, the importance of PfAP-M18 for *P. falciparum* remains unclear as a result of this conflicting data.

Overall, our knowledge of the expression of these aminopeptidases in *P. falciparum* is improving with new techniques, like the antisense method attempted here, helping to provide information about some of the enzymes. However, quite a lot remains to be discovered about this group of enzymes; especially which ones may be essential for the parasites. In particular, methods for investigation of the bestatin-sensitive aminopeptidases

(PfAP-M1 and PfAP-M17) need to be examined to determine the relative importance of these enzymes in digestion of host globin and for parasite growth and development in general.

Chapter 4

Recombinant Expression of
P. falciparum Aminopeptidases including
Purification and Functional Analysis of the M17
Aminopeptidase

4.1. INTRODUCTION

The previous chapter described the identification of four aminopeptidase genes in the *P. falciparum* genome and the confirmation of their expression in erythrocytic-stage parasites. Various aminopeptidase activities have been reported in *Plasmodium* (outlined in Chapter 1) but it remains unclear which one(s) of the four gene products is/are active in the parasite. The characterisation of each of these enzymes is needed to distinguish which, if any, are involved in haemoglobin degradation and therefore, might be potential targets for development of new antimalarials. The limited quantity of protein available for purification from *P. falciparum* parasites means that recombinant production is preferable, if possible, to produce sufficient quantities for biochemical characterisation and investigation of inhibitor susceptibility. A number of reports have documented the successful expression and purification of recombinant M17 aminopeptidases of various eukaryotic organisms, including a number of parasites (see Table 4.1) (71, 72, 74, 80, 84, 109, 118, 161). Therefore, an attempt to generate sufficient quantities of *P. falciparum* aminopeptidases for functional studies by recombinant expression was undertaken.

The M1 aminopeptidase (PfAP-M1) has previously been investigated by purification of this protein from parasite extract by a combination of HPLC and ammonium sulphate precipitation (3, 54). Other work on *P. falciparum* aminopeptidases has included the identification of an ~80-kDa aminopeptidase activity in crude cell extracts (34), the HPLC purification of an ~100-kDa aminopeptidase (167) and the partial-purification of the ~80-kDa activity (by affinity chromatography and gel-exclusion chromatography) yielding four bands with apparent molecular masses between 56 and 97 kDa, including one at ~66 kDa (60). All of the above activities were found to be active against alanine and/or leucine substrates, i.e. the suggested preferred substrates of M17 and M1 family aminopeptidases. Also, the activities were susceptible to bestatin, like most M1 and M17 family aminopeptidases. Therefore, while there are reasons to be interested in all four aminopeptidases, the production of recombinant PfAP-M1 and PfAP-M17 was concentrated on, as the previous studies suggested that one or both of these enzymes was most likely to contribute to the activity observed and, therefore, to be relevant to the antimalarial activity of bestatin (120, 168).

This chapter describes the amplification and cloning of the four *P. falciparum* aminopeptidase genes and their attempted expression in *E. coli* cells, using a number of different systems, and includes the alteration of various factors to optimise their expression. The purification of recombinant PfAP-M17 from *E. coli* and baculovirus-infected Sf9

insect cells and the functional analysis of this purified protein are also described. With the exception of a paper published while this thesis was being written (159), this is the first description of the successful purification and characterisation of a recombinant *P. falciparum* aminopeptidase.

4.2. RESULTS

4.2.1. Recombinant production of *P. falciparum* aminopeptidases

A number of obstacles to production of recombinant aminopeptidase were encountered. Therefore, a number of cloning and expression strategies (outlined in Table 4.2) were employed, the majority of these applying to PfAP-M17.

4.2.1.1. Generation of pQE-30-M17 using native gene sequence

The first strategy attempted was cloning into pQE-30, to produce an N-terminal His$_6$-fusion protein. Fragments of the expected size were amplified from genomic DNA for each of *PfAP-M1*, *PfAP-M17*, *PfAP-M18* and *PfAP-M24* genes using *Taq* DNA polymerase (shown in the previous chapter in Figure 3.2), incorporating *Bam*HI and *Sac*I restriction sites. Amplification of the genes was unsuccessful with the high-fidelity *PfuTurbo* DNA polymerase; therefore a *Taq/PfuTurbo* mixture (in a ratio of 25:1) was used to amplify *PfAP-M17* (Figure 4.1), as this has previously been reported to improve proofreading relative to *Taq* polymerase (30). This fragment was cloned into pQE-30, transforming into *E. coli* XL1-Blue cells and confirmed by PCR and digestion with *Bam*HI (Figure 4.2). Expression of recombinant protein was assessed by SDS-PAGE of induced-cell lysates of a putative transformant, followed by Western blotting with a monoclonal anti-His$_6$ antibody. No band of the expected size was obtained (data not shown). Sequencing of this clone revealed a base deletion that produced a frame shift resulting in a premature stop codon, as well as another base change. Sequencing of two further plasmids showed that each had also incorporated two mutations, different from each other and the first clone. This indicated that amplification of the genes with a high-fidelity polymerase was needed, as the proofreading ability of the polymerase mixture did not appear to be much better than that of *Taq* DNA polymerase alone. Examination of the primers showed that they were quite AT-rich at the 3'-end, (due in part to the high AT content of *P. falciparum* DNA, ~80%) and it was thought that re-designing less AT-rich primers might enable amplification of the desired DNA by *PfuTurbo*. However, as SDS-PAGE of induced *E. coli* cell lysates containing pQE-30-M17 constructs did not display the

53

TABLE 3.3. Summary of experiments on *P. falciparum* aminopeptidases using transgenic parasites

	PfAP-M1	PfAP-M17	PfAP-M18[d]
GFP-tagged protein (full-length)	-	Cytosol[c]	Cytosol and possibly parasitophorous vacuole
GFP-tagged protein (truncated)	-	No fluorescence - ED[b]	-
Over-expressor (full-length)	Could not be created[a]	Increased AAP and LAP activity Decreased susceptibility to bestatin[a]	Increased DAP activity
Over-expressor with native promoter (full-length and truncated)	-	ED[c]	-
Anti-sense (knock-down)	Impaired growth[b]	No antisense produced - ED[c]	Impaired growth
Knock-out	No integration – ED[bc]	No integration - ED[bc]	-

[a]Gardiner *et al*, 2006 (58)

[b]experiments carried out by Dr. Don Gardiner, QIMR, Brisbane, personal communication

[c]experiments carried out as part of this study

[d]Teuscher *et al*, 2007 (159)

AAP = alanine aminopeptidase, LAP = leucine aminopeptidase, DAP = aspartyl aminopeptidase

ED = experiment discontinued

- not determined

TABLE 4.1. Overview of approaches previously used to produce recombinant M17 leucine aminopeptidases of eukaryotic organisms

Organism	Vector	Fusion Tag / Location	Host	Active	Comments	Ref
Lycopersicon esculentum	pD540	None	*E. coli* DS957 (PepA deficient)	Yes	LAP-A. Hexamers formed	(71)
	pQE-11	His$_6$ / N-terminal	*E. coli* DS957 (PepA deficient)	Yes	LAP-A. Hexamers formed	(72)
	pQE-30	His$_6$ / N-terminal	*E. coli* (NS)	Yes	LAP-N. Hexamers formed. Unstable after freezing	(161)
Caenorhabditis elegans	pGEX-5X-3	GST / C-terminal	NS	NS		(84)
Coprinus cinereus	pET-21a	His$_6$ / C-terminal	*E. coli* BLR	Yes	Hexamers formed	(80)
Leishmania major	pET-15b	His$_6$ / N-terminal	*E. coli* BL21 (λDE3)	Yes		(118)
Leishmania amazonensis	pET-15b	His$_6$ / N-terminal	*E. coli* BL21 (λDE3)	Yes	Hexamers formed. Tag cleavage by thrombin did not affect activity	(118)
Leishmania donovani	pET-15b	His$_6$ / N-terminal	*E. coli* BL21 (λDE3)	Yes		(118)
Schistosoma mansoni	pBlueBac4.5	His$_6$ / C-terminal	Sf9 insect cells	Yes		(109)
Haemaphysalis longicornis	pGEX4T-3	GST / N-terminal	*E. coli* (NS)	Yes	Tag cleavage by thrombin did not affect activity	(74)

NS = not specified

expression of an induced band of any size, it was decided to try a different expression system.

4.2.1.2. Generation of MBP-fusion aminopeptidases using native gene sequences

The pMAL system, which produces *E. coli* maltose-binding protein (MBP) fusion proteins, has been suggested to aid in the production of high yields of soluble recombinant protein (85) and had proved quite successful in the production of good quantities of soluble *P. falciparum* proteins in our lab (49, 115). Therefore, the *PfAP-M1, PfAP-M17, PfAP-M18* and *PfAP-M24* genes were amplified with *PfuTurbo* DNA polymerase (Figure 4.3), incorporating *Bam*HI and *Hin*dIII, *Eco*RI and *Pst*I, *Bam*HI and *Pst*I and *Eco*RI and *Pst*I restriction site pairs, respectively, and were cloned into pMAL-c2x and confirmed by PCR (data not shown) and sequencing. The resulting plasmids were initially transformed into *E. coli* TB1 cells and SDS-PAGE of induced cell lysates demonstrated faint bands for PfAP-M17, PfAP-M17-18 and PfAP-M17-24 but none for PfAP-M1 (Figure 4.4). Similar results were observed for pMAL-c2x-M17 expressed in *E. coli* BL-21 (DE3) and ER2508 (not expressing endogenous MBP) cells. Western blotting of SDS-polyacrylamide gels, with anti-MBP antibody, of the four MBP-fusion aminopeptidase constructs showed that truncated and possibly degraded proteins were being produced (Figure 4.5, only pMAL-c2x-M17 in BL-21(DE3) pLysS shown). The production of truncates suggested that the low levels of expression might be due to translational stalling cause by the presence of so-called rare codons in *Plasmodium* genes, i.e. ones not commonly used by *E. coli* (7). In an attempt to improve the expression, the pMAL-c2x-M17 gene was transformed into *E. coli* BL-21 Rosetta® cells, containing seven tRNAs for rare codons on the pRARE plasmid. Unfortunately, no improvement in expression levels was observed (data not shown). It should be noted also that while there is a visible difference between the bands in the uninduced and induced lanes on the Coomassie Blue-stained polyacrylamide gel (Figure 4.5 A), there was no noticeable difference seen on the Western blot (Figure 4.5 B). This could mean that the induced band observed on the gel is not the desired MBP-tagged PfAP-M17 protein.

A number of conditions were changed in the hope of improving the production of the recombinant MBP-fusion aminopeptidases, including induction at lower levels of IPTG (0.5 mM) and induction for various times from 2 h up to 12 h. Induction of *E. coli* cells during the late log phase of growth ($A_{600} = 2.0$) was also carried out as this has previously been shown to increase expression (27, 55). However, none of these alterations succeeded in increased recombinant expression.

An attempt was made to express two MBP-fusions of truncates of PfAP-M1 (carried out by Trinity College undergraduate student Laura Staunton, under my supervision). Florent *et al* found two smaller, active forms of this enzyme, 96 and 68 kDa in size, when they partially-purified it from parasite extract (54), suggesting it to be the result of processing the larger (122 kDa) protein to a mature form. The positions of these were narrowed down using antibodies to two regions of the PfAP-M1 protein, corresponding to residues 142–154 and 194–206 (3). (Note: The *PfAP-M1* gene sequence quoted in the original paper is missing 90 bp at the N-terminus compared with that listed on www.plasmodb.org, therefore the protein in the subsequent paper is 30 amino acids shorter and the regions quoted are residues 111–123 and 163–175). Neither peptide was recognised by the first antibody (142–154) but both were recognised by the second (194–206). As it was impossible to know exactly where, between residues 154 and 194, the PfAP-M1(96) peptide began, a primer was designed that would amplify a DNA sequence beginning at position 460 (bp) of PfAP-M1 (Figure 4.6). This, with the original reverse primer used to amplify PfAP-M1 (MBP-M1R), gives a 2799 bp product, corresponding to a 933-amino acid protein with an estimated molecular mass of 108 kDa (not including the MBP-tag). Therefore, this protein is larger than the 96 kDa product purified from parasites but is still referred to with the original number, i.e. PfAP-M1(96), to avoid confusion. The shorter peptide, PfAP-M1(68), was produced by designing a reverse primer (MBP-M1(68)R) that would, in concert with the above-mentioned forward primer (MBP-M1(96)F), produce a protein with an estimated molecular mass of 68 kDa (not including the MBP-tag). This DNA sequence was 1785 bp in length and corresponds to a 595 amino acid protein.

Both gene truncates were amplified with *PfuTurbo*® DNA polymerase and using pMAL-c2x-M1 as a template (Figure 4.7). They were cloned into pMAL-c2x and confirmed by PCR, digestion with *Bam*HI and *Hind*III, and sequencing (data not shown). However, similar results to those seen with the full-length aminopeptidase were obtained when expression of recombinant protein was assessed. SDS-PAGE of lysates of TB1 cells transformed with pMAL-c2x-M1(68) and -M1(96) yielded no visible band or a very faint band of the expected size on Coomassie Blue-stained SDS-PAGE, respectively. As for the other MBP-fusion proteins, Western blotting of SDS polyacrylamide gels showed that truncates of the proteins were being produced. Again, transformation of the pMAL-c2x-M1(68) construct into Rosetta cells did not result in any improvement in expression (data not shown).

Construct[a]	Expression host	Band visible with Coomassie-staining?	Band detected by Western blot?	Comments
		TABLE 4.2. Plasmid constructs and expression hosts used in this study		
pQE-30-M17	*E. coli* XL1-Blue	No	No	mutated clones
pMAL-c2x-M1	*E. coli* K12 TB1	No	no – only truncated products[c]	
pMAL-c2x-M1(68)	*E. coli* K12 TB1	No	no – only truncated products	PfAP-M1 truncate (68 kDa)
	E. coli Rosetta	No	ND	
pMAL-c2x-M1(96)	*E. coli* K12 TB1	very faint	yes + truncated products	PfAP-M1 truncate (96 kDa)[d]
pMAL-c2x-M17	*E. coli* BL-21 (DE3)	Faint	yes + truncated products	
	E. coli ER2508	No	yes + truncated products	
	E. coli K12 TB1	Faint	yes + truncated products	
	E. coli Rosetta	Faint	yes + truncated products	
pMAL-c2x-M18	*E. coli* K12 TB1	Faint	yes + truncated products	
pMAL-c2x-M24	*E. coli* K12 TB1	Faint	yes + truncated products	
pET-16b-M17	*E. coli* DH5α	ND	ND	Transformants not obtained – experiment discontinued
pMAL-c2x-HisB-M17[b]	*E. coli* K12 TB1	No	ND	

Construct[a]	Expression host	Band visible with Coomassie-staining?	Band detected by Western blot?	Comments
pTrcHisB-M17[b]	*E. coli* BL-21 (DE3) pLysS	Yes	Yes	some soluble and active
	E. coli DH5α	Yes	Yes	some soluble
pTrcHisB-tM17[b]	*E. coli* BL-21 (DE3) pLysS	Yes	Yes	some soluble and active
	E. coli TOP 10	Yes	Yes	some soluble and active
pTrcHisB-tM17[b]	Baculovirus-infected *Sf*9 insect cells	Yes	ND	more active than *E. coli*-produced protein

TABLE 4.2. Plasmid constructs and expression hosts used in this study (continued)

[a]constructs were made using native gene sequences unless otherwise stated

[b]synthesised gene, codon-optimised for expression in *P. pastoris*

[c]possibly due to translational stalling

[d]actual predicted molecular mass is 108 kDa (see section 4.2.1.2)

ND = not determined

Figure 4.1. Amplification of *PfAP-M17* with *Taq/PfuTurbo*® DNA polymerase mixture. The labelled lines on the left refer to molecular size markers (kb) while the labelled arrow on the right indicates the amplified band, corresponding to the expected size of *PfAP-M17*, 1.8 kb.
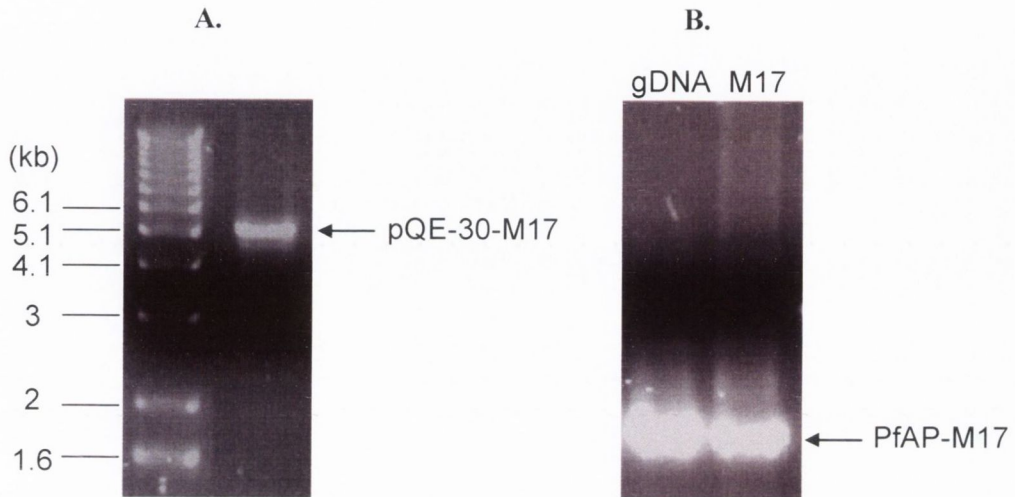
Figure 4.2. Analysis of pQE-30-M17 clones. **A.** Linearisation of pQE-30-M17, the putative transformant, by digestion with *Bam*HI. The arrow indicates the band obtained at the expected size of 5.3 kb. **B.** Amplification of the *PfAP-M17* gene from genomic DNA and pQE-30-M17 is shown in lanes labelled gDNA and M17, respectively. The arrow indicates the bands at the expected size of 1.8 kb. Labelled lines on the left indicate the molecular size markers.
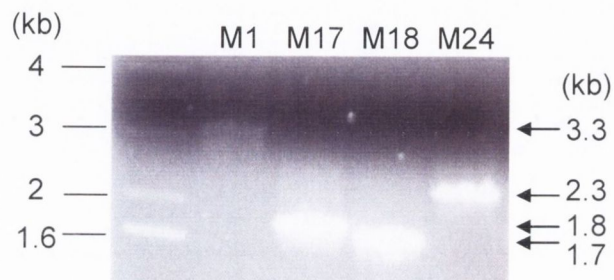
Figure 4.3. Amplification of the four MBP-tagged *P. falciparum* aminopeptidase genes. The labelled arrows on the right refer to the bands amplified at sizes corresponding to the expected sizes of *PfAP-M1*, *PfAP-M17*, *PfAP-M18* and *PfAP-M24* genes, 3.3, 1.8, 1.7 and 2.3 kb, respectively, in lanes labelled M1, M17, M18 and M24, respectively. The labelled lines on the left refer to molecular size markers (kb).
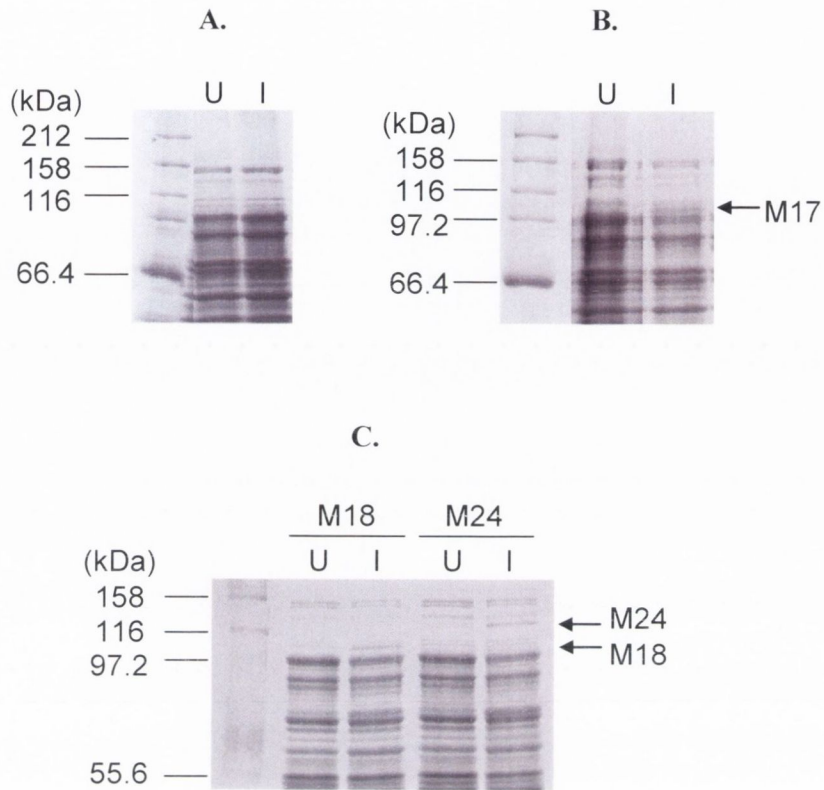
Figure 4.4. SDS-PAGE analysis of *E. coli* TB1 cell lysates containing MBP-fusion aminopeptidase constructs. Lanes contain lysates from cells transformed with **A.** pMAL-c2x-M1, **B.** pMAL-c2x-M17 and **C.** pMAL-c2x-M18 and pMAL-c2x-M24 (labelled M18 and M24, respectively). U refers to uninduced cells and I refers to lysates from cells induced with IPTG (1 mM). Labelled lines on the left refer to the molecular size markers while arrows labelled M17, M18 and M24 indicate bands of the expected sizes of MBP-PfAP-M17 (110.5 kDa), MBP-PfAP-M18 (105.5 kDa) and MBP-PfAP-M24 (127.5 kDa), respectively.
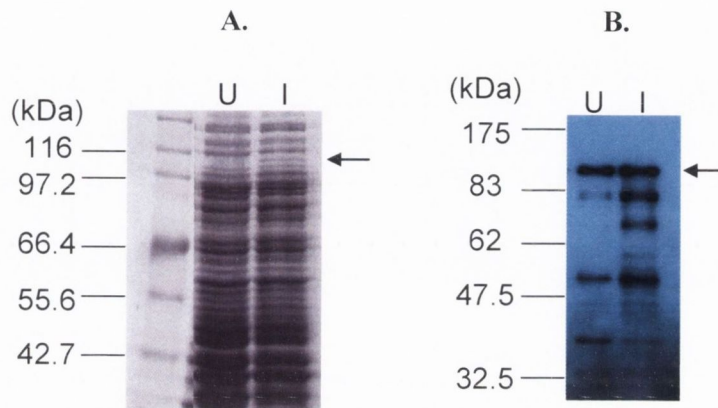
Figure 4.5. Analysis of proteins of *E. coli* BL-21(DE3) pLys containing pMAL-c2x-M17.
A. SDS-polyacrylamide gel of *E. coli* BL-21(DE3) pLys lysate. **B.** Western blot of SDS
polyacrylamide gel loaded similarly to that shown in **A** and probed with anti-MBP
antibody. U refers to uninduced cells and I to cells induced with IPTG (1 mM). The arrows
indicate a band running at the expected size of MBP-PfAP-M17 (110.5 kDa) while labelled
lines refer to molecular size markers.

4.2.1.3. Amplification of *PfAP-M17* for cloning using the pET system

The production of recombinant aminopeptidases as His$_6$-fusion proteins using the pET system was considered but not pursued fully. Primers were designed to amplify *PfAP-M17* and *PfAP-M18*, incorporating *Nde*I and *Bam*HI restriction sites. This was to enable cloning into either the pET-16b or pET-22b vectors, to produce C-terminal or N-terminal His$_6$-fusion proteins, respectively. The *PfAP-M17* gene was amplified (data not shown) from genomic DNA with *PfuTurbo*® DNA polymerase. The cloning of this gene into pET-16b was attempted, transforming into DH5α cells, but none of the putative transformants contained the insert and this experiment was discontinued.

4.2.2. Purification and activity of full-length His$_6$-PfAP-M17 produced in *E. coli* (using a yeast codon-optimised gene)

The pTrcHisB-M17 construct (in *E. coli* DH5α, TOP 10 and BL-21 (DE3) pLysS cells) was kindly provided by Prof. John Dalton. This consisted of the *PfAP-M17* gene, codon-optimised for expression in the yeast *P. pastoris* (purchased from Geneart), cloned into pTrcHisB, an N-terminal His$_6$-tag vector (Figure 4.8). Three asparagine residues (at positions 152, 515 and 546) had been changed to glutamines in this synthesised gene to remove putative glycosylation sites (NXT or NXS). However, it was found that the construct was not expressed in the *P. pastoris* system as it was designed to, but transformation into *E. coli* cells did result in expression (Figure 4.9) of a protein running at approximately the expected size. The band was smaller than the 71 kDa predicted for PfAP-M17 (plus the His$_6$-tag and the additional residues of the pTrcHisB vector) and there were some apparent degradation products observed in the induced lane of the gel. More protein was apparently produced by the *E. coli* strain BL-21 (DE3) pLysS than the DH5α or TOP 10 cells. It was initially thought that the protein was being expressed only as inclusion bodies (J. Dalton, personal communication). However, on investigation in our lab it was found that a certain amount of soluble protein was being produced in both *E. coli* cell types (Figure 4.10).

As it appeared that more soluble protein was expressed in BL-21 (DE3) pLysS cells, PfAP-M17 was purified from these cells. The initial purification, by BL-21 (DE3) pLysS cells, was carried out at room temperature by Ni^{2+} chelate fast protein liquid chromatography, using a 5-ml nickel-nitrilotriacetic acid-agarose Hi-Trap® column. SDS-PAGE analysis of fractions showed that quite a lot of protein remained on the column after washing, eluting up to a concentration of 250 mM imidazole, including a band of the expected size for PfAP-M17 (data not shown). At higher imidazole concentrations,

between 250 and 400 mM, only this band was seen, therefore these fractions were pooled and dialysed overnight into PBS. SDS-PAGE, followed by western blotting with INDIA HisProbe® confirmed the purification of a single His_6-tagged protein running at approximately the predicted size for His_6-PfAP-M17 (Figure 4.11). There was an apparent difference in size observed between the band identified on the Coomassie Blue-stained polyacrylamide gel (Figure 4.11 A) and that on the Western blot (Figure 4.11 B), although the use of a set of differently sized (pre-stained) markers for the Western blotting makes its difficult to direct compare the gel and the blot.

The aminopeptidase activity of purified PfAP-M17 was assessed by measuring the release of the fluorogenic leaving group, 7-amido-4-methyl-coumarin (AMC) from L-leucine-AMC. However, no activity was seen using PfAP-M17 at concentrations up to 20 µg/ml in assays. As it was anticipated that the aminopeptidase would require the presence of a metal ion for activity, the recombinant protein was tested in the presence of a range of divalent metal cations (Ca^{2+}, Co^{2+}, Cu^{2+}, Fe^{2+}, Mg^{2+}, Mn^{2+}, Ni^{2+} and Zn^{2+}) and a slight increase in fluorescence was observed in the presence of cobalt ions (data not shown). To establish that this was due to enzymic activity, increasing amounts of protein (10–100 µg) were incubated with Co^{2+} and a Co^{2+} only control was included. Increasing fluorescence was seen with increasing protein, while no activity was seen with Co^{2+} alone (Figure 4.12). As activity was seen only in the presence of Co^{2+}, all further assays were carried out using this metal co-factor. The specific activity was 1.9 nmol substrate/min/mg recombinant enzyme.

Due to the low activity of the purified PfAP-M17, its activity against a number of AMC substrates, namely alanine, threonine, tyrosine and valine, was assessed to establish if the enzyme would demonstrate better activity against another amino acid. However, no activity was observed (using protein at a concentration of 0.13 mg/ml) against the alanine or valine substrates and only relatively low levels of activity were seen against threonine and tyrosine substrates, with only 10% of the fluorescence of that seen with the leucine substrate (Figure 4.13). This was in contrast to the aminopeptidase activity observed using cytosolic extract (0.006 mg/ml), which demonstrated maximal activity against Ala-AMC. It appeared to have approximately twice as much activity against the Ala-AMC compared with the Leu-AMC but may actually be more since the maximum fluorescence was reached in this assay.

The ability of bestatin, a known inhibitor of M17-family aminopeptidases, to inhibit the activity of PfAP-M17 was assessed (data not shown) and it was found that 5 µM

A.

ATGAAATTAACAAAAGGCTGTGCCTATAAATATATTATTTTCACAGTGTTAATTTTAGCGAATATTCTTTATGATAATAAAAAAAGGTGCA
TGATTAAAAAAAATTTACGTATTAGTTCGTGCGGTATAATAAGTCGCTTGCTCAAATCTAATTCAAATTATAATAGTTTTAATAAGAATTA
TAATTTCACGTCTGCTATATCAGAATTACAATTTTCCAATTTTTGGAATTTAGATATTTTACAAAAGGATATATTTAGTAATATACATAAT
AACAAAAACAAGCCTCAATCATATATAATACATAAAAGACTAATGAGTGAGAAAGGAGATAATAATAATAATAATCACCAAAATAATAATG
GGAATGACAATAAGAAAAGATTAGGATCTGTTGTAAATAATGAAGAAAATACTTGTTCAGATAAAAGAATGAAACCTTTTGAAGAAGGTCA
TGGA**ATTACACAAGTTGATA**AGATGAATAACAACAGTGATCATTTACAACAAAATGGTGTTATGAATTTGAATAGTAATAATGTTGAAAAT
AATAATAATAACAATTCTGTTGTTGTTAAAAAGAACGAACCAAAAATACATTATAGGAAAGATTATAAACCAAGTGGATTTATAATTAATA
ATGTAACATTAAATATTAATATCCATGACAATGAAACTATTGTAAGATCTGTACTTGATATGGATATTAGTAAACACAATGTTGGTGAAGA
TTTAGTTTTTGATGGTGTTGGATTAAAAATTAATGAGATAAGTATTAATAATAAGAAATTAGTTGAAGGAGAAGAATATACCTACGATAAT
GAATTCTTAACTATATATTTTCAAAATTTGTACCAAAATCTAAATTTGCTTTTTCATCAGAAGTTATTATACATCCAGAAACAAATTATGCTC
TTACAGGTTTATATAAATCAAAAAAATATTATTGTTTCTCAATGTGAAGCTACCGGATTCCGTCGTATCACTTTTTTTTATTGACAGACCAGA
TATGATGGCAAAATATGACGTTACAGTAACTGCTGATAAAGAAAAATATCCTGTTTTATTAAGTAATGGTGATAAGGTGAATGAATTTGAA
ATACCAGGTGGTCGTCATGGAGCTAGATTTAATGATCCCCATTTAAAACCATGTTATTTATTTGCTGTTGTAGCTGGTGACCTTAAACATT
TAAGTGCTACATATATTACTAAATATACCAAAAAAAAAGTTGAATTATATGTATTTAGTGAGGAAAAATATGTATCTAAATTACAATGGGC
TTTAGAATGTCTTAAAAAATCGATGGCATTTGATGAAGATTATTTTGGATTGGAATATGATTTGTCTCGTTTAAATTTAGTTGCTGTTTCT
GACTTTAATGTTGGTGCTATGGAAAATAAAGGATTAAATATATTTAATGCTAATTCTTTATTAGCATCCAAAAAAAATTCAATTGATTTTT
CATATGCAAGAATTCTAACGGTCGTAGGACATGAATATTTCCATAATTATACAGGAAATAGAGTTACTCTTAGAGATTGGTTTCAGTTAAC
ATTAAAAGAAGGTCTAACAGTACATAGAGAAAATTTGTTTTCAGAAGAAATGACGAAGACCGTAACTACTCGTTTATCTCATGTAGATTTA
TTAAGAAGTGTTCAATTTTTAGAAGATTCCTCACCATTATCACACCCTATTAGACCAGAATCTTATGTTAGTATGGAAACTTTTATACTA
CTACTGTTTATGATAAAGGTAGTGAAGTTATGAGAATGTATCTTACTATATTAGGTGAAGAATATTATAAAAAAGGTTTTGATATTTATAT
TAAGAAAAATGATGGAAATACTGCTACTTGTGAAGATTTTAATTATGCTATGGAACAAGCATATAAAATGAAAAAAGCAGACAATTCAGCT
AACCTAAACCAATATTTATTATGGTTCTCACAAAGTGGTACTCCACATGTTAGTTTTAAATATAACTACGATGCTGAAAAGAAACAATATA
GTATACATGTTAATCAATATACCAAACCAGATGAAAACCAAAAAGAAAAGAAACCTTTATTTATTCCTATAAGTGTTGGCTTAATTAATCC
AGAAAACGGTAAAGAAATGATATCACAAACCACCTTAGAATTAACAAAAGAAAGTGATACATTTGTATTTAATAATATAGCTGTAAAACCA
ATACCATCCTTATTCAGAGGATTTAGTGCA**CAGTATATATTGAGGATAACTTAACA**GATGAAGAACGTATATTATTATTGAAATATGATA
GTGATGCTTTTGTTCGTTATAACTCATGTACCAATATATATATGAAACAAATATTAATGAATTATAATGAATTCTTAAAAGCTAAAAATGA
AAAATTAGAAAGTTTTAATCTTACACCAGTAAATGCACAATTTATAGATGCTATAAAATATTTATTAGAAGACCCACATGCTGATGCAGGA
TTTAAATCATATATAGTATCCTTACCACAAGATAGATATATAATAAACTTTGTAAGCAATTTAGATACAGACGTATTAGCTGATACTAAAG
AATATATATATAAACAAATCGGAGATAAATTAAATGATGTATATTATAAAATGTTTAAAAGTTTAGAAGCAAAAGCTGATGATTTAACATA
TTTTAATGATGAATCACATGTAGATTTGATCAAATGAATATGAGAACATTAAGAAATACATTATTATCATTATTAAGTAAAGCTCAATAT
CCAAATATATTTAAATGAAATTATTGAACATTCCAAATCACCATATCCATCCAATTGGCTAACTAGTTTATCAGTTTCAGCATATTTCGATA
AATATTTTGAACTTTATGATAAAACTTATAAAACTTATCAAAAGATGATGAATTATTGTTACAAGAATGGTTAAAGACTGTATCAAGATCTGA
TCGTAAAGATATATATGAAATACTTAAAAAAATTAGAAAATGAAGTTTTGAAAGATAGTAAAAATCCAAATGATATTGAGCAGTATATCTT
CCATTTACAAATAATTTAAGAAGATTCCATGATATATCAGGAAAAGGGTATAAATTAATTGCTGAAGTTATTACAAAAACCGATAAATTTA
ATCCTATGGTTGCAACACAATTATGTGAACCATTTAAATTATGGAATAAACTAGATACAAAAAGACAAGAATTAATGCTTAACGAAATGAA
CACAATGTTACAAGAACCAAACATATCAAATAACTTAAAGGAATATTTATTAA**GATTAACAAATAAATTATAA**

B.
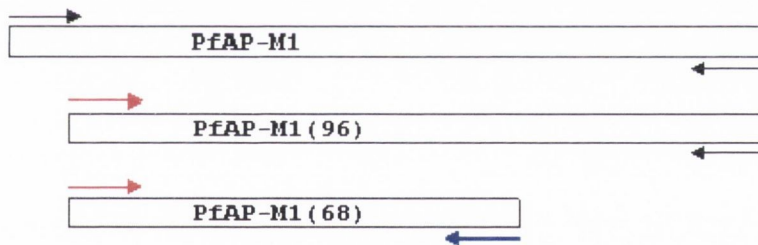
Figure 4.6. Production of truncated forms of *PfAP-M1*. **A.** DNA coding sequence of PfAP-M1 showing positions of primers used to amplify *PfAP-M1*, *PfAP-M1(96)* and *PfAP-M1(68)* for cloning into pMAL-c2x. The points of annealing of the primer pair used to amplify the full-length *PfAP-M1* gene (MBP-M1F and MBP-M1R) are highlighted in (black) bold. Those for the forward primer, MBP-M1(96)F, used (with MBP-M1R) to amplify the *PfAP-M1(96)* gene truncate and for the reverse primer, MBP-M1(68)R, used (with MBP-M1(96)F) to amplify the *PfAP-M1(68)* gene truncate are shown in red and blue, respectively. Arrows show the direction of PCR amplification. **B.** Schematic representation of details described in A.
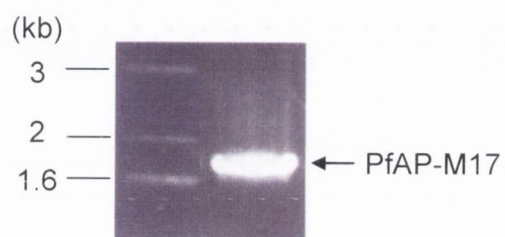
Figure 4.7. Amplification of the truncated forms of *PfAP-M1* with *PfuTurbo*® DNA polymerase mixture. The labelled lines on the left refer to molecular size markers (kb) while the labelled arrows on the right indicate the bands at the expected sizes for *PfAP-M1(68)* and *PfAP-M1(96)*, 1.8 and 2.8 kb, respectively.

```
PfAP-M17        --------------------------------MYFSSLCKFLPISEKEKIYLNI
pTrcHisB-M17    MGGSHHHHHHGMASMTGGQQMGRDLYDDDDKDPYFSSLCKFLPISEKEKIYLNI
                                               *********************
                              EK


VKKRFCKSNIYYNNNNNNIINYNKRGLKFYPFCNNLKKNINFVNINNKKGINFHSINKERKMASEVPQ
VKKRFCKSNIYYNNNNNNIINYNKRGLKFYPFCNNLKKNINFVNINNKKGINFHSINKERKMASEVPQ
*********************************************************** ********
                                                           83


VVSLDPTSIPIEYNTPIHDIKVQVYDIKGGCNVEEGLTIFLVNNPGKENGPVKISSKVNDKNVSEFLK
VVSLDPTSIPIEYNTPIHDIKVQVYDIKGGCNVEEGLTIFLVNNPGKENGPVKISSKVNDKQVSEFLK
***********************************************************. ******
                                                           152


DENMEKFNVKLGTSKHFYMFNDNKNSVAVGYVGCGSVADLSEADMKRVVLSLVTMLHDNKLSKLTVVF
DENMEKFNVKLGTSKHFYMFNDNKNSVAVGYVGCGSVADLSEADMKRVVLSLVTMLHDNKLSKLTVVF
******************************************************************


EINVDKNLFRFFLETLFYEYMTDERFKSTDKNVNMEYIKHLGVYINNADTYKEEVEKARVYYFGTYYA
EINVDKNLFRFFLETLFYEYMTDERFKSTDKNVNMEYIKHLGVYINNADTYKEEVEKARVYYFGTYYA
******************************************************************


SQLIAAPSNYCNPVSLSNAAVELAQKLNLEYKILGVKELEELKMGAYLSVGKGSMYPNKFIHLTYKSK
SQLIAAPSNYCNPVSLSNAAVELAQKLNLEYKILGVKELEELKMGAYLSVGKGSMYPNKFIHLTYKSK
******************************************************************


GDVKKKIALVGKGITFDSGGYNLKAAPGSMIDLMKFDMSGCAAVLGCAYCVGTLKPENVEIHFLSAVC
GDVKKKIALVGKGITFDSGGYNLKAAPGSMIDLMKFDMSGCAAVLGCAYCVGTLKPENVEIHFLSAVC
******************************************************************


ENMVSKNSYRPGDIITASNGKTIEVGNTDAEGRLTLADALVYAEKLGVDYIVDIATLTGAMLYSLGTS
ENMVSKNSYRPGDIITASNGKTIEVGNTDAEGRLTLADALVYAEKLGVDYIVDIATLTGAMLYSLGTS
******************************************************************


YAGVFGNNEELINKILNSSKTSNEPVWWLPIINEYRATLNSKYADINNISSSVKASSIVASLFLKEFV
YAGVFGNNEELINKILQSSKTSNEPVWWLPIINEYRATLNSKYADINQISSSVKASSIVASLFLKEFV
****************.**********************************.******************
                515                                   546
QNTAWAHIDIAGVSWNFKARKPKGFGVRLLTEFVLNDAL 605
QNTAWAHIDIAGVSWNFKARKPKGFGVRLLTEFVLNDAL 637
**************************************
```

Figure 4.8. Alignment of PfAP-M17 sequence with the synthesised gene, codon-optimised for expression in *P. pastoris*, cloned into pTrcHisB. The symbols * and : indicate identical and conserved residues, respectively. The hexahistidine tag (HHHHHH) is underlined. The three asparagine (N) residues that were changed to glutamines (Q), at positions 152, 515, 546, are shown in red. The start of the truncated form of the enzyme, at residue 83 (K) is outlined. The point of cleavage by enterokinase (EK), following the sequence DDDDK, is indicated by a red arrow.

Figure 4.9. SDS-PAGE analysis of *E. coli* cells transformed with pTrcHisB-M17. Lanes labelled DH5α and BL-21 indicate lysates from *E. coli* DH5α and BL-21(DE3) pLysS cells, respectively. U refers to uninduced cells and I to cells induced with IPTG (1 mM). The arrow indicates the band observed in both induced lanes, running lower than the predicted size of 71 kDa, and the labelled lines refer to molecular size markers.
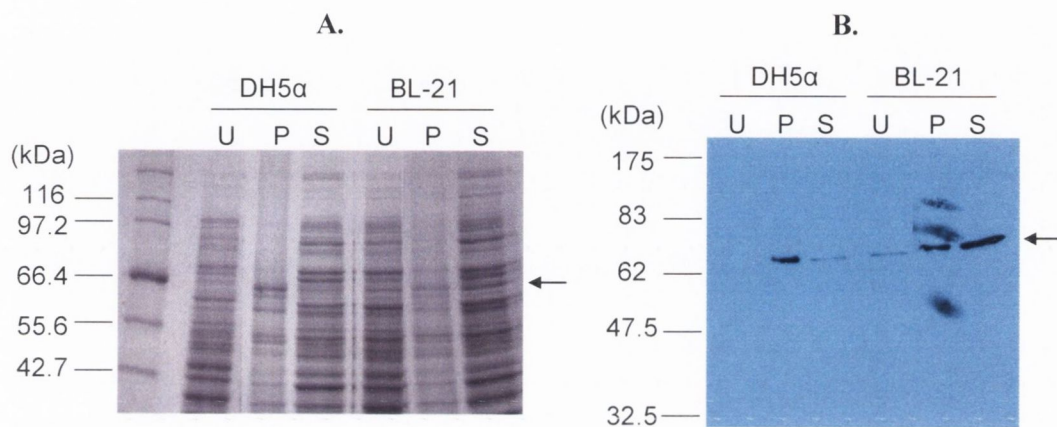
Figure 4.10. Analysis of *E. coli* DH5α and BL-21(DE3) pLysS cells transformed with pTrcHisB-M17. **A.** SDS polyacrylamide gel of cell lysates. **B.** Western blot of SDS polyacrylamide gel loaded similarly to that shown in **A** and probed with anti-MBP antibody. Lanes labelled DH5α and BL-21 indicate lysates from *E. coli* DH5α and BL-21(DE3) pLysS cells, respectively. U refers to lysate from uninduced cells, while P refers to the insoluble fraction (pellet) and S the soluble fraction (supernatant) of lysates from cells induced with IPTG (1 mM). The arrow indicates the band observed in both pellet and supernatant fractions, running a bit lower than the expected size of 71 kDa and the labelled lines refer to molecular size markers.

bestatin was sufficient to completely abolish the recombinant leucine aminopeptidase activity.

To determine if the low levels of enzyme activity were due to loss of activity during the purification process, the aminopeptidase activity of the BL-21 (DE3) pLysS lysate containing the construct was assessed. The results of this experiment indicated that recombinant PfAP-M17 was not very active in the bacterial lysate, even before the purification process had begun. Aminopeptidase activity was detected, as *E. coli* contains aminopeptidases of its own, but lysates with and without the construct demonstrated identical profiles against the range of substrates (data not shown) with the activity of the *E. coli* aminopeptidases presumably masking any PfAP-M17 activity.

Subsequent Ni^{2+}-chelate chromatography purification of the PfAP-M17 protein was carried out at 4 °C, using a 1-ml nickel-agarose resin column and included dialysis of the protein into a solution containing a trace amount of $ZnCl_2$. These alterations produced a more active protein that did demonstrate a base level of activity before incubation with Co^{2+}. This recombinant PfAP-M17 was found to have a K_M of 12.3 ± 1.7 µM but a relatively low k_{cat}/K_M of 98/M/s. The enzyme was quite unstable, prone to precipitation and lost activity over time when stored at 4 °C, while frozen aliquots were found to lose all activity.

4.2.2.1. Generation of MBP-HisB-PfAP-M17

One possible cause considered for the low activity was that some of the protein was misfolding while being produced in the *E. coli* cells. To attempt improvement of this, the yeast-codon-optimised gene was subcloned into the pMAL-c2x vector as this vector has previously been shown to promote correct folding of proteins (85). However, no band was visible when induced cells were analysed by Coomassie-stained SDS-PAGE (not shown) and, therefore, this avenue was not pursued further.

4.2.3. Purification and activity of truncated His_6-PfAP-M17 (tPfAP-M17) produced in *E. coli* (using a yeast codon-optimised gene)

A truncated form of PfAP-M17, termed tPfAP-M17, was kindly provided (in *E. coli* TOP 10 cells) by Prof. John Dalton. This construct consisted of an N-terminal truncate, lacking the first 82 residues, of the yeast-codon-optimised gene described above, cloned into pTrcHisB (Figure 4.8). This construct (pTrcHisB-tM17) was transformed into BL-21 (DE3) pLysS cells as this strain had previously been seen to produce more of the full-length protein. SDS-PAGE analysis of lysates containing the full-length and truncated

constructs (pTrcHisB-M17 and pTrcHisB-tM17, respectively) indicated that the latter was produced in a much greater quantity than the former (Figure 4.14). Investigation of the amount of soluble protein being produced showed that a large amount was present in the soluble fraction, especially in comparison to the full-length protein (Figure 4.15). The truncated recombinant protein was purified from BL-21 (DE3) pLysS cells at 4 °C, by Ni^{2+} chelate chromatography using a 1-ml column (Figure 4.16). This recombinant enzyme had similar activity to the full-length protein with a K_M of 7.6 ± 0.4 µM and a k_{cat}/K_M of 169 /M/s.

4.2.3.1. Attempted cleavage of the His_6-tag

One cause considered for the low activity associated with this recombinant protein was that the presence of the His_6-tag might be interfering with the possible hexamerisation of the enzyme, known to be necessary for the activity of most M17 aminopeptidases. As the pTrcHisB vector contains an enterokinase cleavage site (cleaves after lysine of Asp-Asp-Asp-Asp-Lys, Figure 4.8), removal of the tag with this enzyme was attempted. The purified enzyme (7, 20 or 30 µg) was incubated with 1 unit of enterokinase at different temperatures (4, 23 and 37 °C), with samples taken over a range of times (from 30 min up to 21 h), in an effort to optimise the cleavage of the tag. However, no change in molecular mass was apparent from SDS-PAGE analysis and no increase in aminopeptidase activity was observed from samples treated with enterokinase (data not shown). Cleavage of the control protein, supplied with the enterokinase was successful, confirming that the enzyme had not been de-activated.

4.2.3.2. Investigation of the stability of tPfAP-M17

A number of storage conditions were assessed for their ability to improve the stability of the recombinant tPfAP-M17, purified from *E. coli*, including storage in DMSO, glucose and glycerol at 4, -20 and -70 °C (Figure 4.17). The activity of the enzyme was monitored over a 12-day period, after which time the activity of the control (protein stored at 4 °C in 50 mM Tris-HCl, pH 8.0) had completely reduced to zero from 43 mFu/sec (Figure 4.17A). Overall, the activity of all samples of tPfAP-M17 was reduced by at least 50% activity after 12 days. Samples stored at -70 °C initially seemed to have retained more activity than those at -20 °C but there was no notable difference after 12 days. Protein stored in 50% glycerol demonstrated no activity at any point. It did not seem that storage of the tPfAP-M17 in any of the conditions tested would enable its long-term storage and stability.
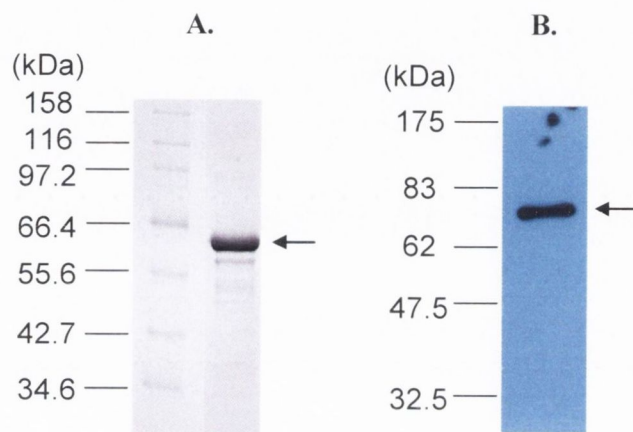
Figure 4.11. Analysis of recombinant PfAP-M17 purified from *E. coli* BL-21(DE3) pLysS cells. Labelled lines refer to molecular size markers. **A.** SDS polyacrylamide gel of purified His_6-PfAP-M17. The arrow indicates the band running a bit lower than the predicted size of 71 kDa. **B.** Western blot of SDS polyacrylamide gel probed with INDIA HisProbe®. The arrow indicates the band running at approximately the predicted size.
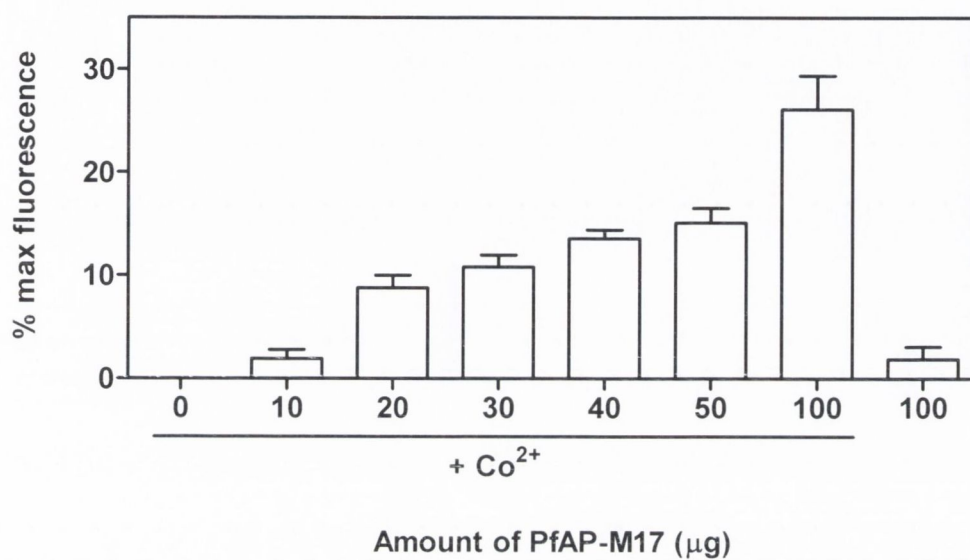
Figure 4.12. Increased activity of recombinant PfAP-M17 in the presence of Co^{2+} ions. The numbers 0 to 100 refer to the amount of PfAP-M17 (μg) added in the presence of 0.5 mM $CoCl_2$ (+ Co^{2+}). The bar on the right refers to the reaction not containing any Co^{2+} ions. Activity is shown as a percentage of fluorescence where the maximum of 999 is designated 100% and 0% activity is equal to the fluorescence of the blank.

A.

B.
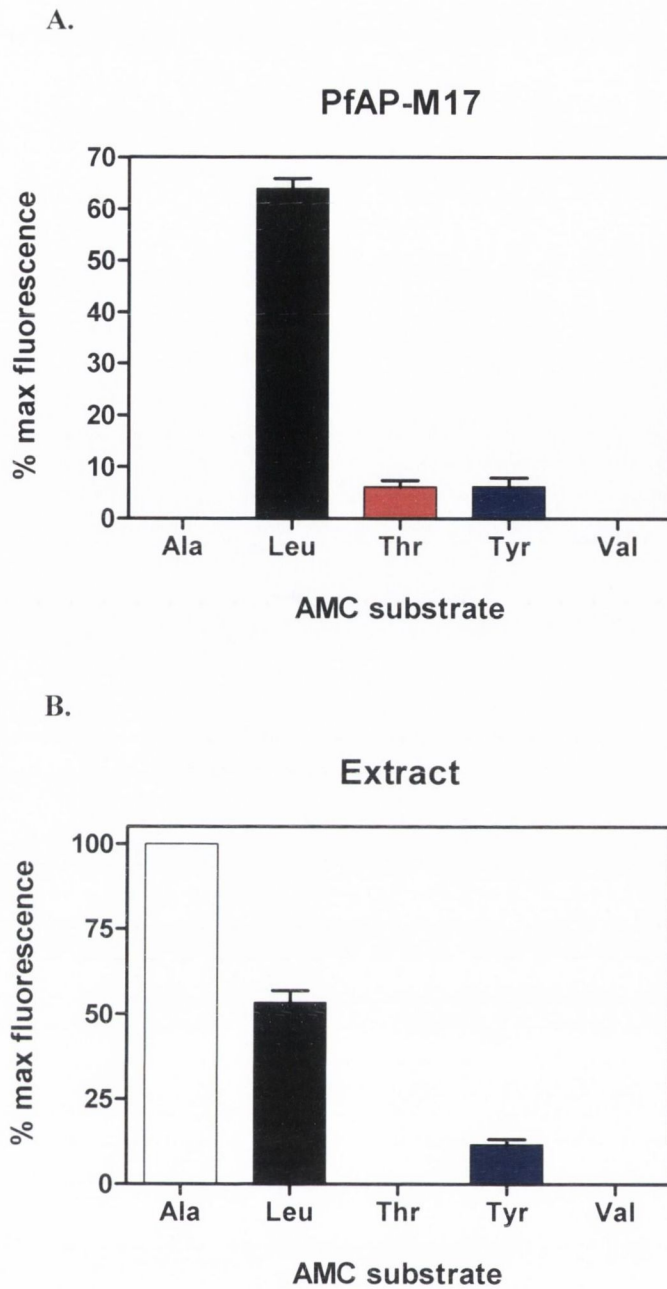
Figure 4.13. Substrate preference of *P. falciparum* M17 aminopeptidase and extract. **A.** Recombinant PfAP-M17 (0.13 mg/ml), purified from *E. coli* and **B.** *P. falciparum* cytosolic extract (0.006 mg/ml) were assayed for their activity against different AMC substrates. Ala, Leu, Thr, Tyr and Val refer to alanine, leucine, threonine, tyrosine and valine AMC substrates, respectively. Activity is shown as a percentage of fluorescence with the maximum of 999 designated as 100% and the fluorescence of the blank equal to 0%.

4.2.4. Purification and characterisation of truncated His$_6$-PfAP-M17 (tPfAP-M17) produced in baculovirus-infected *Sf9* insect cells (using a yeast codon-optimised gene)

4.2.4.1. Purification and activity of tPfAP-M17

Baculovirus-infected *Sf9* (*Spodoptera frugiperda*) insect cells carrying this synthetic, codon-optimised, truncated *PfAP-M17* gene sequence (cloned into the C-terminal His$_6$-tag pENTR vector) were purchased from the SRC Protein Expression Facility, Queensland, Australia. These cells were lysed by freeze-thaw and recombinant tPfAP-M17 was purified by Ni^{2+}-chelate chromatography at 4 °C. Analysis by SDS-PAGE demonstrated a single band running slightly below the expected size of 61.6 kDa (Figure 4.18). It can be seen that while a certain amount of protein was lost in the insoluble fraction a reasonable amount was found in the soluble fraction, enabling the purification of the soluble recombinant protein. The protein was assayed for activity against Leu-AMC in the presence of CoCl$_2$ and had a similar K_M to the other recombinant proteins of 9.9 ±1.1 µM but a much higher catalytic efficiency with a k_{cat}/K_M of 3,669/M/s.

4.2.4.2. Analysis of quaternary structure of tPfAP-M17

The purified tPfAP-M17 protein solution was analysed by high performance liquid chromatography (HPLC) gel filtration (Figure 4.19). Fractions (80 µl) were collected every two minutes and analysed for leucine aminopeptidase activity, following incubation in 0.5 mM CoCl$_2$. Two major peaks of absorbance were observed for the recombinant tPfAP-M17 (data not shown), eluting at 22 (not shown) and 28.5 min. The first of these was the larger, corresponded to a molecular mass much larger than that of the molecular mass of apoferritin (440 kDa), the highest standard run, and did not demonstrate any LAP activity. The second peak corresponded quite well to fractions that exhibited activity against Leu-AMC and protein eluting at this point was determined to be ~393 kDa in size, close to the expected size of a tPfAP-M17 hexamer (370 kDa). No activity was seen in fractions corresponding to the molecular mass of the tPfAP-M17 monomer (61.6 kDa). There was a slight difference in the positions of the protein elution and of the LAP activity profile and between the peaks of the two profiles. It is possible that this is due to the delay between the measuring of the absorbance of the sample in the column and its collection after passing through the column. In addition, as the peak of the LAP activity is likely to lie between the

60

28 and 30 min time points, more frequent collection of fractions would have given a better indication of the exact overlap between the two profiles.

4.2.4.3. Effect of divalent metal ions on tPfAP-M17 leucine aminopeptidase activity

Recombinant tPfAP-M17 was pre-incubated with a series of divalent metal ions (Table 4.3). The leucine aminopeptidase activity of the enzyme was activated by most of the metal ions tested. Co^{2+} ions were most preferred, followed by Mn^{2+} and Ni^{2+} while Cu^{2+} ions (1.0 mM) inhibited enzyme activity.

The recombinant tPfAP-M17 was incubated with 1,10-phenanthroline in an attempt to produce the metal-depleted enzyme (apo-enzyme). Incubation and subsequent dialysis into PBS resulted in a reduction of activity to 8% of that of the control protein incubated in the absence of 1,10-phenanthroline, i.e. a rate of only 26 mFu/sec compared the control rate of 337 mFu/sec. This was also re-activated by most of the cations tested (at 0.1 mM), showing a similar order of preference, except in this instance Zn^{2+} ions were seen to be the next best activators after Co^{2+}.

Titration of Co^{2+} in an assay with the tPfAP-M17 holoenzyme indicated that activity was maximally enhanced at a concentration of 2.5 mM. Inhibitory effects were not seen in the range tested, up to a concentration of 10 mM (data not shown).

4.2.4.4. Substrate preference of purified enzyme

The activity of tPfAP-M17 (1.34 µg/ml) against a number of AMC substrates was assessed (Figure 4.20). As seen for the full-length protein produced in *E. coli* it demonstrated maximal activity against the leucine substrate with a rate of 843 mFu/sec. It also had some activity, 187 mfu/sec, against the phenylalanine substrate but negligible activity against the alanine, aspartate, glutamate and proline substrates, with rates of 4, 0, 2 and 6 mFu/sec, respectively.

4.2.4.5. Investigation of temperature and pH optima of tPfAP-M17

The temperature dependence and stability of tPfAP-M17 were determined by pre-incubation of recombinant enzyme with $CoCl_2$ at various temperatures before assaying activity against Leu-AMC (Figure 4.21). The activity of the enzyme was found to increase with increasing temperature, from 25 °C up to 45 °C, before slightly decreasing at 50 °C (A). The enzyme was found to be stable after incubation up to 60 °C but not up to 80 °C (B).

61
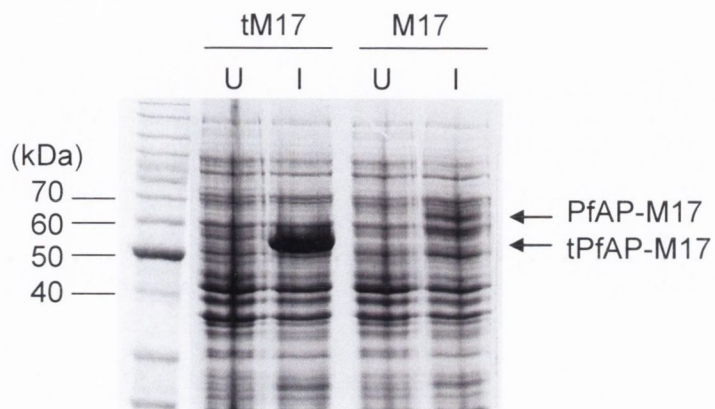
Figure 4.14. SDS-PAGE analysis of *E. coli* BL-21(DE3)pLysS cells transformed with pTrcHisB-tM17 and pTrcHisB-M17. Lanes labelled tM17 and M17 refer to lysates from cells transformed with the pTrcHisB-tM17 and pTrcHisB-M17 constructs, respectively. U refers to uninduced cells and I to cells induced with IPTG (1 mM). Arrows labelled PfAP-M17 and tPfAP-M17 indicate the bands observed in induced-cell lanes, running a bit lower than the expected sizes for full-length (71 kDa) and truncated PfAP-M17 (62 kDa), respectively. The labelled lines on the left refer to molecular size markers.
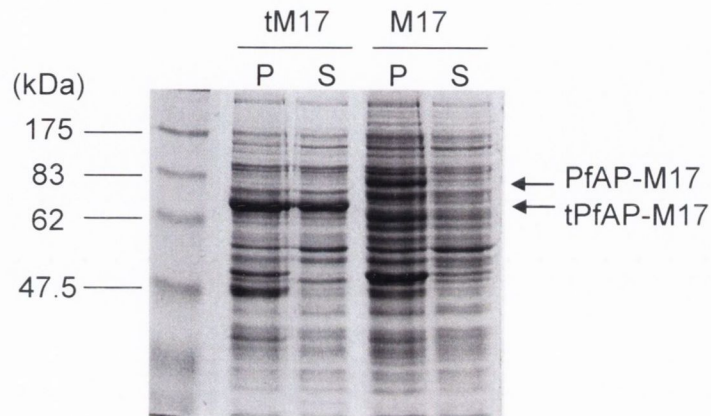
Figure 4.15. SDS-PAGE analysis of fractions of *E. coli* BL-21(DE3)pLysS cells transformed with pTrcHisB-tM17 and pTrcHisB-M17. Lanes labelled tM17 and M17 refer to lysates from cells transformed with the pTrcHisB-tM17 and pTrcHisB-M17 constructs, respectively. P refers to the insoluble fraction (pellet) and S the soluble fraction (supernatant) of lysates from cells induced with IPTG (1 mM). Arrows labelled PfAP-M17 and tPfAP-M17 indicate the bands observed in induced lanes, running a bit lower than the expected sizes for full-length (71 kDa) and truncated PfAP-M17 (62 kDa), respectively. The labelled lines on the left refer to molecular size markers.
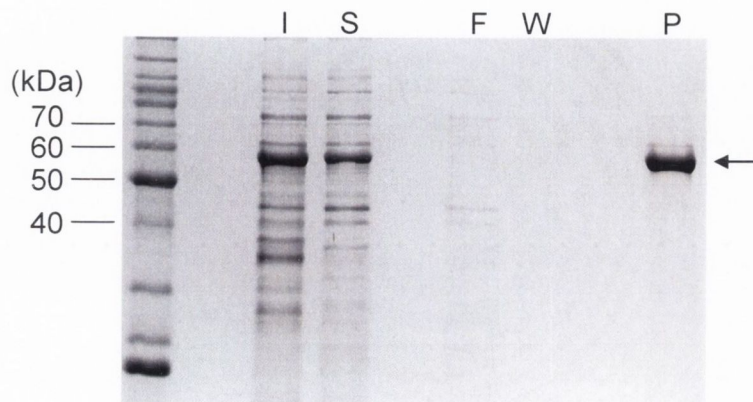
Figure 4.16. Purification of recombinant tPfAP-M17 from *E. coli* BL-21 (DE3) pLysS cells. Lanes labelled I, S, F, W and P indicate those containing the insoluble fraction, soluble fraction, flow through from column, wash from column and purified tPfAP-M17, respectively (10 µl volumes). Labelled lines on the left refer to molecular size markers (kDa) while the arrow on the right indicates the band (tPfAP-M17) running a bit lower the expected size of 61.5 kDa.
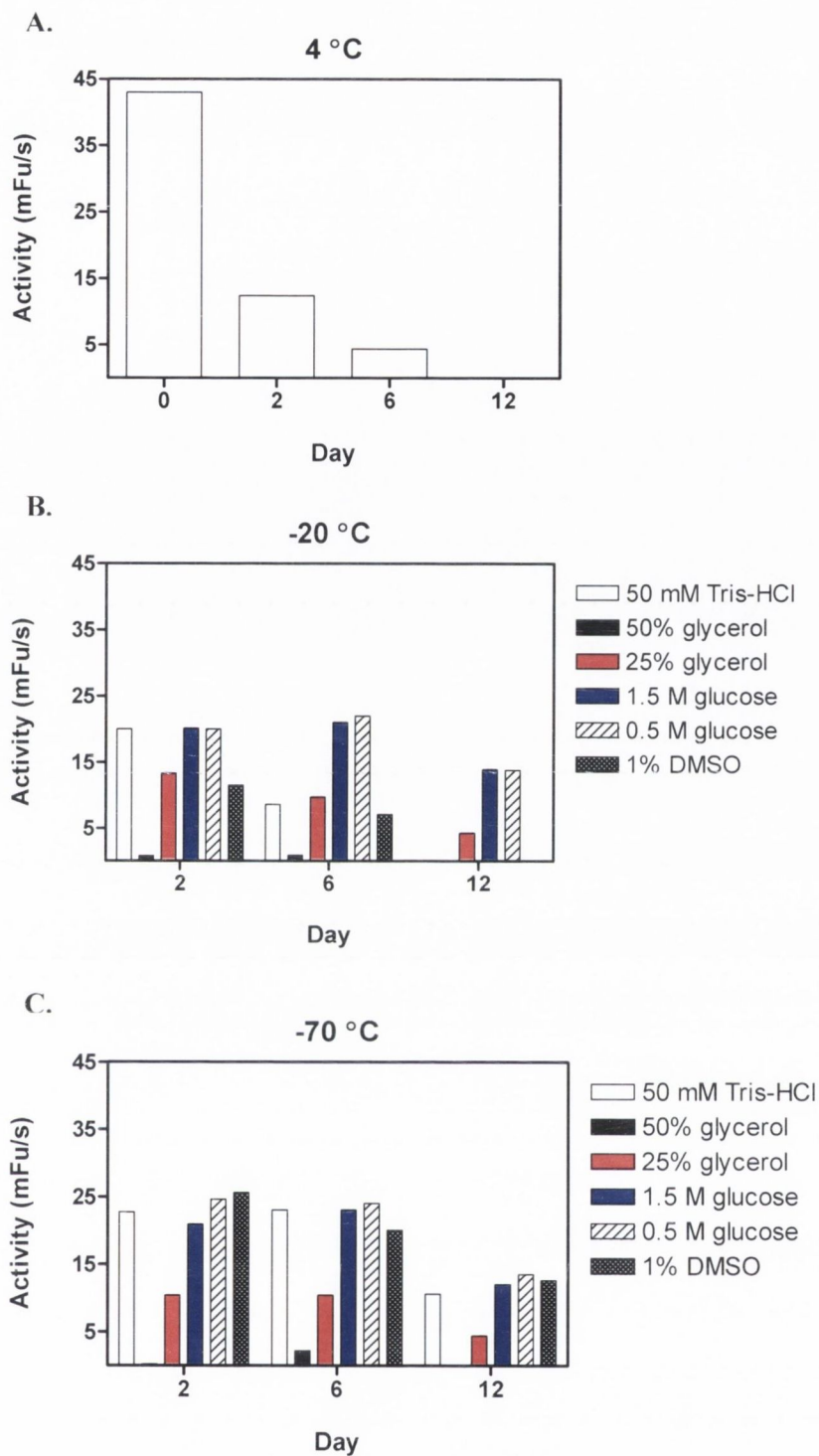
Figure. 4.17. Investigation of the effect of different storage conditions on the stability of recombinant tPfAP-M17 purified from *E. coli*. Aliquots of tPfAP-M17 were stored in **A.** Tris-HCl (50 mM, pH 8.0) at 4 °C or in Tris-HCl (50 mM, pH 8.0), glycerol (50% or 25%(v/v)), glucose (1.5 M or 0.5 M) or DMSO (1%(v/v)) at **B.** -20 °C or **C.** -70 °C for 2, 6 and 12 days before assaying for leucine aminopeptidase activity. (mFu/s = millifluorescence units per second).
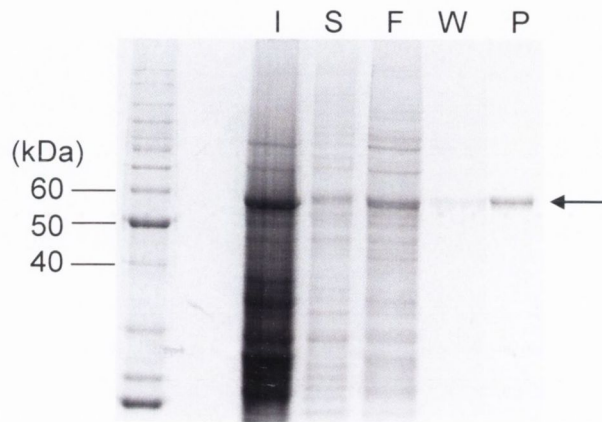
Figure 4.18. Purification of recombinant tPfAP-M17 from baculovirus-infected *Sf9* cells. Lanes labelled I, S, F, W and P indicate those containing the insoluble fraction, soluble fraction, flow through from column, wash from column and purified tPfAP-M17 (diluted 1:5), respectively (10 µl volumes). Labelled lines on the left refer to molecular size markers (kDa) while the arrow on the right indicates the band (tPfAP-M17) running a bit lower the expected size of 61.5 kDa.

A.

B.
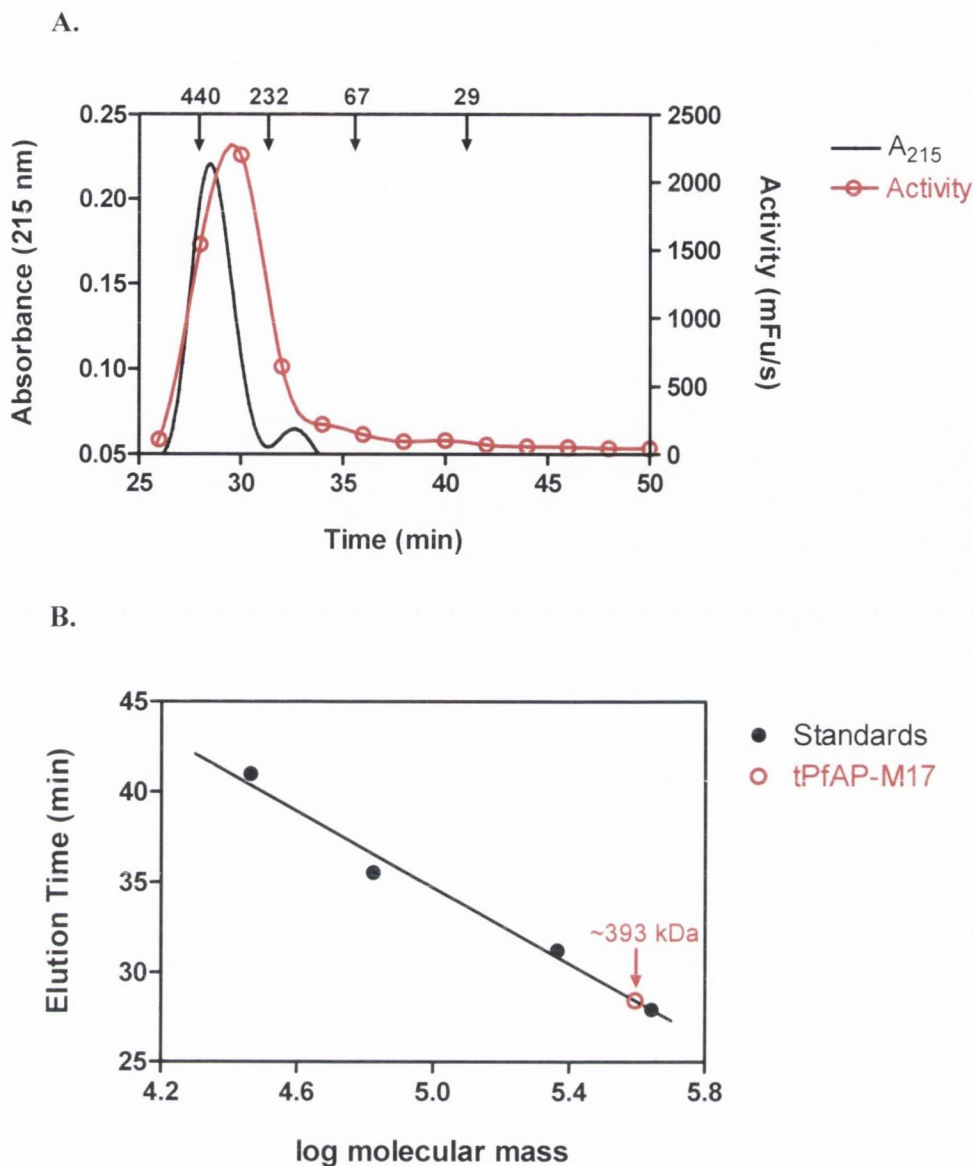
Figure 4.19. HPLC gel filtration of recombinant tPfAP-M17. **A.** The elution profile of the tPfAP-M17 protein is shown in black (left axis, A_{215}), while the LAP activity of fractions collected from the column is shown in red (right axis, mFu/s = millifluorescence units per second). Black, labelled arrows indicate the peaks of the absorbance for the elution mix of the four molecular size standards (apoferritin, β-amylase, bovine serum albumin and carbonic anhydrase), with the numbers referring to masses of 440, 232, 67 and 29 kDa, respectively. **B.** A plot of the log of molecular mass versus elution time was used to estimate the size of the protein peak obtained from the separation of tPfAP-M17, corresponding to the LAP activity. The molecular size standards are shown in black while the red arrow indicates the position of the tPfAP-M17, shown in red and corresponding to a mass of ~393 kDa.

The pH profile of tPfAP-M17 was determined by pre-incubation of recombinant enzyme with $CoCl_2$ at 37 °C, before incubating and assaying activity against Leu-AMC in AMT buffers at pH 4–10.5 (Figure 4.22). The enzyme was found to be active in the neutral to alkaline pH range, 6 to 10.5, with a pH optimum of 8.4.

4.2.4.6. Effect of peptidase inhibitors on tPfAP-M17 leucine aminopeptidase activity

A number of peptidase inhibitors were assessed for their effect on the enzyme activity of recombinant tPfAP-M17 (Table 4.4). The purified protein was incubated with bestatin, an aminopeptidase inhibitor, and 1,10 phenanthroline and EDTA, metal chelators that can inhibit metallopeptidases, in the presence and absence of $CoCl_2$, before addition of Leu-AMC. As expected, bestatin was a potent inhibitor of aminopeptidase activity, reducing it to 1.5% at a concentration of 5 µM. The metal chelators were not as effective at low concentrations. Ten mM 1,10-phenanthroline abolished enzyme activity but only reduced it two-fold when present at a concentration of 1.0 mM. Similarly, 10 mM EDTA reduced LAP activity to only 6% (in the presence of Co^{2+}) but was not very inhibitory at lower concentrations. No inhibition of activity was seen in the presence of phenylmethylsulphonyl fluoride (PMSF), a serine peptidase inhibitor (data not shown).

4.3. DISCUSSION

In-depth studies of *P. falciparum* aminopeptidases have been hampered by the lack of suitable quantities of purified protein for characterisation. Purification from parasites is time-consuming, due to the need to culture large volumes of parasites and the purification procedures are generally quite labour intensive. Establishing a recombinant expression and purification system should enable large amounts of pure aminopeptidase to be isolated relatively easily. Consequently, the aim of the work described in this chapter was to find a system suitable for the cloning and recombinant production of the aminopeptidases as a means of providing sufficient amount for characterisation and functional studies. The M17 aminopeptidase (PfAP-M17) was particularly concentrated on and a number of different strategies were looked at to produce this protein recombinantly.

Quite a lot of time was invested in producing MBP-fusion aminopeptidases as it was thought that this system might successfully produce large quantities of soluble, active protein. This sytem had proved successful for the production of other *P. falciparum* proteins, in our lab and others (138), including another peptidase involved in haemoglobin

degradation, falcipain-2 (66). Unfortunately this system demonstrated quite low levels of expression for all four aminopeptidases and two truncates of PfAP-M1. Alteration of conditions including IPTG concentration and induction time and transformation into other *E. coli* strains (BL-21 (DE3) pLysS, ER2508, Rosetta) did not increase the expression. It has been suggested that induction of *E. coli* cultures at the post-log phase helps to produce more soluble protein as the slower production of recombinant protein, as a result of the lower rate of growth of the bacteria, enables more of the protein to be folded correctly. This method has successfully been used to improve the recombinant production of a *P. falciparum* encoded protein (erythrocyte membrane protein 1, PfEMP1) (50) but when it was attempted here, allowing *E. coli* cells to grow until they reached an $A_{600} = 2.0$ before induction with IPTG, no improvement in expression was observed. It seems apparent from this work that the MBP system is particularly unsuitable for recombinant production of *P. falciparum* aminopeptidases. The lack of expression from the construct consisting of the synthetic codon-optimised gene sub-cloned from pTrcHisB into pMAL-c2x supports this. It may be that the size of the MBP-fusion tag in addition to the aminopeptidases (ranging from 66–126 kDa) results in a protein that is too large to produce. It has been suggested that the molecular mass of *Plasmodium* proteins can be a factor in determining the ease of recombinant production (111).

The high AT content (80–90%) of the *P. falciparum* genome (59) often results in codons not commonly used in *E. coli*, and it is thought that the presence of these rare codons (e.g. AGA and AGG) in *Plasmodium* (and other parasites) is a contributory factor in the difficulties encountered in producing recombinant protein, because of the limited availability of the appropriate tRNAs (139). This has been supported by the improved expression levels obtained by co-transforming cells with the RIG-plasmid, containing three rare tRNAs (7). However, recent studies involving large-scale attempts of production of recombinant *Plasmodium* (111) and apicomplexan (170) proteins for crystallisation have indicated that codon bias does not play as important a role as thought previously. It remains unclear if codon usage does influence the ability to produce recombinant protein but in this study it was found that transformation of constructs into the Rosetta strain (containing tRNAs for seven rare codons on the pRARE plasmid), did not improve the expression of the MBP-fusion aminopeptidases, at least. The synthetic gene used here (in the pTrcHisB-M17 construct) did appear to be produced in larger amounts than constructs made using native gene sequences. However, a true comparison would require cloning of the native sequences into the same vector, pTrcHisB. Indeed, cloning of this synthetic gene into the pMAL-c2x vector (in an attempt to aid correct folding) resulted in no visible

Table 4.3. Effect of divalent metal ions on recombinant tPfAP-M17 activity

Metal Ion	Concentration (mM)	Percent Activity (%)	
		Holoenzyme[a]	Apoenzyme[b]
None	-	100	100
Ca^{2+}	0.01	173 ± 3	
	0.1	158 ± 1	116
	1	144 ± 2	
Co^{2+}	0.01	1327 ± 4	
	0.1	2708 ± 45	4215
	1	2350 ± 30	
Cu^{2+}	0.01	257 ± 7	
	0.1	196 ± 3	191
	1	59 ± 1	
Fe^{2+}	0.01	159 ± 7	
	0.1	238 ± 3	164
	1	214 ± 11	
Mg^{2+}	0.01	203 ± 7	
	0.1	477 ± 9	221
	1	890 ± 7	
Mn^{2+}	0.01	663 ± 15	
	0.1	1866 ± 17	740
	1	2608 ± 16	
Ni^{2+}	0.01	377 ± 1	
	0.1	671 ± 17	601
	1	1132 ± 38	
Zn^{2+}	0.01	422 ± 24	
	0.1	472 ± 4	1674
	1	474 ± 10	

[a]Data reflect the mean $\pm$ SEM (n = 3) of the percent activity of the recombinant tPfAP-M17. Control (100% activity) = rate of 73 ± 6 mFu/s.

[b]Data reflect the percent activity of the tPfAP-M17 (n = 1), following treatment with 1,10-phenanthroline. Control i.e. apoenzyme activity without addition of metal (100% activity) = rate of 25 mFu/s.

Table. 4.4. Effect of peptidase inhibitors on recombinant tPfAP-M17 activity

Reagent	Concentration (mM)	Percent Activity	
		Without Co(II)[a]	With Co(II)[b]
None	-	100	100
Bestatin	0.5	0 ± 0	0 ± 0
	0.05	0.3 ± 0.3	0.1 ± 0.1
	0.005	1 ± 1	1.0 ± 0.1
1,10-phenanthroline	10	0.6 ± 0.6	0.3 ± 0
	1	43 ± 1	52 ± 0
	0.1	95 ± 3	80 ± 2
	0.01	107 ± 3	81 ± 0
EDTA	10	80 ± 3	6 ± 0
	1	90 ± 2	88 ± 1
	0.1	112 ± 3	104 ± 9
	0.01	90 ± 2	93 ± 1

[a]Data reflect the mean percent activity $\pm$ SEM (n = 3) of tPfAP-M17 without pre-incubation with Co^{2+}. Control (100% activity) = rate of 51 ± 1 mFu/s.

[b]Data reflect the mean percent activity $\pm$ SEM (n = 3) of tPfAP-M17 with pre-incubation with Co^{2+}. Control (100% activity) = rate of 1710 ± 4 mFu/s.
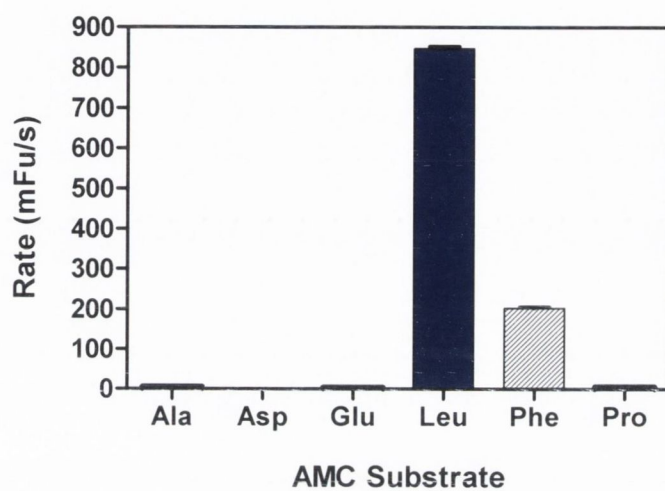
Figure 4.20. Substrate preference of tPfAP-M17. Recombinant tPfAP-M17 (1.34 µg/ml), purified from *Sf9* cells, was assayed with different AMC substrates. Ala, Asp, Glu, Leu, Phe and Pro refer to alanine, aspartate, glutamate, leucine, phenylalanine and proline AMC substrates, respectively. (mFu/s = millifluorescence units per second).

A.

B.
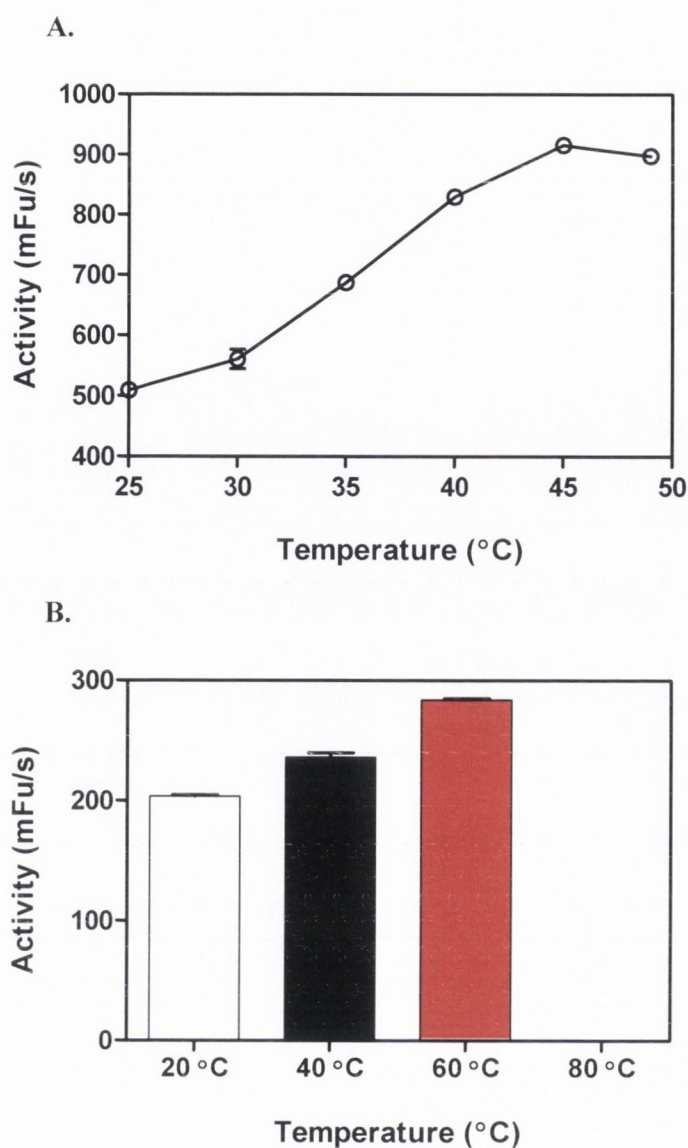
Figure 4.21. Effect of temperature on tPfAP-M17 leucine aminopeptidase activity. **A.** The temperature dependence was determined by pre-incubation of recombinant tPfAP-M17 (0.1 μM) with $CoCl_2$ (1 mM), at the indicated temperatures, for 15 min, before addition of Leu-AMC and measurement of the rate of LAP activity at the indicated temperatures (n = 3). **B.** The temperature stability was determined by pre-incubation of tPfAP-M17 with $CoCl_2$, at the indicated temperatures, for 30 min, before addition of Leu-AMC and measurement of the rate of LAP activity at 37 °C (n = 3). (mFu/s = millifluorescence units per second).
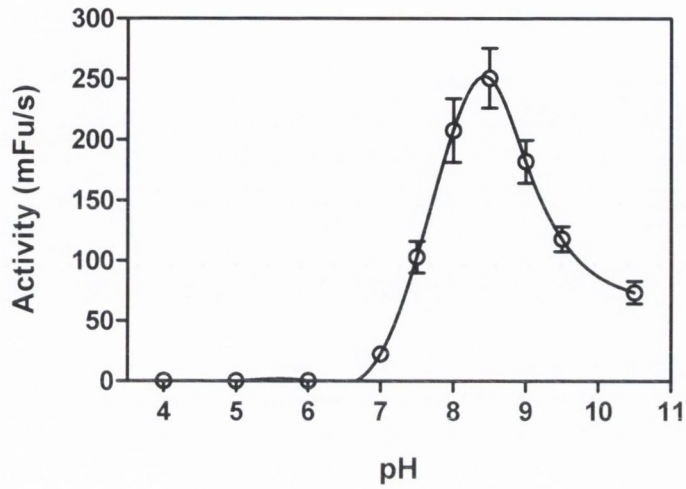
Figure 4.22. Effect of pH on tPfAP-M17 leucine aminopeptidase activity. The pH profile of the enzyme was determined by pre-incubation of recombinant tPfAP-M17 (0.2 μM) with $CoCl_2$ (1 mM), for 15 min, before incubation and measurement of LAP activity, at the various pHs indicated, by addition of Leu-AMC (n = 3). (mFu/s = millifluorescence units per second).

induced band. Therefore, it would appear that the altered codon bias of the gene does not necessarily improve expression and that other factors relating to the type of vector system used may be more important.

Producing the PfAP-M17 protein as a truncate resulted in increased levels of expression in *E. coli*. It may be that the reduction in molecular mass and/or the subsequent lower pI, 6.5 compared to 8.5, contributed to the improved expression as seen with other *P. falciparum* proteins (111). This truncate was produced by removing an asparagine-rich N-terminal region of 82 residues. Many *Plasmodium* proteins (39) are seen to contain N-terminal extensions of low-complexity, containing hydrophilic amino acids, with asparagine residues among the most commonly seen. These regions of low complexity are said to be due to replication slippage, resulting from the high A+T content of the genome, and high rates of recombination (39). They are thought to encode nonglobular, unfolded domains that are not part of the core of the protein but might be involved in evasion of the immune response (127). Truncation of PfAP-M17 did not affect the activity of the protein to any great extent with less than a two-fold difference seen between the k_{cat}/K_M of PfAP-M17 and tPfAP-M17 purified from *E. coli* (98 and 169/M/s, respectively). In fact, as mentioned in the previous chapter, the apparent production of a shorter protein (by approximately 10–15 kDa) *in vivo* (seen in this study and by Dalal *et al*) has led to the suggestion that PfAP-M17 may be processed to this smaller size in the parasites (36). All three PfAP-M17 recombinant preparations, i.e. full-length and truncated protein produced in *E. coli* and truncated protein purified from *Sf9* cells demonstrated similar K_M values of ~10 µM for the leucine substrate. However, a big difference in catalytic activity was observed between protein purified from the bacterial and insect cells. Recombinant tPfAP-M17 purified from the latter had a k_{cat}/K_M of 3996/M/s, more than twenty-fold more active than the former.

Clearly, this insect cell-produced enzyme is more active than that isolated from *E. coli*. It may be that production of the protein in a eukaryotic system yields a better-folded enzyme, resulting in this improved activity. This expression system has also recently been used to successfully produce soluble, active, recombinant PfAP-M18 (159). Additionally, the tPfAP-M17 purified from insect cells resulted in a more stable enzyme than that from bacterial cells. The *E. coli*-produced protein was found to be unstable, precipitating over time and losing activity. It was also found to lose activity upon freezing, something that has been demonstrated before for the tomato leucine aminopeptidase (161). Improvement of the stability of the protein by storage in a number of conditions previously seen to aid stability (41) did not yield much difference. It was thought that cleavage of the tag from

64

the recombinant protein might improve the activity but, unfortunately, this was not achieved.

The assembly of M17 aminopeptidases into hexamers is well documented (158) (see Table 4.1. for some examples). The HPLC analysis of the recombinant tPfAP-M17 indicates that the *P. falciparum* M17 enzyme does indeed form multimers, quite possibly hexamers, as the peak of activity eluting at ~393 kDa (close to the expected size of 370 kDa) coincided quite well with fractions demonstrating LAP activity. (There was an apparent delay between the protein elution profile and the LAP activity profile, possibly due to the time taken for the sample to pass through the column.) This observation of the multimerisation of tPfAP-M17 indicated that the removal of the 82 residue N-terminal extension did not interfere with the folding of the protein or the multimerisation and neither did the additional amino acids and His_6-fusion tag. The requirement of the multimerisation for activity was confirmed by the lack of activity of fractions corresponding to the estimated molecular mass of the monomer (61.5 kDa). Given the apparent need for the formation of these hexamers and their subsequent large apparent molecular mass would indicate that none of the previously described aminopeptidase activities included the PfAP-M17 aminopeptidase. The largest molecular mass of an aminopeptidase reported for *P. falciparum* was ~186 kDa and others ranged between this and 63 kDa. Therefore, all previously described aminopeptidase activities could possibly correspond to the processed forms of PfAP-M1 described previously (3, 54). It may be that the PfAP-M17 aminopeptidase activity was not detected in some of the size-based purifications from parasite extract as it had eluted much earlier than expected for its monomer. For example, the highest molecular mass standard used during the partial purifications of aminopeptidase from *P. falciparum* was 67 kDa (60).

Combining the results of the assays with recombinant PfAP-M17 purified from *E. coli* and insect cells indicates that the enzyme has maximal activity against leucine, followed by phenylalanine (22% compared to cleavage of leucine) and tyrosine and threonine (10% activity) but has negligible activity against alanine, valine, proline, aspartate and glutamate. This lack of activity against alanine and valine was unexpected, as M17-family aminopeptidases are suggested to be active against most hydrophobic residues. However, this type of restricted substrate specificity has been observed previously e.g. the leucine aminopeptidase of *Leishmania* species cleaved leucine, cysteine and methionine but had very little activity against alanine substrates and none against many amino acids including valine (118). This lack of activity against alanine contradicts the results seen with transgenic parasites over-expressing PfAP-M17 where increased activity against an

alanine substrate was observed (58). However, while the presence of the extra copy of the gene was confirmed, an overall increase in the production of PfAP-M17 protein in the transgenic parasite was not demonstrated, making these results difficult to interpret. Also, it may be that overproduction of PfAP-M17 causes some alteration in the production of PfAP-M1 for some reason and that this is the reason for the increased activity against the alanine-containing substrate.

Further work, involving separation of *P. falciparum* parasite extract by HPLC, was carried out by our collaborators (153), indicated that PfAP-M17 does not have activity against alanine substrates. Extract incubated with $CoCl_2$ demonstrated two peaks of leucine aminopeptidase activity of sizes of ~82 kDa and ~320 kDa, presumed to correspond to fractions containing the M1 and M17 enzymes, respectively. The 82-kDa peak also had alanine aminopeptidase activity but the 320-kDa one did not. This confirmed the results observed in the assays carried out with recombinant tPfAP-M17. Again, it would indicate that most of the previously reported activities were documenting PfAP-M1 to some degree as they were active against alanine substrates.

The narrow substrate profile of PfAP-M17 and its overlapping activity with PfAP-M1 seems to suggest that the production of free leucine is important for the parasites. One possible explanation for this apparent bias comes from work on the uptake of isoleucine into cells (108), the only amino acid not present in human haemoglobin and possibly the only one required to be supplied exogenously for *P. falciparum* to survive in culture (36, 100). Isoleucine is suggested to be transported into parasites via an initial ATP-independent pathway and a second ATP-dependent system that is also capable of tranporting leucine across the membrane. In fact, the uptake of isoleucine was increased into parasites pre-loaded with leucine, suggesting that the system may exchange haemoglobin-derived leucine (one the two most abundant amino acids in the protein) for exogenous isoleucine.

Recombinant PfAP-M17 demonstrated markedly increased aminopeptidase activity in the presence of metal ions, as expected. Co^{2+} ions were found to be the best activator of the enzyme. This was not expected as other members of this family, e.g. the bovine lens M17 leucine aminopeptidase, require zinc as their metal co-factor. Indeed, further work by our collaborators, using inductively coupled plasma mass spectrometry (ICP-MS) to detect the metal ion present in the active site, indicated that it is Zn^{2+} (J. Lowther, personal communication). This type of activation of a recombinant Zn^{2+}-containing enzyme by Co^{2+} has been observed many times before (4), including for the *Leishmania* M17 aminopeptidase (118) and, more recently, for the *P. falciparum* M18 aminopeptidase (159).

It is likely to be the result of a metallohybrid where Zn^{2+} is bound to the "tight" metal binding site of the enzyme and the Co^{2+} is bound to the "readily exchangeable" site. This might explain why the apoenzyme was seen to be activated well by Zn^{2+} but the holoenzyme was not. It is possible that the Co^{2+} may be bound in both sites as it has been seen to be the only other divalent metal capable of binding to the "tight" metal binding site of M17 aminopeptidases (4).

Also, it may be possible that the Zn^{2+} concentrations used in this study were in fact too high, as only concentrations down to 10 μM were tested. This preference for cobalt has been seen previously for falcilysin, a *P. falciparum* M16-family metallopeptidase involved in earlier stages of haemoglobin degradation in the digestive vacuole. Studies with the apoenzyme of this protein (purified from parasites) demonstrated that Co^{2+} concentrations of 100 μM generated the highest levels of activity while Zn^{2+} restored activity at 1 μM but inhibited activity at higher concentrations (45).

The pH profile seen here for the recombinant PfAP-M17 is not unexpected considering the previous reports of aminopeptidase activities in *Plasmodium* species. The lack of activity below a pH of 6 confirms that this enzyme would not be active in the acidic environment of the digestive vacuole and supports the idea that peptides generated by other peptidases would need to be transported into the cytosol somehow. The pH optimum of the enzyme is consistent with the cytosolic location of PfAP-M17 seen in the previous chapter.

This work describes the first characterisation of a recombinant *P. falciparum* aminopeptidase. The PfAP-M18 aminopeptidase has also recently been recombinantly produced and characterised (159). Production of recombinant PfAP-M1 and PfAP-M24 aminopeptidases would also provide much more information about the relative importance of all of these enzymes. Overall, it is apparent that the baculovirus-infected insect cell system proved most useful in this study to produce recombinant PfAP-M17, allowing for its functional analysis and aiding in the investigation of which aminopeptidase(s) are important in the parasites. However, an *E. coli*-based system would be much more preferable for recombinant production and further work could include more investigation into this, possibly considering the pET system to produce a C-terminally tagged His_6-fusion protein. The provision of large quantities of recombinant PfAP-M17 at low cost might enable crystallisation of the protein which would provide important information about the structure of the enzyme, and possibly, aid in the design of inhibitors.

Chapter 5

Anti-Malarial and Anti-Aminopeptidase Activities
of M17 Aminopeptidase Inhibitors

5.1. INTRODUCTION

It has been demonstrated that cytosolic extract from *Plasmodium* parasites contains aminopeptidase activity against leucine and alanine-containing substrates (amongst others) (see Table 1.1 for a summary). These amino acids correspond to the suggested preferred substrates of both M1 and M17 aminopeptidases, both of which are present in *P. falciparum* (PfAP-M1 and PfAP-M17, respectively) and it was unclear if only one enzyme or a combination of the two was contributing to these activities. The relative importance of PfAP-M1 and PfAP-M17 to the parasites is of particular interest, since of the aminopeptidases present in *P. falciparum* only these two (i.e. M1 and M17 family enzymes) are expected to be inhibited by bestatin, an aminopeptidase inhibitor with antimalarial activity (120, 168).

Studies with purified PfAP-M1 and with an ~80-kDa aminopeptidase (which may or may not be PfAP-M1) demonstrated activities against both leucine and alanine substrates (3, 34). In contrast, it was seen (in the previous chapter, sections 4.2.2 and 4.2.4.4) that recombinant PfAP-M17 protein had good leucine aminopeptidase activity but very poor alanine aminopeptidase activity. This leucine aminopeptidase activity was greatly increased by incubation with divalent metal ions, particularly Co^{2+} and Mn^{2+}. Additional work by our collaborators showed that parasite extract incubated with $CoCl_2$ and separated by HPLC showed two peaks of leucine aminopeptidase activity of sizes of ~82 kDa and ~320 kDa, presumed to correspond to fractions containing the M1 and M17 enzymes, respectively. The 82-kDa peak also had alanine aminopeptidase activity but the 320-kDa one did not (153). The extract prepared in the absence of $CoCl_2$ showed very much reduced activity from the 320-kDa peak but more activity from the 82-kDa one (J. Lowther, personal communication). Therefore, it appears that PfAP-M17 contributes only to the leucine aminopeptidase activity of the parasite extracts while PfAP-M1 is involved in both the leucine and alanine aminopeptidase activites.

The leucine aminopeptidase activity of *P. falciparum* cytosolic extract is inhibited by bestatin (3, 34, 60) but again it is unclear whether one or both of PfAP-M1 and PfAP-M17 is/are the target(s) for this compound. So far, there have been no reported knock-outs of either the *PfAP-M1* or *PfAP-M17* aminopeptidase genes in *P. falciparum* to aid in determining the relative importance of these enzymes. Transgenic parasites carrying the *PfAP-M17* gene on a multi-copy plasmid demonstrated reduced susceptibility to bestatin, suggesting that PfAP-M17 might be the major target of this agent. However, the over-expression of *PfAP-M17* was not quantified and an indirect effect on PfAP-M1 due to

increased *PfAP-M17* copy number could not be ruled out. No line over-producing PfAP-M1 was obtained (58).

Therefore, in order to assess the validity of the PfAP-M17 enzyme as a target, a series of structurally-related alpha-aminoalkylphosphonates and phosphonopeptides, designed specifically to target the active site of M17 aminopeptidases, were employed as chemical tools. Knowledge of the differing substrate specificities and cation-dependencies of the M1 and M17 enzymes was used to dissect out the inhibition of the two activities in parasite cytosolic extracts and inhibition of recombinant PfAP-M17 was used to confirm these results. This chapter describes the antimalarial and anti-aminopeptidase activities of this series of phosphonic derivatives. A homology model of PfAP-M17 was also generated in an attempt to examine the interactions of inhibitors with the enzyme.

5.2.   RESULTS

5.2.1. Inhibition of growth of cultured *P. falciparum* by α-aminoalkylphosphonates and phosphonopeptides

The series of α-aminoalkylphosphonate and phosphonopeptide compounds was tested against cultured *P. falciparum* using the lactate dehydrogenase assay (described in section 2.2.5). They had varying potencies against the parasites, ranging from inactive at the highest concentrations possible to low micromolar 50% inhibitory concentrations (IC_{50}) (Table 5.1). The two most active compounds were the alicyclic phosphonates D14 and D12 with IC_{50} values of 14 μM and 15 μM, respectively. These were closely followed by D7 and D17, phosphonic acid analogues of phenylalanine, with extended aliphatic chains of one or three methylene groups, respectively (IC_{50} = 22 and 21 μM, respectively). D36, a monophenyl ester derivative of D7, was synthesised (by Dr. Marcin Drag) in the hope of improving uptake into parasites but it did not demonstrate any improved activity. A number of the compounds had very low or negligible antimalarial activity, inhibiting parasite growth by less than 10% at the highest concentration tested (256 μM).

5.2.2. Inhibition of aminopeptidase activity of *P. falciparum* parasite extract

The ability of the series of compounds to inhibit the leucine aminopeptidase (LAP) and alanine aminopeptidase (AAP) activities of parasite cytosolic extracts was investigated. Compounds were tested at two fixed concentrations, 10 μM and 0.1 μM, by incubating them with cytosolic extract before addition of the fluorogenic substrate, Leu-AMC or Ala-AMC. A range of activities against LAP activity was seen (Table 5.2), with the best five

compounds, D14, D12, D17, D7 and D36, inhibiting the activity by $\geq$ 90 % when assayed at 10 µM, while the least effective compounds could only inhibit the LAP activity by a few percent or not at all. The compounds are ordered by decreasing antimalarial activity (i.e. by increasing IC_{50}: see Table 5.1) in Table 5.2 and demonstrate a corresponding trend of decreasing percent inhibition of enzyme activity, indicating a good correlation between antimalarial and anti-LAP activity. There were a couple of minor exceptions to the general trend of agreement including D18, which might be expected to have better antimalarial activity (e.g. closer to D2 or D13) given its anti-aminopeptidase activity. Conversely, D21 might be expected to inhibit the parasite extract to a higher degree given its IC_{50} value.

A similar inhibition of the AAP activity of the extract by the compounds was observed, as was a similar correlation with antimalarial activity. This indicated that the compounds might be having some effect on the M1 aminopeptidase of *P. falciparum*, as PfAP-M17 has been shown to have very low AAP activity (sections 4.2.2 and 4.2.4.4 and J. Lowther, personal communication).

5.2.3. Contributions of PfAP-M17 and PfAP-M1 to aminopeptidase activities of parasite cytosolic extract

In order to investigate whether the activity being inhibited by the compounds was the M17 or M1 aminopeptidase activity or a mixture of the two, parasite extract was tested for leucine and alanine aminopeptidase activity in the presence of $CoCl_2$, which was expected on the basis of previous results to boost PfAP-M17 (sections 4.2.2 and 4.2.4.3) but reduce PfAP-M1 activity (J. Lowther, personal communication). Following incubation with $CoCl_2$, the overall LAP activity of the extract was reduced markedly to 21% of its original activity but the AAP activity was virtually abolished, down to 4% (Figure 5.1). Therefore, assaying parasite extract without $CoCl_2$ and with Ala-AMC as the substrate should measure almost exclusively PfAP-M1, while assaying extract in the presence of $CoCl_2$ and with Leu-AMC as the substrate will measure predominantly PfAP-M17.

5.2.4. Inhibition of LAP activity of parasite extract in the presence and absence of Co^{2+} ions

A number of the compounds were then assessed for their ability to inhibit the LAP activity of parasite extract in the presence of $CoCl_2$. The same general trend of inhibition of enzyme in extract incubated with $CoCl_2$ to that of the extract without $CoCl_2$ was seen (Table 5.3). Overall, there was however a strong trend for the compounds to show some increased inhibition of LAP activity in the presence of $CoCl_2$, suggesting that most of them

were (unlike bestatin) better inhibitors of PfAP-M17 than PfAP-M1. D21 is particularly noteworthy as it was mentioned above as a compound with good antimalarial activity but relatively poor aminopeptidase inhibition (in the absence of $CoCl_2$): it showed a marked increase in LAP inhibition when Co^{2+} was added. By contrast, inhibition by D17 does not vary so it may not be any more specific for PfAP-M17 than PfAP-M1.

5.2.5. Correlation of anti-malarial activity and anti-aminopeptidase activity

A clear linear relationship was seen between the antimalarial activity of the compounds and the anti-LAP activity when the percent inhibition (at 10 μM inhibitor) of extract in the presence of $CoCl_2$ was plotted against the log IC_{50} (Figure 5.2). The data were analysed using Spearman non-parametric correlation and were found to have an r value of -0.8531 (p = 0.0008), suggesting a good negative correlation between log IC_{50} of the compounds and their percent inhibition of the LAP activity of the extract (with $CoCl_2$), i.e. as the anti-malarial activity decreases so too does the inhibition of the extract LAP activity.

5.2.6. Inhibition of leucine aminopeptidase activity of recombinant tPfAP-M17
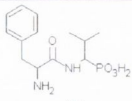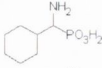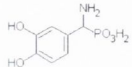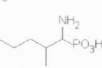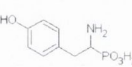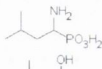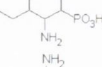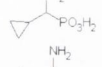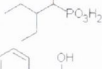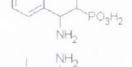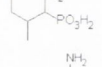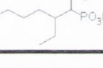
A selection of the compounds was tested for their ability to inhibit the LAP activity of the truncated recombinant PfAP-M17 (tPfAP-M17) purified from baculovirus-infected insect cells (described in section 4.2.4.1). A very similar profile of percent inhibition of LAP activity of the recombinant and the extract (incubated in $CoCl_2$) was seen (Table 5.4, with additional data from Drag *et al* (42)). As a result, there is correspondingly good correlation between inhibition of recombinant enzyme and anti-malarial activity. A slight exception to this is D17, which as discussed above may be roughly equiactive against PfAP-M17 and PfAP-M1. This contention is further supported by its relatively good inhibition of the mammalian M1-family enzyme aminopeptidase N compared with the other compounds. D14 is the best inhibitor of recombinant tPfAP-M17 and it also has the best antimalarial activity of all the compounds tested. However, it is the poorest inhibitor of pkLAP, with a K_i of 9.57 μM, indicating that it may be somewhat selective for PfAP-M17 over the mammalian enzyme.

The K_i values for inhibition of LAP activity of recombinant PfAP-M17 by the most active compounds (i.e. D14, D12, D17 and D7) and bestatin were calculated (Table 5.4.). The activity of tPfAP-M17 was assayed at two or more substrate concentrations with a range of concentrations of the particular inhibitor. Dixon plots of $1/V_s$ versus inhibitor concentration (where V_s is the final steady-state velocity of the reaction) were plotted (see

71

TABLE 5.1. Activities of α-aminoalkylphosphonates and phosphonopeptides on cultured *P. falciparum*

Compound	Structure	Configuration	IC$_{50}$ (μM)[a]	% Inhibition of parasite growth[b]
D14		RS	14	-
D12		RS	15	-
D17		RS	21	-
D7		RS	22	-
D36		RS	25	-
D5		RS	53	-
D21		R >99%	54	-
D3		RS	57	-
D2		RS	65	-
D13		RS	119	-
D20		RS:SS 1:1	135	-
D38[c]		R	>128	30 ± 13
D24		RS:SR 1:1	>128	11 ± 5
D6		RS	>256	34 ± 6
D28		RR:RS 1:1	>256	22 ± 9
D18		RS	>256	17 ± 0
D33		SS:SR 1:1	>256	17 ± 6
D10		R >99%	>256	15 ± 2
D1		RS	>256	14 ± 4
D26		SS >98%	>256	14 ± 4
D30		RR:RS	>256	14 ± 5
D19		RS:SS 1:1	>256	10 ± 6
D8		RS	>256	8 ± 3

TABLE 5.1. Activities of α-aminoalkylphosphonates and phosphonopeptides on cultured *P. falciparum* (continued)

Compound	Structure	Configuration	IC_{50} $(\mu M)^a$	% Inhibition of parasite growth[b]
D34		RS:SS 1:1	>256	7 ± 3
D22		S >99%	>256	7 ± 2
D35		RS	>256	5 ± 4
D31		SS:SR 1:1	>256	2 ± 2
D4		RS	>256	1 ± 1
D23		S >99%	>256	1 ± 1
D25		SSS:RSS 8:2	>256	1 ± 1
D9		RS	>256	0 ± 0
D11		S >99%	>256	0 ± 0
D27		RS:SR 1:1	>256	0 ± 0
D29		SS:SR 1:1	>256	0 ± 0
D32		RR:RS 1:1	>256	0 ± 0

[a]Geometric mean IC_{50} were calculated from six determinations from three separate experiments.

[b]Compounds for which no IC_{50} could be calculated are shown in order of increasing inhibition of parasite growth at a fixed, highest possible concentration. Results represent the arithmetic mean ± SEM (n ≥ 4) of the percent inhibition of parasite growth at the highest concentration of compound tested (i.e. 128 μM for D24 and D38, and 256 μM for all others).

[c]D38 corresponds to the phosphonic analogue of leucine, LeuP (96).

Compound	LAP activity		AAP activity	
	10 µM	0.1 µM	10 µM	0.1 µM
Bestatin	98 ± 1	33 ± 2	97 ± 0	29 ± 2
D14	95 ± 1	17 ± 3	95 ± 1	15 ± 1
D12	94 ± 0	17 ± 3	94 ± 1	13 ± 1
D17	97 ± 1	28 ± 5	97 ± 1	28 ± 3
D7	93 ± 1	15 ± 2	95 ± 0	15 ± 3
D36	90 ± 0	8 ± 2	92 ± 1	12 ± 0
D5	71 ± 1	6 ± 3	76 ± 1	0 ± 4
D21	12 ± 4	0 ± 1	8 ± 3	2 ± 0
D3	43 ± 1	2 ± 1	52 ± 1	2 ± 0
D2	39 ± 0	5 ± 7	43 ± 0	0 ± 0
D13	27 ± 3	3 ± 7	20 ± 3	0 ± 0
D20	4 ± 2	0 ± 5	0 ± 5	0 ± 1
D38	15 ± 0	0 ± 3	24 ± 2	0 ± 1
D24	17 ± 1	-	-	-
D6	6 ± 2	-	-	-
D28	9 ± 0	-	-	-
D18	37 ± 1	-	-	-
D33	11 ± 2	-	-	-
D10	10 ± 6	-	-	-
D1	8 ± 2	-	-	-
D26	6 ± 1	-	-	-
D30	11 ± 1	-	-	-
D19	9 ± 2	-	-	-
D8	6 ± 3	-	-	-
D34	12 ± 1	-	-	-
D22	8 ± 3	-	-	-
D35	7 ± 4	-	-	-
D31	3 ± 3	-	-	-
D4	8 ± 1	-	-	-
D23	2 ± 6	-	-	-
D25	5 ± 0	-	-	-
D9	6 ± 4	-	-	-
D11	6 ± 2	-	-	-
D27	5 ± 2	-	-	-
D29	9 ± 1	-	-	-
D32	1 ± 3	-	-	-

TABLE 5.2. Inhibition of aminopeptidase activity of parasite cytosolic extract — % Inhibition[a]

[a]Results represent the mean ± SEM (n ≥ 4) of leucine aminopeptidase (LAP) and alanine aminopeptidase (AAP) activity of parasite cytosolic extract after incubation with compounds at 10 µM or 0.1 µM.

- not determined.

TABLE 5.3. Inhibition of LAP activity of parasite extract in the absence and presence of CoCl₂

| Compound | % Inhibition[a] | | | |
| | - CoCl₂ | | + CoCl₂ | |
	10 µM	0.1 µM	10 µM	0.1 µM
Bestatin	98 ± 1	33 ± 2	93 ± 1	6 ± 2
D14	95 ± 1	17 ± 3	91 ± 0	51 ± 2
D12	94 ± 0	17 ± 3	91 ± 1	43 ± 5
D17	97 ± 1	28 ± 5	92 ± 0	25 ± 3
D7	93 ± 1	15 ± 2	92 ± 0	41 ± 2
D36	90 ± 0	8 ± 2	73 ± 3	19 ± 11
D5	71 ± 1	6 ± 3	70 ± 5	20 ± 9
D21	12 ± 4	0 ± 1	67 ± 3	50 ± 8
D3	43 ± 1	2 ± 1	73 ± 1	38 ± 1
D2	39 ± 0	5 ± 7	71 ± 1	46 ± 5
D13	27 ± 3	3 ± 7	69 ± 1	21 ± 9
D20	4 ± 2	0 ± 5	0 ± 6	1 ± 0
D38	15 ± 0	0 ± 3	52 ± 0	9 ± 3

[a]Results represent the mean ± SEM (n ≥ 4) of leucine aminopeptidase (LAP) activity of parasite cytosolic extract after incubation with compounds (at 10 µM or 0.1 µM). Extract was assayed in the absence (-) and presence (+) of CoCl₂ (1 mM).
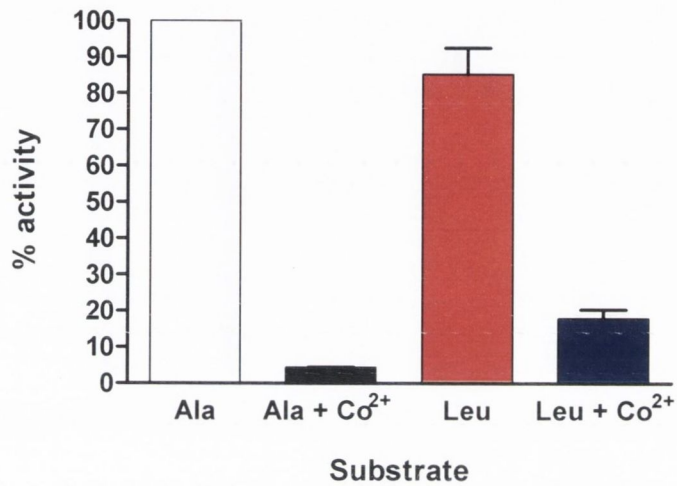
Figure 5.1. Aminopeptidase activity of *P. falciparum* cytosolic extract. Extract was incubated in 50 mM Tris-HCl, pH 8.0, with or without $CoCl_2$ (1 mM) at 37 °C for 15 min before addition of substrate, Ala-AMC or Leu-AMC, to a final concentration of 10 µM. Activity is expressed as a percentage of the alanine aminopeptidase activity of the extract in the absence of $CoCl_2$.

Figure 5.3. for the plot of D14 as an example) and the K_i values determined from the x-axis coordinate of the point of intersection of the graphs. The phosphonate compounds with the lowest K_i values were D14 and D7, at 0.16 and 0.18 μM, respectively, approximately twice the value obtained for bestatin (0.07 μM). D7 demonstrated similar inhibition of the mammalian pkLAP (0.14 μM) while, in contrast, D14 showed a marked preference (nearly 60 fold) for the *P. falciparum* enzyme over the mammalian one. D17 demonstrated a relatively high K_i value for tPfAP-M17, 0.94 μM, supporting the idea that its antimalarial activity may be in part due to some action against PfAP-M1.

5.2.7. Homology modelling of *P. falciparum* M17 aminopeptidase

The lack of available crystallographic data for PfAP-M17 means that its structure cannot be assessed e.g. to determine interactions with inhibitors. Therefore, the crystal structure of the bovine lens LAP was used to construct a homology model of PfAP-M17 in an attempt to examine the potential interactions of the inhibitors tested here with the enzyme's active site.

The sequence of PfAP-M17 was aligned with the sequences of M17 aminopeptidases for which crystal structures are available from the Research Collaboratory for Structural Bioinformatics (RCSB) Protein Data Bank, namely the bovine lens leucine aminopeptidase (blLAP), *E. coli* aminopeptidase A (PepA) and the *C. elegans* leucine aminopeptidase (LAP1) (see Figure 5.4. for alignment with blLAP). The level of identity between PfAP-M17 and the other aminopeptidases was not very high (38, 35 and 31%, respectively) which can cause problems for homology modelling. However, as can be seen in Figure 5.4, there was higher sequence identity in the catalytically important C-terminal region. All of the residues considered important for metal ion binding (coloured green and red) in blLAP (K250, D255, D273, D332 and E334) are conserved in PfAP-M17 (K374, D379, D399, D459 and E461). All, except one, of those involved in interactions with bestatin are also conserved between blLAP (K262, M270, N330, A333, T359, L360, G362, I421 and A451) and PfAP-M17 (K386, M396, N457, A460, T486, L487, G489, I547 and A577) (24, 25). The bovine lens aminopeptidase was chosen as the template for homology modelling as it had the best identity with PfAP-M17. In addition, a number of crystal structures are available for this protein, both unliganded and in complex with different inhibitors, including LeuP (96), one of compounds assayed above (called D38 in this study).

A homology model for PfAP-M17 was generated using this crystal structure of blLAP in complex with LeuP (PDB ID: 1LCP) as described in section 2.11.2. The

structure of 1LCP and the model generated from using this as a template are illustrated in Figure 5.5 A and B, respectively. Due to the N-terminal extension of PfAP-M17 (compared with other M17 aminopeptidases), the model begins at residue 70 (shown in Figure 5.4) as the modelling software could not map these initial residues with no template structure. As might be expected, the N-terminal domain of the PfAP-M17 model (Figure 5.5 B) was quite disordered (green regions) but the C-terminal domain was more ordered (α-helices and β-sheets) and displayed more similarities to the blLAP structure.

5.2.8. Examination of inhibitor interactions with PfAP-M17 homology model

As the template structure chosen for homology modelling contained the co-crystallised ligand LeuP, it was possible to place other inhibitors in the same approximate area of the active site of the PfAP-M17 model to attempt investigation of potential interactions. Inhibitor structures were drawn using the MOE 2006.08 molecule builder and were aligned to the structure of the LeuP molecule taken directly from the bovine lens aminopeptidase template (1LCP) active site. Comparison of the predicted interactions between bestatin and the structures of blLAP and the PfAP-M17 model (Figure 5.6) demonstrated that residues suggested to be involved in inhibitor binding in blLAP (see Figure 5.4) were highlighted by the software package in both structures. This indicated that this method might be suitable for analysis of the binding of the series of inhibitors tested. The predicted interactions for residues of the PfAP-M17 model with the α-aminoalkylphosphonate and phosphonopeptide inhibitors were quite similar but did demonstrate some differences. For example, the interactions predicted for the best inhibitor (D14) and one of the poorest (D25) indicated that the latter may be lacking some hydrophobic side chain interactions compared to the former e.g. with I393 (Figure 5.7).

5.3. DISCUSSION

The best inhibitors of M17-family aminopeptidases (based primarily on work with the M17-family aminopeptidase from porcine kidney (pkLAP)) are analogues of short peptides e.g. the well-known bestatin. Amino acid analogues are also good inhibitors, e.g. *L*-leucinal, and the phosphonic acid analogue of *L*-leucine (LeuP), with the latter group being more specific for metallopeptidases (69). Both groups of inhibitors act as transition state analogues, binding to the metal ions in the active site of the enzyme (63). The series of compounds tested here are phosphonic acid derivatives, some of which were synthesised following the structure-based design of inhibitors against mammalian M17 aminopeptidase
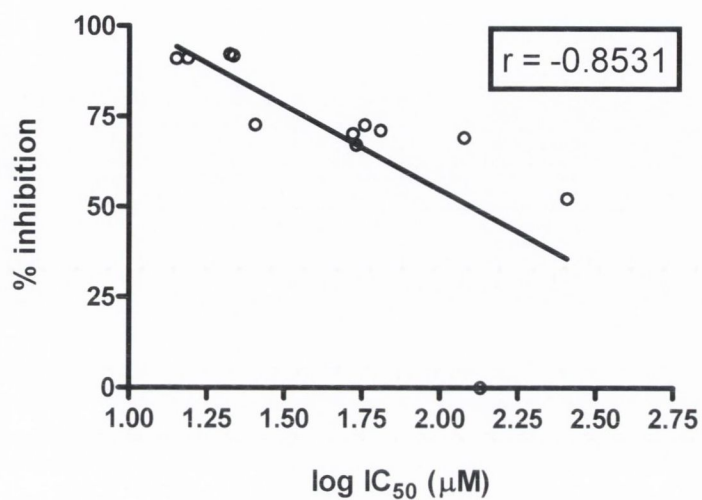
Figure 5.2. Correlation of antimalarial activity and inhibition of parasite extract leucine aminopeptidase activity (in the presence of Co^{2+}). The percent inhibition of parasite extract pre-incubated with $CoCl_2$ (1 mM) of the twelve most active compounds (at 10 μM) was plotted against their log IC_{50} for parasite growth. Spearman rank correlation was used to analyse the data (r = -0.8531, p = 0.0008).

TABLE 5.4. Inhibition of LAP activity of parasite extract and recombinant tPfAP-M17 incubated with CoCl$_2$

Compound	% Inhibition[a]				K_i (µM)		
	Parasite extract		tPfAP-M17		tPfAP-M17	pkLAP[b]	APN[b]
	10 µM	0.1 µM	10 µM	0.1 µM			
Bestatin	-	6 ± 2	-	34 ± 4	0.07	-	-
D14	-	51 ± 2	-	67 ± 7	0.16	9.57	41.6
D12	-	43 ± 5	-	61 ± 1	0.45	0.21	37.1
D17	-	25 ± 3	-	27 ± 3	0.94	0.33	3.69
D7	-	41 ± 2	-	47 ± 1	0.18	0.14	15.9
D21	67 ± 3	-	94 ± 6	-	-	7.89	161
D13	69 ± 1	-	86 ± 6	-	-	0.75	54.7
D22	50 ± 1	-	61 ± 3	-	-	6.96	>2000
D23	26 ± 3	-	9 ± 13	-	-	0.23	53
D25	0 ± 7	-	0 ± 4	-	>10	-	-

[a]Results represent the ± SEM of leucine aminopeptidase (LAP) activity of parasite cytosolic extract (n ≥ 4) and of recombinant tPfAP-M17 (n = 2) after incubation with compounds (at 10 µM or 0.1 µM) and CoCl$_2$ (1 mM).

[b]Results from Drag et al, 2005 (42), pkLAP = porcine kidney leucine aminopeptidase, APN = porcine kidney microsomal aminopeptidase N.
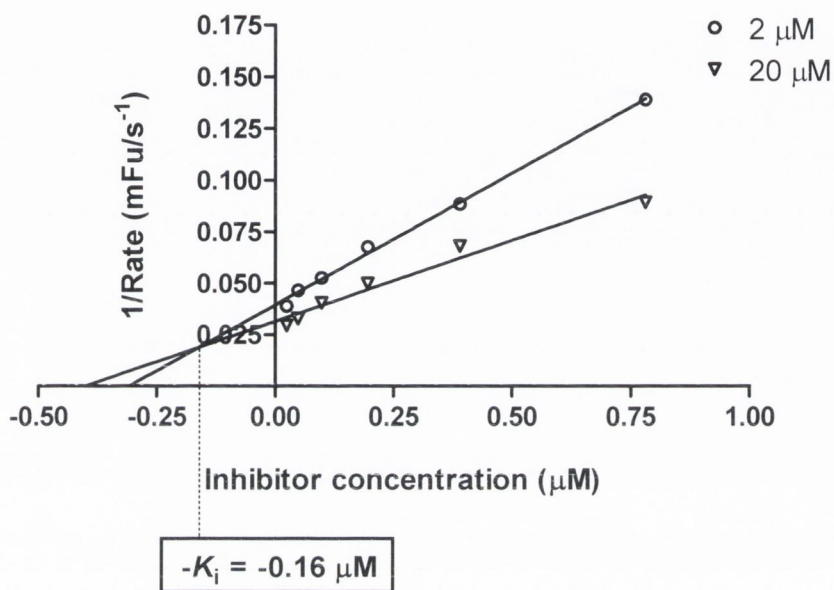
Figure 5.3. Dixon plot of inhibition of tPfAP-M17 activity by D14. The rate of activity of tPfAP-M17 was tested in the presence of a range of inhibitor concentrations and two substrate concentrations, 2 and 20 µM. The K_i of 0.16 µM corresponds to the x-axis coordinate of the point of intersection of the plots for the two substrate concentrations.

```
PfAP-M17   MYFSSLCKFLPISEKEKIYLNIVKKRFCKSNIYYNNNNNNIINYNKRGLKFYPFCNNLKK 60
blLAP      ------------------------------------------------------------
                            ↓                      ↓

PfAP-M17   NINFVNINNKKGINFHSINKERKMASEVPQVVSLDPTSIPIEYNTPIHDIKVQVYDIKGG 120
blLAP      ---------TKGLVLGIYSKEK--EEDEPQFTSAGEN-----FNKLVSGKLREILNISG- 43
                     .**: :     .**:    .: **..*  .       :*. :  .    :: :*.*

PfAP-M17   CNVEEGLTIFLVNNPGKENGPVKISSKVNDKNVSEFLKDENMEKFNVKLGTSKHFYMFND 180
blLAP      --------------PPLKAGKTRTFYGLHEDFPSVVVVG----LGKKTAGIDEQENWHEG 85
                           *   : *  .:   :::.  * .: .      :  .  *  .::    .:.

PfAP-M17   NKNSVAVGYVGCGSVADLSEADMKRVVLSLVTMLHDNKLSKLTVVFEINVDKNLFRFFLE 240
blLAP      KENIRAAVAAGCRQIQDLEIPSVEVDPCGDAQAAAEGAVLGLYEYDDLKQKR-------- 137
                ::*  *.  .** .: **. ..::   .  .   :. : *    ::: .:

PfAP-M17   TLFYEYMTDERFKSTDKNVNMEYIKHLGVYINNADTYKEEVEKARVYYFGTYYASQLIAA 300
blLAP      ----KVVVSAKLHGSED-------------------QEAWQRGVLFASGQNLARRLMET 173
                : :.. :::.::.                 :*   ::. ::   *    * :*: :

PfAP-M17   PSNYCNPVSLSNAAVELAQKLNLEYKILG--VKELEELKMGAYLSVGKGSMYPNKFIHLT 358
blLAP      PANEMTPTKFAEIVEENLKSASIKTDVFIRPKSWIEEQEMGSFLSVAKGSEEPPVFLEIH 233
                *:*   .*..::: . *  :. .:: .::    . :** :**::***.*** *  *:.:

PfAP-M17   YK-SKGDVKKKIALVGKGITFDSGGYNLKAAPGSMIDLMKFDMSGCAAVLGCAYCVGTLK 417
blLAP      YKGSPNASEPPLVFVGKGITFDSGGISIKAAN--MDLMRADMGGAATICSAIVSAAKLD 291
                ** * .  :  .:.:**********.***  .:***..  .:***.: **.*.*::  ....*.

PfAP-M17   PENVEIHFLSAVCENMVSKNSYRPGDIITASNGKTIEVGNTDAEGRLTLADALVYAEKLG 477
blLAP      LP-INIVGLAPLCENMPSGKANKPGDVVRARNGKTIQVDNTDAEGRLILADALCYAHTFN 350
                ::*   *:..:**** *  :: :***::  * *****:* *****.* ***** **..:.

PfAP-M17   VDYIVDIATLTGAMLYSLGTSYAGVFGNNEELINKILNSSKTSNEPVWWLPIINEYR-AT 536
blLAP      PKVIINAATLTGAMDIALGSGATGVFTNSSWLWNKLFEASIETGDRVWRMPLFEHYTRQV 410
                 .  *:: ******.  :**:. :*** *.. * **:::*   :.: ** :*::::.*   .

PfAP-M17   LNSKYADINNISSSVKASSIVASLFLKEFVQNTAWAHIDIAGVSWN-----FKARKPKGF 591
blLAP      IDCQLADVNNIGKYRSAGACTAAAFLKEFVTHPKWAHLDIAGVMTNKDEVPYLRKGMAGR 470
                ::.: **:***..   .*.: .*: ****** :. ***:*****   *    :  :   *

PfAP-M17   GVRLLTEFVLNDAL 605
blLAP      PTRTLIEFLFRFSQ 484
                .* * **::. :
```

Figure 5.4. Sequence alignment of the M17 aminopeptidases of *P. falciparum* and bovine lens. The sequences of the *P. falciparum* (PfAP-M17) and bovine lens (blLAP) M17 aminopeptidases were aligned. The symbols *, : and . indicate identical, conserved and semi-conserved residues, respectively. The NTDAEGRL motif is outlined. Residues highlighted (bold) in green and red indicate those involved in binding the readily-exchangeable and non-readily exchangeable zinc ions, respectively. The other highlighted (bold) residues are those involved in binding bestatin in the active site, with residues coloured blue providing stabilisation to the backbone, while those coloured purple and black are involved in interactions with the leucyl and phenylalanyl side chains of bestatin, respectively. With the exception of the substitution of the M454 of blLAP for S580 in PfAP-M17, all residues found to be important in the former are conserved in the latter. The black arrow indicates the first residue of the PfAP-M17 homology model (Figure 5.5) while the red arrow indicates the position of the truncation of the recombinant tPfAP-M17.

(70). Comparing the results of the antimalarial and anti-aminopeptidase extract and recombinant activity assays for these compounds and the data previously obtained for mammalian M1 and M17 aminopeptidase inhibition enables the identification of the properties likely to confer potency and selectivity against PfAP-M17.

The inhibitors had a range of antimalarial potencies down to low micromolar IC_{50} values. The most potent compounds were those with long, hydrophobic side chains (D14, D12, D17 and D7). As can be seen from these compounds, replacement of the aromatic ring with the more flexible alicyclic one does not alter the antimalarial activity greatly. By contrast, the least active group of compounds generally had shorter side chains. These results suggest that the S1 pocket of the PfAP-M17 enzyme may be quite large since it is able to accommodate compounds with bulky side chains. Also, the surface of the S1 cleft seems to be involved in multiple interactions with the bound inhibitors, as effectors with extended side chains were the most active ones. The data outlined here also suggest that the interactions are of a hydrophobic nature as the presence of the hydroxy group on the compounds tested decreased the inhibitory potency. This observation correlates with results obtained in previous studies for mammalian (porcine kidney) LAP, where the inhibitors with bulky substituents were the best inactivators of the enzyme (42). The most active group of compounds all contained a $(CH_2)_2$ group at the α, β and γ positions, indicating that no branching is required for good activity. The presence of the free amine at the alpha position is also indispensable for the effective interaction between inhibitors and the PfAP-M17 aminopeptidase, as observed by the very weak inactivation by compounds with a hydroxy group at this position (D24–D27).

The comparison of the inhibitory activity of the R enantiomers (corresponding to the natural L amino acids) tested here (D21, D38 and D10) versus their counter-partners with S configurations (D22, D23 and D11) shows a preference for the R ones. This is in agreement with the expected chiral specificity of enzymes, especially aminopeptidases, which usually favour substrates with natural L chirality. However, although the weakest R oriented molecule (D10) is a better inhibitor than the best S compound tested here (D22), the degree of the specificity is not as distinct as that observed for other enzymes (43).

The more active compounds chiefly inhibited the PfAP-M17 aminopeptidase but also had activity against the M1 enzyme to a certain degree. There was a strong correlation between antimalarial activity and the effects on aminopeptidase activity in extracts under conditions favouring PfAP-M17 over PfAP-M1. Based on these data, it also seems that the compounds with IC_{50} values in the 50–70 μM range (D5, D21, D3 and D2) might be slightly more specific for PfAP-M17. Within this group of inhibitors it seems that the

presence of the methoxy group in the *para-* position (in D5, D3 and D2) is important, as increased inhibition of activity was seen with the inhibitors that contained this functional group. Alteration to a free hydroxyl group in this position (D1, D35 and D4) or another (D6 and D35) decreased the activity dramatically. There was also good agreement between M17 aminopeptidase inhibition in extracts and recombinant tPfAP-M17 produced in insect cells. The fact that the compound D14 that had marked selectivity for PfAP-M17 over pkLAP was also the best inhibitor of parasite growth suggests that this structure should be further investigated in the hope of increasing the potency of this more selective inhibitor of the parasite enzyme. It seems that apparent differences in the S1 subsites of parasite and human enzymes could be exploited to design more potent and selective inhibitors for further investigation.

The results described in this chapter indicate that PfAP-M17 may be a valid antimalarial target to be considered for further investigation. The inhibition of the recombinant enzyme by bestatin confirms that PfAP-M17 is a target for this compound, supporting the results obtained with transgenic parasites over-expressing the protein (58). A clear correlation was seen between the inhibition of growth of cultured parasites and inhibition of leucine aminopeptidase activity of both cytosolic extract and recombinant tPfAP-M17 by the compounds tested here. Inhibition of PfAP-M17 in concert with other targets should probably be considered as some degree of redundancy with other aminopeptidases e.g. PfAP-M1 seems quite likely.

The results outlined here also hint that inhibition of PfAP-M1 may have a negative effect on parasite growth as many of the compounds demonstrated good inhibition of the alanine aminopeptidase activity of parasite extract. Inhibition of PfAP-M1 was not entirely unexpected, as although these compounds were designed as specific M17 aminopeptidase inhibitors, some of them had been seen to have some activity against the mammalian M1-family enzyme aminopeptidase N (42). Owing to the lack of active recombinant PfAP-M1 and the difficulty and low yield of its purification (3, 54), we did not test this enzyme in complete isolation from PfAP-M17 so these data cannot be used to validate PfAP-M1 as an antimalarial target. However, the following chapter describes further investigation into the potential of PfAP-M1 as a target by the assessment of the antimalarial and anti-aminopeptidase activity of a series of compounds designed as inhibitors of M1-family aminopeptidases.

The homology model of PfAP-M17 generated here provides a good general framework of the structure of the enzyme. Despite the relatively low level of identity between the bovine lens M17 aminopeptidase and the *P. falciparum* one it was clear that
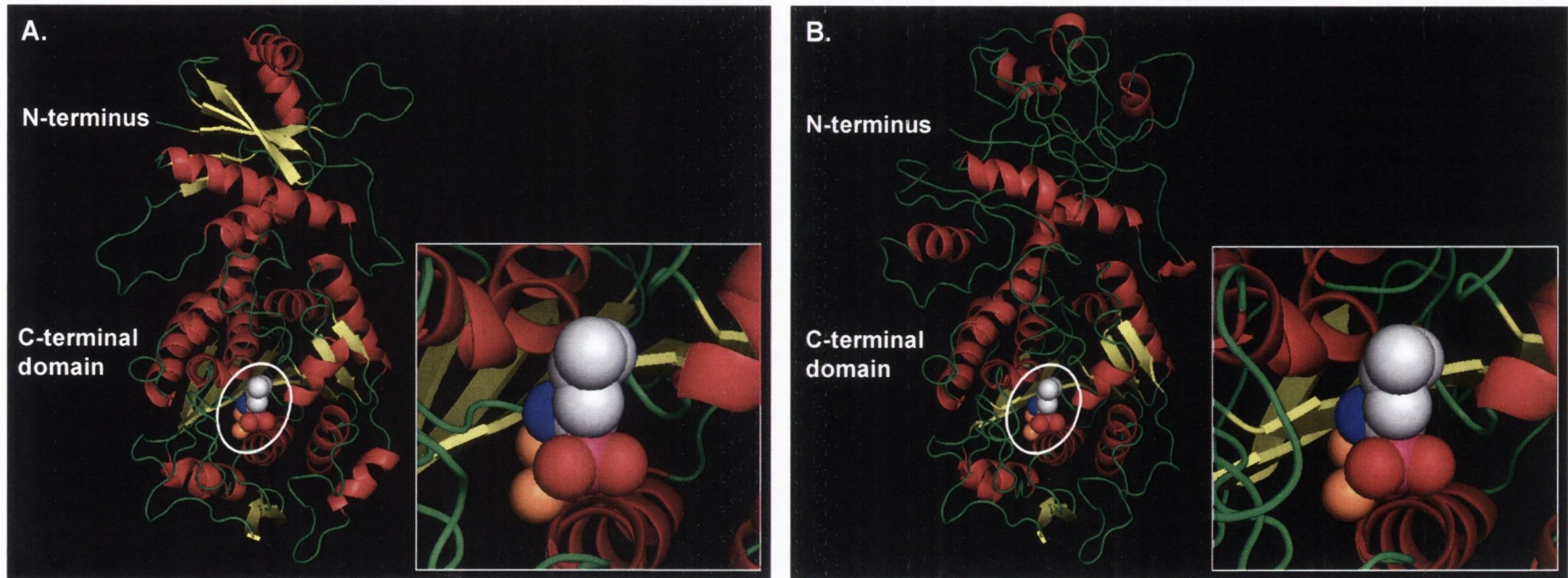
Figure 5.5. Ribbon diagrams of the structures of the bovine lens M17 leucine aminopeptidase (blLAP) and the *P. falciparum* M17 leucine aminopeptidase (PfAP-M17) homology model. Regions coloured red, yellow and green indicate α-helices, β-sheets and loops, respectively. The N-termini of the structures are indicated, as are the C-terminal domains. The inhibitor LeuP (space-filled and circled) can be seen in the active sites (enlarged in the boxed insets), with the carbon, oxygen, nitrogen and phosphorous atoms coloured grey, red, blue and pink, respectively, while the zinc atoms are coloured gold. **A.** The crystal structure of bovine lens M17 aminopeptidase with the LeuP inhibitor bound (PDB ID 1LCP) was used as the template for homology modelling of PfAP-M17. **B.** Homology model of PfAP-M17 based on the crystal structure of bovine lens M17 aminopeptidase (1LCP). The position of LeuP in the active site is based on its position in 1LCP.
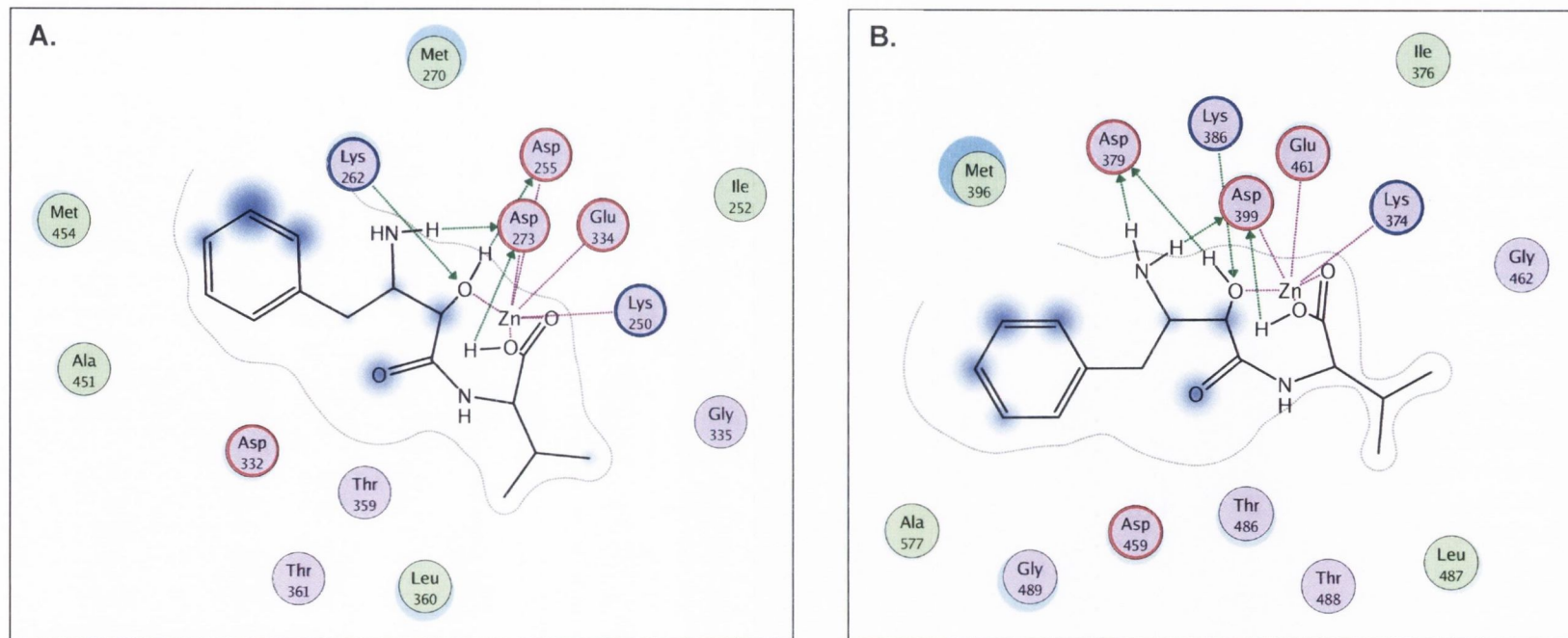
Figure 5.6. Predicted interactions (by MOE software) between bestatin and **A.** the bovine lens M17 aminopeptidase (blLAP) and **B.** the homology model of the *P. falciparum* M17 aminopeptidase (PfAP-M17). The interactions between bestatin and residues in the active site of blLAP and the PfAP-M17 model proposed by the homology modelling software are shown. Green arrows indicate side-chain acceptors and donors while purple lines indicate metal contacts. Residues ringed in red and blue are acidic and basic, respectively, while those coloured purple and green are polar and hydrophobic, respectively. Areas of the inhibitor molecule shaded in blue indicate exposed regions.
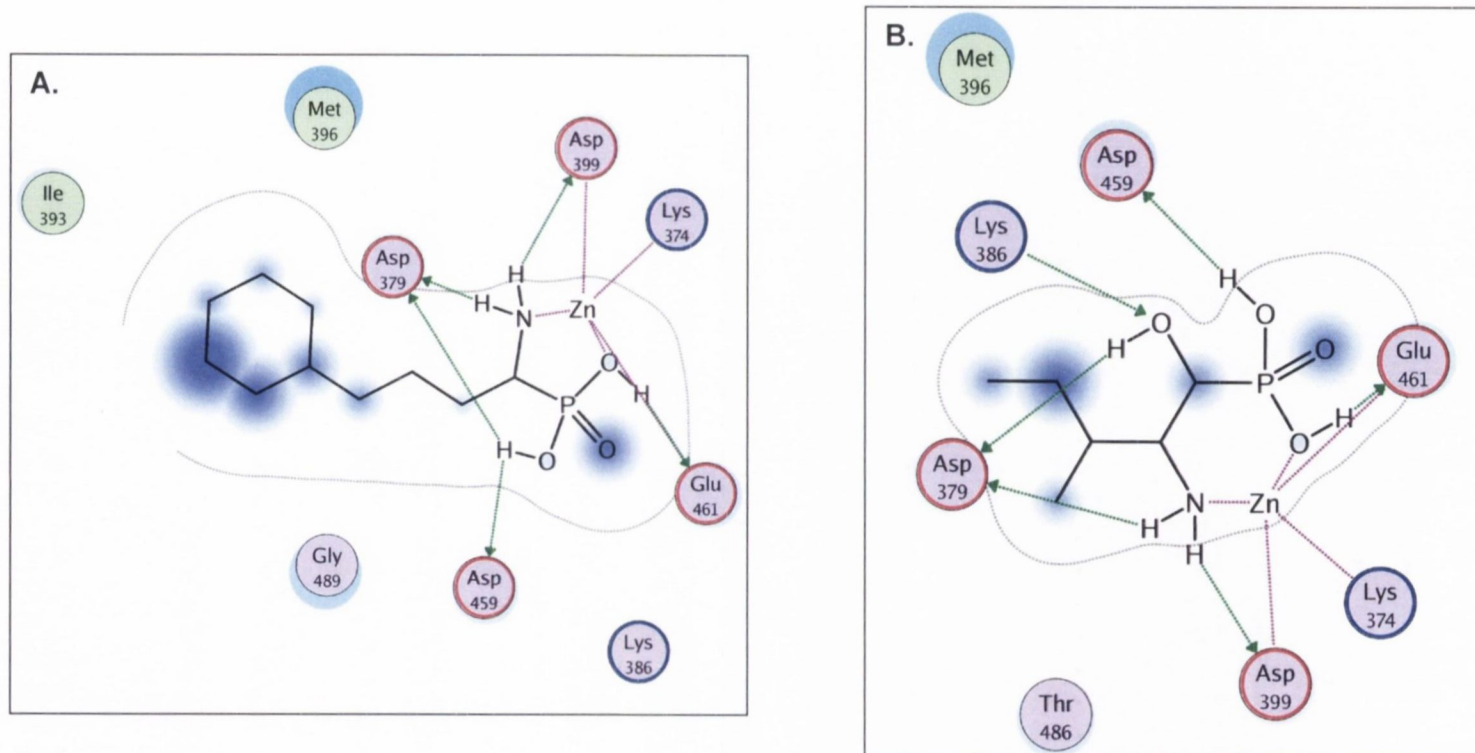
Figure 5.7. Predicted interactions (by MOE software) between the homology model of the *P. falciparum* M17 aminopeptidase (PfAP-M17) and **A.** D14 and **B.** D25. The interactions between the residues in the active site of the PfAP-M17 model and the inhibitors D14 and D25, proposed by the homology modelling software, are shown. Green arrows indicate side-chain acceptors and donors while purple lines indicate metal contacts. Residues ringed in red and blue are acidic and basic, respectively, while those coloured purple and green are polar and hydrophobic, respectively. Areas of the inhibitor molecule shaded in blue indicate exposed regions.

the most important residues were highly conserved and that overall the N-terminal region of the proteins were quite similar. The PfAP-M17 model was somewhat useful when it was used to investigate inhibitor binding, as differences in their activities could not be accounted for by differences in predicted interactions between them and the aminopeptidase model. However, it may be that a homology model of PfAP-M17 will not be suitable for investigation of novel inhibitors unless a more closely related template is crystallised, as it has been suggested that a sequence identity of at least 70% is needed for ligand docking and drug design since only medium accuracy models are generated from template sequences with identity of 30–50% (9). As mentioned in the previous chapter, producing sufficient recombinant PfAP-M17 of suitable quality for crystallisation studies would be ideal to overcome this and would aid in the design of novel inhibitors. The structure could then be used to screen known inhibitors of PfAP-M17 to develop a pharmacophore i.e. a template structure that contains all elements necessary for inhibition of the particular target. This would enable the structure-based design of PfAP-M17 inhibitors.

Chapter 6

Anti-Malarial and Anti-Aminopeptidase
Activities of M1 Aminopeptidase Inhibitors

6.1. INTRODUCTION

The majority of this work has so far concentrated on the *P. falciparum* M17 aminopeptidase, PfAP-M17. However, the M1 aminopeptidase, PfAP-M1, cannot be ruled out as a possible drug target as enzymes in this family are also susceptible to bestatin. The enzyme has a predicted size of 126 kDa but has been suggested to be processed to two smaller fragments, 96 and 68 kDa in size (54). Partially-purified enzyme was most active *in vitro* on substrates containing lysine, closely followed by alanine, arginine and leucine (3). It had a neutral pH optimum, was activated by Zn^{2+}, and was inhibited by the metal chelator 1,10-phenanthroline and by bestatin and amastatin. PfAP-M1 was found to be expressed during the trophozoite and schizont stages and to be located predominantly in the cytosol. It was also found as condensed spots in mature schizonts and merozoites, leading the authors to suggest that it may play a role in erythrocyte re-invasion by parasites in addition to its proposed role in haemoglobin degradation (3).

A number of inhibitors of M1 aminopeptidases have been described (see (14, 179) for extensive reviews) in relation to the treatment of a variety of conditions ranging from various cancers to inflammatory diseases like arthritis and central nervous system disease like Alzheimer's. Most of these are peptidomimetics that are thought to act as transition state analogues, binding to the Zn^{2+} in the enzymes' active sites. They include natural inhibitors like bestatin (163) and amastatin (6) and other related compounds isolated from different *Streptomyces* species. Synthetic peptide inhibitors include α-aminoaldehydes (5), β-aminothiols (16) and α-aminophosphonates (63). However, peptide-based inhibitors have many clinical drawbacks like low bioavailability and short half-lives (179); therefore the development of non-peptide compounds is an active area. This smaller group of M1 aminopeptidase inhibitors includes cyclic imides (114), α-keto amides (121), flavone-8-acetic acid derivatives (99) and the 3-amino-2-tetralone inhibitors (140) (see Figure 6.1 for structure) that are the starting point of the compounds described in this work.

Previous work on inhibitors of PfAP-M1 includes a series of non-peptidic, quinoline-based compounds containing an isobutyl group to mimic the leucine side chain and carboxylic acids or hydroxamate groups for binding of the catalytic metal. These inhibitors were also designed to inhibit haemozoin formation by the parasites, via the quinoline moiety. Three of the hydroxamates (compounds 33, 34 and 35) had good antimalarial and anti-PfAP-M1 activity, inhibiting parasite growth with IC_{50} values of 178, 317 and 151 nM, respectively and enzyme activity with values of 2500, 854 and 1540 nM, respectively. However, the specificity of the inhibitors needed improving as they were

nearly as active against the porcine kidney aminopeptidase N (AP-N) (IC_{50} = 1345, 28 and 1628 nM, respectively) (52). The development of a series of malonic hydroxamates did produce inhibitors more selective for PfAP-M1 (compounds 57 and 66), with IC_{50} values of 27 and 6 nM, respectively, compared with 3616 and 1372 μM, respectively for mammalian APN, but these compounds had modest antimalarial activities (IC_{50} = ~50 μM and ~20 μM, respectively) (51).

The work in this chapter describes the antimalarial and anti-aminopeptidase activities of a series of 3-amino-2-tetralone and 3-amino-2-benzosuberone derivatives (containing benzene rings fused to a cyclohexane or cycloheptane ring, respectively) that were designed to be specific inhibitors of M1 aminopeptidase. Some of these compounds have previously been tested ((2), C. Tarnus, personal communication) against a number of mammalian aminopeptidases including two M1-family members, aminopeptidase N (AP-N) and leukotriene A_4 hydrolase (LTA_4H), and cytosolic leucine aminopeptidase, an M17-family member. It was hoped to validate PfAP-M1 as an antimalarial drug target and establish structure-antimalarial activity relationships for these compounds.

6.2. RESULTS

6.2.1. Inhibition of growth of cultured *P. falciparum* by 3-amino-2-tetralone and 3-amino-2-benzosuberone derivatives

The series of 3-amino-2–tetralone and 3-amino-2-benzosuberone derivatives was tested against asynchronous, cultured *P. falciparum* (Table 6.1), using the lactate dehydrogenase assay (106) as described in section 2.2.5. Dose-response curves were constructed from absorbance readings after 72 h incubation and the 50% inhibitory concentrations (IC_{50}) determined graphically. All of the compounds had measurable activity. They demonstrated varying potencies against the parasites, ranging from only ~20–40% inhibition of growth at the highest concentrations possible to low micromolar IC_{50}.

The most active compounds were T18, T16, T17 and T12 (IC_{50} = 11, 15, 15 and 16 μM, respectively). Compounds T13, T6, T4, T5, T14 and T15 were also relatively good inhibitors of parasite growth with IC_{50} values in the range of ~25–30 μM. Percent inhibition of parasite growth was calculated for those compounds that did not inhibit the parasite growth to 50% at the highest concentration tested i.e. for which it was not possible to calculate an IC_{50}. T1, T2, T3, T8, T9 and T11 were found to inhibit parasite growth by only ~20–40% at these highest achievable concentrations (64 μM or 128 μM).
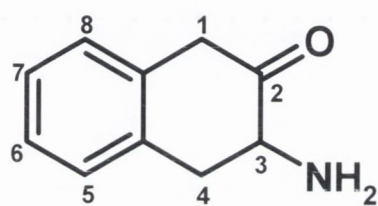
Figure. 6.1. Structure of 3-amino-2-tetralone. The various positions that can be substituted are numbered 1–8.

TABLE 6.1. Activities of 3-amino-2-tetralone and 3-amino-2-benzosuberone derivatives against cultured *P. falciparum*

Compound	Structure	IC$_{50}$ (μM)[a]	% Inhibition of parasite growth[b]
T18		11	-
T16		15	-
T17		15	-
T12		16	-
T13		24	-
T6		25	-
T4		26	-
T5		27	-
T14		30	-
T15		31	-

TABLE 6.1. Activities of 3-amino-2-tetralone and 3-amino-2-benzosuberone derivatives against cultured *P. falciparum* (continued)

Compound	Structure	IC$_{50}$ (µM)[a]	% Inhibition of parasite growth[b]
T7		45	-
T10		54	-
T9		>64	31 ± 7
T11		>64	22 ± 3
T1		>128	37 ± 5
T3		>128	32 ± 7
T8		>128	32 ± 14
T2		>128	18 ± 9

[a] Geometric mean IC$_{50}$ were calculated from six determinations from three separate experiments.

[b] Compounds for which no IC$_{50}$ could be calculated are shown in order of increasing inhibition of parasite growth at a fixed, highest possible concentration. Results represent the arithmetic mean ± SEM (n ≥ 6) of the percent inhibition of parasite growth at the highest concentration of compound tested (i.e. 64 µM for T9 and T11 and 128 µM for all others).

- not applicable

6.2.2. Inhibition of aminopeptidase activity of *P. falciparum* parasite extract

The ability of the series of compounds to inhibit the aminopeptidase activities of parasite cytosolic extracts was investigated. As already discussed in the previous chapter (section 5.2.3), parasite extract is expected to contain both PfAP-M1 and PfAP-M17 activities but analysis of extract activity against Ala-AMC in the absence of $CoCl_2$ will measure mostly the activity of the former. Compounds were tested at 10 μM, and any that inhibited to a good extent were also tested at 0.1 μM, by incubating them with cytosolic extract before addition of the fluorogenic substrate, Ala-AMC or Leu-AMC. The range of activities against AAP and LAP activity seen is outlined in Table 6.2 where the compounds are listed in order of decreasing antimalarial activity (i.e. by increasing IC_{50}: see Table 6.1).

Looking first at the inhibition of AAP activity, the most active compound was T18, which completely abolished the extract AAP activity at 10 μM and was the only compound to have a substantial effect at 0.1 μM. This was followed by T17, T14, T16 and T15 inhibited the activity by ≥ 79%. The least effective compounds were T11, T8, T9, T7, T2 and T4, inhibiting the AAP activity by < 5% at 10 μM.

There is quite good agreement between the inhibition of the AAP and LAP activities of the extract. However, the compounds tested at 0.1 μM, especially T18 and T17, inhibited the LAP activity to a slighter higher extent than the AAP activity. As some of this LAP activity is likely to be due to the enzyme activity of PfAP-M17 this might indicate that some of the compounds have some activity against this aminopeptidase as well.

Although the best aminopeptidase inhibitor was also the strongest antimalarial, in other respects, there was no obvious relationship between the antimalarial activity of these compounds and their aminopeptidase inhibition. This is clear from the lack of corresponding trend in decreasing anti-aminopeptidase activity as the antimalarial activity is seen to decrease in Table 6.2 and can also be seen in a plot of percent inhibition of AAP activity (at 10 μM) vs log IC_{50} (Figure 6.2).

6.2.3. Inhibition of leucine aminopeptidase activity of recombinant tPfAP-M17

The lack of relationship between the antimalarial activity of the compounds and the inhibition of the AAP and LAP activities suggested that some of the compounds might be acting against another target, one possibility being the *P. falciparum* M17 aminopeptidase. Therefore, a selection of the compounds was assessed for their ability to inhibit the leucine aminopeptidase activity of the recombinant *P. falciparum* M17 leucine aminopeptidase (tPfAP-M17, a truncated (58-kDa) form of the protein produced in baculovirus-infected

insect cells, described in section 4.2.4.1) (Table 6.3). The compounds were tested at 10 μM by pre-incubation with the recombinant protein, in the presence of $CoCl_2$, for 10 min, prior to the addition of Leu-AMC. Of the five compounds tested only one demonstrated any inhibition of the activity of the PfAP-M17 enzyme. T12 inhibited the activity by nearly 50% but T18, T4, T1 and T8 inhibited it by ≤ 5%. This inhibition of PfAP-M17 by T12 may account for the increased antimalarial activity of this compound compared to other compounds that inhibit the extract to a similar degree, e.g. T10. It is interesting that although T18 did not inhibit the recombinant to any degree it was capable of inhibiting the overall LAP activity of the extract by 98%.

The lack of availability of recombinant PfAP-M1 and the difficulties associated with purifying the enzyme from parasites (54) meant that it was not possible to assess the activity of these compounds against this peptidase in isolation.

6.3.   DISCUSSION

The series of compounds examined here was derived from the cyclised phenylalanine derivative, 3-amino-2-tetralone. Previous work indicated that the carbonyl group in position 2 and the amino group in position 3 were important for inhibitor activity, at least against AP-N, and lead the authors to suggest that this conformationally constrained bicyclic structure acts as a bidentate ligand, with the functional groups in these positions interacting with the catalytic metal ion (140). The compounds tested here consisted of one set of inhibitors (T1–T8) containing the usual cyclohexane of 3-amino-2-tetralone attached to the benzene ring and one, the 3-amino-2-benzosuberone derivatives, with a heptane ring in its place (T9–T18). The first group contains some derivatives in which the carbonyl oxygen was replaced with nitrogen (T3–T6) and only one compound, T2, contained the two functional groups in positions 2 and 3. T9 and T11 were the only two compounds in the cycloheptane group that did not maintain these functional groups. It was assumed that the series was targeting PfAP-M1 as they were designed to be M1 inhibitors.

Looking initially at the antimalarial activity of the compounds (Table 6.1) it can be seen that the most active ones were aminobenzosuberone (cycloheptane) derivatives. T18, T12 and T13 contain phenyl groups, at the end of a long carbon chain in the case of the latter two agents, while T17 and T16 contain bromine atoms in positions 6 and 9, respectively. The next three best compounds contain the original cyclohexane ring but lack

TABLE 6.2. Inhibition of aminopeptidase activity of parasite cytosolic extract by 3-amino-2-tetralone and 3-amino-2-benzosuberone derivatives

Compound	% inhibition of parasite extract[a]			
	AAP activity		LAP activity	
	10 µM	0.1 µM	10 µM	0.1 µM
Bestatin	97 ± 0	29 ± 2	98 ± 1	33 ± 2
T18	100 ± 0	15 ± 1	98 ± 0	79 ± 1
T16	81 ± 5	1 ± 3	79 ± 2	13 ± 3
T17	98 ± 1	0 ± 2	97 ± 1	39 ± 4
T12	56 ± 10	0 ± 0	34 ± 3	1 ± 0
T13	8 ± 4	-	14 ± 2	-
T6	14 ± 6	-	11 ± 7	-
T4	3 ± 3	-	13 ± 6	-
T5	9 ± 4	-	12 ± 8	-
T14	93 ± 2	2 ± 2	95 ± 1	13 ± 2
T15	79 ± 1	0 ± 3	82 ± 1	13 ± 3
T7	2 ± 3	-	2 ± 2	-
T10	59 ± 3	0 ± 1	50 ± 5	13 ± 2
T9	1 ± 2	-	1 ± 1	-
T11	0 ± 4	-	0 ± 1	-
T1	68 ± 0	0 ± 1	62 ± 2	14 ± 2
T3	7 ± 2	-	12 ± 6	-
T8	1 ± 2	-	2 ± 3	-
T2	3 ± 4	-	8 ± 8	-

[a]Results represent the mean ± SEM (n ≥ 4) of the alanine aminopeptidase (AAP) activity and leucine aminopeptidase (LAP) of parasite cytosolic extract after incubation with compounds at 10 µM or 0.1 µM.

- not determined.
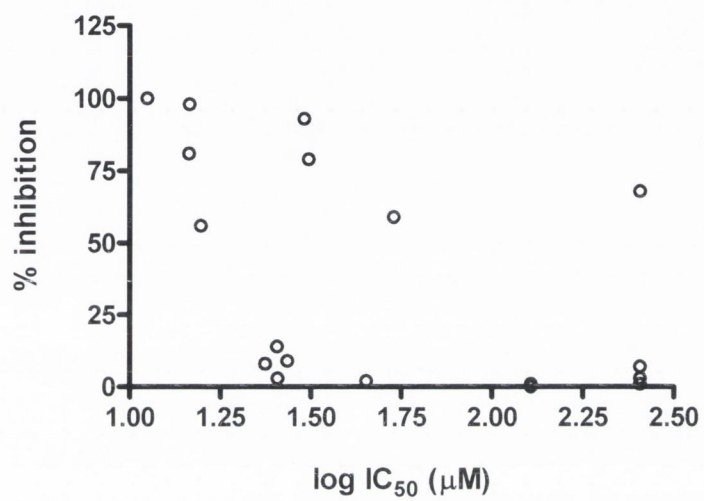
Figure 6.2. Plot of antimalarial activity and inhibition of parasite extract alanine aminopeptidase activity. The percent inhibition of parasite extract of the eighteen compounds (at 10 μM) was plotted against their log IC_{50} for parasite growth. No clear relationship was apparent.

TABLE 6.3. Inhibition of aminopeptidase activity of parasite extract and recombinant tPfAP-M17

Compound	% Inhibition of parasite extract[a]		tPfAP-M17 LAP activity[b]
	AAP activity	LAP activity	
T18	100 ± 0	98 ± 0	0 ± 4
T12	56 ± 10	34 ± 3	47 ± 1
T4	3 ± 3	13 ± 6	0 ± 3
T1	68 ± 0	62 ± 2	5 ± 4
T8	1 ± 2	2 ± 3	5 ± 11

[a]Results represent the mean ± SEM of alanine aminopeptidase (AAP) and leucine aminopeptidase (LAP) activity of parasite cytosolic extract ($n \geq 4$) after incubation with compounds at 10 µM.

[b]Results represent the mean ± SEM of recombinant tPfAP-M17 ($n = 2$) after incubation with compounds at 10 µM in the presence of $CoCl_2$ (1 mM).

the carbonyl oxygen in position 2 (T6, T4 and T5). They contain a phenyl group attached to a carbon side chain and increasing the length of this chain does not affect the activity.

Of the compounds at the bottom of the table T8, T9 and T11 do not contain the amine (in position 3) and T9 and T11 lack the carbonyl group (in position 2), that were seen previously to be required for M1 aminopeptidase inhibition in the cyclohexane tetralone derivatives (140). T1 is a negatively charged hydroxamic acid derivative and may demonstrate a lack of inhibition of parasite growth due to a difficulty entering cells. Overall the potency of the compounds is comparable to the series of M17 aminopeptidase inhibitors (α-aminoalkylphosphonates and phosphonopeptide derivatives) described in the previous chapter.

Varying degrees of correlation between anti-malarial and anti-aminopeptidase activity are seen with this series of compounds. They can be generally divided into four separate groups. Firstly, there are those that had relatively good levels of both activities, including T18, T16, T17, T14, T15 and T10. These compounds are aminobenzosuberone derivatives, containing the amine and carbonyl groups in positions 2 and 3, respectively. The presence of the heptane ring in all of the inhibitors indicates that this may be a useful modification to target M1 aminopeptidase. These compounds are also good inhibitors of AP-N (Table 6.4).

Secondly, there are the compounds that had relatively poor levels of both activities. This group includes T3, T8, T2, T11 and T9. If these compounds are targeting PfAP-M1 then these compounds would presumably be poor inhibitors of aminopeptidase activity for the same reasons that they have poor antimalarial activity.

The third group of compounds demonstrated a poor correlation between anti-malarial and anti-aminopeptidase activity, having relatively good activity against parasite growth but modest or poor activity against the extract aminopeptidase i.e. T12, T13, T6, T4, T5 and T7. Most of the compounds (the first five in the list above) contain a phenyl group at the end of a long hydrocarbon chain. T12 and T13 have the side chain in position 1 of their heptane ring with the latter containing an extra CH_2 group compared to the former. As T12 does demonstrate some inhibition of the parasite aminopeptidase activity it is possible that this addition to the sidechain length (in T13) results in one which is too long to be accommodated by the enzyme. T4, T5 and T6 have the chain in position 2 of the original 6-membered ring. It has been suggested that 3-amino-2-tetralone derivatives with phenyl substitutions like this may interact with the S1 pocket of M1 aminopeptidase (140) that tends to favour aromatic side chains but this is obviously not the case here, and alterations in carbon side chain length did not measurably increase the anti-aminopeptidase

81

activities of these compounds, with all inhibiting to < 15% at 10 μM. All of these compounds were also quite poor inhibitors of all other aminopeptidases tested (Table 6.4) although they were generally more selective for M1 aminopeptidases (AP-N and LTA$_4$H) and in this case the longer side chain (T13) was necessary to reach the highest level of inhibition (K_i = 12 μM). Overall, it is unclear why these compounds should be good inhibitors of parasite growth but it seems likely that they are active against some other target, possibly another metallopeptidase. For example, T7, as a cyclic hydroxamic acid may exert its inhibitory effect by acting as a non-specific chelator.

The final group has only one member, T1, a compound with poor anti-malarial activity but good anti-aminopeptidase activity. As already mentioned, this compound is a negatively charged hydroxamic acid derivative and may not be able penetrate the parasite cells to reach the PfAP-M1 enzyme, if, as indicated by the enzyme assay, it does target this enzyme.

The lack of correlation in some cases between antimalarial and anti-aminopeptidase activity prompted the testing of a selection of the compounds, one from each of the above-mentioned groups, against recombinant PfAP-M17. It is well-known that there are compounds, e.g. bestatin, that demonstrate inhibition across these two aminopeptidase families. T1, T4, T8 and T18 showed no effect against tPfAP-M17 (at 10 μM), confirming that the compounds are more likely to be targeting PfAP-M1 than PfAP-M17. However, the lack of inhibition of the recombinant tPfAP-M17 by T18 might be unexpected in light of its ability to inhibit the overall LAP activity of the parasite extract very highly. This might suggest that PfAP-M17does not contribute to the LAP activity in the parasite extract but conflicts with the results seen in the previous chapter that suggest that the inhibition of the LAP activity of PfAP-M17 does effect the growth of parasites. T12 did demonstrate some inhibition against PfAP-M17, in contrast to the other four compounds. Therefore, it is possible that it is targeting both enzymes to some degree. Its inhibition of AAP activity suggests that it cannot only be inhibiting PfAP-M17. T12 is a cycloheptane derivative of a compound previously found to have good activity against AP-N (140). It is also still possible that this compound is acting against another target altogether, separately or in concert with its inhibition of PfAP-M1 and PfAP-M17.

Unfortunately, there appears to be a good correlation between the inhibition of parasite and mammalian M1 aminopeptidase (AP-N). The top five compounds in terms of both antimalarial activity and anti-aminopeptidase activity were T18, T16, T17, T14 and T15 with IC$_{50}$ values of 11, 15, 15, 30 and 31, respectively and AAP percent inhibition values, at 10 μM, of 100, 81, 98, 93 and 79, respectively. This corresponds to the best five

Table 6.4. Inhibition of LAP activity of mammalian aminopeptidases[a]

Compound	K_i (µM)		
	AP-N	LTA$_4$H	LAPc
T18	0.007	30	-
T16	0.02	ND	-
T17	0.04	>100	-
T12	22	>1000	-
T13	12	>1000	-
T6	80	30	>100
T4	260	500	>100
T5	55	8	>100
T14	0.05	>100	-
T15	0.2	>1000	-
T7	>1000	>1000	>1000
T10	1	>1000	-
T9	>1000	>1000	-
T11	>1000	>1000	-
T1	4	>1000	10
T3	130	>1000	>1000
T8	>1000	>1000	1000
T2	>1000	>1000	>1000

[a]Results from Schalk *et al* (140) and C. Tarnus (personal communication). AP-N = porcine kidney aminopeptidase N, LTA$_4$H = human recombinant leukotriene A$_4$ hydrolase, LAPc = bovine kidney cytosolic leucine aminopeptidase.

- not determined

inhibitors of AP-N with K_i values of 0.007, 0.02, 0.04, 0.05 and 0.2 µM, respectively. Therefore, while T18 is a very good inhibitor of the parasite AAP activity it is also very active against its mammalian counterpart. This lack of selectivity is an area that would need to be addressed were this series of compounds to be contemplated as a basis for antimalarial drug development.

In summary, in terms of identifying structures for future development of inhibitors, the amine and carbonyl groups were confirmed to be important for activity here. In addition, the benzsuberone compounds (containing the heptane ring) demonstrated better activity than those with the original cyclohexane structure. Substitutions with phenyl groups were generally more active against cultured parasites but may be active against another target.

Overall, it cannot be concluded from this work whether targeting the M1 aminopeptidase of *P. falciparum* is a valid route for development of chemotherapeutic agents. While most of the compounds that inhibited the extract aminopeptidase activity did demonstrate some degree of antimalarial activity (with T1 being the exception) no definite relationship between inhibition of parasite growth and aminopeptidase activity could be established. In addition, the degree of parasite growth inhibition is not necessarily reflected in the aminopeptidase inhibition e.g. T18 might be expected to have a lower IC_{50} considering its abolition of extract AAP activity. Issues regarding uptake into the erythrocyte and parasite may account for this and the lack of relationship observed for some compounds. However, the lack of anti-aminopeptidase activity displayed by some compounds with relatively good antimalarial activity cannot be explained by this.

Other data indicate that PfAP-M1 may be an an important peptidase for the parasite and, therefore, a valid antimalarial target. This includes the inability to produce knock-out strains of *PfAP-M1*, described in chapter 3 (section 3.2.5) and by others (36) and the apparent impairment of growth of a *PfAP-M1* antisense strain (D. Gardiner, personal communication). However, further work is needed to assess fully this peptidase as a potential drug target. It is also worth considering that the inhibition of PfAP-M1 in concert with other targets (peptidases or aminopeptidases for example), may be necessary, as it is possible that one or more of the other aminopeptidases might take over some of its functions.

Chapter 7

General Discussion

7.1.   *PLASMODIUM* AMINOPEPTIDASES

The work in this thesis describes the investigation of the aminopeptidases of *P. falciparum*, with particular emphasis on the M17 leucine aminopeptidase (PfAP-M17) of the parasite. Before beginning this work, a number of studies had provided a certain amount of information on the *Plasmodium* aminopeptidases (see Table 1.1 for a summary). It was thought that there were between one and four distinct aminopeptidase activities present in the parasite. All of the aminopeptidase activities studied were found to cleave leucine and/or alanine-containing substrates (some were only tested against one or other substrate) leading to a particular interest in the M1- and M17-family enzymes. These peptidases have often been termed alanyl and leucyl aminopeptidases, respectively, due to their expected preference for these residues. The aminopeptidase activities reported ranged between 60 and 190 kDa in size, had neutral pH optima (with many of them shown to be inactive at acidic pHs) and, as expected, most of them were inhibited by metal chelators and/or bestatin. The lack of activity of these enzymes at acidic pH raised the suggestion that they must be active in the parasite cytosol rather than the acidic digestive vacuole. In addition, studies demonstrated that digestive vacuoles isolated from *P. falciparum* contain negligible aminopeptidase activity (60, 87) and haemoglobin-derived peptides, but no amino acids, were seen to be produced in the vacuoles. This led to the belief that the target peptides of aminopeptidases must be transported to the cytosol in order to be acted on by these neutral enzymes. Controversially, this model has very recently been contradicted by work that suggests two of the aminopeptidases are active in the digestive vacuole (36).

7.2.   CHARACTERISATION OF THE *P. FALCIPARUM* M17 AMINOPEPTIDASE

One major obstacle to gaining a proper understanding of the relative importance of the different aminopeptidases in *P. falciparum* has been the expected overlapping properties of M1 and M17 aminopeptidases. The similarities between the biochemical properties of these enzymes, and, therefore, PfAP-M1 and PfAP-M17, e.g. substrate preference and susceptibility to bestatin, and the difficulties associated with the purification of these individual peptidases from parasites hindered the uncovering of the relative importance of these enzymes. In addition, initially, it seems that investigators were expecting PfAP-M17 to have a molecular mass corresponding to that of its monomer, ~68 kDa, (i.e. very similar to one of the processed forms of PfAP-M1) rather than ~408 kDa, the expected size of a hexamer.

The production of recombinant enzyme was seen as key for investigation of these enzymes independently and, quite a large amount of time and effort was invested here in attempting this. In particular, a number of avenues were employed in the hope of producing PfAP-M17 in recombinant form. The potential difficulties associated with the production of recombinant eukaryotic proteins in bacterial systems and with parasite and *Plasmodium* proteins in particular are well documented ((1, 7, 37, 50, 111, 170) and references within). A variety of reasons have been proposed for these problems with *Plasmodium* proteins including the AT-richness of the genome, leading to a codon bias quite different from prokaryotic organisms, toxicity of the proteins to host cells, incorrect folding and the fact that they are often much larger than the orthologues in other species, often due to the presence of disordered regions of low complexity.

This work demonstrates the benefits associated with the production of *P. falciparum* proteins in insect systems, as previously seen by others (111). Expression of the aminopeptidases as MBP-fusions in *E. coli* was not significantly improved by factors like altering IPTG concentration or induction times at the stationary phase or by the use of strains that are designed to overcome codon-bias problems. However, recent work on recombinant production of numerous apicomplexan parasite proteins (170) achieved quite good levels of expression using *E. coli*. Ideally, the use of an *E. coli*-based system would be preferable to baculovirus-infected insect cells as the latter is somewhat limiting in terms of yield, labour and expense while the former is relatively quick, easy and generally enables the production of large quantities of recombinant protein. The pET-system considered in this study (but not pursued fully) might be worth further investigation, particularly the vector pET-22b that enables the fusion of a C-terminal His$_6$-tag since both the PfAP-M17 (described here) and PfAP-M18 proteins (159) were successfully produced in insect cells with this type of tag. Also, this series of vectors has been used previously to produce eukaryotic M17 aminopeptidases (see Table 4.1).

The results of the characterisation of PfAP-M17 carried out in this study and with our collaborators (153) indicate that all of the *P. falciparum* aminopeptidase activity described previously (34, 60, 73, 120, 167, 169) might correspond to processed forms of PfAP-M1 or its orthologue in other *Plasmodium* species (3, 54), as many of them demonstrated activity against quite a broad range of substrates. At the very least, they were all active against alanine substrates while the recombinant enzyme data, in combination with the HPLC analysis described here and elsewhere (153), demonstrated that PfAP-M17 is not. In addition, the active proteins ranged from ~60–190 kDa in size, which is much smaller than the molecular mass corresponding to the active, hexameric form of PfAP-M17.

Therefore, it appears that this work contains the first reports on the M17 aminopeptidase of *P. falciparum*.

7.3. VALIDATION OF *P. FALCIPARUM* AMINOPEPTIDASES AS POTENTIAL ANTIMALARIAL DRUG TARGETS

The aminopeptidases of *P. falciparum* have been of particular interest, as bestatin, a known metallo-aminopeptidase inhibitor, was shown to prevent the growth of cultured parasites (120, 169). This led to the possibility of targeting them for the development of antimalarial drugs. It was unclear which aminopeptidases were targeted by bestatin but it was thought likely to be one or other of PfAP-M1 and PfAP-M17, or both. Partially-purified PfAP-M1 was found to be inhibited by bestatin, as expected (3). A decrease in bestatin susceptibility of cultured transgenic parasites over-expressing PfAP-M17 supported the suggestion that this enzyme was also a target (58). However, the level of over-expression was not quantified and an indirect effect on the expression of *PfAP-M1* due to an increase in *PfAP-M17* copy number could not be ruled out. This study has now confirmed that bestatin is active against PfAP-M17 as it inhibited the leucine aminopeptidase activity of cytosolic extract (incubated with $CoCl_2$ to boost PfAP-M17 but reduce PfAP-M1 activity) and recombinant tPfAP-M17 enzyme.

The importance of the PfAP-M1 or PfAP-M17 enzymes for parasite growth and development (as indicated by the antimalarial activity of bestatin) may be reflected in the lack of ability to produce knock-outs of either gene (described here and by Dalal *et al* (36)). If this is the case, the reduction of expression of these enzymes by the antisense method would be ideal as it should theoretically enable the examination of parasites as the enzyme expression is knocked down over time. This method was successful in reducing the expression of PfAP-M18 (159) and did apparently produce a corresponding detrimental effect on parasite growth. However, it was unsuccessful in this instance in knocking-down the expression of PfAP-M17, as no antisense strand seemed to be produced, so no conclusions could be drawn in relation to the importance of PfAP-M17 for the parasites.

The validation of PfAP-M17 as a potential antimalarial target was assisted by assaying a series of structurally-related compounds designed to be M17 inhibitors. A clear correlation was observed between the inhibition of cultured parasites and the inhibition of leucine aminopeptidase activity of cytosolic extract (incubated with $CoCl_2$). The correspondingly good inhibition of leucine aminopeptidase activity of recombinant tPfAP-

M17 by the best inhibitors supported this. The inhibition of the alanine aminopeptidase activity of the parasite extract indicated that PfAP-M1 might also be a target since PfAP-M17 does not appear to cleave this amino acid. An attempt was made to investigate this further with a series of compounds designed to be M1-family aminopeptidase inhibitors but no clear correlation was evident. In addition, the difficulty in the purification of PfAP-M1 directly from parasites (54) and the lack of availability of a recombinant makes the assessment of this enzyme more difficult. One conflicting piece of data generated by the study with these M1 inhibitors was the observation of the ability of one of them, T18, to almost completely abolish (by 98%) the LAP activity of the parasite extract while having no effect on the LAP activity of the recombinant tPfAP-M17. This raises a question about the contribution of PfAP-M17 to the LAP activity measured in the parasite extract. However, as the results described above do indicate that the enzyme is important and that inhibition of its LAP activity corresponds to inhibition of parasite growth, this issue remains unclear.

It might seem that PfAP-M1 may be a more important aminopeptidase for the parasites in terms of the numbers of amino acids it can cleave. However, recent work by Martin and Kirk (108) may indicate an importance for PfAP-M17 even with its relatively narrow substrate specificity. In contrast to previous work (40) *P. falciparum* 3D7 parasites have recently been demonstrated to be capable of surviving in culture with only isoleucine supplied in the medium (36, 100), the only amino acid not found in human haemoglobin. Martin and Kirk demonstrated that isoleucine is transported into the parasite via an initial, rapid ATP-independent process and a more gradual ATP-dependent manner, presumed to be a new permeability pathway induced by the parasite. They found that leucine was a substrate for the transporter and that extracellular isoleucine can be exchanged for intracellular leucine to enable the uptake of the former (108). This may explain why there are two enzymes in the parasite capable of releasing leucine and indeed, why one of these seems almost solely dedicated to the release of this amino acid. If isoleucine is the only amino acid required to be supplied exogenously for parasite survival and if the influx of this amino acid relies on sufficient intracellular leucine, then it would make sense that the parasite would have a back-up.

In contrast, recombinant PfAP-M18 seems not to be affected by bestatin ((36), J. Lowther, personal communication), as is expected for an M18-family enzyme. Overall, the importance of PfAP-M18 for the parasites is unclear. Parasite extract has been demonstrated to cleave aspartate and glutamate residues from synthetic peptides corresponding to those derived from endopeptidase cleavage of haemoglobin (60). The

lack of ability of cleavage of aspartate and glutamate substrates by recombinant PfAP-M17 described in this study and PfAP-M1 purified from parasites (3) indicates that PfAP-M18 is the only enzyme capable of acting on these amino acids. As these residues make up just over 10% of the amino acids of human haemoglobin (see Figure 7.1) this would suggest that this enzyme should be important for the process of haemoglobin degradation and, therefore, for the parasites in general. This is supported by work involving the reduction of expression of the gene encoding this enzyme by transfection of parasites with an antisense plasmid (159). In contrast, experiments attempting to knock out all four *P. falciparum* aminopeptidases were only capable of producing parasites deficient in PfAP-M18 (36). In addition, no antimalarial activity was observed by compounds that could inhibit recombinant PfAP-M18 (159). Therefore, this would indicate that the enzyme is not essential for parasite survival, possibly due to a redundancy of function, although it seems unlikely that any of the other aminopeptidases identified in the parasite could carry out the cleavage of these acidic residues. Further investigation of this enzyme is needed to establish its importance for the parasites.

PfAP-M24 is less well characterised than any of the other aminopeptidases and as such its role in *P. falciparum* is less clear than the others. Aminopeptidases of this family (M24B) are involved in cleaving N-terminal residues linked to proline in peptides (as small as tripeptides, but not dipeptides). As this linkage to proline is thought to protect residues from the action of general aminopeptidases (33) it is possible that PfAP-M24 may be needed by the parasites to enable the continued action of other *P. falciparum* aminopeptidases on oligopeptides with proline in the second position. The inability of Dalal *et al* to knock out this enzyme led them to suggest that it, like PfAP-M1 and PfAP-M17, might be important for the parasites' survival (36). In contrast, however, the lack of antimalarial activity of apstatin, an M24 aminopeptidase inhibitor (128), observed in our lab (IC_{50} >128 µM: C. Gavigan, PhD thesis, Trinity College Dublin, 2001) would indicate that this enzyme may not be very important. However, while apstatin is known to generally inhibit this type of aminopeptidases, its action on PfAP-M24 specifically is unknown. It would be useful to produce this enzyme recombinantly to enable the assessment of apstatin (and other analogues (105)) against it and examine any correlation with antimalarial activity.

7.4.   THE FUNCTIONAL ROLES OF AMINOPEPTIDASES IN *P. FALCIPARUM*

While it does seem that the aminopeptidases of *P. falciparum* are important for the parasite it is still not absolutely clear what exact functions they carry out. The most likely suggested role is an involvement in the processing of small oligopeptides, including dipeptides, to free amino acids as part of the terminal stages of parasite haemoglobin degradation. Evidence to support this comes mostly from previous work carried out in our lab and includes the finding that aminopeptidase activity is maximal at the trophozoite stage, i.e. the point of maximal haemoglobin digestion, and that aminopeptidase inhibition by bestatin was most active at the late ring/early trophozoite stage. Most interestingly, this work demonstrated the ability of partially-purified aminopeptidase to cleave synthetic peptides corresponding to those produced by the action of endopeptidases in the digestive vacuole (60). In addition, the observed synergy between aminopeptidase and aspartic and cysteine peptidase inhibitors (bestatin, pepstatin, and E-64 and benzyloxycarbonyl-phenyl-alanyl-alanyl diazomethylketone, respectively) (60) indicated that these peptidases may share a common pathway i.e. haemoglobin degradation. However, the possibility that this shared pathway is a different process distinct from haemoglobin digestion cannot be ruled out, especially in light of the fact that not all of the aspartic and cysteine peptidases (plasmepsins and falcipains, respectively) are thought to be involved in haemoglobin degradation. Only four out of the ten plasmepsins (11) and only two out of four falcipains (146) are considered to be active in this pathway, with one of the latter actually thought to be important for invasion instead.

A proposed model for aminopeptidase activity in haemoglobin degradation is outlined in Figure 7.1. Studies with synthetic peptides based on some of the expected products of endopeptidase cleavage of haemoglobin indicated that parasite extract can cleave a wide variety of residues including alanine, leucine, phenylalanine, arginine, lysine, serine, tyrosine, threonine, valine and proline. Aspartate and glutamate were also readily cleaved while the cleavage of histidine and asparagine were found to be quite low (60). A model for aminopeptidase activity on oligopeptides produced in the digestive vacuole would involve broad-spectrum cleavage of residues by PfAP-M1, which was found to cleave the first eight residues of those listed above (54). More specific activity might be carried out by the other aminopeptidases with PfAP-M17 cleaving leucine, phenylalanine and threonine and tyrosine to some degree and PfAP-M18 cleaving only the aspartate and glutamate residues. PfAP-M24 may unblock peptides that other aminopeptidases cannot act on by cleaving residues attached to proline. Dalal *et al* suggest that this enzyme may act in concert with the dipeptidyl aminopeptidase identified in the digestive vacuole (86) since this enzyme cannot remove dipeptides with proline in the

A.

B.
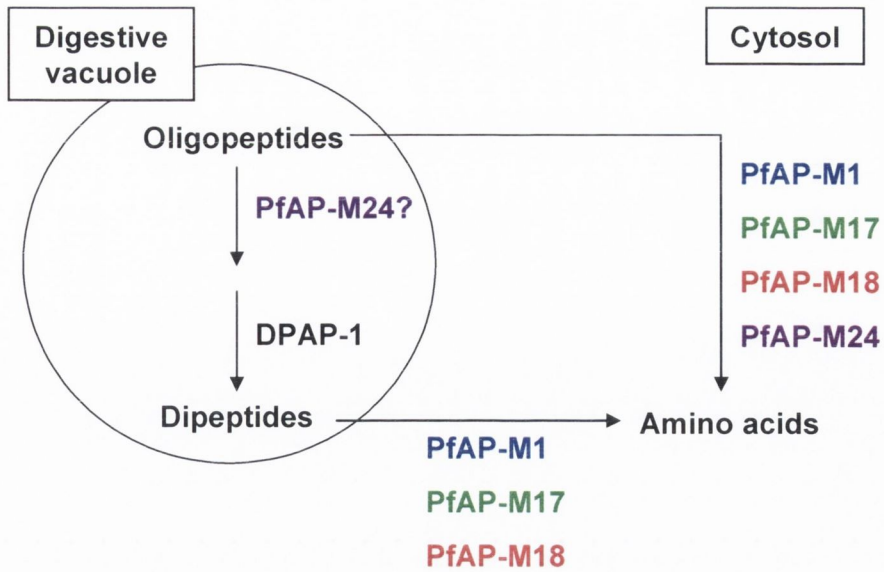
α-chain: VLSPADKTNVKAAWGKVGAHAGEYGAEALERMFLSFPTTKTYFPHFDLSHG
              AQVKGHGKKVADALTNAVAHVDDMPNALSALSDLHAHKLRVDPVNFKLLSH
              CLLVTLAAHLPAEFTPAVHASLDKFLASVSTVLTSKYR

β-chain: VHLTPEEKSAVTALWGKVNVDEVGGEALGRLLVVYPWTQRFFESFGDLSTP
              DAVMGNPKVKAHGKKVLGAFSDGLAHLDNLKGTFATLSELHCDKLHVDPEN
              FRLLGNVLVCVLAHHFGKEFTPPVQAAYQKVVAGVANALAHKYH

PfAP-M1: Lys (K), Ala (A), Arg (R), Ser (S) and Asn (N) (and Leu (L), Phe (F) and Tyr (Y), in green)
PfAP-M17: Leu (L), Phe (F), Thr (T) and Tyr (Y)
PfAP-M18: Asp (D) and Glu (E)
PfAP-M24B: all residues linked to Pro (P)

Figure 7.1. Proposed model for the role of *P. falciparum* aminopeptidases in haemoglobin degradation in the parasites. **A.** the proposed action of the various aminopeptidases on oligopeptides and dipeptides produced by the action of other peptidases. **B.** the residues within human haemoglobin that would be expected to be cleaved by PfAP-M1, PfAP-M17, PfAP-M18 and PfAP-M24 coloured in blue, green, red and purple, respectively. All leucine, phenylalanine, threonine and tyrosine residues are coloured green, indicating cleavage by PfAP-M17 but they could also be acted on by PfAP-M1. All residues linked to proline are coloured purple to indicate putative action by PfAP-M24. Some of the residues in black may possibly be acted on by M1 aminopeptidase but cleavage of these residues has not been assessed. DPAP-1 refers to dipeptidyl aminopeptidase 1.

second position but can cleave those with it in the first. In support of this idea they found (using yellow fluorescent protein (YFP)-tagged protein) that the enzyme was located in the digestive vacuole and that the vacuoles demonstrated aminopeptidase activity. However, the location studies cannot really be relied on as they observed cleavage of the tag from both enzymes that were seen located in the digestive vacuole.

A possible role for aminopeptidases in merozoite invasion has also been suggested as bestatin was seen to be capable of preventing invasion of erythrocytes (123). However, Gavigan *et al* saw that bestatin was capable of affecting trophozoite maturation at concentrations less than those needed to inhibit invasion. They concluded that the observed lack of rings seen in bestatin-treated cultures was due to an inhibition of schizont maturation rather than any effect on invasion (60). The finding by Florent *et al* that PfAP-M1 was labelled as condensed spots in schizonts and merozoites led the authors to speculate that it might be a possible candidate for involvement in invasion but this has not been confirmed (54).

In addition to their apparent functions in the terminal stages of haemoglobin degradation, it seems very likely that even if some or all of the aminopeptidases of *Plasmodium* are involved in this specialised role, they are also involved in other more general house-keeping functions. Aminopeptidases are found to play a variety of roles in such a diverse array of organisms (157) that it would seem inevitable that they would also be involved in other non-specialised processes in *P. falciarum*. For example, a number of parasites that do not reside inside erythrocytes and are, therefore, not involved in any degradation of haemoglobin contain a very similar range of aminopeptidase orthologues as those seen in *Plasmodium* e.g. the apicomplexans *Toxoplasma gondii* (www.toxodb.org) and *Cryptosporidium parvum* (www.cryptodb.org). Therefore, it may well be that some or all of the aminopeptidases are also important in various other house-keeping activities that require processing of peptides besides haemoglobin digestion.

7.5.   FUTURE DIRECTIONS

The peptidases of many organisms have been investigated and employed as targets for preventing disease, infectious and otherwise (48, 77, 162). The successes associated with many of these targets (e.g. HIV peptidase inhibitors and angiotensin-converting enzyme inhibitors) means that peptidases are being considered as targets in a variety of fields. Whatever the exact functions of *P. falciparum* aminopeptidases in the parasite, there

are many indicators that they are important for parasite growth and that they are worthy of targeting for drug development. Given the overlapping of function for some of the enzymes, it seems likely that a combined targeting of the aminopeptidases as a drug target would be the most efficient. There are already some compounds that are active against both the M1 and M17 aminopeptidases (eg. bestatin and many of the compounds tested in this study). Therefore it might be possible to develop a compound that targets both of these enzymes or indeed to look at combining inhibitors that act on other peptidases in the haemoglobin degradation pathway, especially considering the synergy previously observed.

While relatively recent advances, like the sequencing of the *P. falciparum* genome and transfection techniques that enable the manipulation of these genes, have definitely aided our ability to study the parasites, a number of obstacles still remain. For example, the difficulties encountered (here and by others) with the production of recombinant proteins and with experiments involving transgenic parasites delayed and/or prevented work in some instances. Ongoing investigation of new and/or improved methods for studying *P. falciparum* is important to achieve the levels of knowledge required to tackle this organism. However, while problems like those mentioned above mean that a certain amount still remains to be discovered about the aminopeptidases of *P. falciparum* and their role in the parasite, this work has furthered our knowledge about them and about the M17 aminopeptidase in particular.

REFERENCES

1. **Aguiar, J. C., J. LaBaer, P. L. Blair, V. Y. Shamailova, M. Koundinya, J. A. Russell, F. Huang, W. Mar, R. M. Anthony, A. Witney, S. R. Caruana, L. Brizuela, J. B. Sacci, Jr., S. L. Hoffman, and D. J. Carucci.** 2004. High-throughput generation of *P. falciparum* functional molecules by recombinational cloning. Genome Res **14:**2076-82.

2. **Albrecht, S., A. Defoin, E. Salomon, C. Tarnus, A. Wetterholm, and J. Z. Haeggstrom.** 2006. Synthesis and structure activity relationships of novel non-peptidic metallo-aminopeptidase inhibitors. Bioorg Med Chem **14:**7241-57.

3. **Allary, M., J. Schrével, and I. Florent.** 2002. Properties, stage-dependent expression and localization of *Plasmodium falciparum* M1 family zinc-aminopeptidase. Parasitology **125:**1-10.

4. **Allen, M. P., A. H. Yamada, and F. H. Carpenter.** 1983. Kinetic parameters of metal-substituted leucine aminopeptidase from bovine lens. Biochemistry **22:**3778-83.

5. **Andersson, L., T. C. Isley, and R. Wolfenden.** 1982. Alpha-aminoaldehydes: transition state analogue inhibitors of leucine aminopeptidase. Biochemistry **21:**4177-80.

6. **Aoyagi, T., H. Tobe, F. Kojima, M. Hamada, T. Takeuchi, and H. Umezawa.** 1978. Amastatin, an inhibitor of aminopeptidase A, produced by actinomycetes. J Antibiot (Tokyo) **31:**636-8.

7. **Baca, A. M., and W. G. Hol.** 2000. Overcoming codon bias: a method for high-level overexpression of *Plasmodium* and other AT-rich parasite genes in *Escherichia coli*. Int J Parasitol **30:**113-8.

8. **Bairoch, A.** 2000. The ENZYME database in 2000. Nucleic Acids Res **28:**304-5 (http://www.expasy.org/enzyme/).

9. **Baker, D., and A. Sali.** 2001. Protein structure prediction and structural genomics. Science **294:**93-6.

10. **Ball, E. G., R. W. Mc Kee, C. B. Anfinsen, W. O. Cruz, and Q. M. Geiman.** 1948. Studies on malarial parasites ix: chemical and metabolic changes during growth and multiplication in vivo and in vitro. J Biol Chem **175:**547-71.

11. **Banerjee, R., J. Liu, W. Beatty, L. Pelosof, M. Klemba, and D. E. Goldberg.** 2002. Four plasmepsins are active in the *Plasmodium falciparum* food vacuole,

including a protease with an active-site histidine. Proc Natl Acad Sci U S A **99:**990-5.

12.   **Bannister, L., and G. Mitchell.** 2003. The ins, outs and roundabouts of malaria. Trends Parasitol **19:**209-13.

13.   **Barrett, A. J., N. D. Rawlings, and E. A. O'Brien.** 2001. The MEROPS database as a protease information system. J Struct Biol **134:**95-102.

14.   **Bauvois, B., and D. Dauzonne.** 2006. Aminopeptidase-N/CD13 (EC 3.4.11.2) inhibitors: chemistry, biological evaluations, and therapeutic prospects. Med Res Rev **26:**88-130.

15.   **Bell, A.** 2000. Recent developments in the chemotherapy of malaria. IDrugs **3:**310-7.

16.   **Bergin, J. D., and C. H. Clapp.** 1989. Inhibition of aminopeptidase M by alkyl D-cysteinates. J Enzyme Inhib **3:**127-31.

17.   **Berry, C.** 1999. Proteases as drug targets for the treatment of malaria, p. 165-187. *In* B. M. Dunn (ed.), Proteases of infectious agents. Academic Press, San Diego.

18.   **Blackman, M. J.** 2000. Proteases involved in erythrocyte invasion by the malaria parasite: function and potential as chemotherapeutic targets. Curr Drug Targets **1:**59-83.

19.   **Bojang, K. A., P. J. Milligan, M. Pinder, L. Vigneron, A. Alloueche, K. E. Kester, W. R. Ballou, D. J. Conway, W. H. Reece, P. Gothard, L. Yamuah, M. Delchambre, G. Voss, B. M. Greenwood, A. Hill, K. P. McAdam, N. Tornieporth, J. D. Cohen, and T. Doherty.** 2001. Efficacy of RTS,S/AS02 malaria vaccine against *Plasmodium falciparum* infection in semi-immune adult men in The Gambia: a randomised trial. Lancet **358:**1927-34.

20.   **Bonilla, J. A., T. D. Bonilla, C. A. Yowell, H. Fujioka, and J. B. Dame.** 2007. Critical roles for the digestive vacuole plasmepsins of *Plasmodium falciparum* in vacuolar function. Mol Microbiol **65:**64-75.

21.   **Bradford, M. M.** 1976. A rapid and sensitive method for the quantitation of microgram quantities of protein utilizing the principle of protein-dye binding. Anal Biochem **72:**248-54.

22.   **Breman, J. G.** 2001. The ears of the hippopotamus: manifestations, determinants, and estimates of the malaria burden. Am J Trop Med Hyg **64:**1-11.

23.   **Breman, J. G., M. S. Alilio, and A. Mills.** 2004. Conquering the intolerable burden of malaria: what's new, what's needed: a summary. Am J Trop Med Hyg **71:**1-15.

24. **Burley, S. K., P. R. David, R. M. Sweet, A. Taylor, and W. N. Lipscomb.** 1992. Structure determination and refinement of bovine lens leucine aminopeptidase and its complex with bestatin. J Mol Biol **224:**113-40.

25. **Burley, S. K., P. R. David, A. Taylor, and W. N. Lipscomb.** 1990. Molecular structure of leucine aminopeptidase at 2.7-A resolution. Proc Natl Acad Sci U S A **87:**6878-82.

26. **Carpenter, F. H., and J. M. Vahl.** 1973. Leucine aminopeptidase (Bovine lens). Mechanism of activation by Mg^{2+} and Mn^{2+} of the zinc metalloenzyme, amino acid composition, and sulfhydryl content. J Biol Chem **248:**294-304.

27. **Chae, Y. K., K. S. Cho, W. Chun, and K. Lee.** 2003. Protein production by stationary phase induction (SPI). Protein Pept Lett **10:**369-74.

28. **Charet, P., E. Aissi, P. Maurois, S. Bouquelet, and J. Biguet.** 1980. Aminopeptidase in rodent *Plasmodium*. Comp Biochem Physiol **65B:**519-524.

29. **Chen, X., C. R. Chong, L. Shi, T. Yoshimoto, D. J. Sullivan, Jr., and J. O. Liu.** 2006. Inhibitors of *Plasmodium falciparum* methionine aminopeptidase 1b possess antimalarial activity. Proc Natl Acad Sci U S A **103:**14548-53.

30. **Cline, J., J. C. Braman, and H. H. Hogrefe.** 1996. PCR fidelity of *pfu* DNA polymerase and other thermostable DNA polymerases. Nucleic Acids Res **24:**3546-51.

31. **Clyde, D. F., H. Most, V. C. McCarthy, and J. P. Vanderberg.** 1973. Immunization of man against sporozite-induced falciparum malaria. Am J Med Sci **266:**169-77.

32. **Coombs, G. H., D. E. Goldberg, M. Klemba, C. Berry, J. Kay, and J. C. Mottram.** 2001. Aspartic proteases of *Plasmodium falciparum* and other parasitic protozoa as drug targets. Trends Parasitol **17:**532-7.

33. **Cunningham, D. F., and B. O'Connor.** 1997. Proline specific peptidases. Biochim Biophys Acta **1343:**160-86.

34. **Curley, G. P., S. M. O'Donovan, J. McNally, M. Mullally, H. O'Hara, A. Troy, S. A. O'Callaghan, and J. P. Dalton.** 1994. Aminopeptidases from *Plasmodium falciparum*, *Plasmodium chabaudi chabaudi* and *Plasmodium berghei*. J Eukaryot Microbiol **41:**119-23.

35. **Dagle, J. M., and D. L. Weeks.** 2001. Oligonucleotide-based strategies to reduce gene expression. Differentiation **69:**75-82.

36. **Dalal, S., and M. Klemba.** 2007. Roles for two aminopeptidases in vacuolar hemoglobin catabolism in *Plasmodium falciparum*. J Biol Chem [Epub ahead of print] PMID: 17895246

37. **Daly, R., and M. T. Hearn.** 2005. Expression of heterologous proteins in *Pichia pastoris*: a useful experimental tool in protein engineering and production. J Mol Recognit **18:**119-38.

38. **Das, A., H. G. Elmendorf, W. I. Li, and K. Haldar.** 1994. Biosynthesis, export and processing of a 45 kDa protein detected in membrane clefts of erythrocytes infected with *Plasmodium falciparum*. Biochem J **302:**487-96.

39. **DePristo, M. A., M. M. Zilversmit, and D. L. Hartl.** 2006. On the abundance, amino acid composition, and evolutionary dynamics of low-complexity regions in proteins. Gene **378:**19-30.

40. **Divo, A. A., T. G. Geary, N. L. Davis, and J. B. Jensen.** 1985. Nutritional requirements of *Plasmodium falciparum* in culture. I. Exogenously supplied dialyzable components necessary for continuous growth. J Protozool **32:**59-64.

41. **Dowd, A. J., M. Dooley, C. Fagain, and J. P. Dalton.** 2000. Stability studies on the cathepsin L proteinase of the helminth parasite, *Fasciola hepatica*. Enzyme Microb Technol **27:**599-604.

42. **Drag, M., J. Grembecka, M. Pawelczak, and P. Kafarski.** 2005. alpha-Aminoalkylphosphonates as a tool in experimental optimisation of P1 side chain shape of potential inhibitors in S1 pocket of leucine- and neutral aminopeptidases. Eur J Med Chem **40:**764-71.

43. **Drag, M., M. Pawelczak, and P. Kafarski.** 2003. Stereoselective synthesis of 1-aminoalkanephosphonic acids with two chiral centers and their activity towards leucine aminopeptidase. Chirality **15 Suppl:**S104-7.

44. **Edwards, G., and G. A. Biagini.** 2006. Resisting resistance: dealing with the irrepressible problem of malaria. Br J Clin Pharmacol **61:**690-3.

45. **Eggleson, K. K., K. L. Duffin, and D. E. Goldberg.** 1999. Identification and characterization of falcilysin, a metallopeptidase involved in hemoglobin catabolism within the malaria parasite *Plasmodium falciparum*. J Biol Chem **274:**32411-7.

46. **Ellis, K. J., and J. F. Morrison.** 1982. Buffers of constant ionic strength for studying pH-dependent processes. Methods Enzymol **87:**405-26.

47. **Ersmark, K., B. Samuelsson, and A. Hallberg.** 2006. Plasmepsins as potential targets for new antimalarial therapy. Med Res Rev **26:**626-66.

48.   **Fear, G., S. Komarnytsky, and I. Raskin.** 2007. Protease inhibitors and their peptidomimetic derivatives as potential drugs. Pharmacol Ther **113:**354-68.

49.   **Fennell, B. J., J. A. Naughton, E. Dempsey, and A. Bell.** 2006. Cellular and molecular actions of dinitroaniline and phosphorothioamidate herbicides on *Plasmodium falciparum*: tubulin as a specific antimalarial target. Mol Biochem Parasitol **145:**226-38.

50.   **Flick, K., S. Ahuja, A. Chene, M. T. Bejarano, and Q. Chen.** 2004. Optimized expression of *Plasmodium falciparum* erythrocyte membrane protein 1 domains in *Escherichia coli*. Malar J **3:**50.

51.   **Flipo, M., T. Beghyn, V. Leroux, I. Florent, B. P. Deprez, and R. F. Deprez-Poulain.** 2007. Novel selective inhibitors of the zinc plasmodial aminopeptidase PfA-M1 as potential antimalarial agents. J Med Chem **50:**1322-34.

52.   **Flipo, M., I. Florent, P. Grellier, C. Sergheraert, and R. Deprez-Poulain.** 2003. Design, synthesis and antimalarial activity of novel, quinoline-based, zinc metallo-aminopeptidase inhibitors. Bioorg Med Chem Lett **13:**2659-62.

53.   **Florens, L., M. P. Washburn, J. D. Raine, R. M. Anthony, M. Grainger, J. D. Haynes, J. K. Moch, N. Muster, J. B. Sacci, D. L. Tabb, A. A. Witney, D. Wolters, Y. Wu, M. J. Gardner, A. A. Holder, R. E. Sinden, J. R. Yates, and D. J. Carucci.** 2002. A proteomic view of the *Plasmodium falciparum* life cycle. Nature **419:**520-6.

54.   **Florent, I., Z. Derhy, M. Allary, M. Monsigny, R. Mayer, and J. Schrével.** 1998. A *Plasmodium falciparum* aminopeptidase gene belonging to the M1 family of zinc-metallopeptidases is expressed in erythrocytic stages. Mol Biochem Parasitol **97:**149-60.

55.   **Galloway, C. A., M. P. Sowden, and H. C. Smith.** 2003. Increasing the yield of soluble recombinant protein expressed in *E. coli* by induction during late log phase. Biotechniques **34:**524-6, 528, 530.

56.   **Gardiner, D. L., D. C. Holt, E. A. Thomas, D. J. Kemp, and K. R. Trenholme.** 2000. Inhibition of *Plasmodium falciparum* clag9 gene function by antisense RNA. Mol Biochem Parasitol **110:**33-41.

57.   **Gardiner, D. L., J. S. McCarthy, and K. R. Trenholme.** 2005. Malaria in the post-genomics era: light at the end of the tunnel or just another train? Postgrad Med J **81:**505-9.

58. **Gardiner, D. L., K. R. Trenholme, T. S. Skinner-Adams, C. M. Stack, and J. P. Dalton.** 2006. Overexpression of leucyl aminopeptidase in *Plasmodium falciparum* parasites. Target for the antimalarial activity of bestatin. J Biol Chem **281**:1741-5.

59. **Gardner, M. J., N. Hall, E. Fung, O. White, M. Berriman, R. W. Hyman, J. M. Carlton, A. Pain, K. E. Nelson, S. Bowman, I. T. Paulsen, K. James, J. A. Eisen, K. Rutherford, S. L. Salzberg, A. Craig, S. Kyes, M. S. Chan, V. Nene, S. J. Shallom, B. Suh, J. Peterson, S. Angiuoli, M. Pertea, J. Allen, J. Selengut, D. Haft, M. W. Mather, A. B. Vaidya, D. M. Martin, A. H. Fairlamb, M. J. Fraunholz, D. S. Roos, S. A. Ralph, G. I. McFadden, L. M. Cummings, G. M. Subramanian, C. Mungall, J. C. Venter, D. J. Carucci, S. L. Hoffman, C. Newbold, R. W. Davis, C. M. Fraser, and B. Barrell.** 2002. Genome sequence of the human malaria parasite *Plasmodium falciparum*. Nature **419**:498-511.

60. **Gavigan, C. S., J. P. Dalton, and A. Bell.** 2001. The role of aminopeptidases in haemoglobin degradation in *Plasmodium falciparum*-infected erythrocytes. Mol Biochem Parasitol **117**:37-48.

61. **Gelb, M. H.** 2007. Drug discovery for malaria: a very challenging and timely endeavor. Curr Opin Chem Biol **11**:440-5.

62. **Genton, B., I. Betuela, I. Felger, F. Al-Yaman, R. F. Anders, A. Saul, L. Rare, M. Baisor, K. Lorry, G. V. Brown, D. Pye, D. O. Irving, T. A. Smith, H. P. Beck, and M. P. Alpers.** 2002. A recombinant blood-stage malaria vaccine reduces *Plasmodium falciparum* density and exerts selective pressure on parasite populations in a phase 1-2b trial in Papua New Guinea. J Infect Dis **185**:820-7.

63. **Giannousis, P. P., and P. A. Bartlett.** 1987. Phosphorus amino acid analogues as inhibitors of leucine aminopeptidase. J Med Chem **30**:1603-9.

64. **Ginsburg, H.** 1990. Some reflections concerning host erythrocyte-malarial parasite interrelationships. Blood Cells **16**:225-35.

65. **Gluzman, I. Y., S. E. Francis, A. Oksman, C. E. Smith, K. L. Duffin, and D. E. Goldberg.** 1994. Order and specificity of the *Plasmodium falciparum* hemoglobin degradation pathway. J Clin Invest **93**:1602-8.

66. **Goh, L. L., P. Loke, M. Singh, and T. S. Sim.** 2003. Soluble expression of a functionally active *Plasmodium falciparum* falcipain-2 fused to maltose-binding protein in *Escherichia coli*. Protein Expr Purif **32**:194-201.

67. **Goldberg, D. E., A. F. Slater, R. Beavis, B. Chait, A. Cerami, and G. B. Henderson.** 1991. Hemoglobin degradation in the human malaria pathogen

Plasmodium falciparum: a catabolic pathway initiated by a specific aspartic protease. J Exp Med **173**:961-9.

68.   **Green, P. J., O. Pines, and M. Inouye.** 1986. The role of antisense RNA in gene regulation. Annu Rev Biochem **55**:569-97.

69.   **Grembecka, J., and P. Kafarski.** 2001. Leucine aminopeptidase as a target for inhibitor design. Mini Rev Med Chem **1**:133-44.

70.   **Grembecka, J., W. A. Sokalski, and P. Kafarski.** 2000. Computer-aided design and activity prediction of leucine aminopeptidase inhibitors. J Comput Aided Mol Des **14**:531-44.

71.   **Gu, Y. Q., F. M. Holzer, and L. L. Walling.** 1999. Overexpression, purification and biochemical characterization of the wound-induced leucine aminopeptidase of tomato. Eur J Biochem **263**:726-35.

72.   **Gu, Y. Q., and L. L. Walling.** 2000. Specificity of the wound-induced leucine aminopeptidase (LAP-A) of tomato activity on dipeptide and tripeptide substrates. Eur J Biochem **267**:1178-87.

73.   **Gyang, F. N., B. Poole, and W. Trager.** 1982. Peptidases from *Plasmodium falciparum* cultured in vitro. Mol Biochem Parasitol **5**:263-73.

74.   **Hatta, T., K. Kazama, T. Miyoshi, R. Umemiya, M. Liao, N. Inoue, X. Xuan, N. Tsuji, and K. Fujisaki.** 2006. Identification and characterisation of a leucine aminopeptidase from the hard tick *Haemaphysalis longicornis*. Int J Parasitol **36**:1123-32.

75.   **Haynes, R. K., and S. Krishna.** 2004. Artemisinins: activities and actions. Microbes Infect **6**:1339-46.

76.   **Hill, R. J., W. Konigsberg, G. Guidotti, and L. C. Craig.** 1962. The structure of human hemoglobin. I. The separation of the alpha and beta chains and their amino acid composition. J Biol Chem **237**:1549-54.

77.   **Holz, R. C., K. P. Bzymek, and S. I. Swierczek.** 2003. Co-catalytic metallopeptidases as pharmaceutical targets. Curr Opin Chem Biol **7**:197-206.

78.   **Hooper, N. M.** 1994. Families of zinc metalloproteases. FEBS Lett **354**:1-6.

79.   **Horrocks, P., K. Dechering, and M. Lanzer.** 1998. Control of gene expression in *Plasmodium falciparum*. Mol Biochem Parasitol **95**:171-81.

80.   **Ishizaki, T., A. Tosaka, T. Nara, N. Aoshima, S. Namekawa, K. Watanabe, F. Hamada, A. Omori, and K. Sakaguchi.** 2002. Leucine aminopeptidase during meiotic development. Eur J Biochem **269**:826-32.

81.   **Jambou, R., E. Legrand, M. Niang, N. Khim, P. Lim, B. Volney, M. T. Ekala, C. Bouchier, P. Esterre, T. Fandeur, and O. Mercereau-Puijalon.** 2005. Resistance of *Plasmodium falciparum* field isolates to in-vitro artemether and point mutations of the SERCA-type PfATPase6. Lancet **366:**1960-3.

82.   **Jana, S., and J. Paliwal.** 2007. Novel molecular targets for antimalarial chemotherapy. Int J Antimicrob Agents **30:**4-10.

83.   **Jongeneel, C. V., J. Bouvier, and A. Bairoch.** 1989. A unique signature identifies a family of zinc-dependent metallopeptidases. FEBS Lett **242:**211-4.

84.   **Joshua, G. W.** 2001. Functional analysis of leucine aminopeptidase in *Caenorhabditis elegans*. Mol Biochem Parasitol **113:**223-32.

85.   **Kapust, R. B., and D. S. Waugh.** 1999. *Escherichia coli* maltose-binding protein is uncommonly effective at promoting the solubility of polypeptides to which it is fused. Protein Sci **8:**1668-74.

86.   **Klemba, M., I. Gluzman, and D. E. Goldberg.** 2004. A *Plasmodium falciparum* dipeptidyl aminopeptidase I participates in vacuolar hemoglobin degradation. J Biol Chem **279:**43000-7.

87.   **Kolakovich, K. A., I. Y. Gluzman, K. L. Duffin, and D. E. Goldberg.** 1997. Generation of hemoglobin peptides in the acidic digestive vacuole of *Plasmodium falciparum* implicates peptide transport in amino acid production. Mol Biochem Parasitol **87:**123-35.

88.   **Krugliak, M., J. Zhang, and H. Ginsburg.** 2002. Intraerythrocytic *Plasmodium falciparum* utilizes only a fraction of the amino acids derived from the digestion of host cell cytosol for the biosynthesis of its proteins. Mol Biochem Parasitol **119:**249-56.

89.   **Kyes, S., R. Pinches, and C. Newbold.** 2000. A simple RNA analysis method shows *var* and *rif* multigene family expression patterns in *Plasmodium falciparum*. Mol Biochem Parasitol **105:**311-5.

90.   **Laemmli, U. K.** 1970. Cleavage of structural proteins during the assembly of the head of bacteriophage T4. Nature **227:**680-5.

91.   **Lambros, C., and J. P. Vanderberg.** 1979. Synchronization of *Plasmodium falciparum* erythrocytic stages in culture. J Parasitol **65:**418-20.

92.   **Langreth, S. G., J. B. Jensen, R. T. Reese, and W. Trager.** 1978. Fine structure of human malaria in vitro. J Protozool **25:**443-52.

93.   **Le Gouill, C., and C. V. Dery.** 1991. A rapid procedure for the screening of recombinant plasmids. Nucleic Acids Res **19:**6655.

94.   **Le Roch, K. G., J. R. Johnson, L. Florens, Y. Zhou, A. Santrosyan, M. Grainger, S. F. Yan, K. C. Williamson, A. A. Holder, D. J. Carucci, J. R. Yates, 3rd, and E. A. Winzeler.** 2004. Global analysis of transcript and protein levels across the *Plasmodium falciparum* life cycle. Genome Res **14:**2308-18.

95.   **Le Roch, K. G., Y. Zhou, P. L. Blair, M. Grainger, J. K. Moch, J. D. Haynes, P. De La Vega, A. A. Holder, S. Batalov, D. J. Carucci, and E. A. Winzeler.** 2003. Discovery of gene function by expression profiling of the malaria parasite life cycle. Science **301:**1503-8.

96.   **Lejczak, B., P. Kafarski, and J. Zygmunt.** 1989. Inhibition of aminopeptidases by aminophosphonates. Biochemistry **28:**3549-55.

97.   **Leung, D., G. Abbenante, and D. P. Fairlie.** 2000. Protease inhibitors: current status and future prospects. J Med Chem **43:**305-41.

98.   **Lew, V. L., T. Tiffert, and H. Ginsburg.** 2003. Excess hemoglobin digestion and the osmotic stability of *Plasmodium falciparum*-infected red blood cells. Blood **101:**4189-94.

99.   **Lindsay, C. K., D. E. Gomez, and U. P. Thorgeirsson.** 1996. Effect of flavone acetic acid on endothelial cell proliferation: evidence for antiangiogenic properties. Anticancer Res **16:**425-31.

100. **Liu, J., E. S. Istvan, I. Y. Gluzman, J. Gross, and D. E. Goldberg.** 2006. *Plasmodium falciparum* ensures its amino acid supply with multiple acquisition pathways and redundant proteolytic enzyme systems. Proc Natl Acad Sci U S A **103:**8840-5.

101. **Llinas, M., Z. Bozdech, E. D. Wong, A. T. Adai, and J. L. DeRisi.** 2006. Comparative whole genome transcriptome analysis of three *Plasmodium falciparum* strains. Nucleic Acids Res **34:**1166-73.

102. **Loria, P., S. Miller, M. Foley, and L. Tilley.** 1999. Inhibition of the peroxidative degradation of haem as the basis of action of chloroquine and other quinoline antimalarials. Biochem J **339:**363-70.

103. **Lowther, W. T., and B. W. Matthews.** 2002. Metalloaminopeptidases: common functional themes in disparate structural surroundings. Chem Rev **102:**4581-608.

104. **Mackintosh, C. L., J. G. Beeson, and K. Marsh.** 2004. Clinical features and pathogenesis of severe malaria. Trends Parasitol **20:**597-603.

105. **Maggiora, L. L., A. T. Orawski, and W. H. Simmons.** 1999. Apstatin analogue inhibitors of aminopeptidase P, a bradykinin-degrading enzyme. J Med Chem **42:**2394-402.

106.   **Makler, M. T., J. M. Ries, J. A. Williams, J. E. Bancroft, R. C. Piper, B. L. Gibbins, and D. J. Hinrichs.** 1993. Parasite lactate dehydrogenase as an assay for *Plasmodium falciparum* drug sensitivity. Am J Trop Med Hyg **48:**739-41.

107.   **Maniatis, T., E. F. Fritsch, and J. Sambrook.** 1982. Molecular cloning: a laboratory manual. Cold Spring Harbour Laboratory Press, Cold Spring Harbour, NY.

108.   **Martin, R. E., and K. Kirk.** 2007. Transport of the essential nutrient isoleucine in human erythrocytes infected with the malaria parasite *Plasmodium falciparum*. Blood **109:**2217-24.

109.   **McCarthy, E., C. Stack, S. M. Donnelly, S. Doyle, V. H. Mann, P. J. Brindley, M. Stewart, T. A. Day, A. G. Maule, and J. P. Dalton.** 2004. Leucine aminopeptidase of the human blood flukes, *Schistosoma mansoni* and *Schistosoma japonicum*. Int J Parasitol **34:**703-14.

110.   **McKerrow, J. H., C. Caffrey, B. Kelly, P. Loke, and M. Sajid.** 2006. Proteases in parasitic diseases. Annual Review of Pathology: Mechanisms of Disease **1:**497-536.

111.   **Mehlin, C., E. Boni, F. S. Buckner, L. Engel, T. Feist, M. H. Gelb, L. Haji, D. Kim, C. Liu, N. Mueller, P. J. Myler, J. T. Reddy, J. N. Sampson, E. Subramanian, W. C. Van Voorhis, E. Worthey, F. Zucker, and W. G. Hol.** 2006. Heterologous expression of proteins from *Plasmodium falciparum*: results from 1000 genes. Mol Biochem Parasitol **148:**144-60.

112.   **Menard, D., M. D. Matsika-Claquin, D. Djalle, F. Yapou, A. Manirakiza, V. Dolmazon, J. Sarda, and A. Talarmin.** 2005. Association of failures of seven-day courses of artesunate in a non-immune population in Bangui, Central African Republic with decreased sensitivity of *Plasmodium falciparum*. Am J Trop Med Hyg **73:**616-21.

113.   **Miura, K., D. B. Keister, O. V. Muratova, J. Sattabongkot, C. A. Long, and A. Saul.** 2007. Transmission-blocking activity induced by malaria vaccine candidates Pfs25/Pvs25 is a direct and predictable function of antibody titer. Malar J **6:**107.

114.   **Miyachi, H., M. Kato, F. Kato, and Y. Hashimoto.** 1998. Novel potent nonpeptide aminopeptidase N inhibitors with a cyclic imide skeleton. J Med Chem **41:**263-5.

115.   **Monaghan, P., and A. Bell.** 2005. A *Plasmodium falciparum* FK506-binding protein (FKBP) with peptidyl-prolyl cis-trans isomerase and chaperone activities. Mol Biochem Parasitol **139:**185-95.

116.   **Montgomery, M. K., S. Xu, and A. Fire.** 1998. RNA as a target of double-stranded RNA-mediated genetic interference in *Caenorhabditis elegans*. Proc Natl Acad Sci U S A **95:**15502-7.

117.   **Moorthy, V. S., M. F. Good, and A. V. Hill.** 2004. Malaria vaccine developments. Lancet **363:**150-6.

118.   **Morty, R. E., and J. Morehead.** 2002. Cloning and characterization of a leucyl aminopeptidase from three pathogenic *Leishmania* species. J Biol Chem **277:**26057-65.

119.   **Murata, C. E., and D. E. Goldberg.** 2003. *Plasmodium falciparum* falcilysin: a metalloprotease with dual specificity. J Biol Chem **278:**38022-8.

120.   **Nankya-Kitaka, M. F., G. P. Curley, C. S. Gavigan, A. Bell, and J. P. Dalton.** 1998. *Plasmodium chabaudi chabaudi* and *P. falciparum*: inhibition of aminopeptidase and parasite growth by bestatin and nitrobestatin. Parasitol Res **84:**552-8.

121.   **Ocain, T. D., and D. H. Rich.** 1992. alpha-Keto amide inhibitors of aminopeptidases. J Med Chem **35:**451-6.

122.   **Oeuvray, C., H. Bouharoun-Tayoun, H. Gras-Masse, E. Bottius, T. Kaidoh, M. Aikawa, M. C. Filgueira, A. Tartar, and P. Druilhe.** 1994. Merozoite surface protein-3: a malaria protein inducing antibodies that promote *Plasmodium falciparum* killing by cooperation with blood monocytes. Blood **84:**1594-602.

123.   **Olaya, P., and M. Wasserman.** 1991. Effect of calpain inhibitors on the invasion of human erythrocytes by the parasite *Plasmodium falciparum*. Biochim Biophys Acta **1096:**217-21.

124.   **Olliaro, P. L., and D. E. Goldberg.** 1995. The *Plasmodium* digestive vacuole: metabolic headquarters and choice drug target. Parasitol Today **11:**294-7.

125.   **Olliaro, P. L., and Y. Yuthavong.** 1999. An overview of chemotherapeutic targets for antimalarial drug discovery. Pharmacol Ther **81:**91-110.

126.   **Omara-Opyene, A. L., P. A. Moura, C. R. Sulsona, J. A. Bonilla, C. A. Yowell, H. Fujioka, D. A. Fidock, and J. B. Dame.** 2004. Genetic disruption of the *Plasmodium falciparum* digestive vacuole plasmepsins demonstrates their functional redundancy. J Biol Chem **279:**54088-96.

127.   **Pizzi, E., and C. Frontali.** 2001. Low-complexity regions in *Plasmodium falciparum* proteins. Genome Res **11:**218-29.

128.	**Prechel, M. M., A. T. Orawski, L. L. Maggiora, and W. H. Simmons.** 1995. Effect of a new aminopeptidase P inhibitor, apstatin, on bradykinin degradation in the rat lung. J Pharmacol Exp Ther **275:**1136-42.

129.	**Rawlings, N. D., and A. J. Barrett.** 1993. Evolutionary families of peptidases. Biochem J **290:**205-18.

130.	**Rawlings, N. D., and A. J. Barrett.** 1999. MEROPS: the peptidase database. Nucleic Acids Res **27:**325-31.

131.	**Rawlings, N. D., F. R. Morton, and A. J. Barrett.** 2006. MEROPS: the peptidase database. Nucleic Acids Res **34:**D270-2 (www.merops.ac.uk).

132.	**Rawlings, N. D., D. P. Tolle, and A. J. Barrett.** 2004. Evolutionary families of peptidase inhibitors. Biochem J **378:**705-16.

133.	**Rosenberg, R., R. A. Wirtz, I. Schneider, and R. Burge.** 1990. An estimation of the number of malaria sporozoites ejected by a feeding mosquito. Trans R Soc Trop Med Hyg **84:**209-12.

134.	**Rosenthal, P. J.** 2004. Cysteine proteases of malaria parasites. Int J Parasitol **34:**1489-99.

135.	**Rosenthal, P. J.** 2002. Hydrolysis of erythrocyte proteins by proteases of malaria parasites. Curr Opin Hematol **9:**140-5.

136.	**Rosenthal, P. J., and R. G. Nelson.** 1992. Isolation and characterization of a cysteine proteinase gene of *Plasmodium falciparum*. Mol Biochem Parasitol **51:**143-52.

137.	**Rosenthal, P. J., P. S. Sijwali, A. Singh, and B. R. Shenai.** 2002. Cysteine proteases of malaria parasites: targets for chemotherapy. Curr Pharm Des **8:**1659-72.

138.	**Sati, S. P., S. K. Singh, N. Kumar, and A. Sharma.** 2002. Extra terminal residues have a profound effect on the folding and solubility of a *Plasmodium falciparum* sexual stage-specific protein over-expressed in *Escherichia coli*. Eur J Biochem **269:**5259-63.

139.	**Sayers, J. R., H. P. Price, P. G. Fallon, and M. J. Doenhoff.** 1995. AGA/AGG codon usage in parasites: implications for gene expression in *Escherichia coli*. Parasitol Today **11:**345-6.

140.	**Schalk, C., H. d'Orchymont, M. F. Jauch, and C. Tarnus.** 1994. 3-Amino-2-tetralone derivatives: novel potent and selective inhibitors of aminopeptidase-M (EC 3.4.11.2). Arch Biochem Biophys **311:**42-6.

141. **Scornik, O. A., and V. Botbol.** 2001. Bestatin as an experimental tool in mammals. Curr Drug Metab **2:**67-85.

142. **Shenai, B. R., and P. J. Rosenthal.** 2002. Reducing requirements for hemoglobin hydrolysis by *Plasmodium falciparum* cysteine proteases. Mol Biochem Parasitol **122:**99-104.

143. **Shenai, B. R., P. S. Sijwali, A. Singh, and P. J. Rosenthal.** 2000. Characterization of native and recombinant falcipain-2, a principal trophozoite cysteine protease and essential hemoglobinase of *Plasmodium falciparum*. J Biol Chem **275:**29000-10.

144. **Sherman, I. W.** 1979. Biochemistry of *Plasmodium* (malarial parasites). Microbiol Rev **43:**453-95.

145. **Sijwali, P. S., K. Kato, K. B. Seydel, J. Gut, J. Lehman, M. Klemba, D. E. Goldberg, L. H. Miller, and P. J. Rosenthal.** 2004. *Plasmodium falciparum* cysteine protease falcipain-1 is not essential in erythrocytic stage malaria parasites. Proc Natl Acad Sci U S A **101:**8721-6.

146. **Sijwali, P. S., J. Koo, N. Singh, and P. J. Rosenthal.** 2006. Gene disruptions demonstrate independent roles for the four falcipain cysteine proteases of *Plasmodium falciparum*. Mol Biochem Parasitol **150:**96-106.

147. **Sijwali, P. S., B. R. Shenai, J. Gut, A. Singh, and P. J. Rosenthal.** 2001. Expression and characterization of the *Plasmodium falciparum* haemoglobinase falcipain-3. Biochem J **360:**481-9.

148. **Singh, B., L. Kim Sung, A. Matusop, A. Radhakrishnan, S. S. Shamsul, J. Cox-Singh, A. Thomas, and D. J. Conway.** 2004. A large focus of naturally acquired *Plasmodium knowlesi* infections in human beings. Lancet **363:**1017-24.

149. **Singh, N., P. S. Sijwali, K. C. Pandey, and P. J. Rosenthal.** 2006. *Plasmodium falciparum*: biochemical characterization of the cysteine protease falcipain-2'. Exp Parasitol **112:**187-92.

150. **Skinner-Adams, T. S., P. L. Hawthorne, K. R. Trenholme, and D. L. Gardiner.** 2003. GATEWAY vectors for *Plasmodium falciparum* transfection. Trends Parasitol **19:**17-8.

151. **Spielmann, T., and H. P. Beck.** 2000. Analysis of stage-specific transcription in *Plasmodium falciparum* reveals a set of genes exclusively transcribed in ring stage parasites. Mol Biochem Parasitol **111:**453-8.

152. **Spielmann, T., M. W. Dixon, M. Hernandez-Valladares, M. Hannemann, K. R. Trenholme, and D. L. Gardiner.** 2006. Reliable transfection of *Plasmodium*

falciparum using non-commercial plasmid mini preparations. Int J Parasitol **36:**1245-8.

153.   **Stack, C. M., J. Lowther, E. Cunningham, S. Donnelly, D. L. Gardiner, K. R. Trenholme, T. S. Skinner-Adams, F. Teuscher, J. Grembecka, A. Mucha, P. Kafarski, L. Lua, A. Bell, and J. P. Dalton.** 2007. Characterization of the *Plasmodium falciparum* M17 leucyl aminopeptidase. A protease involved in amino acid regulation with potential for antimalarial drug development. J Biol Chem **282:**2069-80.

154.   **Stowers, A. W., M. C. Kennedy, B. P. Keegan, A. Saul, C. A. Long, and L. H. Miller.** 2002. Vaccination of monkeys with recombinant *Plasmodium falciparum* apical membrane antigen 1 confers protection against blood-stage malaria. Infect Immun **70:**6961-7.

155.   **Strater, N., and W. N. Lipscomb.** 1995. Transition state analogue L-leucinephosphonic acid bound to bovine lens leucine aminopeptidase: X-ray structure at 1.65 A resolution in a new crystal form. Biochemistry **34:**9200-10.

156.   **Taylor, A.** 1993. Aminopeptidases: structure and function. Faseb J **7:**290-8.

157.   **Taylor, A.** 1993. Aminopeptidases: towards a mechanism of action. Trends Biochem Sci **18:**167-71.

158.   **Taylor, A., K. W. Volz, W. N. Lipscomb, and L. J. Takemoto.** 1984. Leucine aminopeptidase from bovine lens and hog kidney. Comparison using immunological techniques, electron microscopy, and X-ray diffraction. J Biol Chem **259:**14757-61.

159.   **Teuscher, F., J. Lowther, T. S. Skinner-Adams, T. Spielmann, M. W. Dixon, C. M. Stack, S. Donnelly, A. Mucha, P. Kafarski, S. Vassiliou, D. L. Gardiner, J. P. Dalton, and K. R. Trenholme.** 2007. The M18 Aspartyl Aminopeptidase of the Human Malaria Parasite *Plasmodium falciparum*. J Biol Chem **282:**30817-26.

160.   **Trager, W., and J. B. Jensen.** 1976. Human malaria parasites in continuous culture. Science **193:**673-5.

161.   **Tu, C. J., S. Y. Park, and L. L. Walling.** 2003. Isolation and characterization of the neutral leucine aminopeptidase (LapN) of tomato. Plant Physiol **132:**243-55.

162.   **Turk, B.** 2006. Targeting proteases: successes, failures and future prospects. Nat Rev Drug Discov **5:**785-99.

163.   **Umezawa, H., T. Aoyagi, H. Suda, M. Hamada, and T. Takeuchi.** 1976. Bestatin, an inhibitor of aminopeptidase B, produced by actinomycetes. J Antibiot (Tokyo) **29:**97-9.

164.	**Umezawa, H., M. Ishizuka, T. Aoyagi, and T. Takeuchi.** 1976. Enhancement of delayed-type hypersensitivity by bestatin, an inhibitor of aminopeptidase B and leucine aminopeptidase. J Antibiot (Tokyo) **29:**857-9.

165.	**Vallee, B. L., and D. S. Auld.** 1993. New perspective on zinc biochemistry: cocatalytic sites in multi-zinc enzymes. Biochemistry **32:**6493-500.

166.	**Vallee, B. L., and D. S. Auld.** 1990. Zinc coordination, function, and structure of zinc enzymes and other proteins. Biochemistry **29:**5647-59.

167.	**Vander Jagt, D. L., B. R. Baack, and L. A. Hunsaker.** 1984. Purification and characterization of an aminopeptidase from *Plasmodium falciparum*. Mol Biochem Parasitol **10:**45-54.

168.	**Vander Jagt, D. L., W. S. Caughey, N. M. Campos, L. A. Hunsaker, and M. A. Zanner.** 1989. Parasite proteases and antimalarial activities of protease inhibitors. Prog Clin Biol Res **313:**105-18.

169.	**Vander Jagt, D. L., L. A. Hunsaker, and N. M. Campos.** 1987. Comparison of proteases from chloroquine-sensitive and chloroquine-resistant strains of *Plasmodium falciparum*. Biochem Pharmacol **36:**3285-91.

170.	**Vedadi, M., J. Lew, J. Artz, M. Amani, Y. Zhao, A. Dong, G. A. Wasney, M. Gao, T. Hills, S. Brokx, W. Qiu, S. Sharma, A. Diassiti, Z. Alam, M. Melone, A. Mulichak, A. Wernimont, J. Bray, P. Loppnau, O. Plotnikova, K. Newberry, E. Sundararajan, S. Houston, J. Walker, W. Tempel, A. Bochkarev, I. Kozieradzki, A. Edwards, C. Arrowsmith, D. Roos, K. Kain, and R. Hui.** 2007. Genome-scale protein expression and structural biology of *Plasmodium falciparum* and related Apicomplexan organisms. Mol Biochem Parasitol **151:**100-10.

171.	**Walker, D. J., J. L. Pitsch, M. M. Peng, B. L. Robinson, W. Peters, J. Bhisutthibhan, and S. R. Meshnick.** 2000. Mechanisms of artemisinin resistance in the rodent malaria pathogen *Plasmodium yoelii*. Antimicrob Agents Chemother **44:**344-7.

172.	**Waller, R. F., and G. I. McFadden.** 2005. The apicoplast: a review of the derived plastid of apicomplexan parasites. Curr Issues Mol Biol **7:**57-79.

173.	**WHO.** May 2007. Malaria. Fact sheet No. 94., (http://www.who.int/mediacentre/factsheets/fs094/en/).

174.	**Williams, J. A., J. A. Langeland, B. S. Thalley, J. B. Skeath, and S. B. Carroll.** 1995. Expression of foreign proteins in *E. coli* using plasmid vectors and purification of specific polyclonal antibodies, p. 15-58 *In* D. M. Glover and B. D.

Hames (ed.), DNA Cloning: A Practical Approach Volume 2: Expression Systems. Oxford University Press Inc., New York.

175. **Wirth, D. F.** 2002. Biological revelations. Nature **419:**495-6.

176. **Wongsrichanalai, C., A. L. Pickard, W. H. Wernsdorfer, and S. R. Meshnick.** 2002. Epidemiology of drug-resistant malaria. Lancet Infect Dis **2:**209-18.

177. **Wu, Y., X. Wang, X. Liu, and Y. Wang.** 2003. Data-mining approaches reveal hidden families of proteases in the genome of malaria parasite. Genome Res **13:**601-16.

178. **Wyatt, D. M., and C. Berry.** 2002. Activity and inhibition of plasmepsin IV, a new aspartic proteinase from the malaria parasite, *Plasmodium falciparum*. FEBS Letters **513:**159-162.

179. **Xu, W., and Q. Li.** 2005. Progress in the development of aminopeptidase N (APN/CD13) inhibitors. Curr Med Chem Anticancer Agents **5:**281-301.

180. **Zhang, P., D. E. Nicholson, J. M. Bujnicki, X. Su, J. J. Brendle, M. Ferdig, D. E. Kyle, W. K. Milhous, and P. K. Chiang.** 2002. Angiogenesis inhibitors specific for methionine aminopeptidase 2 as drugs for malaria and leishmaniasis. J Biomed Sci **9:**34-40.

181. **Zuckerman, A., D. Spira, and J. Hamburger.** 1967. A procedure for the harvesting of mammalian plasmodia. Bull World Health Organ **37:**431-6.